

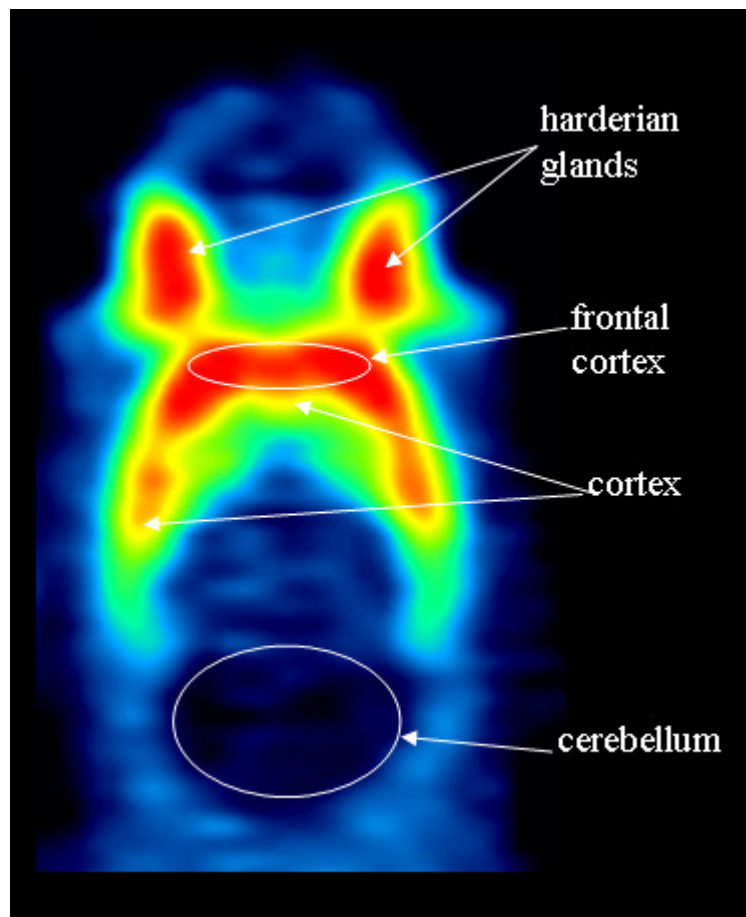
**Synthesis and evaluation of ^{18}F -radiopharmaceuticals
within the serotonergic receptor system
for molecular imaging**

Dissertation zur Erlangung des Grades
„Doktor der Naturwissenschaften“
im Promotionsfach Chemie

am Fachbereich Chemie, Pharmazie und Geowissenschaften
der Johannes Gutenberg-Universität
in Mainz

Matthias Herth
geb. in Mainz

Mainz 2009



Transversale µPET Aufnahme eines Rattenhirns zur Visualisierung des 5-HT_{2A} Rezeptorsystems.

Erklärung

Hiermit versichere ich, dass ich die vorliegende Dissertation eigenständig verfasst und keine anderen als die angegebenen Hilfsmittel verwendet habe.

Die Dissertation habe ich weder als Arbeit für eine staatliche oder andere wissenschaftliche Prüfung eingereicht noch ist sie oder ein Teil dieser als Dissertation bei einer anderen Fakultät oder einem anderem Fachbereich eingereicht worden.

Mainz, Mai 09

Abstract

Molecular imaging technologies as Positron Emission Tomography (PET) are playing a key role in drug discovery, development and delivery due to the possibility to quantify e.g. the binding potential *in vivo*, non-invasively and repetitively. In this context, it provides a significant advance in the understanding of many CNS disorders and conditions. The serotonergic receptor system is involved in a number of important physiological processes and diseases such as depression, schizophrenia, Alzheimer's disease, sleep or sexual behaviour. Especially, the 5-HT_{2A} and the 5-HT_{1A} receptor subtypes are in the focus of fundamental and clinical research due to the fact that many psychotic drugs interact with these neuronal transmembrane receptors.

This work describes the successful development, as well as *in vitro* and *in vivo* evaluation of 5-HT_{2A} and 5-HT_{1A} selective antagonistic PET-radiotracers.

The major achievements obtained in this thesis are:

1. the development and *in vitro* evaluation of several 5-HT_{2A} antagonistic compounds, namely MH.MZ ($K_i = 9.0$ nM), (R)-MH.MZ ($K_i = 0.72$ nM) and MA-1 ($K_i = 3.0$ nM).
2. the ¹⁸F-labeling procedure of these compounds and their optimization, whereby radiochemical yields > 35 % in high specific activities (> 15 GBq/μmol) could be observed. Synthesis time inclusive secondary synthon synthesis, the radioactive labeling procedure, separation and final formulation took no longer than 120 min and provided the tracer in high radiochemical purity.
3. the *in vivo* μPET evaluation of [¹⁸F]MH.MZ and (R)-[¹⁸F]MH.MZ resulting in promising imaging agents of the 5-HT_{2A} receptor status; from which (R)-[¹⁸F]MH.MZ seems to be the most promising ligand.
4. the determination of the influence of P-gp on the brain biodistribution of [¹⁸F]MH.MZ showing a strong P-gp dependency but no regional alteration.
5. the four-step radiosynthesis and evaluation of [¹⁸F]MDL 100907 resulting in another high affine tracer, which is, however, limited due to its low radiochemical yield.
6. the development and evaluation of 3 novel possible 5-HT_{2A} imaging agents combining structural elements of altanserin, MDL 100907 and SR 46349B demonstrating different binding modes of these compounds.
7. the development, the labeling and *in vitro* evaluation of the novel 5-HT_{1A} antagonistic tracer [¹⁸F]AH1.MZ ($K_i = 4.2$ nM).

Kurzdarstellung

Molekular bildgebende Verfahren wie die Positronen-Emissions-Tomography (PET) spielen eine wichtige Rolle bei vielen biologischen und medizinischen Fragestellungen. Dabei kann die PET *in vivo*, wiederholbar und nicht-invasiv z.B. das Bindungspotential von Tracern bestimmen und somit zu einem besseren Verständnis z.B. von neurologischen Krankheiten oder mentalen Zuständen dienen. Das serotonerge System ist an vielen physiologischen Prozessen und Krankheiten beteiligt. Besondere Bedeutung kommt dem 5-HT_{2A} und dem 5-HT_{1A} Rezeptorsubtypen zu. Viele Antipsychotika interagieren mit diesen Rezeptoruntereinheiten. Diese Arbeit befasst sich mit der erfolgreichen Entwicklung, der *in vitro* und *in vivo* Evaluierung von 5-HT_{2A} und 5-HT_{1A} selektiver antagonistischer PET-Radiotracer.

Die wichtigsten Ergebnisse werden im Folgenden aufgelistet:

1. die Entwicklung und *in vitro* Evaluierung mehrerer 5-HT_{2A} antagonistischer Verbindungen, MH.MZ ($K_i = 9.0$ nM), (R)-MH.MZ ($K_i = 0.72$ nM) und MA-1 ($K_i = 3.0$ nM) mit hoher Affinität und Selektivität.
2. die ¹⁸F-Markierung der genannten Liganden und deren Optimierung, die zu radiochemischen Ausbeuten (RCY) > 35 % in hohen spezifischen Aktivitäten (> 15 GBq/μmol) und hohen radiochemischen Reinheiten führten. Synthesezeit inklusive Synthonsynthese, Markierung, Abtrennung und Formulierung dauerte ~ 120 min.
3. die *in vivo* μPET Evaluierung von [¹⁸F]MH.MZ und (R)-[¹⁸F]MH.MZ, aus der resultiert, dass beide markierten Verbindungen als vielversprechende Tracer für den 5-HT_{2A} Rezeptorstatus dienen können; (R)-[¹⁸F]MH.MZ mit dem größeren Potential.
4. die Bestimmung des P-gp Einflusses auf die Hirnverteilung von [¹⁸F]MH.MZ mit dem Ergebnis, dass der Ligand eine starke P-gp Abhängigkeit aufweist. Jedoch konnten keine regionalen Biodistributionsunterschiede von [¹⁸F]MH.MZ determiniert werden.
5. eine 4-stufige radioaktive Synthese und Evaluierung von [¹⁸F]MDL 100907. Die Verbindung zeigte hochaffines Verhalten.
6. die Entwicklung und Evaluierung von 3 möglichen 5-HT_{2A} Verbindungen, die Strukturelemente von Altanserin, MDL 100907 und SR 46349B vereinigen. Die Charakterisierung legt nahe, dass die Rezeptorbindung in unterschiedlicher räumlicher Orientierung erfolgt.
7. die Entwicklung, Markierung und *in vitro* Evaluierung eines neuen 5-HT_{1A} antagonistischen Tracers [¹⁸F]AH1.MZ ($K_i = 4.2$ nM).

This thesis is based on the following 8 manuscripts:

- I. Herth, M.M.; Debus, F.; Piel, M.; Palner, M. Knudsen, G.M.; Lüddens, H.; Rösch, F.
Total Synthesis and Evaluation of [¹⁸F]MHMZ.
Bioorg. Med. Chem. Lett. 2008, 18, 151.
- II. Mühlhausen, U.; Ermert, J.; Herth, M.M.; Coenen, H.H.
Synthesis, Radiofluorination and First Evaluation of [¹⁸F]MDL 100907 as a Serotonin 5-HT_{2A} Receptor Antagonist for PET.
J. Label. Compd. Radiopharm. 2009, 52, 6.
- III. Herth, M.M.; Kramer, V.; Rösch, F.
Synthesis of Novel WAY 100635 derivatives containing a Norbornene Group and Radiofluorination of [¹⁸F]AH1.MZ, as a Serotonin 5-HT_{1A} Receptor Antagonist for Molecular Imaging.
J. Label. Compd. Radiopharm. 2009, DOI: 10.1002/jlcr.1589
- IV. Herth, M.M.; Piel, M.; Debus, F.; Schmitt, U.; Lüddens, H.; Rösch, F.
Preliminary in vivo and ex vivo Evaluation of the 5-HT_{2A} Imaging Probe [¹⁸F]MH.MZ.
Nucl. Med. Biol. 2009, DOI:10.1016/j.nucmedbio.2009.01.012
- V. Herth, M.M.; Kramer, V.; Piel, M.; Palner, M.; Reiß, P.; Knudsen, G.M.; Rösch, F.
Synthesis and in vitro Affinities of Various MDL 100907 Derivatives as Potential ¹⁸F-Radioligands for 5-HT_{2A} Receptor Imaging with PET.
Bioorg. Med. Chem. 2009, DOI:10.1016/j.bmc.2009.03.021
- VI. Kramer, V.; Herth, M.M.; Palner, M.; Knudsen, G.M.; Rösch, F.
Determination of Structure-Activity Relationships of MDL 100907, Altanserin and SR 46349B.
Bioorg. Med. Chem. Lett. 2009, (in preparation)
- VII. Debus, F.; Herth, M.M.; Buchholz, H.-H.; Bausbacher, N.; Kramer, V.; Moderegger, D.; Lüddens, H.; Rösch, F.
¹⁸F-Labeling and Evaluation of Novel MDL 100907 Derivatives as Potential 5-HT_{2A} Antagonists.
Nucl. Med. Biol. 2009, (in preparation)
- VIII. Schmitt, U.; Lee, D; Herth, M.M.; Piel, M.; Buchholz, H.-G.; Rösch, F.; Hiemke, C.; Lüddens, H; Debus, F.
P-glycoprotein Influence on the Brain-Uptake of a 5-HT_{2A} Ligand: [¹⁸F]MH.MZ.
JPET 2009, (submitted)

1	INTRODUCTION	- 1 -
1.1	Positron Emission Tomography (PET)	- 2 -
1.1.1	Basic principles for receptor binding	- 4 -
1.1.2	PET kinetic analysis – compartment modelling	- 5 -
1.2	¹⁸F-Production and labelling strategies	- 10 -
1.3	The serotonergic system	- 14 -
1.3.1	Biosynthesis and metabolism of serotonin	- 14 -
1.3.2	Anatomy and physiology of the serotonergic receptors and the serotonergic transporter	- 16 -
1.3.3	Interactions of drugs within the serotonergic system	- 22 -
1.4	PET molecular imaging of the serotonergic system	- 25 -
1.5	Discussion of routinely used 5-HT_{2A/1A} antagonistic PET tracers	- 31 -
1.6	Interaction of serotonergic PET-tracers with P-gp (plasma glycoprotein)	- 35 -
2	AIMS	- 38 -
3	MANUSCRIPTS	- 61 -
3.1	Total synthesis and evaluation of [¹⁸F]MHMZ	- 61 -
3.2	Synthesis, radiofluorination and first evaluation of [¹⁸F]MDL 100907 as a serotonin 5-HT_{2A} receptor antagonist for PET	- 72 -
3.3	Preliminary in vivo and ex vivo evaluation of the 5-HT_{2A} imaging probe [¹⁸F]MH.MZ	- 88 -
3.4	Synthesis and in vitro affinities of various MDL 100907 derivatives as potential ¹⁸F-radioligands for 5-HT_{2A} receptor imaging with PET	- 110 -
3.5	Determination of structure-activity relationships of MDL 100907, altanserin and SR 46349B	- 147 -
3.6	¹⁸F-Labeling and evaluation of novel MDL 100907 derivatives as potential 5-HT_{2A} antagonists for molecular imaging	- 157 -

3.7	Analysis of P-glycoprotein influence on the brain- uptake of a 5-HT_{2A} ligand: [¹⁸F]MH.MZ	- 174 -
3.8	Synthesis of novel WAY 100635 derivatives containing a norbornene group and radiofluoroination of [¹⁸F]AH1.MZ, as a serotonin 5-HT_{1A} receptor antagonist for molecular imaging	- 190 -
4	CONCLUSION	- 205 -
5	OUTLOOK	- 216 -
6	EPILOGUE	- 218 -
7	DANKSAGUNG	FEHLER! TEXTMARKE NICHT DEFINIERT.
8	CURRICULUM VITAE	- 220 -

1 Introduction

The perception of impulses represents an advantage for creatures regarding to the Darwinian theory of evolution. Therefore, diverse specialized cells or tissues, e.g. neuroreceptors or sensor-cells enable communication by cross-linking among each other and thus forming the nervous system.

Signal transmission among these cells has to be a basic postulate for a working nervous system. It is achieved by neurotransmitters, e.g. serotonin (5-hydroxytryptamine (5-HT)) and electrochemical processes. However, without this neuronal communication, mental or motor activities, also senses, would not be conceivable. On the other hand, manipulation of these signal transmission, e.g. within the brain, leads to varied behaviour. Drugs of misuse, such as MDMA (N-methyl-3,4-methylenedioxyamphetamine, ecstasy) and to some extent cocaine, are known to exert their effect via the serotonin reuptake site,¹ whereas LSD (lysergic acid diethylamide) functions as a 5-HT_{2A} agonist.^{2,3}

Moreover, selective serotonin reuptake inhibitors (SSRIs) modulate the synaptic serotonin levels by blocking the presynaptic serotonin transporter (SERT). The subsequent increased serotonin level within the synaptic cleft results in augmented population of serotonin receptors. This issue results in an improved disease pattern in depressive patients. Therefore, SERT functions as a primary target site for many antidepressant drugs.⁴ For example imipramin, a selective noradrenalin and serotonin reuptake inhibitor, is applied as an effective drug in many clinical trials.⁵

The “catecholamine hypothesis” of affective disorders reported by Schildkraut et al. in 1965 indicates that a deficit of catecholamines leads to major depression.⁶ Later experiments demonstrated the important role of serotonin within this clinical picture and led to the “serotonin-hypothesis” of depression.^{7,8,9,10,11} Serotonergic receptors regulate the behavioral patterns of mood, sexuality, memory or learning.^{12,13} The serotonergic neurotransmission is also associated with many other psychiatric mental diseases as the Alzheimer’s disease (AD)¹⁴ or schizophrenia.^{15,16} Moreover, all clinically approved atypical antipsychotic drugs are potent 5-HT_{2A}receptor antagonists.¹⁷

Positron emission tomography (PET) is an appropriate tool to measure *in vivo* directly, non-invasively and repetitively the binding potential, the receptor availability, and uptake kinetics of radiotracers for neuroreceptors. For these reasons, *in vivo* mapping of various serotonergic

receptors, especially of the 5-HT_{2A} and 5-HT_{1A} subtypes, is most valuable for the understanding of alterations within the serotonergic system. It might provide a significant advance in the understanding of the above mentioned disorders and conditions as well as it might prove its usefulness in monitoring antidepressant therapy.

A number of neurotransmitter analogues labeled with β^+ - emitter containing radioligands have already been synthesized as radiopharmaceuticals for molecular imaging of the 5-HT_{2A} and the 5-HT_{1A} receptor status. To date, *in vivo* studies have been performed with several 5-HT_{2A} selective antagonists such as [¹¹C]MDL 100907¹⁸ and [¹⁸F]altanserin¹⁹; selective 5-HT_{1A} antagonists used *in vivo* are [¹¹C]WAY 100635²⁰ and [¹⁸F]MPPF.²¹

However, PET studies of the 5-HT_{1A} and 5-HT_{2A} receptors still is limited by the characteristics of these radioligands and i.e. various shortcomings. Consequently, there is considerable interest in the development of more suitable PET radioligands for these receptors.

1.1 Positron Emission Tomography (PET)

Positron emission tomography is a nuclear medicine imaging technique which allows three-dimensional *in vivo*, non-invasive, quantitative, kinetic and repetitive imaging of functional biochemical processes within the body. Thereby the binding potential, the receptor availability, and the uptake kinetics of radio-tracers can be measured e.g. for neuroreceptors. Especially, the relationship of pharmacokinetic and pharmacodynamic parameters of a drug with behaviour and therapeutic efficacy can be evaluated in PET occupancy studies by applying a β^+ - emitting radioactive analogue of the drug.

Therefore, PET has been widely accepted as a tool for molecular imaging, which is regarded as one of the main paradigms for the twenty-first century biology.^{22,23} It is clinically particularly useful in patients with certain diseases affecting e.g. the brain, the heart as well as various cancer subtypes.

The PET device is able to detect pairs of gamma rays emitted following the decay of a positron-emitting radionuclide, which is attached on a biologically active molecule injected in the living body. In contrast to computed tomography (CT) or magnetic resonance imaging (MRI), which today mainly provide anatomic information, PET enables functional, diagnostic imaging. Compared with other functional imaging methods, PET and also SPECT (Single Photon Emission Computed Tomography) bear the advantages of high sensitivity (the level of detection approaches 10^{-12} M of tracer) and isotropism (*i.e.*, ability to detect expression accurately, regardless of tissue depth), which provide reliability for *in vivo* quantitative

imaging analyses at least for PET. Out of both techniques, PET represents the more precise and more detailed imaging methodology due to higher spatial and temporal resolution as well as due to better quantification possibilities.²⁴

The PET imaging principle makes use of the unique decay characteristics of a number of positron emitting radionuclides. A neutron-deficient isotope inside its atomic nucleus converts a proton into a neutron with subsequent emission of a positron, a particle with the opposite charge of an electron, from the nucleus. After travelling up to a few millimeters, depending on its initial kinetic energy, the positron encounters and annihilates with an electron, forming a positronium and then by decay a pair of annihilation γ -photons (2×511 keV) flashing in opposite directions ($\sim 180^\circ$) (Figure 1).²⁵

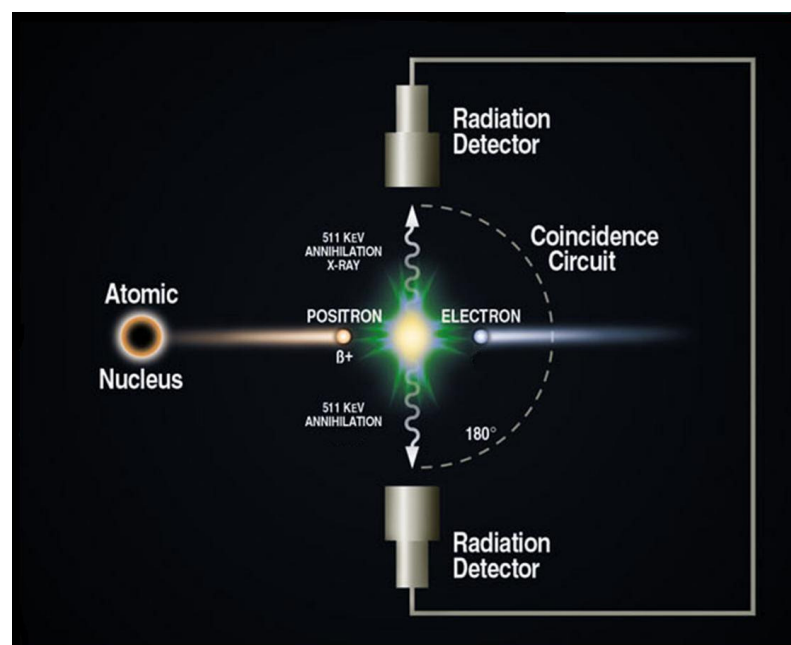


Figure 1: Annihilation and detection process involved in tomographic detection of positron decay²⁶

The simultaneously emitted γ -photons hardly interact with ambient matter of low density (such as water) and can therefore be detected by various scintillator materials creating a burst of light which is then detected by photomultiplier tubes or silicon avalanche photodiodes (Si APD) by a coincidence-detection.²⁷

Due to the decay mode of the positron emitters and the coincidence mode of detection, it is possible to reconstruct their source of origin along a straight line between one detector pair (line of response or LOR). After the correction (correction for random coincidences,

estimation and subtraction of scattered photons, detector dead-time correction, detector-sensitivity correction and attenuation correction) and a reconstruction process a 2D - 3D tomographic areas or volumes are rendered. The signal intensity in each of the image voxels is proportional to the amount of radiotracer therein and thus can be used to do quantitative analyses in the subject by involving transmission scans or CT registration.²⁸ By measuring the tissue concentration of radiotracers in a time sequence the rate of biological processes can be determined and mathematical modeling thereof can be applied.²⁹

1.1.1 Basic principles for receptor binding

The basis of receptor binding studies is the binding of ligand (L) to a receptor (R) to form a ligand-receptor complex (LR).



The K_D equilibrium dissociation constant measures the affinity of a ligand for a receptor, and is equal to k_2/k_1 . Thereby, k_1 is the association rate constant and k_2 is the dissociation rate constant. The K_D is the concentration of radioactive ligand required to occupy 50% of the receptors, whereas B_{max} is a measure of the density of the receptor in a tissue and is equivalent when all of the receptors are occupied by a radioactive ligand (Figure 2).³⁰

$$[\text{LR}] = (B_{max} * [\text{Ligand}]) / (K_D + [\text{Ligand}]) \quad (2)$$

Once steady-state conditions have been reached, the bound radioactive ligand is separated from the free ligand. The amount of receptor-ligand complex (bound) can be estimated by measuring the radioactivity.

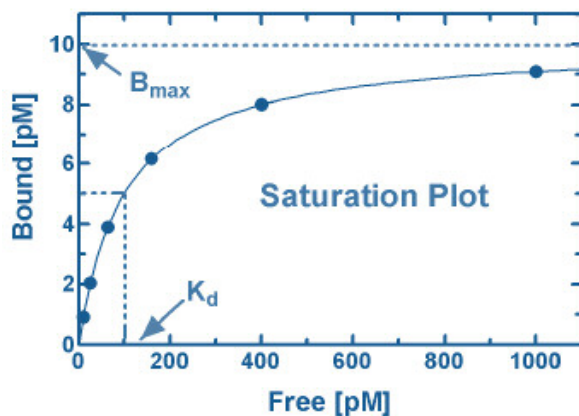


Figure 2: Saturation plot of bound (receptor-ligand-complex) and free ligand³⁰

Many ligands are not available in a radioactive form, therefore the affinity of the unlabeled ligand for the receptor can only be determined indirectly by measuring its ability to compete with, and thus inhibit, the binding of a radioactive ligand to its receptor (Figure 3).³⁰

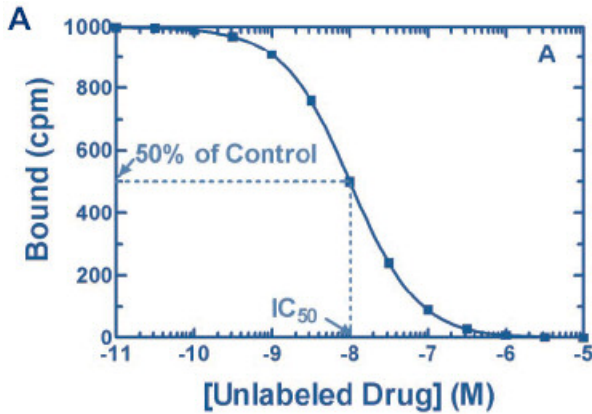


Figure 3: Various concentrations of unlabelled ligand are incubated with the receptor in the presence of a fixed concentration of radioactive ligand. The IC_{50} value is the concentration of unlabeled ligand that inhibits the binding of 50% of the radioactive ligand to the specific binding sites.³⁰

The binding parameter obtained from this experiment is the concentration of unlabeled ligand that inhibits the binding of the radioactive ligand by 50% (IC_{50} -value). The dissociation constant for the unlabeled ligand for the receptor is often referred to as the K_i rather than K_D because it is obtained from inhibition experiments rather than saturation experiments. The K_i -value for the unlabeled ligand can be obtained from the IC_{50} -value using the Cheng-Prusoff equation where L is the concentration of radioactive ligand used and K_D is the affinity of the radioactive ligand for the receptor.

$$K_i = IC_{50} / (1 + [L/K_D]) \quad (3)$$

1.1.2 PET kinetic analysis – compartment modelling

PET enables the visualization of the distribution of radiotracer and also the quantification of biochemical functions. However, in order to exploit the full potential of PET in all detail, the basic kinetic analysis of the biological behaviour of the labelled tracer has to be understood. Thereby, compartmental modelling is the basic principle to analyze dynamic PET data. In order to interpret the observed PET data after applying proper corrections (see 1.1), physiologically separated pools of the labelled tracer are assumed as compartments. Several acceptances underlie the compartmental model. The physiological process and the molecular

interactions are not allowed to be influenced by the injected tracer and should be constant during the PET measurement.

The binding potential (BP) is the most commonly reported outcome measure in PET studies of radioligand interaction with neuroreceptors. The BP corresponds to the ratio of B_{\max} (total receptor concentration) over K_D (the equilibrium dissociation constant of a molecule for a receptor) and can be derived from the Michaelis-Menten equilibrium equation. As described in 1.1.1, at equilibrium, the association and dissociation of the ligand from the receptor are equal, which implies:

$$k_{\text{on}} * [L] * [R] = k_{\text{off}} * [LR] \quad (4)$$

k_{on} = association rate constant

k_{off} = dissociation rate constant

L = free concentration of the radioligand

R = available receptors

LR = ligand receptor complex.

Substitution of LR as B, the total receptor concentration as B_{\max} , the $k_{\text{off}}/k_{\text{on}}$ ratio as K_D , R as $B_{\max} - B$ and rearrangement leads to the following equation.³¹

$$[B] = ([B_{\max}] * [L]) / (K_D + [L]) \quad (5)$$

At tracer amounts, which are used in PET scans, the free concentration of the radioligand [L] is much smaller than K_D and the equation simplifies to:

$$[B] = ([B_{\max}] * [L]) / K_D \quad \text{or} \quad [BP] = [B_{\max}] / K_D = [B] / [L] \quad (6)$$

Thus, at equilibrium, the BP is equal to the ratio of specifically bound ligand to free ligand.³¹

Neuroreceptor-ligand interactions are normally liable to the three tissue compartmental model. However, the number of compartments depends on the biochemical properties of the radioligands. In Figure 4 a typical neuroreceptor-ligand-interaction is presented. It shows the three tissue compartments model. The first compartment is the arterial blood. The radioligand is able to pass from the arterial blood into the second compartment, known as the free compartment. The third compartment is the region of specific binding and the fourth

compartment is a nonspecific-binding compartment that exchanges with the free compartment.

The transport and binding rates of the tracer (k_1 , k_2 , k_3 , k_4 , k_5 and k_6) are assumed to be linearly related to the concentration differences between two compartments, and the following differential equations are described at time t [min]:

$$dC_b(t) / dt = k_3 C_f(t) - k_4 C_b(t) \quad (7)$$

$$dC_f(t) / dt = k_1 C_p(t) + k_6 C_n(t) + k_4 C_b(t) - (k_2 + k_3 + k_5) C_f(t) \quad (8)$$

$$dC_n(t) / dt = k_5 C_f(t) - k_6 C_n(t), \quad (9)$$

where $C_p(t)$, $C_f(t)$, $C_b(t)$ and $C_n(t)$ are radioactivity concentrations at time t [min] for each compartment. Data obtained by PET ($C_{PET}(t)$) are a summation of these compartments as

$$C_{PET}(t) = C_f(t) + C_b(t) + C_n(t) \quad (10)$$

These parameters can be estimated by fitting the model to measured PET data with arterial radioactivity concentration ($C_p(t)$) as input function. Nevertheless, the $C_p(t)$ must be measured separately from PET data acquisition.³²

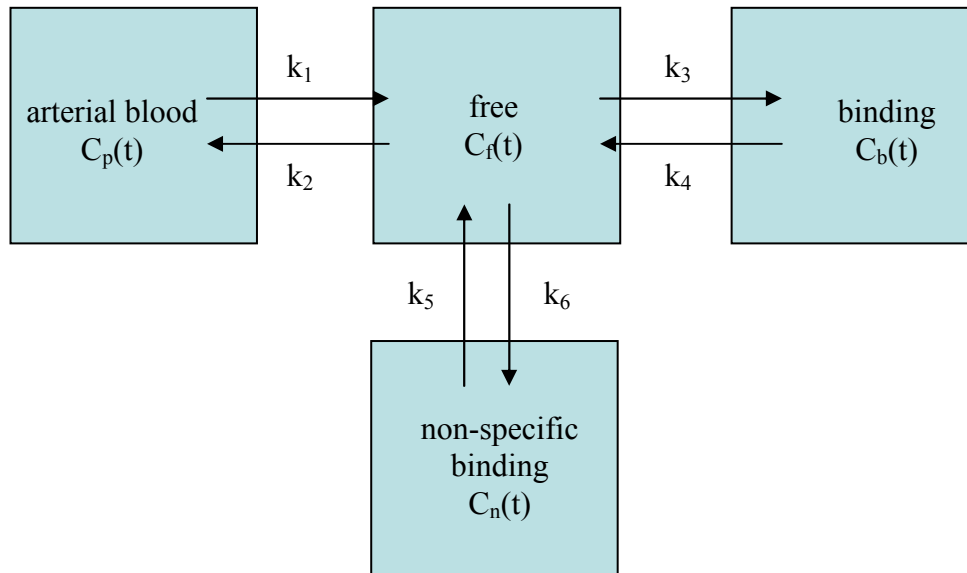


Figure 4: General three tissue (or four-compartment) model. This model consists of components of plasma, free ligand in tissue, specific binding and non-specific binding and six rate constants (k_1 – k_6).

The analysis of these parameter leads to macro parameters as the distribution volume (k_1/k_2), a rate to quantify the distribution of the tracer between plasma and the rest of the body, and the binding potential (k_1k_3/k_2k_4 or k_3/k_4), a quantity to measure the density of available receptors.

However, compartmental analysis needs the arterial activity as the input curve. Arterial sampling is invasive and technically demanding. Therefore, alternative techniques based on compartmental analysis are developed to avoid arterial cannulation and time-consuming metabolite measurements. Recently, a method has been described which allows for quantification of receptor binding kinetics without measuring the arterial input function. This method relies on the presence of a reference tissue, a region without specific binding of the ligand. It is omitting the arterial input function by assuming that all voxels of the interest in the PET data share the same arterial input function.^{33,34,35} The resulting model is called reference tissue model (Figure 5).³⁴

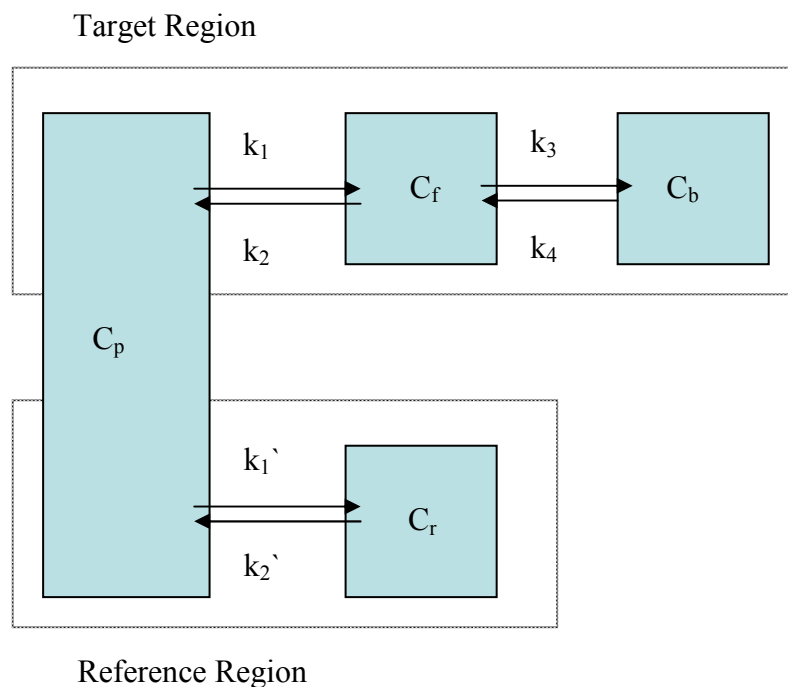


Figure 5: Reference tissue model. The target region and the reference region have the same plasma input function. It uses the C_r , time activity curve of the reference region as an indirect input function.³⁵

However, in the reference tissue model, the time course of the radioligands uptake in the tissue of interest is expressed in terms of its uptake in the tissue, assuming that the level of

nonspecific binding is the same in both tissues. The nonspecific binding is usually in rapid equilibrium with the free compartment and is therefore not distinguished from the free radioligand concentration.

‘The reference tissue compartment model is based on following differential equations:

$$dC_r(t) / dt = k_1' C_p(t) - k_2' C_r(t) \quad (11)$$

$$dC_f(t) / dt = k_1 C_p(t) - k_2 C_f(t) - k_3 C_f(t) + k_4 C_b(t) \quad (12)$$

$$dC_b(t) / dt = k_3 C_f(t) - k_4 C_b(t) \quad (13)$$

where C_p is the metabolite corrected plasma concentration, C_r is the concentration in reference tissue, C_f is the concentration of free (not specifically bound) ligand, C_b is the concentration of specifically bound ligand, k_1 is the rate constant for transfer from plasma to free compartment, k_2 is the rate constant for transfer from free to plasma compartment, k_3 is the rate constant for transfer from free to bound compartment, k_4 is the rate constant for transfer from bound to free compartment, k_1' is the rate constant for transfer from plasma to reference compartment, k_2' is the rate constant for transfer from reference to plasma compartment, and t is time.³⁵

Equation 11 describes the exchange between plasma and reference tissue, while equation 12 and 13 relate to the free and bound compartments of the region of interest, respectively. In practice, only the total concentration $C_t = C_f + C_b$ can be measured. Nevertheless, from equation 12 and 13 it is possible to derive a relationship between C_t and C_p and by using the relationship between C_p and C_r obtained from equation 11, a relationship between C_t and C_r can then be derived.

This relationship contains six parameters (k_1 , k_2 , k_3 , k_4 , k_1' , and k_2'). However, k_1 and k_1' only enter as a ratio ($R_1 = k_1/k_1'$), which accounts for any differences in delivery to the region of interest and the reference tissue. The operational equation can be further simplified by assuming that the volume of distribution of the not specifically bound tracer in both tissues is the same, i.e.,

$$k_1'/k_2' = k_1/k_2. \quad (14)$$

Consequently, k_2' can be replaced by k_2/R_1 . After replacing k_4 by k_3/BP , an operational equation with four parameters (R_1 , k_2 , k_3 , and BP) is obtained.³⁵ From the measured tissue

concentrations $C_i(t)$ and $C_r(t)$, best estimates of these parameters can be achieved using standard nonlinear regression analysis.³⁶

Although this technique has several advantages, especially non-invasiveness, it generally involves more assumptions and needs caution for use. For example, specific binding in reference regions results in an underestimation of specific binding in the target region.³⁷

1.2 ^{18}F -Production and labelling strategies

The success of PET as an unique imaging tool for clinical and basic research in life sciences for the investigation, localization, and quantification of physiological activities *in vivo* always stems from the development of suitable radiotracers. However, this development begins with the selection of an appropriate radionuclide enabling specialized PET-radiopharmaceuticals for targeting and quantifying specific molecular processes such as neurotransmitter-receptor interactions or enzyme activities within the living system. The choice of the nuclide is dependent on the half-life in relation to the kinetics of the process to be monitored or the position to be labelled (Table 1).

Table 1: Important radionuclides for PET - imaging³⁸

nuclide	half-life	Decay mode and probability [%]		E_{β^+} max. [MeV]	Mean of E_{β^+} [MeV]	max. distance in H_2O [mm]
^{11}C	20.4 min	β^+	99.8	0.96	0.385	4.1
^{13}N	9.97 min	β^+	99.8	1.19	0.491	5.4
^{15}O	2.04 min	β^+	99.9	1.70	0.735	8.2
^{18}F	110 min	β^+	96.9	0.63	0.242	2.4

Without a doubt, the short-lived positron emitting radionuclides that have had the greatest impact in PET for radiotracer synthesis are carbon-11 and fluorine-18. This is understandable due to the fact that carbon is a element of life, and can be substituted for its stable counterpart without influencing the bioactivity of the molecule. While fluorine-18 is not a significant element in living systems, its half-life and unique chemical properties make its use for labelling of considerable value. In addition experimentally achieved specific activities tend to be higher as compared to those of other frequently used isotopes. Moreover, unlike carbon-11, fluorine-18 possesses a much lower positron energy resulting only in a maximum range of 2.4

mm and thus making it a very attractive radioisotope for high-resolution PET measurements. However, nowadays the spatial resolution of human PET scanners unlike as for μ -PET scanners reaches distances between 3 and 4 mm. Nevertheless, in the near future higher resolutions even for human PET scanners will be possible e.g. by improvement of mathematical algorithms, time-of-flight scanners or combined MRI/PET-scanners. An additional advantage of fluorine-18 is its significant longer half-life (110 min) than carbon-11 (20 min), thus providing additional time to perform more complex synthetic manipulations or biological experiments, not to speak from transportation of the formulated tracer to external research facilities. However, even when an ^{18}F -compound closely resembles the parent, alterations of the biochemical behaviour cannot be excluded. Thus, an extensive and detailed evaluation process is required.

In conclusion, the existence of ^{18}F -tracers enables chemical and medicinal departments to probe specific targets in more detail regarding to the higher resolution, the higher specific activity and the half-life of this positron emitter. If pharmacokinetics are comparable to an ^{11}C -tracer, the ^{18}F -derivative displays the more valuable in view of clinical applications.

Today, fluorine-18 is cyclotron produced by bombardment with protons on enriched oxygen-18 [$^{18}\text{O}(\text{p},\text{n})^{18}\text{F}$] or with deuterons on neon-20 [$^{20}\text{Ne}(\text{d},\alpha)^{18}\text{F}$]. The method of choice depends on several factors including, whether it is desirable for the fluorine-18 source to be aqueous or anhydrous, whether the radiolabelled synthon needs to be nucleophilic or electrophilic, and whether that synthon needs to possess a high specific activity.³⁹ As a general rule to follow, proton irradiation of enriched water will yield an aqueous source of ^{18}F -fluoride for nucleophilic displacements with high specific activities while deuteron irradiation of neon will yield an anhydrous source of electrophilic fluorine-18 typically as elemental fluorine. However it is possible to render an aqueous source of ^{18}F -fluoride anhydrous as well as interconvert the nucleophilic fluoride into electrophilic reagents.³⁹

a) Preparation of fluorine-18 labelled elemental fluorine

Elemental ^{18}F -labelled fluorine is produced through the deuteron bombardment of a high-pressure neon gas target containing 0.1 to 2% of F_2 -carrier.⁴⁰ The method suffers from low specific activity due to the carrier addition with practical limits around 444 GBq/mmol.⁴¹

Probably, the most important electrophilic reaction is the labelling procedure of L-6- ^{18}F fluorodopa (Figure 6). Typically, the electrophilic ^{18}F -fluorination requires electron rich educts, e.g. aromatic systems, alkenes or a carbanion.

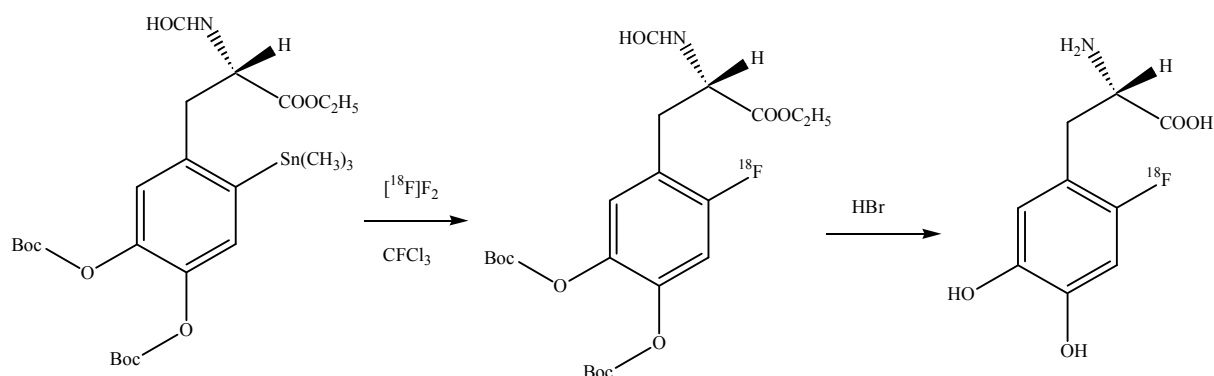


Figure 6: Electrophilic fluorination of L-[^{18}F]6-fluorodopa⁴²

b) Preparation of fluorine-18 as a fluoride ion

Radiofluorinations based on nucleophilic processes almost exclusively rely on no-carrier-added (n.c.a.) ^{18}F -fluoride. Thereby one key issue is how to render the ^{18}F -fluoride in a suitable solvent that is devoid of an excess of water which surrounds the produced ion due to the production route of an $^{18}\text{O}(\text{p},\text{n})^{18}\text{F}$ reaction on water targets.

Typically, most nucleophilic radiofluorinations will tolerate trace levels of water in the reaction medium so it is not essential to render the ^{18}F -fluoride entirely anhydrous.³⁹ Simple distillation can lead to a concentration of anionic and cationic contaminants from the target materials that can influence reactivity of the ^{18}F -fluoride.⁴³

These problems regarding the isolating process of ^{18}F -fluoride can be overcome by processing the target water through an ion exchange resin. This enables not only to recover the target ^{18}O -water, but also to remove some of the target water metal ion contaminants.³⁹ Finally, ^{18}F -fluoride can be extracted from target water using a potassium ion/cryptand complex immobilized on a stationary support.⁴⁴

Another key issue is how to maintain ^{18}F -fluoride solubility. A counter-ion is usually required that possesses sufficient solubility within the reaction media to maintain fluoride solubility.

Typically, ^{18}F -fluoride is extracted from the anion exchange resin using a dilute alkali metal carbonate solution. Potassium carbonate is preferred. However, the K^+ -counter-ion possesses limited solubility in some reaction solvents. Larger alkali metals such as caesium or rubidium do offer some enhancement to fluoride solubility.^{45,46,47} A number of alternate methodologies have been investigated to provide enhancement to solubility, as well as to reactivity. Some of these involve adding complexing agents to enhance cation solubility. For example, addition of 18-crown-6 ether will greatly improve ^{18}F -fluoride reactivity in certain instances such as radiofluorinating progesterone.⁴⁸ Use of aminopolyether Kryptofix 2.2.2. as a complexing

agent will also improve K^+ -solubility, and greatly enhance nucleophilic radiofluorinations with ^{18}F -fluoride on both aliphatic and aromatic substrates.

The most important nucleophilic reaction is the labelling procedure of 2- ^{18}F fluorodesoxy-D-glucose (2- ^{18}F FDG) (Figure 7).

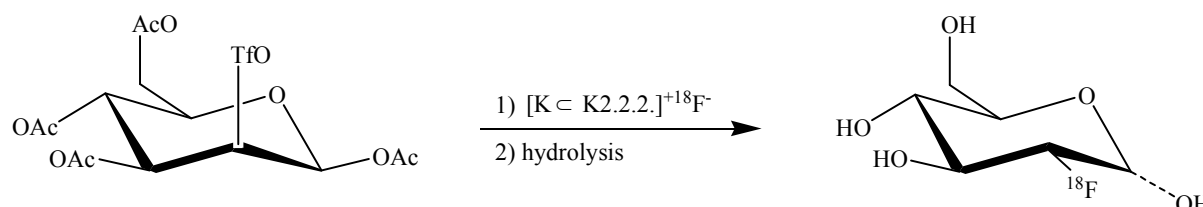


Figure 7: Nucleophilic fluorination of 2- ^{18}F FDG

c) Preparation of fluorine-18 containing small molecules as secondary synthon precursors

Very often nucleophilic synthesis routes are not accomplishable and interconversion of the nucleophilic fluoride into electrophilic reagents is necessary. A classic example is the aryl radiofluorination of phenolic compounds. Due to the acidity of the phenolic hydrogen, abstraction of hydrogen by fluoride will dominate over substitution. An alternate labelling strategy evolved for introducing fluorine-18 onto larger molecules by first attaching the radioisotope to a prosthetic group (Figure 8).

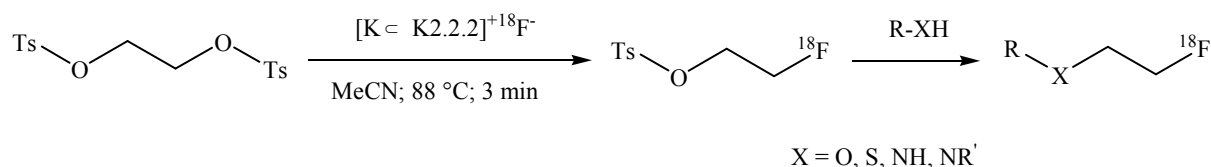


Figure 8: Scheme of the general interconversion of the nucleophilic fluoride into an electrophilic alkylating reagent and a labelling reaction of this synthon

Many prosthetic groups are well known for acylation, amidation or alkylation. However, the most significant agents are thereby alkylating synthons as ^{18}F [FETos or 4- ^{18}F]fluorophenacyl bromide.

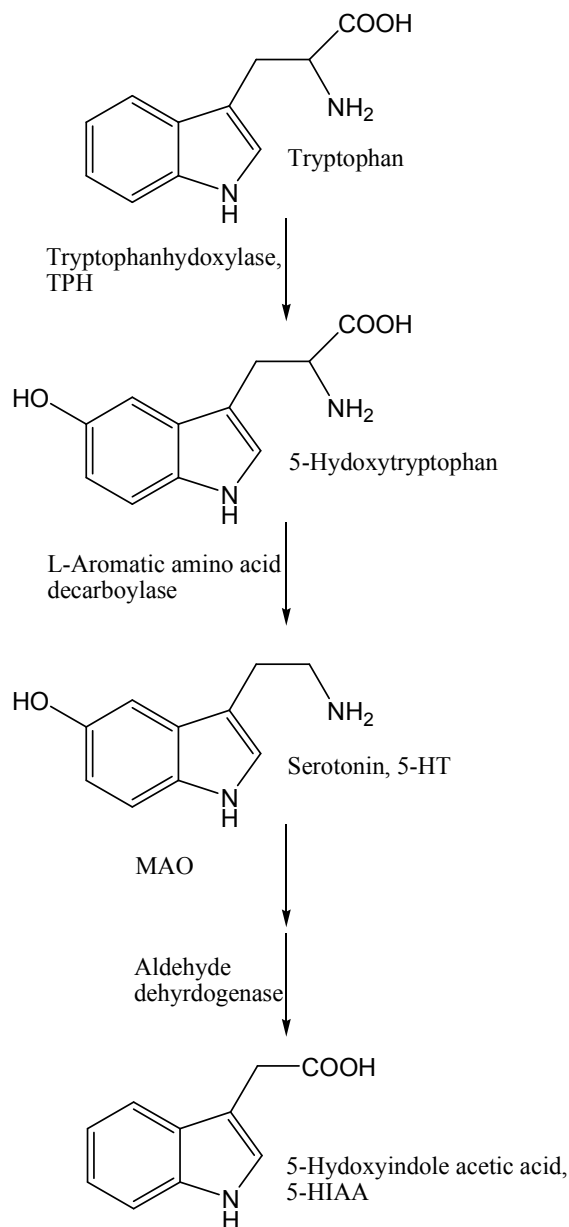
1.3 The serotonergic system

Serotonin (5-hydroxytryptamine, (5-HT)) is involved in the regulation of all behavioural, cognitive and physiological brain functions, including affect, aggression, anxiety, appetite, cognition, emesis, endocrine function, gastrointestinal function, mood, motor function, neurotrophism, pain, perception, sensory function, sex, sleep, and vascular function,^{49,50} as well as in the pathophysiology of many psychiatric and neurological disorders.^{51,52,53} However, it is not fully understood to what extent serotonin regulates or modulates these functions specifically. Moreover, serotonin 5-HT_{2A} receptors in the frontal cortex and in the hippocampus modulate local circuitry. Both of these brain areas are known to be involved importantly in associative learning across a number of species and learning paradigms.⁵⁴ Many clinically used drugs for the treatment of psychiatric disorders, e.g. depression and schizophrenia, are thought to act, at least partially, through serotonergic mechanisms. Actually, of the top 10 CNS drugs by total sales in the year 2003, 7 modulate serotonergic neurotransmission as part of their mechanism of action (olanzapine; sertraline; venlafaxine, risperidone; buspropion; paroxetine; quetiapine).⁵⁰ However, the involvement of serotonin in such an extensive range of functions implies that serotonin may function as both a classical neurotransmitter and a modulator of other neurotransmission systems. Moreover, this broad spectrum of various functions of the serotonergic system is explainable because of the anatomy of the serotonergic system, in which serotonergic cell bodies clustered in the brainstem raphe nuclei are positioned through their vast projections to influence all regions of the neuraxis. Another reason lies in the molecular diversity and differential cellular distribution of the many serotonergic receptor subtypes that are expressed in brain and other tissues. During the past decades, molecular cloning techniques and the subsequent development of receptor-subtype knockout mice, as well as development of compounds that are more highly selective at individual receptor subtypes, a greater understanding of serotonergic function continued to emerge. However, even with this wide armamentarium of 5-HT-modulating drugs, our understanding of the basic functions of serotonin in the CNS remains limited.⁵⁰

1.3.1 Biosynthesis and metabolism of serotonin

Serotonin is an indolamine with a hydroxyl group at the 5 position and a terminal amine group on the carbon chain. It is at physiological conditions protonated. It is hydrophilic and therefore unable to cross the blood-brain-barrier (BBB). Consequently, it has to be

synthesized locally in serotonergic neurons from the essential amino acid tryptophan by two separate enzymes. First, the precursor tryptophan is transported across the BBB by the transporter for neutral amino acids and second, tryptophan is converted by tryptophan hydroxylase (TPH) to 5-hydroxytryptophan using molecular oxygen, ascorbic acid, and biotin. 5-hydroxytryptophan is then decarboxylated into serotonin by L-aromatic amino acid decarboxylase (AADC).⁵⁵



The first enzyme in the pathway, tryptophan hydroxylase, is the rate-limiting step in the serotonin synthesis and is subject to regulatory processes. It can be competitively inhibited by parachlorophenylalanin and 6-fluoro-tryptophan of serotonin.⁵⁰ Inhibition of TPH results in a depletion of serotonin and subsequent downregulation of TPH and the serotonergic transporter.⁵⁰ Glucocorticoids as well as enhanced ingestion of tryptophan increase the serotonin synthesis. It is predominantly synthesized in the cytoplasm of the nerve terminals and thereafter accumulated into a secretory vesicle for regulated exocytotic release. After release into the synaptic cleft, serotonin is degraded by the actions of monoamine oxidase (MAO_A) and aldehyde dehydrogenase into its primary metabolite, 5-hydroxyindole acetic acid (5-HIAA), which is excreted in the urine (Figure 9).⁵⁰ Decreased levels of 5-HIAA are found in depressed patients who have recently attempted suicide.

Figure 9: Biosynthesis and metabolism of serotonin⁵⁰

In addition to the metabolism of extracellular serotonin in the synaptic cleft, it is also actively transported back into the presynaptic terminal by a serotonergic transporter (SERT) and recycled into vesicles or degraded by monoamine oxidase (MAO_B) (see Figure 11).^{53,56,57}

1.3.2 Anatomy and physiology of the serotonergic receptors and the serotonergic transporter

The complex serotonergic system is widespread throughout the brain, with the majority of the cell bodies of serotonergic neurons located in the raphe nuclei of the midline brainstem along its entire rostral-caudal axis: the dorsal raphe (DRN) and median raphe (MRN).⁵⁸ The DRN projects preferentially to the cortex, caudate and putamen, thalamus, nucleus accumbens, and dopaminergic nuclei of the midbrain (substantia nigra and ventral tegmental area), whereas the MRN projects thick serotonergic fibers with large varicosities that preferentially innervate the septum, cerebellum, spinal cord, hypothalamus, dorsal hippocampus and other limbic structures.^{59,60} Several brain structures like the amygdala and ventral hippocampus are innervated by the DRN as well as the MRN (Figure 10).^{52,53}

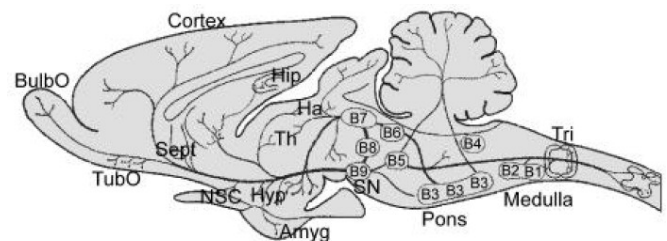
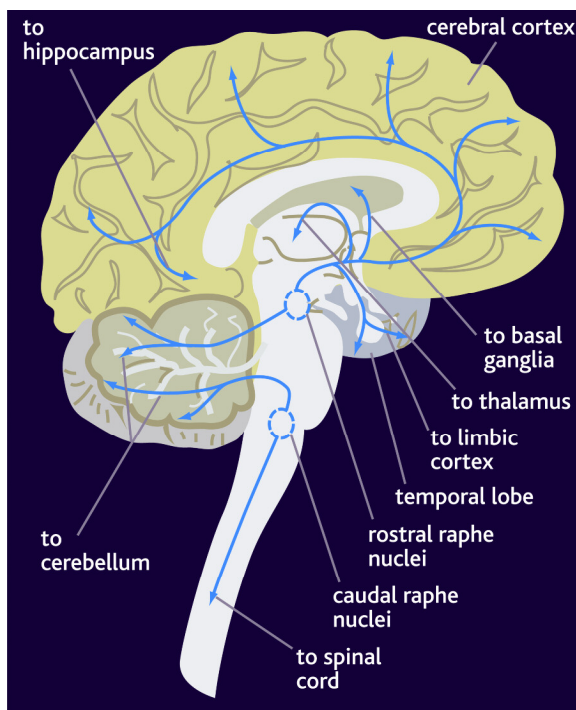


Figure 10: Diagram of the serotonergic pathways in the human brain (left) and in the rat brain (right) originating in the raphe nuclei.^{61,62}

BulbO: Bulbus olfactorius, TubO: Tuberculum olfactorium, Sept: Septum, NSC: Nucleus suprachiasticus, Hyp: Hypothalamus, Hip: Hippocampus, Th: Thalamus, Amyg: Amygdala, Ha: Habenulae, SN: Substantia nigra, Medulla: Medulla oblongata, Tri: Trigemini

The expansiveness of the serotonergic system makes it difficult to precisely ascertain the function of serotonin in the brain, although a modulatory role might be suggested. However, MRN appear primarily to be involved in modulation of sensory input and motor control,⁶³

whereas the nature of DRN interaction with postsynaptic elements, and the widespread distribution of 5-HT terminals in cortical and limbic areas indicate that these projections are most likely to be involved in the regulation of behavioural state and the modulation of more specific behaviours.⁵²

The serotonergic system consists of several presynaptic, postsynaptic receptors and one transporter (SERT) (Figure 11). In the raphe nuclei, the 5-HT_{1A} receptor acts as an autoreceptor and regulates the release of serotonin. The other receptors are distributed in highly distinct brain areas, such that individual brain regions express their own patterns of serotonergic receptor subtypes.^{51,64}

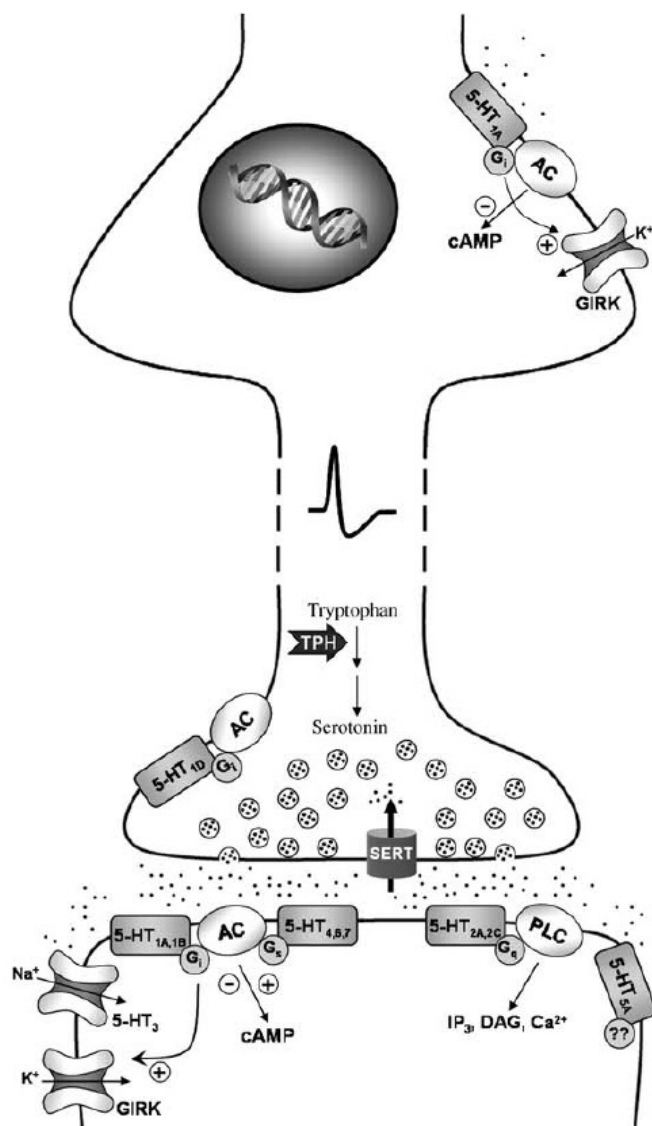


Figure 11: Diagram of a serotonergic neuron⁵⁰

The SERT is mainly located on serotonergic axons and maybe a small number is present on glia cells. Most serotonergic neurons fire with a spontaneous, slow, regular discharge pattern, which activity show up to be at its highest during active waking and low during sleep.⁶⁵

5-HT-Receptors

The at least 14 serotonin receptors can be divided into four receptor families: the three G-protein coupled (A-C) and the ion channel (D) based receptors, the A) 5-HT₁, B) 5-HT₂, C) 5-HT₄, 5-HT₆, 5-HT₇ and D) 5-HT₃ receptors. An overview of the known serotonin classes, their location and function is shown in Table 2.

In the following, this manuscript will focus on the receptor 5-HT₂ and the 5-HT_{1A} receptor family.

Table 2: Localization of 5-HT receptor subtypes (5HT_x) within the brain⁶²

Receptors	Distribution	Transduction mechanism
5-HT _{1A}	hippocampus, amygdala, septum, entorhinal cortex, hypothalamus, raphe nuclei	inhibits adenylate cyclase, releases K ⁺ -canals
5-HT _{1D}	substantia nigra, basalganglia	inhibits adenylate cyclase
5-HT _{1F}	cortex, striatum, hippocampus	inhibits adenylate cyclase
5-HT _{2A}	claustrum, cortex, olfactory bulb, corpus striatum, nucleus accumbens	stimulates phospholipase C, locks K ⁺ -canals
5-HT _{2B}	cerebellum, cortex, amygdala, substantia nigra, nucleus caudatus, thalamus, hypothalamus, retina	stimulates phospholipase C
5-HT _{2c}	globus pallidus, cortex, hypothalamus, septum, substantia nigra	stimulates phospholipase C
5-HT ₃	hippocampus, entorhinal cortex, amygdala, nucleus accumbens, trigeminal nerve, vagus nucleus, area postrema	releases K ⁺ -canals
5-HT ₄	hippocampus, corpus striatum, olfactory bulb, substantia nigra	stimulates adenylate cyclase
5-HT ₇	cortex, septum, thalamus, hypothalamus, amygdala	stimulates adenylate cyclase
5-HT _{5A} , 5-HT _{5B} , 5-HT ₆	unknown	unknown

5-HT₂-Receptor family

The 5-HT₂ receptor family consists of three receptor subtypes, 5-HT_{2A}, 5-HT_{2B} and 5-HT_{2C}, which are similar in terms of their molecular structure, pharmacology and signal transduction pathways and primarily located within the frontal cortex. With few notable exceptions (e.g. motor nuclei and the nucleus tractus solitarius), relatively low concentrations of 5-HT₂ receptors or mRNA expression are found in the brainstem and spinal cord.

Whereas the agonist [³H]serotonin only binds with low affinity, the antagonist [³H]ketanserin binds to the whole 5-HT₂ family with high. As a common attribute, all receptors are coupled positively to phospholipase C, mobilise intracellular calcium and stimulation of these receptors causes cell excitation.⁶⁶ Moreover, all receptors are members of the G-protein-coupled receptor superfamily.

The 5-HT_{2A} receptor: The distribution of 5-HT_{2A} receptors in the CNS has been extensively characterized by autoradiography. To date, the tracer of choice to study the 5-HT_{2A} receptor distribution is usually [³H]MDL 100907. Thereby, high levels of 5-HT_{2A} receptor binding sites could be detected in many forebrain regions (e.g. the neocortex), with lower levels in the basal ganglia, thalamus and hippocampus and no binding in the cerebellum. The 5-HT_{2A} receptors are particularly abundant in the pyramidal neurons primarily from cortical layers IV and V (Figure 12).^{67,68,69,70,71}

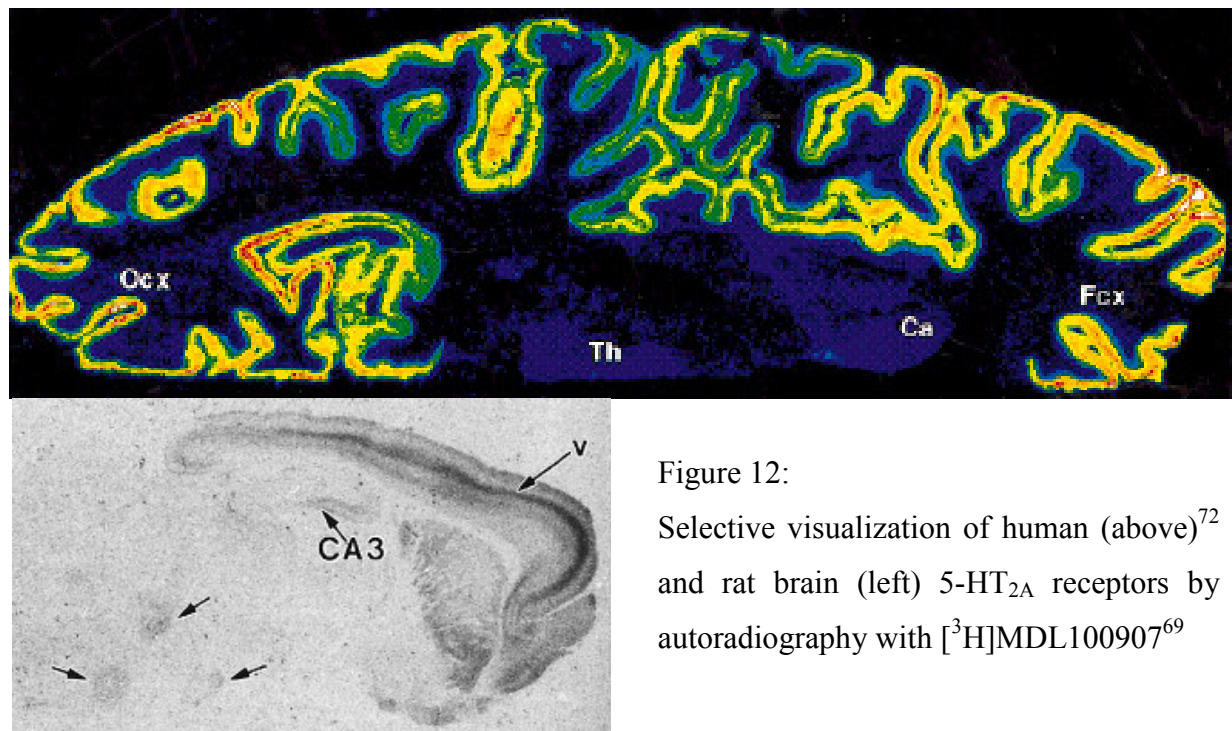


Figure 12:
Selective visualization of human (above)⁷²
and rat brain (left) 5-HT_{2A} receptors by
autoradiography with [³H]MDL100907⁶⁹

Because of the concordance between the distribution of 5-HT_{2A} receptor binding sites, mRNA, and receptor-like immunoreactivity,⁵⁰ the localization of cells expressing 5-HT_{2A} receptors is in regions where the receptors are located postsynaptically. The 5-HT_{2A} receptors are essential for mediating a large number of physiological processes in the periphery and in the CNS, including platelet aggregation, smooth muscle contraction and modulation of mood and perception.

The 5-HT_{2B} receptor: 5-HT_{2B} receptors are found in many tissues, including the stomach fundus, vascular smooth muscle, heart valves, spinal cord, and at low levels in some brain regions like the cerebellum, lateral septum, dorsal hypothalamus, and medial amygdale.^{73,74,75,76,77,78}

The 5-HT_{2C} receptor: The 5-HT_{2C} receptor sequence is fully cloned in rat, mouse, and human.^{79,80,81} It is very little expressed outside of the CNS unlike the 5-HT_{2A} and 5-HT_{2B} receptors. Autoradiographic studies have provided a detailed map of 5-HT_{2C} receptor binding sites in rat and other species.⁵⁸ Thereby, very high levels in the choroid plexus of the 5-HT_{2C} receptor binding sites and a wide distribution pattern in the cortex, basal ganglia, hippocampus, and hypothalamus was detected.⁸² Due to correlation between 5-HT_{2C} receptor mRNA and receptor binding sites, the 5-HT_{2C} receptor is clearly located postsynaptically.⁸³ The 5-HT_{2C} receptor is involved in the regulation of a wide range of behavioural and physiological processes, including regulation of the dopaminergic system and regulation of appetite, and plays a role in drug abuse, anxiety, and depression.⁸⁴

5-HT₁-receptor family

The 5-HT₁ class is the largest among the seven classes of 5-HT receptors. There are five different receptor types: the 5-HT_{1A}, 5-HT_{1B}, 5-HT_{1D}, 5-HT_{1E} and 5-HT_{1F}. All five having a nanomolar affinity for 5-HT and belong to the G-protein coupled receptor superfamily. All of the 5-HT₁ receptors inhibit adenylyl cyclase and modulate ion channels.^{85,86}

5-HT_{1A}-receptor: The highest densities of 5-HT_{1A} binding sites and high levels of 5-HT_{1A} mRNA expression in the brain are in the dorsal raphe nucleus, hippocampal pyramidal cell layer, and cerebral cortex, septum, amygdala, and cortical limbic areas.^{87,88} E.g., autoradiographic visualisation of the 5-HT_{1A} receptor in *post mortem* human and rat brain slices carried out with [³H]WAY 100635 and *p*-[¹⁸F]MPPF showed highest binding in neocortical regions and the hippocampus and low binding in the thalamus and basal ganglia,

whereas no binding was found in the cerebellum (Figure 13).^{72,89} The 5-HT_{1A} receptors are located presynaptically on serotonergic neurons in the raphe nuclei, where they inhibit the firing rate of serotonin via a negative-feedback influence when activated by an excess amount of 5-HT. Thus, they act as autoreceptors in the raphe nuclei.

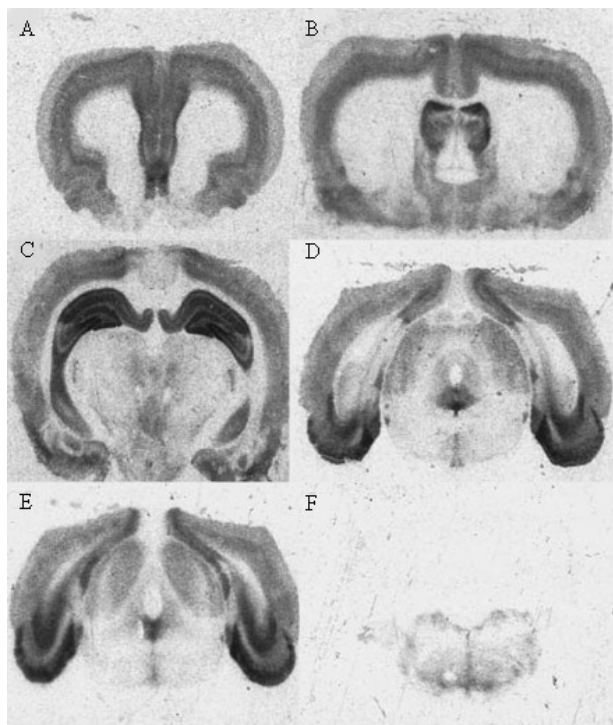
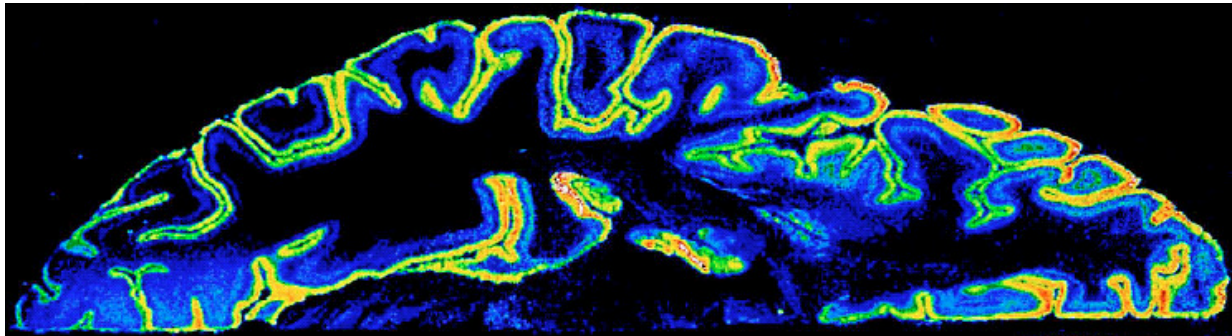


Figure 13:

Selective visualization of human 5-HT_{1A} receptors by autoradiography with [³H]WAY 100635⁷² and visualization by *p*-[¹⁸F]MPPF in rat brain:

*Autoradiograms show strong binding in cortex (A), lateral septum (B), hippocampus (C), dorsal raphe (D), and entorhinal cortex (E) and very low in cerebellum (F).*⁸⁹

Activation of 5-HT_{1A} autoreceptors results in a decrease of 5-HT release in projecting structures.⁹⁰ Beside the 5-HT_{1A} autoreceptors, there are postsynaptic receptors in limbic and cortical regions,⁹¹ which also act via an inhibitory action on neuronal firing.⁹² The molecular mechanisms of action underlying the opening of K⁺-channels are most likely common to all neurotransmitter receptors that couple act via G-proteins. In entorhinal cortex, where the density of 5-HT_{1A} receptors is especially high (and the density of 5-HT_{2A} receptors low), unopposed 5-HT_{1A} receptor mediated hyperpolarizing responses are seen.⁹³ However, cortical neurons in most other regions typically display mixed inhibitory and excitatory responses to

serotonin because of expression by the same pyramidal cells of multiple receptor subtypes (for example, 5-HT_{1A} and 5-HT_{2A/2C}).^{94,95,96,97}

1.3.3 Interactions of drugs within the serotonergic system

Many pharmaceutical applications target the serotonergic system. For example, it is very well known that SSRIs as well as inhibition of the degradation of serotonin by blocking MAO displays antidepressive effects.⁹⁸ To date, SSRIs (selective serotonin reuptake inhibitors) as fluoxetine or paroxetine are used, whereas in the past tricyclics, e.g. clomipramine, disadvantaged by cross-affinities most notably towards the noradrenaline transporter (NET; norepinephrine) but also to the dopamine transporter (DAT) and thus having adverse effects, were applied.⁹⁹

SERT is extremely important clinically as the majority of antidepressants inhibit the activity of this transporter, thus prolonging serotonergic signaling. However, after long-term but not short-term administration of those antidepressants, disinhibitory responses are seen with the selective 5-HT_{1A} antagonist WAY 100635 suggesting an increased 5-HT_{1A}-mediated inhibitory tone on hippocampal pyramidal cells.¹⁰⁰

In addition to psychotherapeutic agents, several drugs of abuse interfere with SERT activity, along with other transporters. These include cocaine, amphetamines, and MDMA; the effects of these agents on SERT have been recently reviewed.¹⁰¹

Anxiolytic-like effects can be initiated in a dose-dependent manner by partial 5-HT_{1A} agonists (buspirone, ipsapirone, gepirone) and to a certain degree by full 5-HT_{1A} receptor agonists (8-OH-DPAT).^{102,103} Nevertheless, to date it is not understood whether the postsynaptic interaction, and thus an increased neurotransmission or the inhibitory activation of autoreceptors, is responsible for the observed effect. Moreover, it has been suggested, that the 5-HT_{2B} receptor has a role in anxiety because the nonselective 5-HT₂ receptor agonist BW723C86 is reported to have anxiolytic properties in the rat social interaction test that can be reversed by a selective 5-HT_{2B} receptor antagonist.^{104,105}

The actions of psilocybin in humans can be blocked at facial motoneurons by either ketanserin or risperidone but not by haloperidol,¹⁰⁶ indicating that the actions of hallucinogens in humans are mediated via activation of 5-HT_{2A} receptors. Early studies in the dorsal raphe nucleus showed that lysergic acid diethylamide (LSD) and other indolamine hallucinogens are powerful agonists at the somatodendritic 5-HT autoreceptor.^{107,108} Especially, LSD showed to act as an agonist at 5-HT_{2A} and 5-HT_{2C} receptors.¹⁰⁹

The involvement of 5-HT_{2A} receptors in schizophrenia was recognized in 1954 with further support coming with the discovery that reserpine, a drug with some efficacy in treating schizophrenia, depletes 5-HT.^{110,111} The discovery that clozapine, a highly effective drug in treating schizophrenia,¹¹² is a 5-HT_{2A} receptor antagonist,^{17,113} which down-regulates 5-HT_{2A} receptors further reinforced these hypothesis.^{114,115} Moreover, the discovery of atypical antipsychotic drugs, a group, bound with higher affinity to 5-HT_{2A} receptors than to dopamine D₂ receptors approved this thesis.¹¹⁶ Indeed, atypical antipsychotic drugs can be classified based on a 5-HT_{2A}/D₂ affinity ratio of >1, while the typical antipsychotic drugs, e.g. haloperidol, all have 5-HT_{2A}/D₂ affinity ratios of <1 and thus often cause extrapyramidal dysfunction. Interestingly, risperidone and olanzapine, both high affinity 5-HT_{2A} receptor blocking antagonists compared to their D₂ affinity, have greater efficiency for treating negative symptoms of schizophrenia and produce fewer extrapyramidal side effects than haloperidol.^{117,118} Selective 5-HT_{2A} receptor antagonists (especially MDL 100907 and SR46349B) have shown promise in animal models to be predictive of atypical antipsychotic action¹¹⁹ and have demonstrated efficacy in treating schizophrenia.¹²⁰ However, future studies have to clarify the suggested mechanism of action.

Migraine can be treated with 5-HT agonists, even the pathophysiology of this disease is mostly understood. However, the primary dysfunction appears to be neuronal and thus forming misled, inflamed veins causing migraine. Thus, a local vasodilatation of extracerebral blood vessels resulting in an activation of surrounding sensoric neurons of the trigeminus system followed by a release of biochemical substances is assumed to cause migraine. Sumatriptan is an agonist of 5-HT_{1B} receptor, directly causes vasoconstriction and thus applied to patients suffered by migraine. Moreover, the selective 5-HT_{1F} agonist LY334370 inhibits neuronal impulses within the trigeminus area and therefore also appears to be therapeutically useful.¹²¹

Extensive serotonin release is caused in chromaffin cells of the gut by chemotherapeutics resulting in an increased activation of 5-HT₃ receptors and thus depolarising visceral neurons which leads to nausea and emesis. 5-HT₃ antagonists, e.g. ondansetron, suppress this mechanism.¹²²

Finally, serotonin is involved in the development of the eating disorder which is frequently combined with serotonergic deregulation.¹²³ Increased eating habits can be treated by SSRIs as fenfluramin, whereas antidepressiva are effective in bulimia patients.¹²⁴ However, the appetite suppressant fenfluramin is now-banned because of pulmonary arterial hypertension and damages of serotonin neurons after long-term application. These side-effects have

recently been reported to mediated via an activation of 5-HT_{2B} receptors as an agonist.¹²⁵ However, amphetamine derivatives such as fenfluramin and methylenedioxy-methamphetamine (MDMA, ecstasy) can also destroy 5-HT terminals leading to a long-lasting depletion of serotonin.^{126,127}

Figure 14 illustrates the possible interaction of various drugs within the serotonergic system.

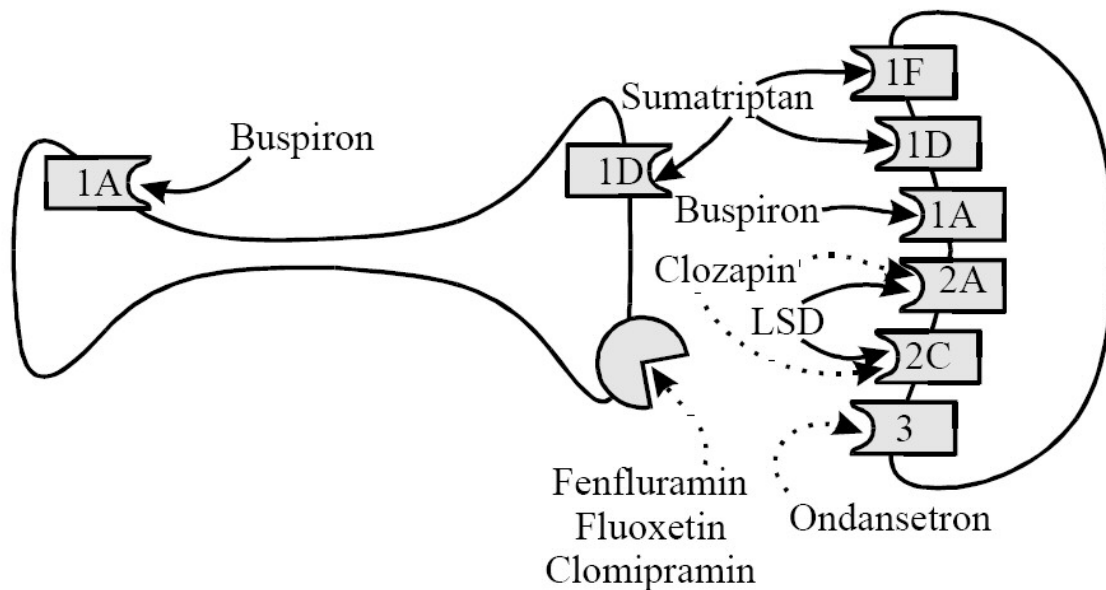


Figure 14: Scheme of interactions of various pharmaceuticals within the serotonergic system¹²⁸

More recently, it has been shown that 5-HT_{2A} receptors are also implicated in mediating viral entry of the JC virus.¹²⁹ The JC virus uses intact 5-HT_{2A} receptors for viral entry into neuronal cells. Blocking these receptors by 5-HT_{2A} selective antagonists inhibits this viral entry. These results imply that 5-HT_{2A} antagonists may represent novel treatments for virus entry and could lead to novel treatment applications concerning the human immunodeficiency virus (HIV) dementia.¹³⁰

Flibanserin is a novel drug used to cure female sexual dysfunction (FSD) or hypoactive sexual desire disorder (HSDD). The molecular basis is unknown, however the mechanism is supposed to be proceed via a potent agonistic mechanism of the 5-HT_{1A} receptor, via an antagonistic medium potent 5-HT_{2A} activation and a very low potent D₄ agonistic binding.

A lot of data were published in the nineties which led to the assumption that 5-HT_{2A} agonists can enhance associative learning, while antagonists like ritanserin and cyproheptadine

impaired it.^{131,132,133,134,135} Harvey et al. comes to the conclusion that the serotonin 5-HT_{2A} receptor is involved importantly in learning, and that alterations in this receptor can lead to abnormalities in cognitive functions in both humans and experimental animals.¹³⁶

1.4 PET molecular imaging of the serotonergic system

The serotonin synthesis rate, the availability and occupancy of the 5-HT_{1A} and the 5-HT_{2A} receptor as well as the reuptake rate of the serotonergic transporter are the most often investigated targets for the treatment of depression. The prevalence of major depression is estimated at 1 % to 10 % of persons 60 years of age or older, whereas depressive symptoms may occur in up to 20 %.^{137,138} In addition, the rate of suicide in this age group is higher than at any other stage of life.¹³⁹ Moreover, due to the fact that the serotonergic system is involved in various diseases and conditions, it is obvious that *in vivo* studies of these receptors and this transporter would provide a significant advance.

Figure 15 shows the currently used PET imaging probes for the 5-HT_{2A/1A}, SERT and the serotonin synthesis rate. All can be synthesized in satisfying radiochemical yields (RCY) and good specific activities (A_s).^{140,141,142,143,144,145,146} However, all act as antagonists, whereas serotonin itself functions as agonist.

[¹⁸F]Altanserin (**1**), [¹¹C]MDL 100907 (**2**) und [¹⁸F]SR 46349B (**3**) are the tracer of choice to image the 5-HT_{2A} receptor status, whereas [¹¹C]WAY 100635 (**4**) and [¹⁸F]FBWAY/[¹⁸F]MPPF (**5**) can be used for the 5-HT_{1A}-receptor.¹⁴⁷ For these imaging probes nanomolar affinities and good specificity towards the mentioned receptor were determined (Table 3).^{142, 148,149, 150}

[¹¹C]McN-5652X (**6**), [¹¹C]DASB (**7**) and [¹⁸F]ACF (**8**) are highly potent blockers of the serotonin reuptake site.¹⁵¹ Moreover, PET techniques have also been applied to the measurement of serotonin synthetic rates *in vivo* by α-[¹¹C]methyl-L-tryptophan (**9**).^{152,153}

In vivo evaluation: [¹⁸F]Altanserin is definitive the 5-HT_{2A} PET tracer with the greatest clinical impact. A number of medicinal studies have already been published.^{63,154,155,156,157,158} Dynamic PET brain imaging of [¹⁸F]altanserin in animals and humans corresponded to the known distribution of 5-HT_{2A} receptors in the brain.^{159,160,161}

Quantitative [¹⁸F]altanserin PET studies in man have suggested a decrement in binding with increasing age. Moreover, Alzheimer's disease patients showed a diffuse markedly lower [¹⁸F]altanserin binding than both the young and elderly controls.⁶³ This widespread reduced

brain 5-HT_{2A} receptor density in AD patients sets in early in the course of the disease and is related to early cognitive and neuropsychiatric symptoms.¹⁶²

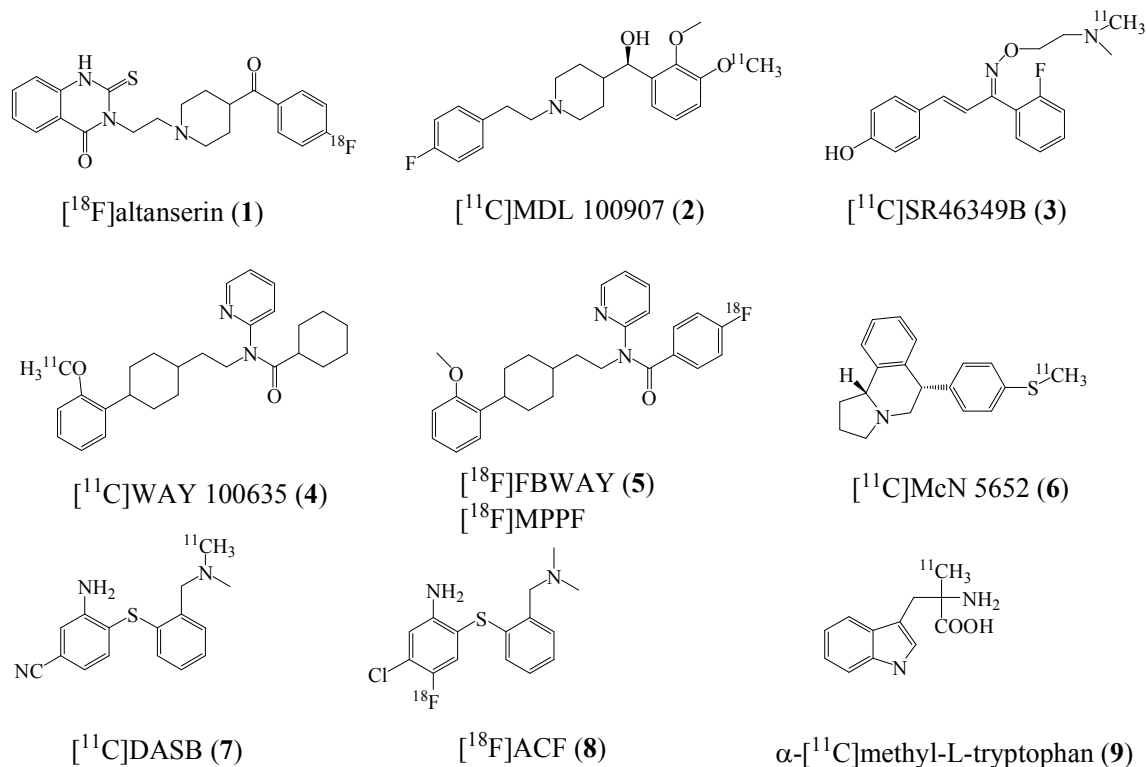


Figure 15: Serotonergic PET-Tracer

Table 3: Receptor affinities [nM] of 5-HT_{2A} and 5-HT_{1A} tracers

	5-HT _{2A}		5-HT _{1A}		5-HT _{2c}	D ₂	α ₁
	K _d	K _i	K _d	K _i	K _i	K _i	K _i
altanserin	~ 0.3	0.13	-	1570	40	62	4.55
(R)-MDL 100907	~ 0.3	0.36	-	> 10000	107	2250	128
SR 46349B	~ 2.9	1.07	-	> 10000	120	280000	3400
WAY 100635	-	578	1.11	0.84	3450	86.8	45
FBWAY	-	130	0.34	3.96	-	-	151

Other promising PET ligands for the 5-HT_{2A} receptor as [¹¹C]MDL 100907 and [¹¹C]SR 46349B are either not generally applied in clinical studies or still in the evaluation process.^{163,18,164} Indeed, [¹¹C]MDL 100907 has similar binding potency but greater specificity for the 5-HT_{2A} receptor as compared with [¹⁸F]altanserin,^{165,166,167} but is disadvantaged of the half-life of carbon-11. However, it is used in several promising *in vivo* studies.¹⁵⁸

Figure 17 shows the binding characteristic of [^{11}C]MDL 100907 in the human brain. Results are very similar to the those obtained using [^{18}F]altanserin.

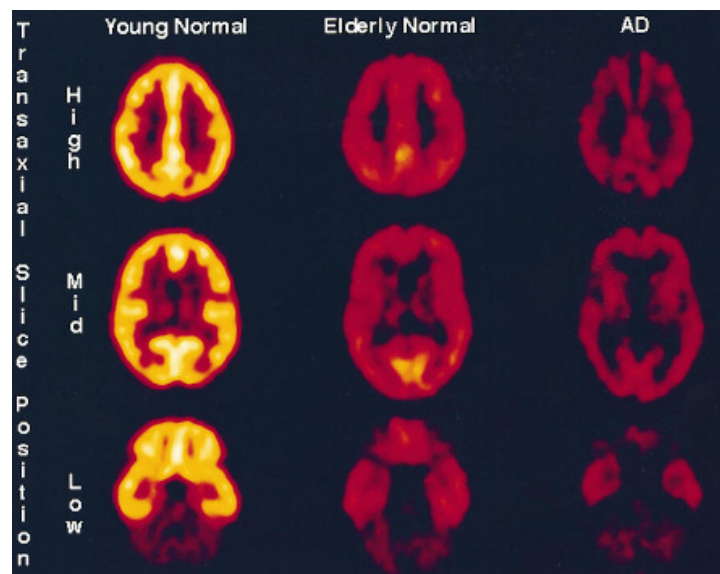


Figure 16: Summed [^{18}F]altanserin PET images in young normal (age: 20), elderly normal (age: 66 years), and AD (age: 67 years) subjects.

Images are displayed normalized to the cerebellum. Cortical 5-HT_{2A} binding is notably greater in the young relative to the elderly subject. The AD subject exhibits diffuse markedly lower [^{18}F]altanserin binding than both the young and elderly controls.⁶³

Bhagmagar et al. suggested by receptor binding measurements with [^{11}C]MDL 100907 that recovered subjects of major depression have an elevated binding potential of cortical 5-HT_{2A} receptors.¹⁶⁸

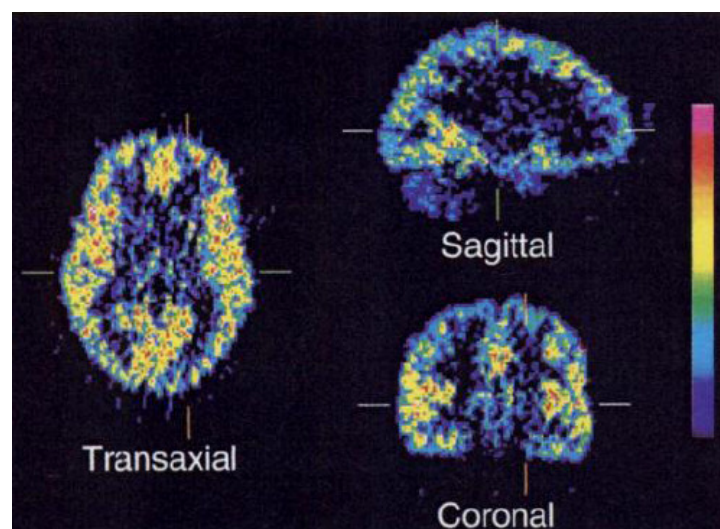


Figure 17: Summed PET images in three dimensions after intravenous injection of [^{11}C]MDL 100907.¹⁵⁸

The other highly potent and specific 5-HT_{2A} receptor antagonist, [¹¹C]SR 46349B, has properties that suggest that it may prove useful as a sensitive means to detect *in vivo* changes in endogenous serotonin levels.^{163,169} In order to study the (dys)function of neurotransmitter systems, it is important to quantify changes in the levels of these neurotransmitters in the living brain. Larisch et al. examined the postsynaptic receptor binding potential of [¹⁸F]altanserin as a possible indicator of synaptic serotonin content after pharmacological challenge.¹⁷⁰ They observed a decreased binding potential and distribution volume of altanserin following clomipramine challenge. This challenge probably increased the synaptic serotonin level, which competed with altanserin leading to the lowered binding potential. The paradigm might, thus, be useful to estimate serotonin release *in vivo*. Pre-treatment with serotonergic antidepressants reduces the effect of clomipramine.¹⁷⁰

[¹¹C]WAY 100635 is the first potent and selective PET tracer to image the 5-HT_{1A} receptor status.^{171,172,173} Later, the first ¹⁸F-labeled derivative, [¹⁸F]FBWAY, was developed. Both tracers are applied in many clinical studies to investigate various diseases and conditions.^{174,175,176,177} Figure 18 represents the distribution of [¹¹C] WAY 100635 within a baboon brain. It corresponds to the known distribution of 5-HT_{1A} receptors within the brain.⁶³

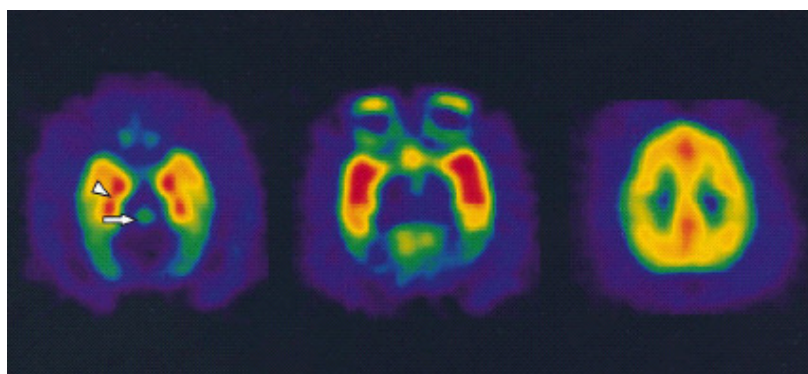


Figure 18: Summed [¹¹C]WAY 100635 PET imaging of the 5-HT_{1A} receptor at three levels in a baboon brain.

Binding to areas of known high density of 5-HT_{1A} receptors, such as the hippocampus (arrowhead) and brainstem raphe nuclei (arrow), is demonstrated.⁶³

Radiotracers for both the 5-HT_{2A} and 5-HT_{1A} sites permit the imaging of cortical areas due to the relatively high concentrations of these receptor subtypes in the cortex. As there is a higher concentration of 5-HT_{1A} receptors in the mesial temporal lobe, compounds that bind to this site such as [¹¹C]WAY 100635 permit the visualization of the hippocampal/ amygdala

complex. These regions may be especially important to evaluate *in vivo* due to the degenerative changes that occur in these regions in aging and AD.

In addition, a decreased 5-HT_{1A} receptor availability in medication-naïve patients with major depressive disorder as well as in patients with temporal lobe epilepsy could be determined by *in vivo* studying using [¹¹C]WAY 100635.^{178,179} Furthermore, an increased 5-HT_{1A} receptor occupancy in the temporal cortices and a decreased one in the amygdala in schizophrenic patients as observed in *post mortem* studies^{180,181} could only be proved by some PET studies. For example, Tauschner et al. measured a higher binding potential of WAY 100635 in schizophrenic patients (Figure 19),¹⁸² whereas Frankle et al. could not approve this issue.¹⁸³

The influence of endogenous serotonin on the *in vivo* binding of [¹¹C]WAY 100635 was also studied. Reserpine-induced serotonin depletion and fenfluramin-induced serotonin increase showed no obvious effect of enhanced serotonin levels on [¹¹C]WAY 100635 binding. These results indicated that the *in vivo* binding of [¹¹C]WAY 100635 in the hippocampus and cerebral cortex mainly reflects postsynaptic 5-HT_{1A} receptor binding, and that this binding is not sensitive to endogenous serotonin.¹⁸⁴ Moreover, there were recently evidences provided with WAY 100635 for a specific interrelation between the 5-HT_{1A} receptor distribution, sex hormones, and aggression in humans. A reduced down-stream control due to higher amounts or activities of frontal 5-HT_{1A} receptors results in more aggressive subjects, which is presumably modulated by sex hormones.¹⁸⁵

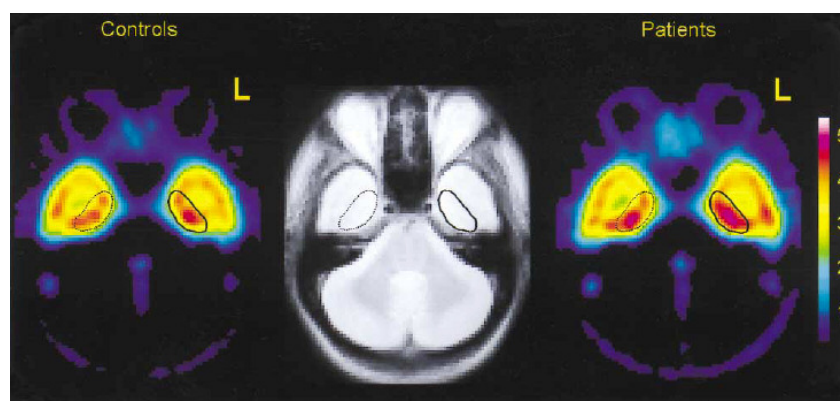


Figure 19: Composite mean 5-HT_{1A} binding potential images obtained with [¹¹C]WAY 100635

14 healthy controls and 14 age-matched patients with schizophrenia indicate higher BP values in mediotemporal regions of interest. Mean BP images and magnetic resonance images had been spatially normalized to the Montreal Neurologic Institute brain space.¹⁸²

Efforts to develop radiolabelled SSRIs have been problematic.¹⁸⁶ Nevertheless, today several PET-tracers such as [¹¹C]McN 5652¹⁸⁷ and diphenyl(thio)ether ([¹¹C]DASB, [¹⁸F]ACF)¹⁵¹ are applied in qualitative and quantitative studies of the SERT showing regional localization binding that is both consistent with the known distribution of the 5-HT reuptake site and is reduced following blockage via specific binding ligands.^{187,188,189}

Figure 20 shows an example of the usefulness of [¹¹C]DASB and [¹¹C]McN 5652 to image the dependency of the drug MDMA and demonstrates the reduction in SERT binding in the MDMA subject with both radioligands.¹⁹⁰

However, the application of [¹¹C]McN 5652 is limited by the slow accumulation of the tracer combined with the short half-life of carbon-11. Moreover, a high binding to unspecific regions is reported prohibiting authentic quantification in low SERT-low-density areas, as e.g. the limbic system.¹⁹¹ DASB and ACF have promising characteristics. They showed superiority in animal studies because of the faster accumulation kinetics.^{192,193} However, out of both [¹¹C]DASB is disadvantaged due to its half-life enabling only short PET scans and the requirement of very fast tracer accumulating in the region of interest.¹⁹⁴

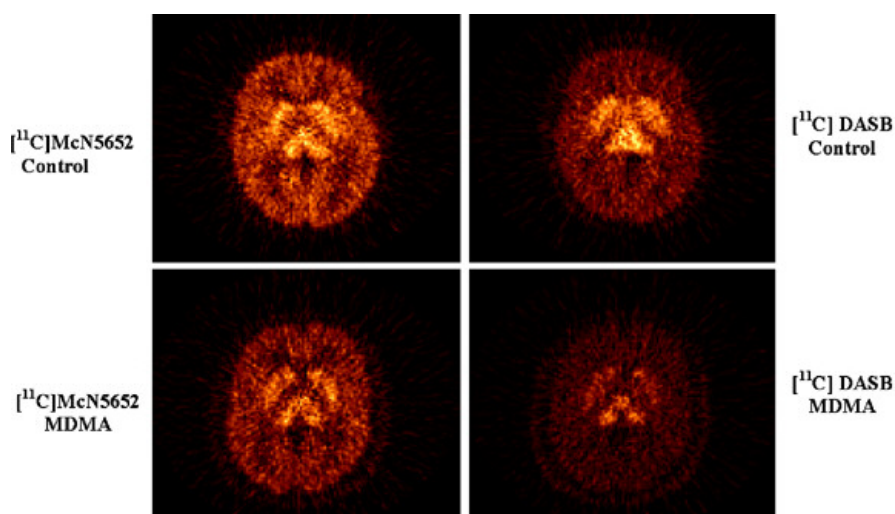


Figure 20: PET images of [¹¹C]McN5652 and [¹¹C]DASB in a representative control subject and a representative MDMA subject demonstrating the reductions in SERT binding in the MDMA subject¹⁹⁰

Another aspect of 5-HT function that can be imaged with PET is serotonin synthesis. Diksic, Nishizawa et al. have used radiolabelled α -methyl-L-tryptophan to track serotonin synthesis.^{152,153,195} PET measurements of serotonin synthetic rates may improve our understanding of the feedback control mechanisms involved in release and reuptake of serotonin, and thus may elucidate the mode of action of antidepressants. Application of this

technique in humans yielded preliminary evidence suggesting disturbed serotonin synthesis in depression and differential regulation of serotonin synthesis in men and women, which may contribute to the increased vulnerability of women to depression (Figure 21).¹⁹⁵

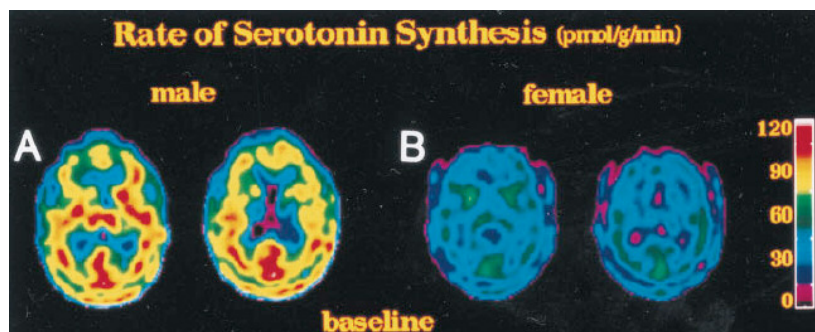


Figure 21: Representative PET images obtained from a male and a female subject

*A and B were obtained from a male and a female subject. The colour bar on the right in the same row gives an indication of synthesis.*¹⁹⁵

1.5 Discussion of routinely used 5-HT_{2A/1A} antagonistic PET tracers

5-HT_{2A} tracers: [¹⁸F]Altanserin, [¹⁸F]SR 46349B and (R)-[¹¹C]MDL 100907 are the most promising tracers to image the 5-HT_{2A} receptor status. All show high affinity towards the 5-HT_{2A} receptor and a good selectivity towards other 5-HT subtypes, other receptors and transporters (Table 3).¹⁵⁰ [¹⁸F]altanserin is the most applied imaging probe in research out of these.

(R)-[¹¹C]MDL 100907's receptor binding to other 5-HT receptor subtypes is very low, and for [¹⁸F]altanserin's moderate to low.⁶³ A further difference between these two tracers is the binding to receptors outside the serotonergic system. Altanserin shows a relatively high affinity for D₂ (62 nM) and especially for adrenergic- α_1 receptors (4.55 nM) (Table 3) whereas the affinity of (R)-MDL 100907 to these receptors is insignificant.¹⁶⁵ Visualisation of these binding differences is possible by autoradiography (Figure 22). A total displacement of [³H]MDL 100907 by ketanserin, a known 5-HT_{2A} antagonist with no affinity toward the D₂ receptor, succeeds, while a displacement of [¹⁸F]altanserin is only partially observed. Specific binding in known high density D₂ receptor areas cannot be replaced significantly.

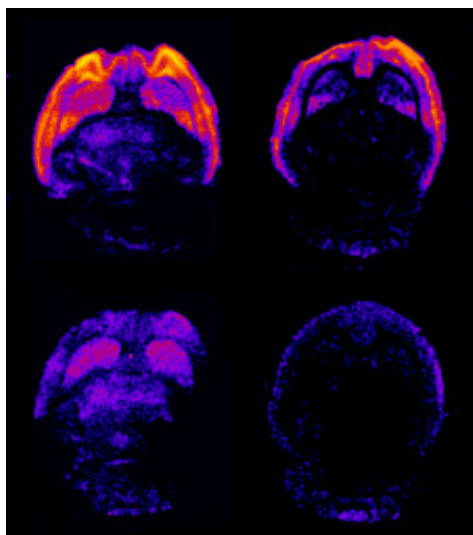


Figure 22: Autoradiography of rat brain slices; $[^{18}\text{F}]$ altanserin (left), $[^{11}\text{C}]$ MDL 100907 (right); total binding (above), specific binding (below)

The advantage of $[^{18}\text{F}]$ altanserin over ^{11}C -labeled imaging probes is the possibility to perform equilibrium scans lasting several hours and to transport the tracer to other facilities based on the 110 min half-life of $[^{18}\text{F}]$ fluorine compared to the 20.4 min half-life of carbon-11. On the other hand, a drawback of $[^{18}\text{F}]$ altanserin is its rapid and extensive metabolism. Four metabolites are formed in humans that cross the blood-brain-barrier.¹⁹⁶ N-dealkylation and reduction of the ketone to the corresponding alcohol are e.g. already described metabolites.¹⁹⁷ Figure 23 describes the postulated enzymatic attack followed by an N-dealkylation.

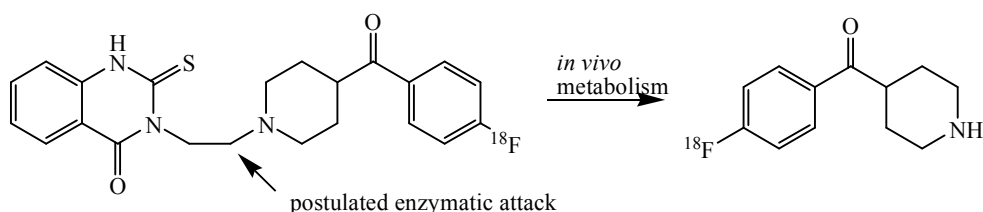


Figure 23: One possible *in vivo* metabolism pathway of $[^{18}\text{F}]$ altanserin

Deuterization of altanserin to $[^{18}\text{F}]$ deuteroaltanserin leads to a reduced metabolism rate of the mentioned N-dealkylation.¹⁹⁷ Thus, the ratio of metabolite to intact tracer in human beings was improved.

An ^{18}F -version of SR 46349B is chemically accessible but limited by a complicated multi-step radioactive reaction route. Thereby, the final tracer has to be separated into their corresponding diastereomeric derivatives. It is thus constricted in its routine application (Figure 24).¹⁹⁸

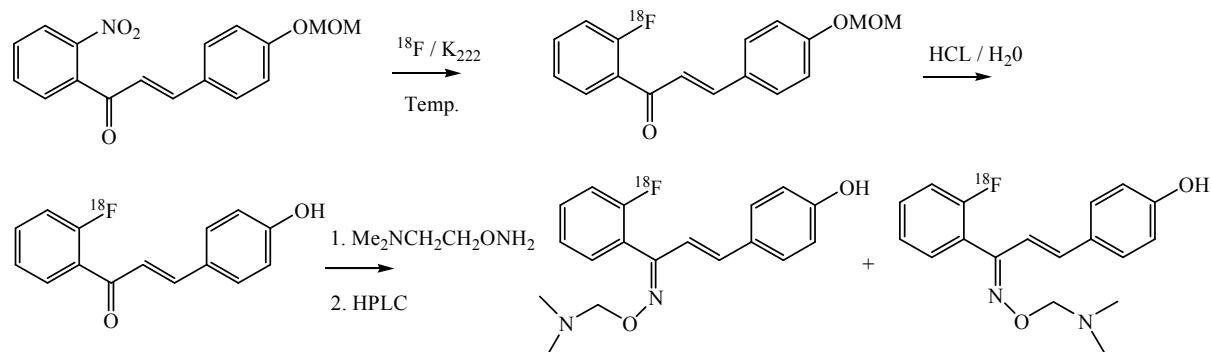


Figure 24: Radioactive synthesis of $[^{18}\text{F}]$ SR 46349B

Today, MDL 100907 only exists as an ^{11}C -variant resulting in a disadvantaged a lower spatial resolution and a shorter half-life compared to ^{18}F -compounds. MDL 100907 has the best binding selectivity⁶³ and the formed radioactive metabolite is not able to cross the BBB.¹⁹⁹ Metabolization of MDL 100907 occurs by a conversion of the 3-methoxygroup to the corresponding phenolic alcohol. Indeed, the resulting non-radioactive metabolite MDL 105725 is a high affine 5-HT_{2A} ligand, but Scot et al.¹⁹⁹ report that the parent compound MDL 100907 is 4 times more effective in crossing the BBB than this metabolite.

Nevertheless, a serious disadvantage of $[^{11}\text{C}]$ MDL 100907 is its slow kinetics combined with the half-life of carbon-11.²⁰⁰ In Figure 25a and 25b the time-activity-curve (TAC) of $[^{11}\text{C}]$ MDL 100907 and $[^{18}\text{F}]$ altanserin in the human brain are displayed. Therein, $[^{11}\text{C}]$ MDL 100907 reaches steady state not until 45 minutes¹⁶⁴, whereas the binding of $[^{18}\text{F}]$ altanserin rapidly decreased already beginning 20 minutes p.i.¹⁵⁴ This points out that altanserin has either a fast metabolism within the brain or radioactive metabolites able to cross the BBB.

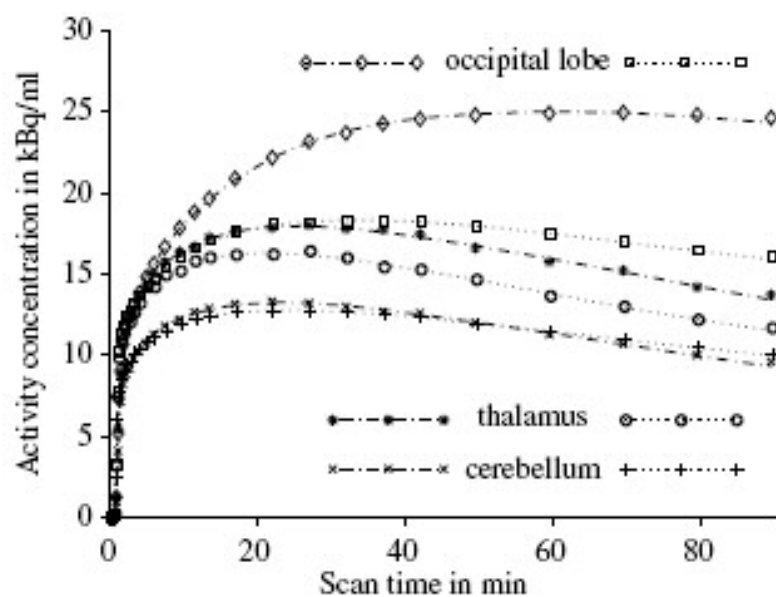


Figure 25 a:

TAC of $[^{11}\text{C}]$ MDL 100907 in the human brain¹⁶⁴:

The symbols on the dashed-dotted lines to the left of the region name refer to the unblocked scan, and the symbols on the dotted lines to the right indicate the blocked scan.

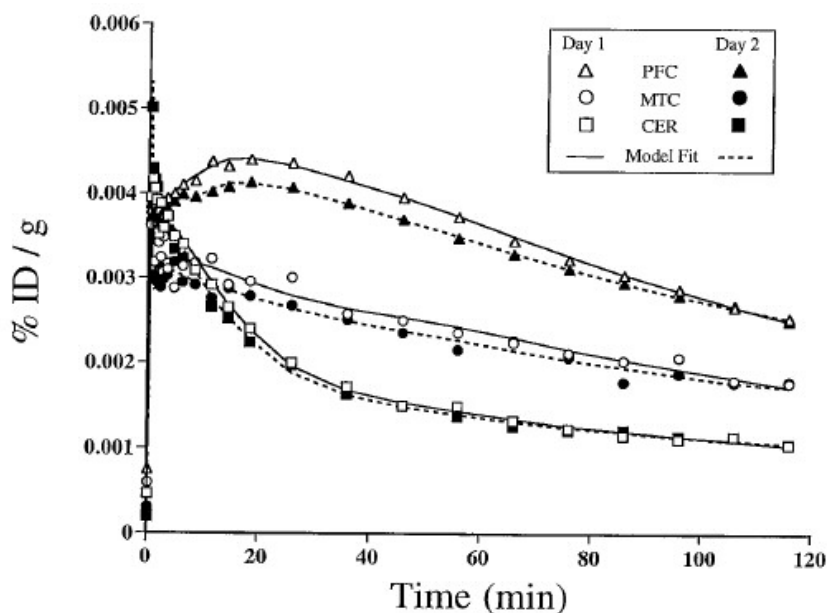


Figure 25 b:

TAC of [^{18}F]altanserin in the human brain¹⁵⁴:

PFC-prefrontal Cortex, *MTC*-mesial zemporale cortex, *CER*-cerebellum

The 5-HT_{2A} antagonists MDL 100907, altanserin and SR 46349B induce no changes in the dopaminergic system.²⁰¹ However, SR 46349B is able to modulate the dopamine release of haloperidol, whereas this issue is neither observed for MDL 100907 as for altanserin.²⁰²

In conclusion, an optimal imaging probe for the 5-HT_{2A} receptor status is still missing. Either cross-affinities, radioactive metabolites, able to cross the BBB, difficult reaction routes or the half-life of the chosen nuclide within the tracer limits the application spectrum.

5-HT_{1A} tracers: Various radioactive metabolites of [^{11}C]WAY 100635 are known which are to some extent able to cross the BBB. The most important one is [^{11}C]WAY 100634. It shows no affinity towards the 5-HT_{1A} receptor, but can cross the BBB (Figure 26) and thus impairing the ratio of specific to unspecific binding.¹⁴⁴

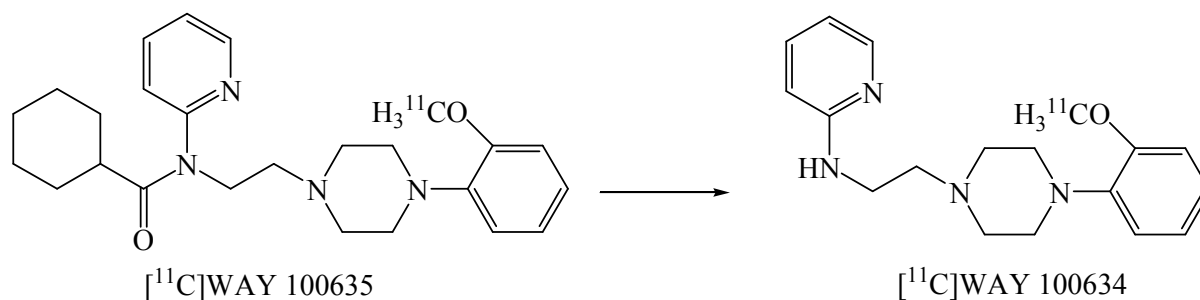


Figure 26: Derivatisation of [^{11}C]WAY 100635 to [^{11}C]WAY 100634

A solution to that dilemma is a different labelling strategy resulting in radiometabolites that are not able to cross the BBB. Figure 27 shows a possible labelling position.²⁰³ This compound [¹⁸F]FBWAY is furthermore able to reach transient equilibrium, whereas Lang et al. demonstrated, that this is impossible for [¹¹C]WAY 100635.¹⁴⁴

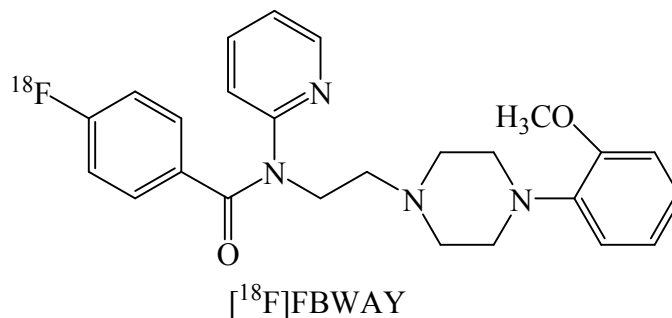


Figure 27: Structure of [¹⁸F]FBWAY

1.6 Interaction of serotonergic PET-tracers with P-gp (plasma glycoprotein)

The permeability of the BBB limits the bioavailability of various drugs and tracers. Indeed, passive diffusion of lipophilic substances is possible but even for some lipophilic compounds crossing has not been observed to a high extent, possibly due to carrier-systems which transport these molecules out of the brain.

ABC carriers, as the P-gp, could be responsible for these processes and thus inhibition of these carrier-systems leads to an increased accumulation of the respective substance. Therefore, identification of drugs acting within the central nervous system (CNS) as potential P-gp substrates or inhibitors are of crucial importance in drug development. PET studies can play an important role in the *in vivo* screening process as a follow-up of high throughput *in vitro* assays.²⁰⁴ For example, by quantitative PET measurement of P-gp function, the dose of modulators required to increase the concentration of CNS drugs may be determined, which may result in improved drug therapy.²¹⁰

Some qualitative- and often intuitive rules are currently used by medicinal chemists to predict the BBB permeation of compounds. Structure-activity-relationship (SAR) models are already published mainly applying classical regression equations. Levin et al. showed a relation between the brain capillary permeability coefficient and $\text{Log}(P(\text{molecular weight})^{-1/2})$ for molecules with molecular weights < 400.^{205,206} Important features on the respective substrates include multiple hydrophobic and hydrogen bond acceptor features, which are widely

dispersed.²⁰⁷ However, results of the SARs have indicated that there may be three or more binding sites of drugs towards P-gp.²⁰⁸ Steady-state kinetic analyses of P-gp mediated ATPase activity using different substrates indicates that these sites can show mixed-type or non-competitive inhibition, indicative of overlapping substrate specificities.²⁰⁹

Several PET rodent studies have shown the influence of P-gp on the pharmacokinetics and brain uptake of radiolabelled compounds, e.g. for the two 5-HT_{1A} receptor ligands, [¹⁸F]MPPF and [¹¹C]WAY 100635. The specific brain uptake of [¹⁸F]MPPF is several times lower (5 to 10 lower) than that of [¹¹C]WAY 100635. After cyclosporine A (CsA) modulation, [¹⁸F]MPPF uptake in the rat brain increased to the level of the ¹¹C-derivative. Cerebral uptake of [¹¹C]WAY 100635 was also increased by modulation, but lower than that observed for [¹⁸F]MPPF (2-3 fold).²¹⁰

In addition, [¹⁸F]altanserin was shown to be strongly P-gp dependent.²¹¹ *Ex vivo* as well as *in vivo* PET studies in rats show that altanserin is limited by low brain uptake and the BP is hardly reproducible. Therefore, Palner et al. conclude that altanserin, in parallel to the above mentioned tracers, is a substrate for P-gp. Pre-treated CsA (cyclosporine A) rats had a 52 % higher total brain uptake of [¹⁸F]altanserin and a 6.46 fold increase in frontal cortex BP compared to control (Figure 28). Moreover, they had lower radioactivity in blood and plasma than controls. Ketanserin treated rats had lower radioactivity levels in plasma but not in blood, probably because of the ketanserin-induced displacement of [¹⁸F]altanserin from 5-HT₂ receptors.

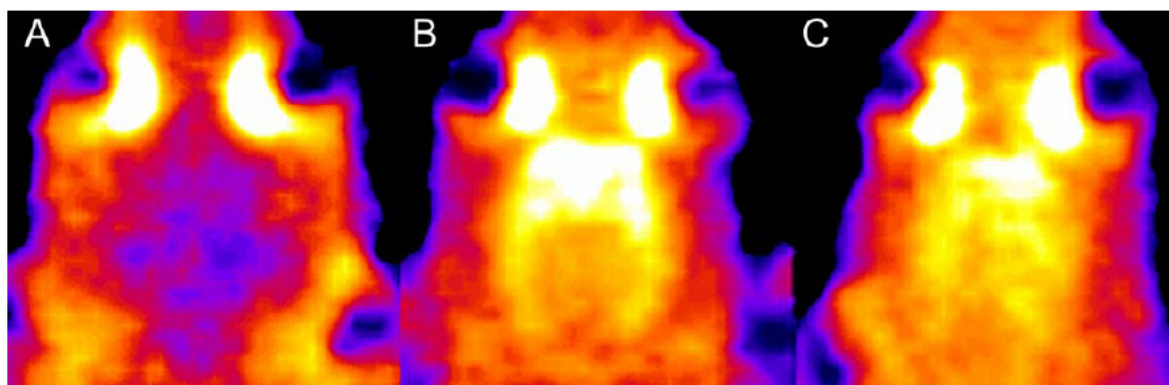


Figure 28: Summed μ PET images of [¹⁸F]altanserin before (A) and after (B) treatment with cyclosporine A and (C) after treatment with cyclosporine A and the 5-HT_{2A} antagonist ketanserin.²¹¹

Besides, P-gp is probably involved in diseases, such as epilepsy, neurodegenerative disorders, inflammations, brain tumors, and HIV encephalopathy, because it allows undesired compounds to enter the brain which then again may cause damage.²¹²

2 Aims

The serotonergic receptor system plays a key role in the transduction of signals within the central nerve system and represents an important target for antidepressants and antipsychotics. Alterations of the 5-HT_{2A/1A} receptor status are involved e.g. in memory, Alzheimer's disease and depression.

Indeed, there are already tracers available for molecular imaging the 5-HT_{2A} receptors (¹¹C]MDL 100907, ¹¹C]SR 46349B and ¹⁸F]altanserin) as well as for the 5-HT_{1A} receptor (¹¹C]WAY 100635 and ¹⁸F]MPPF). However, each of the individual imaging probes is limited either by affinity, specificity, metabolism, pharmacokinetics or by the half-life which only enables PET scans near to the equilibrium.

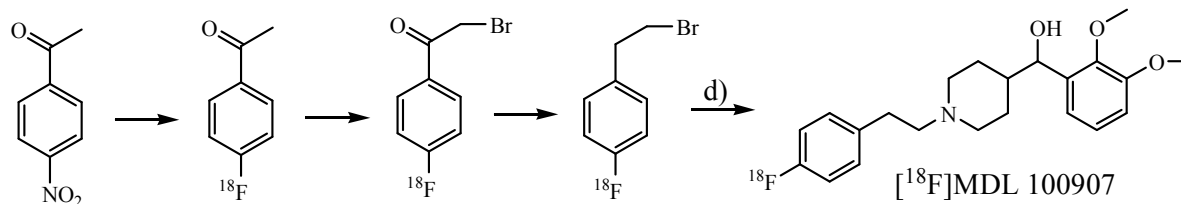
Hence, on the basis of known selective tracers (5-HT_{2A} selective compounds: MDL 100907, altanserin, SR 46349B; 5-HT_{1A} selective compounds: WAY 100635), novel compounds should be synthesized and evaluated to overcome these problems.

5-HT_{2A}:

The first aim of this thesis is to label MDL 100907 with fluorine-18 to combine the advantage of the better selectivity of MDL 100907 and the more valuable isotopic characteristics used in ¹⁸F]altanserin. Therefore, labelling approaches with secondary labelling precursors are chosen to form either the original molecule by replacing the fluorine-19 within MDL 100907 by fluorine-18 or to vary the original structure in terms of fluoroalkylation and thus to label it with fluorine-18 via ¹⁸F]FETos. Afterwards most promising ligands should be labelled with fluorine-18. Figure 29 shows two possible labelling approaches to label either the original MDL 100907 or a derivative by fluorine 18.

The latter approach, however asks for structure-activity-relationship (SAR) studies to identify whether the new compound is affine, selective and shows a reasonable lipophilicity. In extending SAR studies with variety of novel derivatives, two major goals should be achieved. A high affine and selective compound and a medium affine but still selective compound should be synthesized to image either the 5-HT_{2A} receptor itself or to measure the influence of endogenous changes of serotonin towards the receptor.

A)



B)

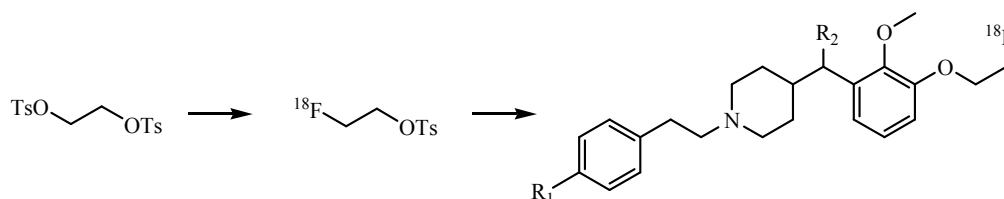


Figure 29: Labelling approaches of MDL 100907 derivatives. A) shows the labelling of the original MDL 100907 molecule, whereas B) shows the indirect labelling via [^{18}F]FETos of a derivative.

Furthermore, a SAR of altanserin, SR 46349 B and MDL 100907 should be carried out to determine whether all compounds bind to the same binding pocket or a combination of structural elements could improve these already high affinity ligands of the 5-HT_{2A} receptor.

The novel synthesized ^{18}F -labeled tracers should be evaluated in *ex vivo* and *in vivo* experiments to obtain relevant pharmacological information for molecular imaging. Especially, autoradiography, PET and organ biodistribution studies should be carried out. Furthermore, due to the known dependency of [^{18}F]altanserin on P-gp and the similar structural relationship of projected ^{18}F -MDL 100907 derivatives, the sensitivity of the novel tracers towards P-gp and the related impact on its brain uptake should be clarified.

5-HT_{1A}:

Another aim is to label novel antagonistic 5-HT_{1A} tracers, which could lead to a considerable improvement of the visualisation of the 5-HT_{1A} receptor system. Therefore, a leading compound, namely 4-[3-[4-(*o*-Methoxyphenyl)piperazin-1-yl]propoxy]-4-azatricyclo-[5.2.1.0_{2,6}]dec-8-ene-3,5-dione, was chosen having outstanding selectivity. Three new derivatives should be synthesized and evaluated for their affinity.

Figure 30 shows the leading compound and its three to synthesized new derivatives.

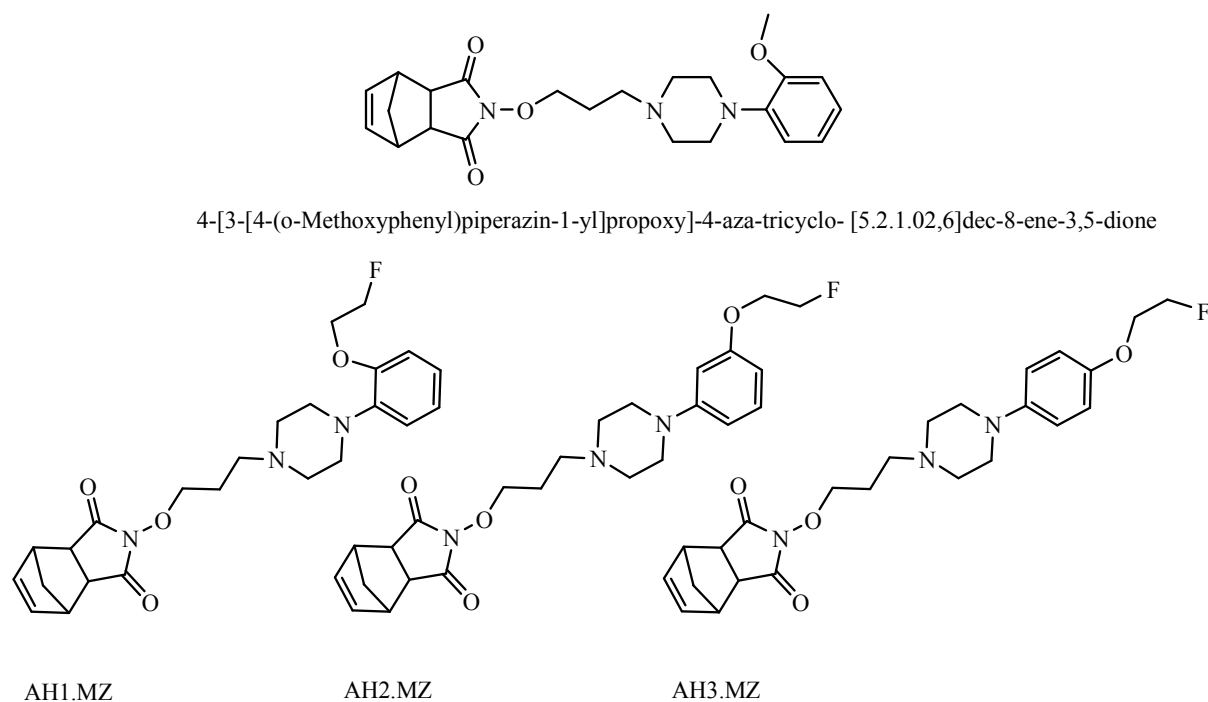


Figure 30: Structures of 4-[3-[4-(o-Methoxyphenyl)piperazin-1-yl]propoxy]-4-aza-tricyclo- [5.2.1.02,6]dec-8-ene-3,5-dione and varied derivatives AH1.MZ, AH2.MZ, AH3.MZ

References

- 01 Cole, J.C.; Sumnall, H.R.. Altered states: The clinical effects of Ecstasy. *Pharmacol. Therapeut.* (2003) 98, 35-58
- 02 Gresch, P.J.; Smith, R.L.; Barrett, R.J.; Sanders-Bush, E. Behavioral tolerance to lysergic acid diethylamide is associated with reduced serotonin-2A receptor signaling in rat cortex. *Neuropsychopharmacology* (2005) 30, 1693-1702
- 03 Marek, G.J.; Aghajanian, G.K. LSD and the phenethylamine hallucinogen DOI are potent partial agonists at 5-HT_{2A} receptors on interneurons in rat piriform cortex. *Pharmacology* (1996) 278, 1373-1382
- 04 Spinks, D.; Spinks, G. Serotonin reuptake inhibition: An update on current research strategies. *Curr. Med. Chem.* (2002) 9, 799-810
- 05 Carlsson, A.; Fuxe, K.; Ungerstedt, U. The effect of imipramine on central 5-hydroxytryptamine neurons. *J. Pharm.Pharmacol.* (1968) 20, 150-151
- 06 Schildkraut, J.J The catecholaminehypothesis of affective disorders: A review of supporting evidence. *Am. J. Psychiatry* . (1965) 122, 509-522
- 07 Charney, D.S.; Menkes, D.B.; Heninger, G.R. Receptor sensitivity and the mechanism of action of antidepressant treatment. Implicationsfor the etiology and therapy of depression. *Arch.Gen. Psychiatry* (1981) 38, 1160-1180
- 08 Coppen, A.J. Biochemical aspects of depression. *Int. Psychiatry Clin.* (1969) 6, 53-81
- 09 Coppen, A.J.; Prange, A.J.; Whybrow, P.C.; Noguera, R. Abnormalities of indoleamines in affective disorders. *Arch. Gen. Psychiatry* (1972) 26, 474-478
- 10 Delgado, P.L. Depression: the case for a monoamine deficiency. *J. Clin. Psychiatry* (2000) 61, 7-11
- 11 Lapin, I.P.; Oxenkrug, G.F. Intensification of the central serotonergic processes as a possible determinant of the thymoleptic effect. *Lancet* (1969) 1, 132-136
- 12 Glennon, R.; Dukat, M. Novel serotonergic agents. *ID Res. Alert* (1997) 2, 107-113
- 13 Kennett, G.A.; Wood, M.D.; Bright, F.; Cilia, J.; Piper, D.C.; Gager, T.; Thomas, D.; Baxter, G.S.; Forbes, I.T.; Ham, P.; Blackburn, T.P. In vitro and in vivo profile of SB 206553, a potent 5-HT_{2C}/ 5-HT_{2B} receptor antagonist with anxiolytic-like properties. *Br. J. Pharmacol.* (1996) 117, 427-434
- 14 Lai, M.K.; Tsang, S.W.; Alder, J.T.; Keene, J.; Hope, T.; Esiri, M.M.; Francis, P.T.; Chen, C.P. Loss of serotonin 5-HT_{2A} receptors in the postmortem temporal cortex

- correlates with rate of cognitive decline in Alzheimer's disease. *Psychopharmacology* (2005) 179, 673-677
- 15 Naughton, M.; Mulrooney, J.B.; Leonard, B.E. A review of the role of serotonin receptors in psychiatric disorders. *Hum Psychopharmacol* (2000) 15, 397-415
 - 16 Schmidt, J.C.; Kehne, J.H.; Carr, A.A. MDL 100907: A selective 5-HT_{2A} receptor antagonist for the treatment of schizophrenia. *CNS Drug Reviews* (1997) 3, 49- 67
 - 17 Meltzer, H.Y.; Matsubara, S.; Lee, J.C. Classification of typical and atypical antipsychotic drugs on the basis of dopamine D-1, D-2 and serotonin₂ pKi values. *J. Pharmacol. Exp. Ther.* (1989) 25, 238-246
 - 18 Gründer, G.; Yokoi, F.; Offord, S.J.; Ravert, H.T.; Dannals, R.F.; Salzman, J.K.; Szymanski, S.; Wilson, P.W.; Howard, D.R.; Wong, D.F.. Time course of 5-HT_{2A} receptor occupancy in the human brain after a single oral dose of the putative antipsychotic drug MDL 100907 measured by PET. *Neuropsychopharmacology* (1997) 17, 175-185
 - 19 Adams, K.H.; Pinborg, L.H.; Svarer, C.; Hasselbalch, S.G.; Holm, S.; Haugbøl, S.; Madsen, K.; Frøkjær, V.; Martiny, L.; Paulson, O.B.; Knudsen, G.M. A database of [¹⁸F]altanserin binding to 5-HT_{2A} receptors in normal volunteers: normative data and relationship to physiological and demographic variables. *NeuroImage* (2004) 21, 1105–1113
 - 20 Meltzer, C.C.; Drevetsa, W.C.; Pricea, J.C.; Mathis, C.A.; Lopresti, B.; Greer, P.J.; Villemagne, V.L.; Holt, D.; Mason, N.S.; Houck, P.R.; Reynolds, C.F.; DeKosky, S.T. Gender-specific aging effects on the serotonin 1A receptor. *Brain Research* (2001) 895, 9–17
 - 21 Plenevaux, A.; Weissmann, D.; Aerts, J.; Lemaire, C.; Brihaye, C.; Degueldre, C.; Le Bars, D.; Comar, D.; Pujol, J.-F.; Luxen, A. Tissue distribution, autoradiography, and metabolism of 4-(29-Methoxyphenyl)-1-[29-[N-(20-Pyridinyl)-p-[¹⁸F]fluorobenz-amido]ethyl]piperazine (p-[¹⁸F]MPPF), a new serotonin 5-HT_{1A} antagonist for Positron Emission Tomography: An In Vivo Study in Rats. *Journal of Neurochemistry* (2000) 75, 803-811
 - 22 Luker, G.; Piwnica-Worms, D. Molecular imaging *in vivo* with PET and SPECT. *Acad Radiol* (2001) 8, 4–14
 - 23 Dobrucki, L.; Sinusas, A. Molecular imaging. A new approach to nuclear cardiology. *J Nucl Med Mol Imaging* (2005) 49, 106–115

- 24 Wolf, G.L. Handbook of targeted delivery of imaging agents, CRC Press, Boca Raton, FL, (1995), 3-23
- 25 Saha, B.S. Fundamentals of Nuclear Pharmacy. 1997, New York, Berlin, Heidelberg: Springer
- 26 Herth, M.M. Diplomarbeit: Synthese und ^{18}F -Markierung von Altanserin und MDL 100907-Derivaten für den 5-HT_{2A}-Rezeptor im serotonergen System. Johannes Gutenberg-Universität zu Mainz 2006
- 27 Phelps, M.E. Positron Emission Tomography. Clinical Brain Imaging: Principles and Application, ed. J. Mazziotta and S. Gilman. 1992, New York: F.A. Davis Company
- 28 Phelps, M. PET: molecular imaging and its biological applications. 2004 New York, Springer-Verlag, Inc.
- 29 Debus, F. Dissertation: Specific PET-ligands for selected 5-HT_{2A} and GABA_A-receptor subtypes. Johannes Gutenberg-Universität zu Mainz 2008
- 30 Deupree, J.D.; Bylund, D.B. Basic principles and techniques for receptor binding. *Tocris Reviews* (2002) No.18
- 31 De Haes, J.U. Dissertation: In vivo imaging of dopamine and serotonin release: response to psychopharmacological challenges. Rijksuniversiteit Groningen 2005
- 32 Watabe, H.; Ikoma, Y.; Kimura, Y.; Naganawa, M.; Shidahara, M.. PET kinetic analysis-compartmental model. *Annals of Nuclear Medicine* (2006) 20, 583-588
- 33 Watabe, H.; Itoh, M.; Cunningham, V.; Lammertsma, A.; Bloomfield, P.; Mejia, M. Noninvasive quantification of rCBF using positron emission tomography. *J Cereb Blood Flow Metab* (1996) 16, 311–319
- 34 Bella, E.D.; Clackdoyle, R.; Gullberg, G. Blind estimation of compartmental model parameters. *Phys Med Biol* (1999) 44, 765–780
- 35 Lammertsma, A.A.; Bench, C.; Hume, S.; Osman, S.; Gunn, K.; Brooks, D. Comparison of methods for analysis of clinical [^{11}C]raclopride studies. *J Cereb Blood Flow Metab.* (1996) 16, 42–52
- 36 Lammertsma, A.A.; Hume, S.P. Simplified reference tissue model for PET receptor studies. *Neuroimage* (1996), 53–158
- 37 Breier, A.; Su, T.; Saunders, R.; Carson, R.; Kolachana, B.; Bartolomeis, de A. Schizophrenia is associated with elevated amphetamine-induced synaptic dopamine concentrations: evidence from a novel positron emission tomography method. *Proc Natl Acad Sci* (1997) 94, 2569-2574

-
- 38 Lederer CM, Shirley, VS, Tables of Isotopes, 7th Edition (1978), John Wiley, New York
- 39 Ferrieri, R.A. Production and application of synthetic precursors labeled with carbon-11 and fluorine-18, BNL-68184 (2005)
- 40 Casella, V.; Ido, T.; Wolf, A.P.; Fowler, J.S.; MacGregor, R.R.; Ruth, T.J. Anhydrous ¹⁸F labeled elemental fluorine for radiopharmaceutical production. *J. Nucl. Med.*, (1980) 21, 750-757
- 41 Blessing, G.; Coenen, H.H.; Franken, K.; Qaim, S.M. Production of [¹⁸F]F₂, H¹⁸F and ¹⁸F_{aq} using the ²⁰Ne(d,α)¹⁸F process. *Appl. Radiat. Isot.* (1986) 37, 1135-1140.
- 42 Dolle, F.; Demphel, S.; Hinnen, F.; Fournier, D.; Vaufrey, F.; Crouzel, C. 6-[¹⁸F]Fluoro-*L*-DOPA by radiofluorodestannylation: a short and simple synthesis of a new labelling precursor; *Label. Compds. Radiopharm.* (1998) 41, 105-114
- 43 Nickles, R.J.; Gatley, S.J.; Votaw, J.R.; Kornguth, M.L. Production of reactive fluorine-18. *Appl. Radiat. Isot.* (1986) 37, 649-651
- 44 Jewett, D.M.; Toorongian, S.A.; Mulholland, G.K.; Watkins, G.L.; Kilbourn, M.K. Multiphase extraction: rapid phase-transfer of [¹⁸F]fluoride for nucleophilic radiolabelling reactions. *Appl. Radiat. Isot.* (1988) 39, 1109-1111
- 45 Shiue, C.Y.; Fowler, J.S.; Wolf, A.P.; Watanabe, M.; Arnett, C.D. Synthesis and specific activity determinations of NCA ¹⁸F-labeled butyrophenonen euroleptics: benperidol, haloperidol, spiroperidol and pipamperone. *J. Nucl. Med.* (1985) 26, 181-186
- 46 Shiue, C.Y.; Bai, L.Q.; Teng, R.; Wolf, A.P. Application of the nucleophilic substitution reactions to the synthesis of NCA ¹⁸F-labeled radioligands. *J. Label. Compds. Radiopharm.* (1986) 23, 1038-1039
- 47 Shiue, C.Y.; Fowler, J.S.; Wolf, A.P.; McPherson, D.W.; Arnett, C.D.; Zecca L. No-carrier-added fluorine-18 labeled N-methylspiroperidol: synthesis and biodistribution in mice. *J. Nucl. Med.* (1986) , 27, 226-234
- 48 Irie, T.; Fukushi, F.; Ido, T.; Nazaki, T.; Kasida, Y. ¹⁸F-Fluorination by crown ethermetal fluoride: labeling [¹⁸F]-2-fluoroprogesterone. *Int. J. AppZ. Radiat. Isot.* (1982) 33, 1449-1452
- 49 Aghajanian, G.K.; Sanders-Bush, E. Serotonin. *Neuropsychopharmacology-The fifth Generation of Process* (2002), 15-35

-
- 50 Gray, J.A.; Roth, B.R. Serotonin synthesis. *Handbook Neuropsychopharmacology* (2007) Volume 1 chapter 8, 257-277
- 51 Barnes, N.M.; Sharp, T. A review of central 5-HT receptors and their function. *Neuropharmacology* (1999) 38, 1083-1152
- 52 Jacobs, B.L.; Azmitia, E.C. Structure and function of the brain serotonin system. *Physiol Rev* (1992) 72, 165-229
- 53 Pineyro, G.; Blier, P. Autoregulation of serotonin neurons: role in antidepressant drug action. *Pharmacol Rev* (1999) 51, 533-591
- 54 Weible, A. P.; McEchron, M.D.; Disterhoft, J.F. Cortical involvement in acquisition and extinction of trace eyeblink conditioning. *Behav. Neurosci.* (2000) 114, 1058-1067
- 55 Wurtman, R.J.; Hefti, F.; Melamed, E. Precursor control of neurotransmitter synthesis. *Pharmacol. Rev.* (1980) 32, 315-335
- 56 Shih, J. C.; Chen, K.; Ridd, M.J. Monoamine oxidase: from genes to behavior. *Ann. Rev. Neurosci.* (1999). 22, 197-217
- 57 Zhou, F. C.; J. H. Tao-Cheng; Segu, L.; Patel, T.; Wang, Y. Serotonin transporters are located on the axons beyond the synaptic junctions: anatomical and functional evidence. *Brain. Res.* (1998) 805, 241-254
- 58 Palacios, J.; Waeber, C.; Hoyer, D.; Mengod, G. Distribution of serotonin receptors. *Ann. NY Acad. Sci.* (1990) 600,36–52
- 59 Azmitia, E. C.; Whitaker-Azmitia, P. M. Awakening the sleeping giant: Anatomy and plasticity of the brain serotonergic system. *J. Clin. Psychiatry* (1991) 52, 4–16
- 60 Kosofsky, B. E.; Molliver, M. E. The serotonergic innervation of cerebral cortex: Different classes of axon terminals arise from dorsal and median raphe nuclei. *Synapse* (1987) 1, 153–168
- 61 http://www.cnsforum.com/imagebank/item/Neuro_path_SN_DA/default.aspx
- 62 Frazer A, Hensler JG (1999); (Hrsg.) *Basic Neurochemistry*. Lippincott-Raven, Philadelphia, PA
- 63 Meltzer, C.C.; Smith, G.; DeKosky, S.; Pollock, B.; Mathis, C.; Moore, R.; Kupfer, D.; Reynolds, C. Serotonin in aging, late-life depression, and Alzheimer's disease: The emerging role of functional imaging. *Neuropsychopharmacology* 18, 407- 430

-
- 64 Saxena, P.R.; De Vries, P.; Villalon, C.M. 5-HT₁-like receptors: a time to bid goodbye. *Trends Pharmacol Sci* (1998) 19, 311-316
- 65 Gartside, S.E.; Hajos-Korcsok, Bagdy, E.; Harsing, L.G.; Sharp, T.; Hajos, M. Neurochemical and electrophysiological studies on the functional significance of burst firing in serotonergic neurons. *Neuroscience* (2000) 98, 295-300
- 66 Roth, B. L.; Berry, S.A.; Kroeze, W.K.; Willins, D.L.; Kristiansen, K. Serotonin 5-HT_{2A} receptors: Molecular biology and mechanisms of regulation. *Crit. Rev. Neurobiol.* (1987) 12, 319–338
- 67 Pazos, A.; Cortes, R.; Palacios, M. Quantitative autoradiographic mapping of serotonin receptors in the rat brain. II. Serotonin-2 receptors. *Brain Res* (1985) 346, 231-249
- 68 Pazos, A.; Probst, A.; Palacios, C. Serotonin receptors in the human brain-IV. Autoradiographic mapping of serotonin-2 receptors. *Neuroscience* (1987) 21, 123-39
- 69 Lopèz-Giménez, J.F; Guadalupe Mengod, G.;Palacios, J.M., Vilaró, M.T. Selective visualization of rat brain 5-HT_{2A} receptors by autoradiography with [³H]MDL 100907. *Nauyn-Schiedeberg`s Arch. Pharmacol* (1997) 356, 446-454
- 70 Roth, B.L.; McLean, S. Characterization of two [³H]ketanserin recognition sites in rat striatum. *J. Neurochem.* (1987) 49, 1833-1838
- 71 Willins, D.L.; Deutch, A. Y.; Roth, B.L. Serotonin 5-HT_{2A} receptors are expressed on pyramidal cells and interneurons in the rat cortex. *Synapse* (1997) 27, 79-82
- 72 Hall, H.; Farde, L.; Halldin, C.; Lundkvist, C.; Sedvall, G. Autoradiographic localization of 5-HT_{2A} receptors in the human brain using [³H]MDL 100907 and [¹¹C]MDL 100907. *Synapse* (2000) 38, 421-431
- 73 Wainscott, D.B.; Lucaites, V.L., Kursar, J.D.; Baez, M.; Nelson, D.L. Pharmacologic characterization of the human 5-hydroxytryptamine_{2B} receptor: Evidence for species differences. *J. Pharmacol. Exp. Ther.* (1996) 276, 720–727
- 74 Ullmer, C.; Schmuck, K.; Kalkman, H.O.; Lubbert, H. Expression of serotonin receptor mRNAs in blood vessels. *FEBS Lett.* (1995) 370, 215–221
- 75 Roy, A.; Brand, N.J.; Yacoub, M.H. Expression of 5-hydroxytryptamine receptor subtype messenger RNA in interstitial cells from human heart valves. *J. Heart Valve Dis.* (2000) 9, 256–260

-
- 76 Helton, L.A.; Thor, K.B.; Baez, M. 5-Hydroxytryptamine_{2A}, 5-hydroxytryptamine_{2B}, and 5-hydroxytryptamine_{2C} receptor mRNA expression in the spinal cord of rat, cat, monkey and human. *Neuroreport* (1994) 5, 2617–2620
- 77 Choi, D.S.; Maroteaux, L. Immunohistochemical localisation of the serotonin 5-HT_{2B} receptor in mouse gut, cardiovascular system, and brain. *FEBS Lett.* (1996) 391, 45–51
- 78 Duxon, M.S.; Flanigan, T.P.; Reavley, A.C.; Baxter, G.S.; Blackburn, T.P.; Fone, K. C. Evidence for expression of the 5-hydroxytryptamine-2B receptor protein in the rat central nervous system. *Neuroscience* (1997) 76, 323–329
- 79 Julius, D.; MacDermott, A.B.; Axel, R.; Jessell, T.M. Molecular characterization of a functional cDNA encoding the serotonin_{1C} receptor. *Science* (1988) 241, 558–564
- 80 Saltzman, A.G.; Morse, B.; Whitman, M.M.; Ivanshchenko, Y.; Jaye, M.; Felder, S. Cloning of the human serotonin 5-HT₂ and 5-HT_{1C} receptor subtypes. *Biochem. Biophys. Res. Commun.* (1991) 181, 1469–1478
- 81 Yu, L.; Nguyen, H.; Le, H.; Bloem, L.J.; Kozak, C.A.; Hoffman, B.J.; Snutch, T.P.; Lester, H.A.; Davidson, N.; Lubbert, H. The mouse 5-HT_{1C} receptor contains eight hydrophobic domains and is X-linked. *Brain Res. Mol. Brain Res.* (1991) 11, 143–149
- 82 Molineaux, S.M.; Jessell, T.M.; Axel, R.; Julius, D. 5-HT_{1C} receptor is a prominent serotonin receptor subtype in the central nervous system. *Proc. Natl. Acad. Sci.* (1989) 86, 6793–6797
- 83 Mengod, G.; Pompeiano, M.; Martinez-Mir, M.I.; Palacios, J.M. Localization of the mRNA for the 5-HT₂ receptor by in situ hybridization histochemistry. Correlation with the distribution of receptor sites. *Brain Res.* (1990) 524, 139–143
- 84 Giorgetti, M.; Tecott, L.H. Contributions of 5-HT_{2C} receptors to multiple actions of central serotonin systems. *Eur. J. Pharmacol.* (2004) 488, 1–9
- 85 Hoyer, D.; Schoeffter, P. 5-HT receptors: subtypes and second messengers. *J. Recept. Res.* (1991) 11, 197–214
- 86 Julius, D. Molecular biology of serotonin receptors. *Annu. Rev. Neurosci.* (1991) 14, 335–360
- 87 Miquel, M.C.; Doucet, E.; Boni, C. Central serotonin_{1A} receptors: respective distributions of encoding mRNA, receptor protein and binding sites by in situ hybridization histochemistry, radioimmunohistochemistry and autoradiographic mapping in the rat brain. *Neurochem Int* (1991) 19, 453–465

-
- 88 Pazos, A.; Palacios, J.M. Quantitative autoradiographic mapping of serotonin receptors in the rat brain.I. Serotonin-1 receptors. *Brain Res* (1985) 346, 205–230
- 89 Plenevaux, A.; Weissmann, D.; Aerts, J.; Lemaire, C.; Brihaye, C.; Degueldre, C.; Le Bars D.; Comar, D.; Pujol, J.F.; Luxen, A. Tissue distribution, autoradiography, and metabolism of 4-(2)-Methoxyphenyl)-1-[2-[N-(20-Pyridinyl)-p-[¹⁸F]Fluorobenz-amido]ethyl]piperazine (p-[¹⁸F]MPPF), a new serotonin 5-HT_{1A} antagonist for Positron Emission Tomography: An in vivo study in rats *J. Neurochem.* (2000), 75, 803-811
- 90 Rueter, L.E.; Fornal, C.A.; Jacobs, B.L. A critical review of 5-HT brain microdialysis and behavior. *Rev. Neurosci.* (1997) 8, 117–137
- 91 Hamon, M. The main features of the central 5-HT_{1A} receptors. In *serotonergic neurons and 5-HT Receptors in the CNS*. H. G. Baumgarten and M. Goether, Eds. Springer (1997), Berlin, 238–268
- 92 Sprouse, J. S.; Aghajanian, G.K. Responses of hippocampal pyramidal cells to putative serotonin 5-HT_{1A} and 5-HT_{1B} agonists: A comparative study with dorsal raphe neurons. *Neuropharmacology* (1988) 27, 707–715
- 93 Grunschlag, C.R.; Haas, H.L.; Stevens, D.R. 5-HT inhibits lateral entorhinal cortical neurons of the rat in vitro by activation of potassium channel-coupled 5-HT_{1A} receptors. *Brain Res* (1997) 770, 10–17
- 94 Araneda, R.; Andrade, R. 5-Hydroxytryptamine₂ and 5-Hydroxytryptamine_{1A} receptors mediate opposing responses on membrane excitability in rat association cortex. *Neuroscience* (1991) 40, 399–412
- 95 Davies, M.F.; Deisz, R.A.; Prince, D.A. Two distinct effects of 5-hydroxytryptamine on single cortical neurons. *Brain Res* (1987) 423, 347–352
- 96 Sheldon, P.W.; Aghajanian G.K. Serotonin (5-HT) induces IPSPs in pyramidal layer cells of rat piriform cortex: evidence for the involvement of a 5-HT₂-activated interneuron. *Brain Res* (1990) 506, 62–69
- 97 Tanaka, E.; North, R.A. Actions of 5-hydroxytryptamine on neurons of the rat cingulate cortex. *J. Neurophysiol.* (1993) 69, 1749–1757
- 98 Murphy, D.L.; Aulakh, C.S.; Garrick, N.A. How antidepressants work: cautionary conclusions based on clinical and laboratory studies of the longer-term consequences of antidepressant drug treatment. *Ciba Found. Symp.* (1986) 123, 106-125

-
- 99 Leonard, B.E. The comparative pharmacological properties of selective serotonin re-uptake inhibitors in animals. *Selective serotonin re-uptake inhibitors*. Wiley & Sons, Chichester, (1996), New York
- 100 Haddjeri, N.; Szabo, S.T.; de Montigny, C. Increased tonic activation of rat forebrain 5-HT_{1A} receptors by lithium addition to antidepressant treatments. *Neuropsychopharmacology* (2000) 22, 346–356
- 101 Rothman, R. B.; Baumann, M. H. Monoamine transporters and psychostimulant drugs. *Eur. J. Pharmacol.* (2003) 479, 23–40
- 102 Lucki, I.; Singh, A.; Kreiss, D.S. Antidepressant-like behavioral effects of serotonin receptor agonists. *Neurosci. Biobehav. Rev.* (1994) 18, 85–95
- 103 De Vry, J. 5-HT_{1A} receptor agonists: Recent developments and controversial issues. *Psychopharmacol.* (1995) 121, 1–26
- 104 Kennett, G. A.; Bright, F.; Trail, B.; Baxter, G.S.; Blackburn, T.P. Effects of the 5-HT_{2B} receptor agonist, BW 723C86, on three rat models of anxiety. *Br. J. Pharmacol.* (1996) 117, 1443–1448
- 105 Kennett, G.A.; Wood, M.D.; Bright, F.; Cilia, J.; Piper, D.C.; Gager, T.; Thomas, D.; Baxter, G.S.; Forbes, I.T.; Ham, P.; Blackburn, T.P. In vitro and in vivo profile of SB 206553, a potent 5-HT_{2C}/5-HT_{2B} receptor antagonist with anxiolytic-like properties. *Br. J. Pharmacol.* (1996) 117, 427–434
- 106 Vollenweider, F. X.; Vollenweider-Scherpenhuyzen, M. F.; Babler, A.; Vogel, H.; Hell, D. Psilocybin induces schizophrenia-like psychosis in humans via a serotonin-2 agonist action. *Neuroreport* (1998) 9, 3897–3902
- 107 Aghajanian, G.K.; Foote, W.E.; Sheard, M.H. Lysergic acid diethylamide: sensitive neuronal units in the midbrain raphe. *Science* (1968) 161, 706–708
- 108 Aghajanian, G.K.; Haigler, H.J.; Bloom, F.E. Lysergic acid diethylamide and serotonin: direct actions on serotonin-containing neurons in rat brain. *Life Sci* (1972) 11, 615–622
- 109 Egan, C.T.; Herrick-Davis, K.; Miller, K.; Glennon, R.A.; Teitler, M. Agonist activity of LSD and lisuride at cloned 5HT_{2A} and 5HT_{2C} receptors. *Psychopharmacology* (1998) 136, 409–414
- 110 Wooley, D. W.; Shaw, E. A biochemical and pharmacological suggestion about certain mental disorders. *Proc. Natl. Acad. Sci.* (1954) 40, 228–231

-
- 111 Pletscher, A.; Shore, P.A.; Brodie, B.B. Serotonin release as a possible mechanism of reserpine action. *Science* (1955) 122, 374–375
- 112 Matz, R.; Rick, W.; Thompson, H.; Gershon, S Clozapine-a potential antipsychotic agent without extrapyramidal manifestations. *Curr. Ther. Res. Clin. Exp.* (1974) 16, 687–695
- 113 Fink, H.; Morgenstern, R.; Oelssner, W. Clozapine- A serotonin antagonist. *Pharmacol. Biochem. Behav.* (1984) 20, 513–517
- 114 Reynolds, G.P.; Garrett, N.J.; Rupniak, N.; Jenner, P.; Marsden, C.D. Chronic clozapine treatment of rats down-regulates cortical 5-HT₂ receptors. *Eur. J. Pharmacol.* (1983) 89, 325–326
- 115 Gray, J. A.; Roth, B. L. Paradoxical trafficking and regulation of 5-HT_{2A} receptors by agonists and antagonists. *Brain Res. Bull.* (2001) 56, 441–451
- 116 Altar, C.A.; Wasley, A.M.; Neale, R.F.; Stone, G.A. Typical and atypical antipsychotic occupancy of D₂ and S₂ receptors: An autoradiographic analysis in rat brain. *Brain Res. Bull.* (1986) 16, 517–525
- 117 Beasley, C. M.; Sanger, T.; Satterlee, W.; Tollefson, G.; Tran, P.; Hamilton, S. Olanzapine versus placebo: results of a double-blind, fixed-dose olanzapine trial. *Psychopharmacol.* (1996) 124, 159–167
- 118 Chouinard, G.; Jones, B.; Remington, G.; Bloom, D.; Addington, D.; MacEwan, G.W.; Labelle, A.; Beauclair, L.; Arnott, W. A Canadian multicenter placebocontrolled study of fixed doses of risperidone and haloperidol in the treatment of chronic schizophrenic patients. *J. Clin. Psychopharmacol.* (1993) 13, 25–40
- 119 Kehne, J. H.; Ketteler, H.J.; McCloskey, T.C.; Sullivan, C.K.; Dudley, M.W.; Schmidt, C.J. Effects of the selective 5-HT_{2A} receptor antagonist MDL 100907 on MDMA-induced locomotor stimulation in rats. *Neuropsychopharmacology* (1996) 15, 116–124
- 120 Meltzer, H.Y.; Arvanitis, L.; Bauer, D.; Rein, W.; Meta-Trial Study Group. Placebo-controlled evaluation of four novel compounds for the treatment of schizophrenia and schizoaffective disorder. *Am. J. Psychiatry.* (2004) 161, 975–984
- 121 Shephard, S.L.; Edvinsson, L.; Cumberbatch, M.; Williamson, D.; Mason, G.; Webb J.; Boyce, S.; Hill, R.; Hargreaves, R.J. Possible antimigraine mechanisms of action of the 5HT_{1F} receptor agonist LY334370. *Cephalalgia* (1999) 19, 851–858

-
- 122 Cubeddu, L.X. Serotonin mechanisms in chemotherapy-induced emesis in cancer patients. *Oncology* (1996) 53, 18-25
- 123 Brewerton, T.D. Toward a unified theory of serotonin dysregulation in eating and related disorders. *Psychoneuroendocrinology* (1995) 20, 561- 590
- 124 Kotler, L.A.; Walsh, B.T. Eating disorders in children and adolescents: pharmacological therapies. *Eur. Child Adolesc. Psychiatry* (2000) 9, 108-116
- 125 Rothman, R.B.; Baumann, M.H.; Savage, J.E.; Rauser, L.; McBride, A.; Hufeisen, S.J.; Roth, B.L. Evidence for possible involvement of 5-HT_{2B} receptors in the cardiac valvulopathy associated with fenfluramine and other serotonergic medications. *Circulation* (2000) 102, 2836–2841
- 126 Harvey, J.A.; McMaster, S.E. Fenfluramine: Evidence for a neurotoxic action on midbrain and a long-term depletion of serotonin. *Psychopharmacol. Commun.* (1975) 1, 217–228
- 127 Schmidt, C.J.; Wu, L.; Lovenberg, W. Methylenedioxymethamphetamine: A potentially neurotoxic amphetamine analogue. *Eur. J. Pharmacol.* (1986) 124, 175–178
- 128 Larisch R (2001); Habilitationsvorschrift: Untersuchungen des serotonergen Systems und der Serotonin 5HT_{2A}-Rezeptoren mit [¹⁸F] Altanserin und PET. Universität zu Düsseldorf 2001
- 129 Elphick, G.F.; Querbes, W.; Jordan, J.A.; Gee, G.V.; Eash, S.; Manley, K.; Dugan, A.; Stanifer, M.; Bhatnagar, A.; Kroeze, W.K.; Roth, B.L.; Atwood, W.J. The human polyomavirus, JCV, uses serotonin receptors to infect cells. *Science* (2004) 306, 1380–1383
- 130 Armbruster, B.N.; Roth, B.L. Mining the receptorome. *J. Biol. Chem.* (2004) 280, 5129–5132
- 131 Titov, S. A.; Shamakina, I., Ashmarin, I.P. Effect of lysyl vasopressin and vasotocin on a disorder of the conditioned avoidance reaction by a serotonin receptor blockader *Biull Eksp Biol Med* (1983) 95, 31-33
- 132 Hensman, R.; Guimaraes F.S.; Wang, M.; Deakin, J.F. Effects of ritanserin on aversive classical conditioning in humans. *Psychopharmacology* (1991) 104, 220-224
- 133 Alhaider, A.A.; Ageel, A.M.; Ginawi, O.T. The quipazine- and TFMPP-increased conditioned avoidance response in rats: role of 5HT_{1C}/5-HT₂ receptors. *Neuropharmacology* (1993) 32, 1427-32

-
- 134 Williams, G. V.; Rao, S.G.; Goldman-Rakic, P.S. The physiological role of 5-HT_{2A} receptors in working memory. *J. Neurosci.* (2002) 22, 2843-2854
- 135 Vitiello, B., Martin, A.; Hill, J.; Mack, C.; Molchan, S.; Martinez, R.; Murphy, D.L.; Sunderland, T. Cognitive and behavioral effects of cholinergic, dopaminergic, and serotonergic blockade in humans. *Neuropsychopharmacology* (1997) 16, 15-24
- 136 Harvey, J. A. Role of the serotonin 5-HT_{2A} receptor in learning. *Learn Mem* (2003) 10, 355-62
- 137 Blazer, D.; Hughes, D.; George, L. The epidemiology of depression in an elderly community population. *Gerontologist* (1987) 27, 281–287
- 138 Borson, S.; Barnes, R.; Kukull, W.; Okimoto, J.; Veith, R.; Inui, T.; Carter, W.; Raskind, M. Symptomatic depression in elderly medical outpatients. I. Prevalence, demography, and health service utilization. *J. Am. Geriatr. Soc.* (1986) 34, 341–347
- 139 Casey, D. Depression in the elderly. *South Med. J.* (1994) 87,559–563
- 140 Leysen Gaps and peculiarities in 5-HT₂ receptor studies. *Neuropsychopharmacology* (1990) 3, 361-369
- 141 Kristiansen, H.; Elfing, B.; Plenge, P.; Pinborg, L.H.; Gillings, N.; Knudsen, G.M. Binding characteristics of the 5-HT_{2A} receptor antagonists altanserin and MDL 100907. *Synapse* (2005) 58, 249–257
- 142 Rinaldi-Carmona, M; Congy, C.; Santucci, V.; Simiand, Gautret, B.; Neliat, G.; Labeeuw, B.; Le Fur, G.; Soubrie, O.; Breliere, J.C. Biochemical and pharmacological properties of SR 46349B, a new potent and selective 5-hydroxytryptamine₂ receptor antagonist. *J. Pharmacology and Experimental Therapeutics* (1992) 262, 759-768
- 143 Burnet, P.W.J.; Eeastwood, S.L., Harrison, P.J. [³H]WAY 100635 for 5-HT_{1A} Receptor Autoradiography in human brain. *Neurochem.* (1997) 30, 565-574
- 144 Lang, L.; Jagoda, E.; Schmall, b; Sassaman, M.; Ma, Y.; Eckelman, W.C. Development of Fluorine-¹⁸F-Labeled 5-HT_{1A} Antagonists. *J. Med. Chem.* (1999) 42. 1576-1586
- 145 Kung, H.F.; Frederick, D., Kim, H-J.; McElgin, W.; Kung, M-P.; Mu ,M.; Mozley, P.D.; Vessotskie, J.M.; Andrew, D.; Kushner, S.A.; Zhunag, Z-P. In vivo binding of [¹²³I]4-(2`methoxyphenyl)-1[2`-(N-2``-pyridinyl)-p-iodobenz-amido]ethylpiperazine, p-MPPI, to 5-HT_{1A} receptors in rat brain, *Synapse* (1994) 18, 359-366

-
- 146 Khawaja, X. Characterization of the binding of [³H]WAY 100635, a novel 5-HT_{1A} receptor antagonist, to rat brain. *J. Neurochem.* (1995) 64, 2716-2726
- 147 Mathis, C.A.; Simpson, N.R.; Mahmood, K.; Kinahan, P.E; Mintun, M.A. [¹¹C]WAY 100635 : A radioligand for imaging 5-HT_{1A} receptors in rat brain. *Life Sci.* (1994) 55, 403-407
- 148 López-Rodríguez, M.L.; Ayala, D.; Benhamú, B.; Morcillo, M.J.; Viso, A. Arylpiperazin derivatives acting at 5-HT_{1A} receptors. *Current Medicinal Chemistry* (2002) 9, 443-469
- 149 Leysen, J.E. Gaps and peculiarities in 5-HT₂ receptor studies. *Neuropsychopharmacology* (1990) 3,361-369
- 150 Heinrich, T.; Böttcher, H.; Prücher, H.; Gottschlich, R.; Ackermann, K-A.; van Amsterdam, C. 1-(1-Phenethylpiperidin-4-yl)-1-phenylethanols as potent and highly selective 5-HT_{2A} antagonists. *Chem.Med.Chem.* (2006) 1, 245-255
- 151 Timo Stoll (2004); Dissertation: Entwicklung und trägerarme ¹⁸F-Markierung selektiver Inhibitoren des Serotonin Transporters. Universität zu Köln (2004)
- 152 Diksic, M.; Nagahiro, S.; Grdisa, M. The regional rate of serotonin synthesis estimated by the d-methyl-tryptophan method in rat brain from a single time point. *J Cereb Blood Flow Metab* (1995) 15, 806–813
- 153 Diksic, M.; Nagahiro, S.; Chaly, T.; Sourkes, T.; Yamamoto, Y.; Feindel, W. Serotonin synthesis rate measured in living dog brain by positron emission tomography. *J. Neurochem* (1991) 56,153–160
- 154 Smith, G.; Price, J.C.; Lopresti, B.J.; Hunag, Y.; Simpson, N.; Holt, D.; Mason, N.S.; Meltzer, C.C.; Sweet, R.A.; Nichols, T.; Sashin, D.; Mathis, C.A. Test–retest variability of serotonin 5-HT_{2A} receptor binding measured with Positron Emission Tomography and [¹⁸F]altanserin in the human brain. *Synapse* (1998) 30, 380-392
- 155 Sheline, Y.I.; Mintun, M.A.; Barcg, D.M.; Wilkins, C.; Snyder, A.Z.; Moerlein, S.M. Decreased hippocampal 5-HT_{2A} receptor binding in older depressed patients using [¹⁸F]altanserin positron emission tomography. *Neuropsychopharmacology* (2004) 29, 2235-2241
- 156 Bailer, U.F.; Price, J.C., Meltzer, C.C.; Mathis, C.A.; Frank, G.K.; Weissfeld, L.; McConaha, C.W.; henry, S.E.; Brooks-Achenbach, S.; Barbarich, N.C., Barbarich, N.C.; Kaye, W.H. Altered 5-HT_{2A} receptor binding after recovery from bulimia-type

- Anorexia Nervosa: Relationships to harm avoidance and drive for thinness. *Neuropsychopharmacology*. (2004)29, 1143-1155
- 157 Qu, Y.; Chang, L.; Klaff, J.; Balbo, A.; Rapoport, S.I. Imaging brain phospholipase A2 activation in awake rats in response to the 5-HT_{2A/2C} agonist. *Neuropsychopharmacology* (2003) 28, 244-252
- 158 Ito, H.; Nyberg, S.; Halldin, C.; Lundkvist, C.; Farde, L.. PET Imaging of central 5-HT_{2A} receptors with carbon-11-MDL 100907. *J.Nuc.Med.* (1998) 39, 208-214
- 159 Biver, F.; Lotstra, F.; Monclus, M.; Dethy, S.; Damhaut, P.; Wikler, D., Luxen, A.; Goldman, S. In vivo binding of [¹⁸F]altanserin to rat brain 5HT₂ receptors: A film and electronic autoradiographic study. *Nucl Med Biol* (1997) 24, 357–360
- 160 Biver, F.; Goldman, S.; Luxen, A.; Monclus, M.; Forestini, M.; Mendlewicz, J.; Lotstra, F. Multicompartmental study of fluorine-18 altanserin binding to brain 5HT₂ receptors in humans using positron emission tomography. *Eur J Nucl Med* (1994) 21, 937–946
- 161 Sadzot, B.; Lemaire, C.; Maquet, P.; Salmon, E.; Plenevaux, A.; Degueldre, C.; Hermanne, J.; Guillaume, M.; Cantineau, R.; Comar, D.; Franck, G. Serotonin 5HT₂ receptor imaging in the human brain using positron emission tomography and a new radioligand, [¹⁸F]altanserin: Results in young normal controls. *Journal of Cerebral Blood Flow & Metabolism* (1995) 15, 787–797
- 162 Hasselbalch, S.G.; Madsen, K.; Svarer, C.; L.H. Pinborg, L.H.; Holm, S.; O.B. Paulson, O.B.; Waldemar, G.; Knudsen, G.M. Reduced 5-HT_{2A} receptor binding in patients with mild cognitive impairment. *Neurobiology of Aging* (2008) 29, 1830–1838
- 163 Dewey, S.; Tan, P.; Smith, G.; King, P.; Pappas, N.; MacGregor, R.; Ding, Y-S.; Shea C.; Alexoff, D.; Martin, T.; Gatley, S.; Fowler, J.; Wolf, A. PET and in vivo microdialysis studies of SR 46349B, a new and selective 5-HT₂ antagonist. *Soc Neurosci Abstr* (1994) 20:1552
- 164 Hinz, R.; Bhagwagar, Z.; Cowen, P.J.; Cunningham, V.J.; Grasby, P.M. Validation of a tracer kinetic model for the quantification of 5-HT_{2A} receptors in human brain with [¹¹C]MDL 100907. *Journal of Cerebral Blood Flow & Metabolism* (2007) 27, 161–172

- 165 Lundkvist, C.; Halldin, C.; Ginovart, N.; Nyberg, S.; Swahn, C-G.; Carr, A.; Brunner F.; Farde, L. [^{11}C]MDL 100907, a radioligand for selective imaging of 5-HT_{2A} receptors with positron emission tomography. *Life Sci* (1996) 58, 187–192
- 166 Mathis, C.A.; Huang, Y.; Simpson, N.R.; Mahmood, K.; Gerdes, J.M.; Price, J.C. [^{11}C]MDL 100,907: A potent and selective antagonist of 5-HT_{2A} receptors labelled with ^{11}C at two different positions. *J Labelled Compd Radiopharm* (1995) 27, 316–318
- 167 Mathis, C.A.; Mahmood, K.; Huang, Y.; Simpson, N.R.; Gerdes, J.M.; Price, J.C. Synthesis and preliminary in vivo evaluation of [^{11}C]MDL 100907: A potent and selective radioligand for the 5-HT_{2A} receptor system. *Med. Chem. Res.* (1996) 6, 1–10
- 168 Bhagwagar, Z.; Hinz, R.; Taylor, M.; Fancy, S.; Cowen, P.; Grasby, P. Increased 5-HT_{2A} receptor binding in euthymic, medication-free patients recovered from depression: A Positron Emission Study with [^{11}C]MDL 100907. *Am J Psychiatry* (2006)163, 1580–1587
- 169 Ashworth, S.; Hume, S.; Lammertsma, A.; Opacka-Juffry, J.; Shah, F.; Pike, V. Development of central 5-HT_{2A} receptor radioligands for PET: Comparison of [^3H]RP 62203 and [^3H]SR 46349B kinetics in rat brain. *Nucl. Med. Biol.* (1996) 23, 245–250
- 170 Larisch, R.; Klimke, A.; Hamacher, K.; Henning, U.; Estalji, S.; Hohlfeld, T.; Vosberg, H.; Tosch, M.; Gaebel, W.; Coenen, H.H.; Mülller-Gärtner, H-W. A Influence of synaptic serotonin level on [^{18}F]altanserin binding to 5HT₂ receptors in man. *Behavioural Brain Research* (2003)139, 21–29
- 171 Hume, S.P.; Ashworth, S.; Opacka-Juffry, J.; Ahier, R.G.; Lammertsma, A.A.; Pike V.W.; Cliffe, I.A.; Fletcher, A.; White, A.C. Evaluation of [O-methyl- ^3H]WAY 100635 as an in vivo radioligand for 5-HT_{1A} receptors in rat brain. *Eur J Pharmacol* (1994) 271, 515–523
- 172 Price, J.; Mathis, C.; Simpson, N.; Mahmood, K.; Mintun, M. Kinetic modeling of serotonin-1A binding in monkeys using [^{11}C]WAY 100635 and PET. Quantification of brain function using PET. San Diego, Academic Press(1996), 257–261
- 173 Mathis, C.A.; Simpson, N.R.; Mahmood, K.; Kinahan, P.E.; Mintun, M.A. [^{11}C]Way 100635: A radioligand for imaging 5-HT_{1A} receptors with positron emission tomography. *Life Sci* (1994) 55, 403–407
- 174 Osman, S.; Lundkvist, C.; Pike, V.; Halldin, C.; McCarron, J.; Swahn, C-G.; Ginovart, N.; Luthra, S.; Bench, C.; Grasby, P.; Wikström, H.; Barf, T.; Cliffe, I.; Fletcher, A.; Farde, L. Characterization of the radioactive metabolites of the 5-HT_{1A} receptor

- radioligande, [O-methyl-¹¹C]WAY 100635, in monkey and human plasma by HPLC: Comparison of the behaviour of an identified radioactive metabolite with parent radioligand in monkey using PET. *Nucl. Med. Biol.* (1996) 23, 627–634
- 175 Parsey, R.V.; Slifstein, M.; Hwang, D.R.; Abi-Dargham, A.; Simpson, N.; Mawlawi, O.; van Heertum, R.; Mann, J.J.; Laruelle, M. Validation and reproducibility of measurement of 5-HT_{1A} receptor parameters with [carbonyl-¹¹C]WAY-100635 in humans: Comparison of arterial and reference tissue input functions. *Journal of Cerebral Blood Flow & Metabolism* (2000) 20, 1111–1133
- 176 Pike, V.; McCarron, J.; Lammertsma, A.; Osman, S.; Hume, S.; Sargent, P.; Bench, C.; Cliffe, I.; Fletcher, A.; Grasby, P. Exquisite delineation of 5-HT_{1A} receptors in human brain with PET and [carbonyl-¹¹C]WAY-100635. *Eur J Pharmacol* (1996) 301, 5–7
- 177 Martinez, D.; Hwang, D.; Mawlawi, O.; Slifstein, M.; Kent, J.; Simpson, N.; Parsey, R.V.; Hasimoto, T.; Huang, Y.; Shinn, A.; van Heertum, R.; Abi-Dargham, A.; Caltabiano, S.; Malizia, O.; Cowley, H.; Mann, J.J.; Laurelle, M.; Differential occupancy of somatodendritic and postsynaptic 5-HT_{1A} receptors by pindolol: A dose-occupancy study with [¹¹C]WAY 100635 and Positron Emission Tomography in humans. *Neuropsychopharmacology* (2001) 24, 209-229
- 178 Hirvonen, J.; Karlsson, H.; Kajander, J.; Lepola, A.; Markkula, J.; Rasi-Hakala, H.; Någren, K.; Salminen, J.K.; Hietala, J. Decreased brain serotonin 5-HT_{1A} receptor availability in medication-naive patients with major depressive disorder: an in-vivo imaging study using PET and [carbonyl-¹¹C]WAY-100635. *Neuropsychopharmacology* (2008) 11,465-476
- 179 Lothe, A.; Didelot, A.; Hammers, A.; Costes, N.; Saoud, M.; Gilliam, F.; Ryvlin, P. Comorbidity between temporal lobe epilepsy and depression: a [¹⁸F]MPPF PET study. *Brain* (2008) 131, 2765-2782
- 180 Yasuno, F.; Suhara, T.; Ichimaya, T.; Takano, A.; Ando, T.; Okubo, Y.. Decreased 5-HT_{1A} receptor binding in amygdale of schizophrenia. *Biol. Psychiatry* (2004) 55, 439-444
- 181 Hashimoto, T.; Nishino, N.; Nakai, H.; Tanaka, C. Increase in serotonin 5-HT_{1A} receptors in prefrontal and temporal cortices of brains from patients with chronic schizophrenia. *Life Sci.* (1991) 48, 355-363

- 182 Tauscher, J.; Kapur, S.; N. Verhoeff, P.L.G.; Hussey, D.F.; Daskalakis, Z.J.; Tauscher-Wisniewski, S.; Wilson, A.A.; Houle, S.; Kasper, S.; Zipursky, R.B.; Brain serotonin 5-HT_{1A} receptor binding in schizophrenia measured by Positron Emission Tomography and [¹¹C]WAY-100635. *Arch Geb Pschiatry* (2002) 59, 514-520
- 183 Frankle, W.G.; Lombardo, I.; Kegels, L.S.; Slifstein, M.; Martin, J.H.; Hunag, Y.; Hwang, D.R.; Reich, E.; Cangianno, C.; Gil, R.; Laruelle, M.; Abi-Dargham, A.. Serotonin 1A receptor availability in patients with schizophrenia and schizo-affective disorder: a positron emission tomography imaging study with [¹¹C]WAY 100635. *Psychopharmacology* (2006) 189, 155-164
- 184 Maeda, J.; Sahara, T.; Ogawa, M.; Okauchi, T.; Kawabe, K.; Zhang, M-R.; Semba, J.; Suzuki, K. In Vivo Binding Properties of [Carbonyl-¹¹C]WAY-100635: Effect of endogenous serotonin. *Synapse* (2001) 40, 122–129
- 185 Witte, A.V.; Flöel, A.; Stein, P.; Savli, M.; Mien, L-K.; Wadsak, W.; Spindelegger, C.; Moser, U.; Fink, M.; Hahn, A.; Mitterhauser, M.; Kletter, K.; Kasper, S.; Lanzenberger, R. Aggression is related to frontal serotonin-1A receptor distribution as revealed by PET in healthy subjects. *Human Brain Mapping* (2009) (accepted)
- 186 Fletcher, S.R.; Burkamp, F.; Blurton, P.; Cheng, S.K.F.; Clarkson, R.; O'Connor, D.; Spinks, D.; Tudge, M.; van Niel, M.B.; Patel, S.; Chapman, K.; Marwood, R.; Shephard, S.; Bentley, G.; Cook, G.P.; Bristow, L.J.; Castro, J.L.; Hutson, P.H.; MacLeod, A.M. 4-(Phenylsulfonyl)piperidines: Novel, selective, and bioavailable 5-HT_{2A} receptor antagonists. *J. Med. Chem.* (2002) 45, 492-503
- 187 Szabo, Z.; Kao, P.; Scheffel, U.; Suehiro, M.; Mathews, W.; Ravert, H.; Musachio, J.; Marengo, S.; Kim, S.; Ricaurte, G.; Wong, D.; Wagner, H.; Dannals, R. Positron emission tomography imaging of serotonin transporters in the human brain using [¹¹C]McN5652. *Synapse* (1995) 20, 37–43
- 188 Ginovart, N.; Wilson, N.N.; Meyer, J.H.; Hussey, D.; Houle, S. [¹¹C]DASB, a tool for in vitro measurement of SSRI-induced occupancy of the serotonin transporter. *Synapse* (2003) 47, 123-133
- 189 Szabo, Z.; McCann, U.D.; Wilson, A.A.; Scheffel, U.; Owonikoko, T.; Mathews, W.B.; Ravert, H.D.; Hilton, J.; Dannals, R.F.; Ricaurte, G.A. Comparison of (+)-[¹¹C]-McN5652 and [¹¹C]-DASB as serotonin transporter radioligands under various experimental conditions. *J. Nuc. Med.* (2002) 43, 678-692

-
- 190 McCann, U.D.; Szabo, Z.; Seckin, E.; Rosenblatt, P.; Methews, W.B.; Ravert, H.T.; Dannals, R.F.; Ricaurte, G.A. Quantitative PET studies of the serotonin transporter in MDMA users and controls using [^{11}C]McN5652 and [^{11}C]DASB. *Neuropsychopharmacology* (2005) 30, 1741-1750
- 191 Laruelle, M.; Slifstein, M.; Huang, Y. Positron emission tomography: imaging and quantification of neurotransmitter availability. *Methods* (2002) 27, 287-299
- 192 Houle, S.; Ginovart, N.; Hussey, D.; Meyer, J.H.; Wilson, A.A. Imaging the serotonin transporter with positron emission tomography: Initial human studies with [^{11}C]DAPP and [^{11}C]DASB. *Eur. J. Nucl. Med.* (2001) 27, 1719-1722
- 193 Wilson, A.,A.; Houle, S. Radiosynthesis of carbon-11 labelled N-methyl-2-(arylthio)benzylamines: Potential radiotracers for the serotonin reuptake receptor. *J. Label. Comp. Radiopharm.* (1999) 42, 1277-1288
- 194 Huang, Y.; Hwang, D.R.; Narendran, R.; Sudo, Y.; Chatterjee, R.; Bar, S.A.; Mawlawi, O., kegeles, L.S.; Wilson, A.A.; Kung, H.F.; Laruelle, M. Comparative evaluation in nonhuman primates of five PET radiotracers for imaging the serotonin transporters: [^{11}C]McN 5652, [^{11}C]ADAM, [^{11}C]DASB, [^{11}C]DAPA, and [^{11}C]AFM. *J. Cerebral Blood Flow Metabol.* (2002) 22, 1377-1398
- 195 Nishizawa, S.; Benkelefat, C.; Young, S.N.; Leyton, M.; Mzengeza, S.; De Montigny, C.; Blier, P.; Diksic, M. Differences between males and females in rates of serotonin synthesis in human brain. *Proc. Natl. Acad. Sci.* (1997) 94, 308–5313
- 196 Stayley, J.K.; van Dyck, C.H.; Tan, P.Z.; Al Tikiti, M.; Ramsby, Q.; klump, H.; Ng, C.; Garg, P.; Soufer, R.; Baldwin, R.M.; Innis, R.B. Comparison of [^{18}F]altanserin and [^{18}F]deuteroaltanserin for PET imaging of serotonin $_2\text{A}$ receptors in baboon brain: pharmacological studies. *Nucl. Med. Biol.* (2001) 28, 271-279
- 197 Tan, PZ.; Baldwin, R.M.; Fu, T.; Charney, D.S.; Innis, R.B. Characterization of radioactive metabolites of 5-HT $_2\text{A}$ receptor PET ligand [^{18}F]altanserin in human and rodent, *Nuc. Med. Biol.* (1999) 26, 601-608
- 198 Tan, P.; Fowler, J.S.; Yu-Shin, D.; Schleyer, D.J.) Rapid syntheses of [^{18}F]SR46348B, a potent and selective 5-HT $_2\text{A}$ receptor antagonist, *J.Labl.cmpds.* (1995) 36, 719-728
- 199 Scot, D.O.; Heath, T.G.J. Investigation of the CNS penetration of a potent 5-HT $_2\text{A}$ receptor antagonist and an active metabolite, *Pharm. Biomed. Anal.* (1998) 17, 17-25

-
- 200 Watabe, H.; Michael, A.; Channing, M.G.; Adams, H.R.; Jagoda, E.; Herscovitch, P.; Eckelman, W.C.; Carson, R.E. Kinetic Analysis of the 5-HT_{2A} Ligand [¹¹C]MDL 100,907. *J. Cerebral Blood Flow Metab.* (2000) 20, 899-909
- 201 Bonaccorso, S.; Meltzer, H.Y.; Li, Z.; Dai, J.; Alboszta, A.R.; Ichikawa, J. SR 46349B Potentiates Haloperidol-induced Dopamine Release. *Neuropsychopharmacology* (2002) 27, 430-441
- 202 Gobert, A.; Millan, M.J. Serotonin 5-HT_{2A} receptor activation enhances dialysis levels of dopamine and noradrenaline, but not 5-HT, in the frontal cortex of freely-moving rats, *Neuropharmacol.* (1999) 38, 315-317
- 203 Pike, V.W.; McCarron, J.A.; Lammerstma, A.A.; Hume, S.P.; Poole, K.; Grasby, P.M.; Malizia A.; Cliffe, I.A.; Fletcher, A.; Bench C.J. First delineation of 5-HT_{1A} receptors in human brain with PET and [¹¹C]WAY 100635. *Eur. J. Pharmacol.* (1995) 283, 1 – 3
- 204 Price, L.H.; Malison, R.T.; McDougale, C.J.; Pelton, G.H.; Heninger, G.R. The neurobiology of tryptophan depletion in depression: Effects of intravenous tryptophan infusion. *Biol. Psychiatry* (1998) 43, 339–347
- 205 Litman, T.; Zuthen, T.; Skovsgaard, T.; Stein, W. Structure-Activity Relationships of P-Glycoprotein Interacting Drugs: Kinetic Characterization of their Effects on ATP-ase Activity. *Biochim. Biophys. Acta* (1997) 1361, 159-168
- 206 Levin, V.A. Relationship of Octanol/Water Partition Coefficient and molecular Weight to Rat Brain Capillary Permeability. *J. Med. Chem.* (1980) 23, 682-684
- 207 Ekins, S.; Kim, R.B.; Leake, B.F.; Dantzig, A.H.; Schuetz, E.G.; Lan, L-B.; Yasuda, K.; Shepard, R.L.; Winter, M.A; Schuetz, J.D.; Wikel, J.A.; Wrighton, S.A. Application of three-dimensional quantitative structure-activity relationships of P-glycoprotein inhibitors and substrates. *Mol Pharmacol* (2002) 61, 974–981
- 208 Shapiro, A.B.; Fox, K.; Lam, P.; Ling, V. Stimulation of P-glycoprotein-mediated drug transport by prazosin and progesterone. Evidence for a third site. *Eur J Biochem* (1999) 259, 841–850
- 209 Wang, R.B.; Kuo, C.L.; Lien, L.L.; Lien, E.J. Structure–activity relationship: analyses of p-glycoprotein substrates and inhibitors. *Journal of Clinical Pharmacy and Therapeutics* (2003) 28, 203–228

-
- 210 Elsinga, P.H.; Hendrikse, N.H.; Bart, J.; van Waarde, A.; Vaalburg, W. Positron Emission Tomography Studies on binding of central nervous system drugs and P-glycoprotein function in the rodent brain. *Mol Imaging Biol* (2005) 7, 37-44
- 211 Palner, M; Syvänen, S.; Kristoffersen; U.S.; Gillings, N.; Kjaer, A.; Knudsen, G.M. The effect of a P-glycoprotein inhibitor on rat brain uptake and binding of [¹⁸F]altanserin: a micro-PET study. *Abstract Brain and Mind Forum 2007*
- 212 Godbout, R.; Chaput, Y.; Blier, P.; de Montigny, C. Tansospirone and its metabolite, 1-(2-pyrimidinyl)-piperazine. Effects of acute and long-term administration of tandospirone on serotonin neurotransmission. *Neuropharmacology* (1991), 30, 679–690

3 Manuscripts

3.1 Total synthesis and evaluation of [¹⁸F]MHMZ

by Matthias M. Herth,^{a,*} Fabian Debus,^b Markus Piel,^a Mikael Palner,^c Gitte M. Knudsen,^c Hartmut Lüddens^b and Frank Rösch^a

^a Institute of Nuclear Chemistry, University of Mainz, Fritz-Strassmann-Weg 2, 55128 Mainz, Germany

^b Department of Psychiatry, Clinical Research Group, Untere Zahlbacher Straße 8, 55131 Mainz, Germany

^c Center for Integrated Molecular Brain Imaging, Rigshospitalet, Blegdamsvej 9, DK-2100 Copenhagen Ø, Denmark

Abstract

Radiochemical labelling of MDL 105725 using the secondary labelling precursor 2-[¹⁸F]fluoroethyltosylate ([¹⁸F]FETos) was carried out in yields of 90% synthesizing [¹⁸F]MHMZ in a specific activity of 50 MBq/nmol with a starting activity of 3 GBq. Overall radiochemical yield including [¹⁸F]FETos synthon synthesis, [¹⁸F]fluoroalkylation and preparing the injectable [¹⁸F]MHMZ solution was 42% within a synthesis time of 100 min. The novel compound showed excellent specific binding to the 5-HT_{2A} receptor ($K_i = 9.0$ nM) *in vitro* and promising *in vivo* characteristics.

Key Words

[¹⁸F]MHMZ; MDL 100907; [¹⁸F]altanserin; 5-HT_{2A}; Antagonist; Positron emission tomography; Autoradiography

Serotonergic 5-HT_{2A} receptors are of central interest in the pathophysiology of schizophrenia and other diseases, including Alzheimer's disease and personality disorders.¹ The serotonergic system is also implicated in sleep, aging, and pain.² *In vivo* studies of 5-HT_{2A} receptor

occupancy would provide a significant advance in the understanding of the mentioned disorders and conditions. Positron emission tomography (PET) is an appropriate tool to measure *in vivo* directly, non-invasively, and repetitively the binding potential of radio tracers for neuroreceptors.

A number of neurotransmitter analogues labelled with β^+ -emitter containing radioligands were synthesized as radiopharmaceuticals for the imaging of the 5-HT_{2A} receptor. To date, *in vivo* studies have been performed with several 5-HT_{2A} selective antagonists such as [¹¹C]MDL 100907,³ [¹⁸F]altanserin,⁴ and [¹¹C]SR46349B⁵.

Within those ligands, [¹⁸F]altanserin and [¹¹C]MDL 100907 represent the radioligands of choice for *in vivo* 5-HT_{2A} PET imaging because of their high affinity and selectivity for the 5-HT_{2A} receptor {altanserin: $K_i = 0.13 \text{ nM}^4$; (R)-MDL 100907: $K_i = 0.57 \text{ nM}^6$ }. Affinities are more than 100-fold higher for other receptors such as 5-HT_{2C}, α_1 , D₁, and D₂. Nevertheless, it was proposed that the selectivity of [¹¹C]MDL 100907 for 5-HT_{2A} receptor is slightly higher than the selectivity for this receptor of [¹⁸F]altanserin.⁸ Both tracers show in *in vitro* and in *in vivo* experiments, high affinity, selectivity, and a good ratio of specific to non-specific binding for 5-HT_{2A} receptors.^{3,7} The advantage of [¹⁸F]altanserin over [¹¹C]MDL 100907 is the possibility to perform equilibrium scans lasting several hours and to transport the tracer to other facilities based on the 110 min half-life of [¹⁸F]fluorine. A drawback of [¹⁸F]altanserin is its rapid and extensive metabolism. Four metabolites are formed in humans that cross the blood–brain-barrier,⁷ whereas metabolites of [¹¹C]MDL 100907 do not enter the brain to any larger extent.⁹

The aim of this study was to develop an ¹⁸F-analogue of MDL 100907 (1) combining advantages of both ligands, the better selectivity of MDL 100907 and the superior isotopic properties of [¹⁸F]fluorine. For this purpose we decided to replace one of the O-methyl groups by an O-2-[¹⁸F]fluoroethyl moiety resulting in [¹⁸F]MHMZ ([¹⁸F]FE1-MDL100907) ((3-[¹⁸F]fluoro-ethoxy-2-methoxyphenyl)-1-[2-(4-fluoro-phenyl)ethyl-4-piperidine-methanol, 2) (Fig. 1).

The methoxy group in the 3-position seemed to be more suitable for labelling because previous [^{11}C]MDL 100907 studies showed that metabolism predominantly resulted in the formation of its 3-OH analogue MDL 105725 ((3-hydroxy-2-methoxy-phenyl)-1-[2-(4-fluorophenyl)ethyl]-4-piperidine-methanol, 3). ^{18}F -Labeling in the 2-position would therefore lead to extensive formation of the labelled 3-OH-analogue (2- ^{18}F fluoro-ethoxy-3-methoxyphenyl)-1-[2-(4-fluoro-phenyl)ethyl]-4-piperidine-methanol that may be expected to cross the blood–brain-barrier or to be metabolized within the brain and thus interfere with the interpretation of the labelled tracer uptake.^{10,11}

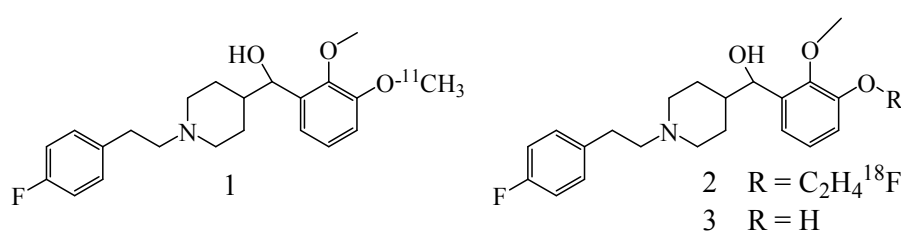


Figure 1. Structures of [^{11}C]MDL 100907 (1), [^{18}F]MHMZ (2), and MDL 105725 (3).

A useful synthetic route to MDL 100907 and its racemic precursor MDL 105725 has been published by Huang et al.³ The route depended upon a key transformation of an ester to a ketone via an amide intermediate (Fig. 2) and was carried out essentially as published³ with minor modifications.

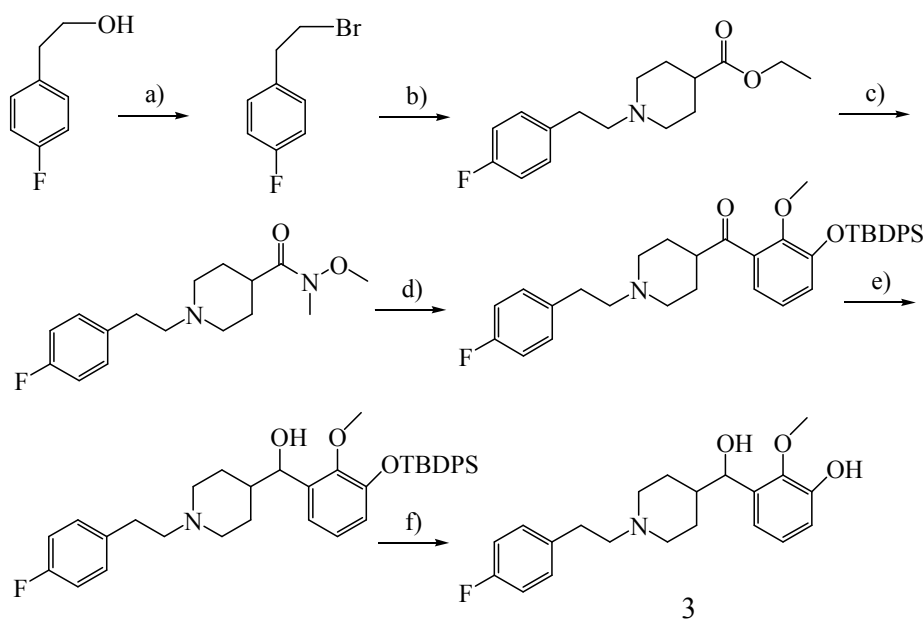


Figure 2. (a) PBr_3 , toluene; (b) K_2CO_3 , DMF; (c) $\text{Me}(\text{MeO})\text{NH}\cdot\text{HCl}$, EtMgBr , THF; (d) $n\text{-BuLi}$, THF, TBDPS-gujacol; (e) NaBH_4 , MeOH; (f) K_2CO_3 , MeOH, H_2O .

Finally, MHMZ was synthesized via a fluoroalkylation of the precursor MDL 105725 in dry DMF by addition of sodium hydride and 1-bromo-2-fluoroethane (Fig. 3) in a yield of 40%. A chiral derivatization of the final product MHMZ was not performed.

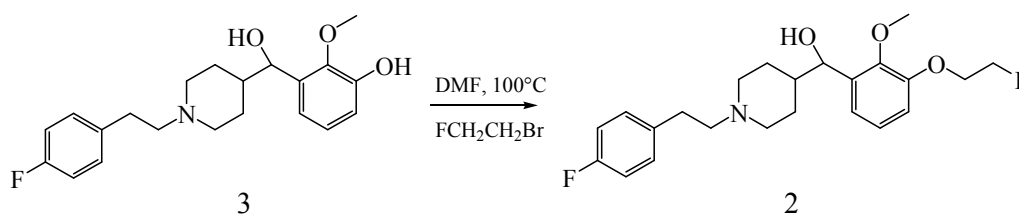


Figure 3. Synthesis of MHMZ.

The purity of MHMZ was examined to be higher than 98% as indicated by HPLC analysis (ET 250/8/4 Nucleosil 5 C18; MeCN/H₂O 40:60, R_f = 8.68 min). These results justified further analyses like determination of the affinity and the route for radioactive syntheses, receptor autoradiography, and metabolism studies.

A radioligand competition binding assay was carried out with GF-62 cells, a clonal cell line expressing high amounts (5–7 pmol/mg) of the 5-HT_{2A} receptor, in test tubes containing [³H]MDL (0.2 nM) and seven different concentrations of test compounds (1 μM–1 pM) in a total of 1mL assay buffer. Ketanserin (1 μM) was used to determine non-specific binding. The 5-HT_{2A} binding affinities of the racemic MHMZ and the reference compounds altanserin and MDL 100907 are shown in Table 1.

Table 1. Receptor binding data of MDL 100907 derivatives and altanserin

Compound	K _i [nM]
MH.MZ	9.00 ± 0.10
altanserin	0.74 ± 0.88
MDL 100907	2.10 ± 0.13

MHMZ showed a 4.5 times lower affinity as compared to the parent compound MDL 100907 but still was in the nanomolar range. The assay was performed n = 4 times.

[^{18}F]Fluoroalkylation of the precursor MDL 105725 was carried out using [^{18}F]FETos, which was produced in an automated module.¹² Optimization of the reaction conditions gave radiochemical yields of about 90% at a reaction temperature of 100 °C in a reaction time of 10 min using 7 mmol precursor and 7 mmol 5 N NaOH as a base in dry DMF as a solvent.

The optimization procedure of the radiochemical yield of [^{18}F]MHMZ is exemplified for the parameter temperature in Figure 4.

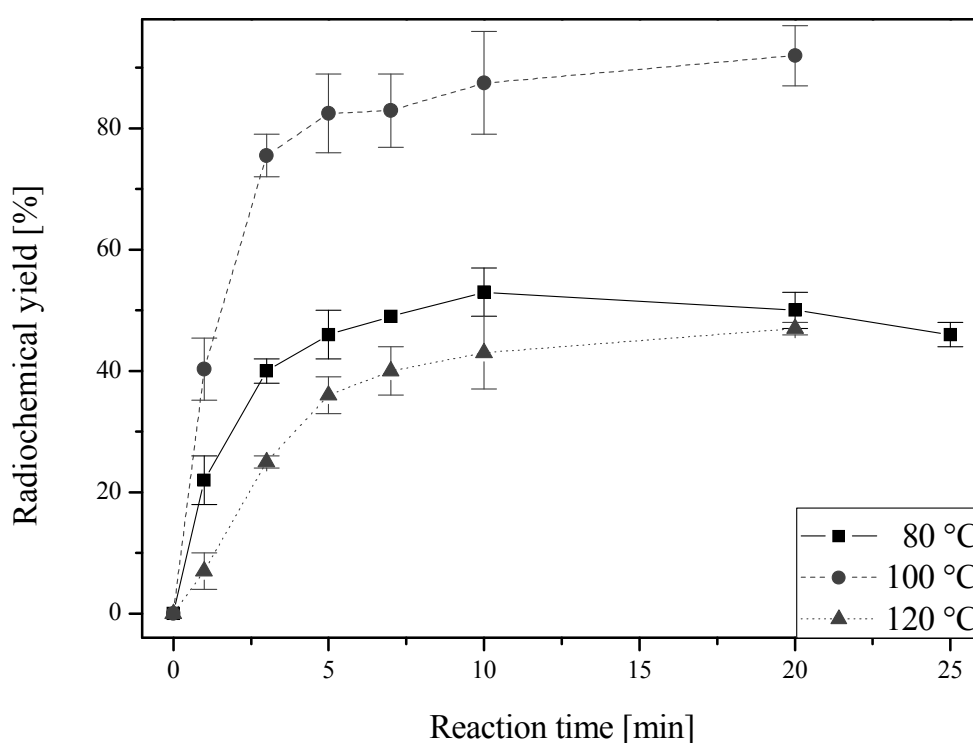


Figure 4. [^{18}F]Fluoroalkylation of 7 mmol MDL 105725 at different reaction temperatures using DMF and 7 mmol 5 N NaOH.

The final formulation of the injectable solution including a semipreparative HPLC (ET 250/8/4 Nucleosil 5 C18; MeCN/H₂O 40:60, R_f = 8.68 min) took no longer than 100 min and provided [^{18}F]MHMZ (2) with a purity >96% as indicated by analytical HPLC analyses. The specific activity was determined to be 50 MBq/nmol with a starting amount of radioactivity of 3 GBq of [^{18}F]fluorine.

Autoradiographic images of the 5-HT_{2A} receptor obtained with [¹⁸F]MHMZ showed excellent visualization results in rat brain sections (Fig. 5). Images were in complete agreement with the distribution obtained with [³H]MDL 100907¹³ (also Fig. 6B and C). Highest binding was detected in lamina V of the frontal cortex, the caudate-putamen, the motor trigeminal nucleus, the facial nucleus, and the pontine nuclei.

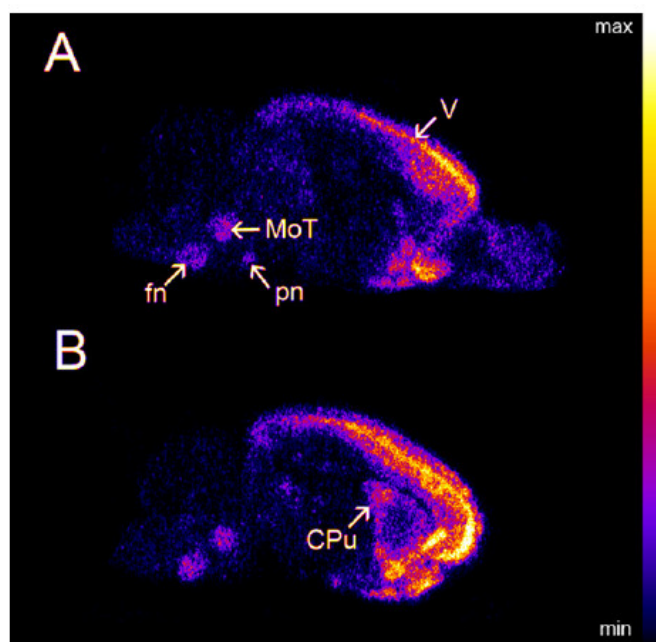


Figure 5. Images of an autoradiography of [¹⁸F]MHMZ binding at 14 μ m thick rat brain sections; (A and B) total binding at a concentration of 5 nM with (A) lateral 0.9 mm and (B) lateral 2.4 mm from bregma. Major binding was detected in lamina V (V) of the frontal cortex, in the caudate-putamen (CPu), and three regions of the brain stem, the motor trigeminal nucleus (MoT), facial nucleus (fn), and the pontine nuclei (pn). Non-specific binding was determined in the presence of 10 μ M ketanserin which led to total inhibition of [¹⁸F]MHMZ binding (cf. C0 Fig. 6). Specific activity was 1.38 MBq/nmol (at the end of the incubation period).

Minor binding was detected in the olfactory system, the mesencephalon, and the hippocampus. Competition autoradiography assays (data not shown) with 5 nM [¹⁸F]MHMZ and 10 μ M of fallypride, WAY 100635, and prazosin showed that [¹⁸F]MHMZ is highly specific for 5-HT_{2A} receptors. Displacement could only be detected with fallypride. Here, co-incubation led to a displacement of 30% (n = 4, \pm 6% SEM) of total binding in the frontal

cortex as well as in the caudate-putamen, which does not imply that [^{18}F]MHMZ recognizes D_2/D_3 receptors but might rather be explained by the known cross affinity of fallypride to 5-HT $_2$ receptors.¹⁴

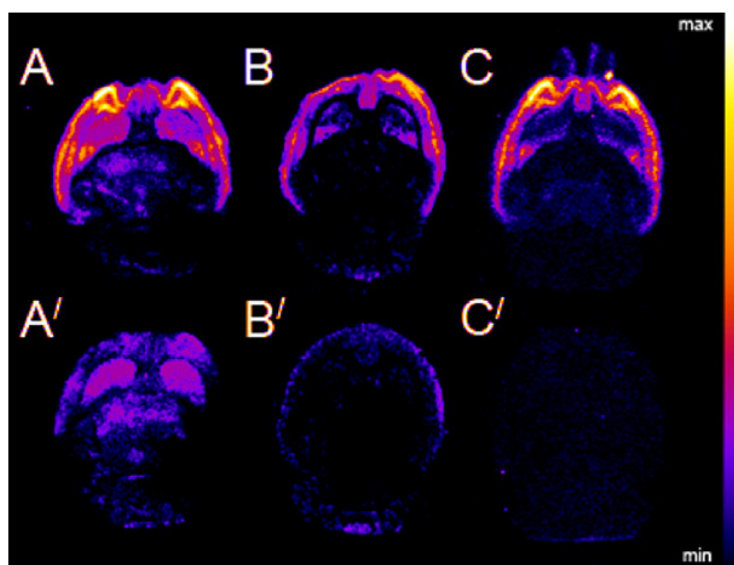


Figure 6. Autoradiographic images of the total binding and non-specific binding, respectively, of (A/A') [^{18}F]altanserin, (B/B') [^3H]MDL 100907 and (C/C') 5 nM [^{18}F]MHMZ at 14 μm rat brain sections. Non-specific binding was determined in the presence of 10 μM ketanserin. Specific activity of [^{18}F]MHMZ and [^{18}F]altanserin was 160 kBq/nmol (at the end of the incubation period). Washing was done 2 \cdot 10 min for (A/A') in ice-cold reaction buffer, 2 \cdot 2 min at room temperature with (B/B') and 3 \cdot 2 min at room temperature (4 min with buffer containing 0.01% Triton X-100). Reaction buffer was 50 mM Tris buffer, pH 7.4, containing 120 mM NaCl and 5 mM KCl.

Binding parameters of [^{18}F]MHMZ of different regions of the rat brain obtained with autoradiography assays at sagittal sections are displayed in Table 2. Binding in the cerebellum was at the level of non-specific binding so levels of binding in different brain regions are also given relative to that.

A comparison of the binding of [^{18}F]altanserin and [^{18}F]MHMZ (Fig. 6) displays that [^{18}F]MHMZ is in no way inferior to [^{18}F]altanserin in terms of specificity for 5-HT $_{2A}$ receptors. Figure 6 also shows the complete agreement of the binding of [^3H]MDL 100907 and [^{18}F]MHMZ.¹⁵

Table 2: Binding parameters obtained with [^{18}F]MHMZ from binding experiments at 14 μm sagittal sections of the rat brain ($x = \text{means} \pm \text{SEM}$)

	n	pmol/mm ³	Region/cerebellum
Frontal cortex			
Laminae I-IV	4	23.30 \pm 1.69	26.9 \pm 0.9
Lamina V	4	61.60 \pm 5.24	59.5 \pm 2.8
Laminae Via + VIb	4	27.27 \pm 2.76	31.4 \pm 1.3
Caudate-putamen	4	16.80 \pm 2.33	19.2 \pm 1.4

The metabolite analyses of rat plasma (Fig. 7) showed that [^{18}F]MHMZ underwent fast metabolism. Plasma samples were taken at 5, 10, 30, and 60 min and analyzed by radio-TLC. One polar metabolite was found in rat plasma which is not likely to cross the blood–brain-barrier because of its hydrophilicity. The percentage of unmetabolized fractions was 43%, 32%, 16%, and 7% at 5, 10, 30, and 60 min, respectively.

In conclusion, precursors and reference compounds of [^{18}F]MHMZ were synthesized in high yields. The new ^{18}F -labeled compound could be obtained as an injectable solution in overall radiochemical yields of about 42% within a synthesis time of about 100 min in a purity of >96% and high specific activities. This is very similar to the radiosynthesis of [^{18}F]altanserin, which takes 75–100 min and results in a radiochemical yield between 30% and 50%.⁴

First autoradiographic studies showed excellent *in vitro* binding with high specificity of [^{18}F]MHMZ for 5-HT $_{2A}$ receptors and very low non-specific binding. [^{18}F]MHMZ undergoes fast metabolism resulting in one very polar active metabolite. Except from the slightly

decreased affinity the reported *in vitro* data seem to be comparable with those of [^3H]MDL 100907. Our data suggest that the aim of developing a novel ^{18}F -analogue of MDL 100907 (1) combining the better selectivity of MDL 100907 as compared to altanserin and the superior isotopic properties for the clinical routine of [^{18}F]fluorine as compared to [^{11}C]carbon could be achieved.

All together, new auspicious results concerning the synthesis and of the *in vitro* studies of [^{18}F]MHMZ justify further experiments like *ex vivo* brain regional distribution and *in vivo* small animal PET studies to verify the potential of this new 5-HT $_2\text{A}$ imaging ligand.

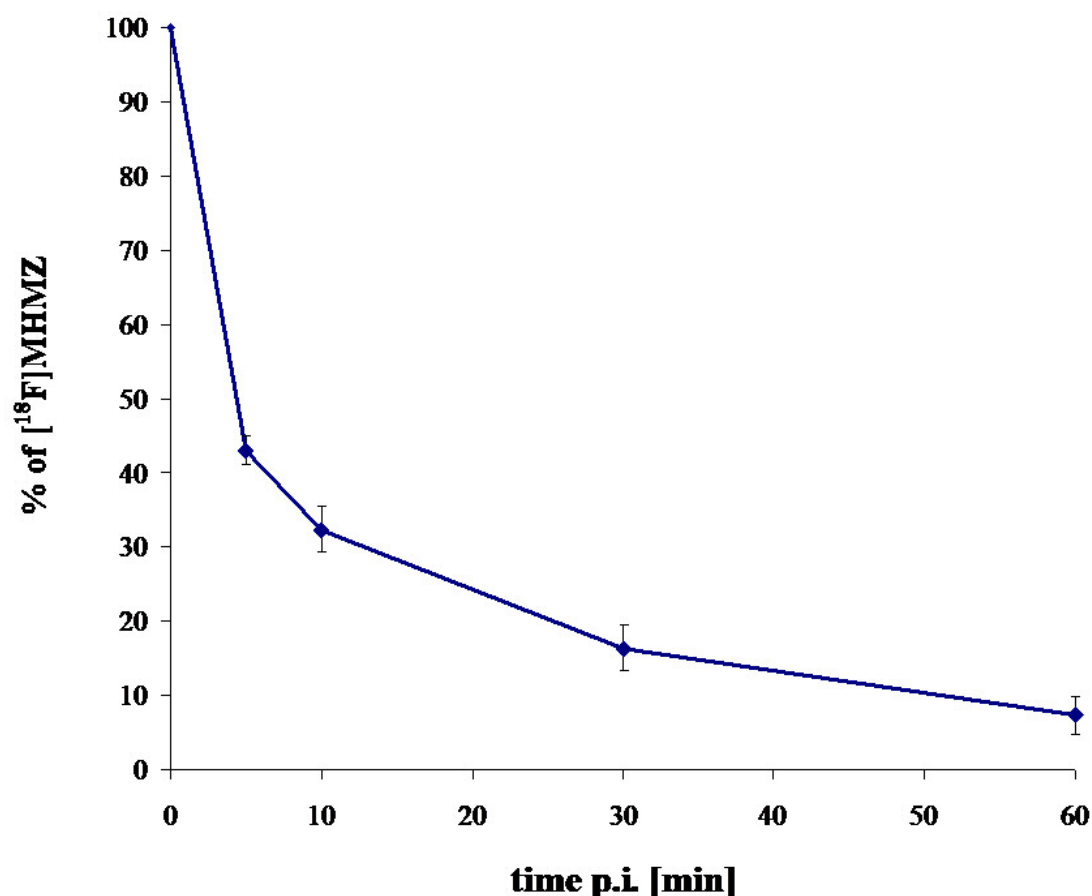


Figure 7. (A) Plasma clearances of [^{18}F]MHMZ at 5, 10, 30, and 60 min ($n = 3$ per time point; means \pm SD shown). (B) Radioactivity in TLC plate of plasma samples at 5 min p.i. is shown. Spots for [^{18}F]MHMZ (T) ($R_f = 0.76$) and its metabolite (M) ($R_f = 0.16$) were clearly visible.

Acknowledgments

The authors thank S. Höhnemann and P. Riss for the syntheses of [^{18}F]FETos. We also like to thank the VCI (Verband der chemischen Industrie e.V.) for the donation of solvents. Financial support by Friedrich–Naumann–Stiftung, the European Network of Excellence (EMIL), and the Deutsche Forschungsgemeinschaft (DFG) is gratefully acknowledged.

References and notes

1. Kristiansen, H.; Elfing, B.; Plenge, P.; Pinborg, L. H.; Gillings, N.; Knudsen, G. M. *Synapse* 2005, 58, 249.
2. Lemaire, C.; Cantineau, R.; Guillaume, M.; Plenevaux, A.; Christiaens, L. J. *Nucl. Med.* 1991, 32, 2266.
3. Huang, Y.; Mahmood, K.; Mathis, C. A. *J. Labelled Compd. Radiopharm.* 1999, 42, 949.
4. Hamacher, K.; Coenen, H. H. *Appl. Radiat. Isot.* 2006, 64, 989.
5. Alexoff, D. L.; Shea, C.; Fowler, J. S.; King, P.; Gatley, S. J.; Schleyer, D. J.; Wolf, A. *P. Nucl. Med. Biol.* 1995, 22, 892.
6. Heinrich, T.; Boetcher, H.; Pruecher, H.; Gottschlich, R.; Ackermann, K.-A.; van Amsterdam, C. *Chem. Med. Chem.* 2006, 1, 245.
7. Tan, P.-Z.; Baldwin, R. M.; Fu, T.; Charney, D. S.; Inis, R. B. *J. Labelled Compd. Radiopharm.* 1998, 42, 457.
8. Meltzer, C. C.; Smith, G.; DeKosky, S. T.; Pollock, B. G.; Mathis, A. M.; Moore, R. Y.; Kupfer, D. J.; Reynolds, C. F. *Neuropsychopharmacology* 1997, 18, 407.
9. Scot, D.; Heath, T. G. *J. Pharm. Biomed. Anal.* 1998, 17, 17.
10. Ullrich, T.; Ice, K. C. *Bioorg. Med. Chem.* 2000, 8, 2427.
11. Lundkvist, C.; Halldin, C.; Ginovart, N.; Swahn, C.-G.; Carr, A. A.; Brunner, F.; Farde, L. *Life Sci.* 1996, 58, 187.
12. Bauman, A.; Piel, M.; Schirmacher, R.; Rösch, F. *Tetrahedron Lett.* 2003, 44, 9165.
13. Lopez-Gimenez, J. F.; Mengod, D.; Palacios, J. M.; Vilario, M. T. *Naunyn-Schmiedeberg's Arch. Pharmacol.* 1997, 356, 446.
14. Stark, D.; Piel, M.; Hübner, H.; Gmeiner, P.; Gründer, G.; Rösch, F. *Biorg. Med. Chem.* 2007, 15, 6819.

-
15. Autoradiography experiments were carried out at room temperature in reaction buffer (50 mM Tris/HCl buffer, pH 7.4, containing 120 mM NaCl, and 5 mM KCl) with [³H]MDL 100907 and [¹⁸F]MHMZ and on ice with [¹⁸F]altanserin. Sections with [¹⁸F]MHMZ were washed 2 · 2 min in reaction buffer containing 0,01% Triton X-100 and 1*2 min in reaction buffer, shortly dipped into deionized water, and quickly dried in a stream of cold air. Sections with [¹⁸F]altanserin were washed in pure ice-cold reaction buffer 2*10 min, sections with [³H]MDL 100907 were washed in pure buffer 2*2 min. Sections were exposed to Fuji phosphor screen for 3 h when ¹⁸F was used and for 5 days when ³H was used. Screens were read out with a Fuji FLA-7000 scanner. For ¹⁸F quantification was done after calibration by a standard curve which was obtained by a dilution series of the radiotracer. Calibration was repeated for each fresh radiotracer synthesis. Calibration for sections with ³H was done with Amersham microscale standards. Calibration, quantification and data evaluation was done with Multi Gauge, Fujifilm image analysis software.

3.2 Synthesis, radiofluorination and first evaluation of [¹⁸F]MDL 100907 as a serotonin 5-HT_{2A} receptor antagonist for PET

by Ute Mühlhausen*^a, Johannes Ermert,^a Matthias M. Herth,^b Heinz H. Coenen^a

^aInstitute of Neurosciences and Biophysics (INB-4): Nuclear Chemistry, Research Center Jülich GmbH, D-52425 Jülich, Germany

^bInstitute of Nuclear Chemistry, University of Mainz, Fritz-Strassmann-Weg 2, D-55128 Mainz, Germany

Abstract

In some psychiatric disorders 5-HT_{2A} receptors play an important role. In order to investigate those *in vivo* there is an increasing interest in obtaining a metabolically stable, subtype selective and high affinity radioligand for receptor binding studies using PET. Combining the excellent *in vivo* properties of [¹¹C]MDL 100907 for PET imaging of 5-HT_{2A} receptors and the more suitable half-life of fluorine-18, MDL 100907 was radiofluorinated in 4 steps using 1-(2-bromoethyl)-4-[¹⁸F]fluorobenzene as a secondary labelling precursor. The complex reaction required an overall reaction time of 140 min and (±)-[¹⁸F]MDL 100907 was obtained with a specific activity of at least 30 GBq/μmol (EOS) and an overall radiochemical yield of 1 to 2 %. In order to verify its binding to 5-HT_{2A} receptors, *in vitro* rat brain autoradiography was conducted showing the typical distribution of 5-HT_{2A} receptors and a very low nonspecific binding of about 6 % in frontal cortex, using ketanserin or spiperone for blocking. Thus [¹⁸F]MDL 100907 appears to be a promising new 5-HT_{2A} PET ligand.

Introduction

Serotonergic 5-HT_{2A} receptors are of central interest in the complex pathophysiology of human cerebral disorders such as anxiety, depression, Alzheimer's disease and schizophrenia.^{1, 2, 3} In order to investigate the role of these receptors there is an increasing interest in obtaining a selective and high affinity radiolabelled ligand for direct *in vivo*

receptor binding studies using positron emission tomography (PET). For this purpose several radiotracers have been developed, of which [^{11}C]MDL 100907 and [^{18}F]altanserin proved to be most useful.

Both MDL 100907 and altanserin bind to the 5-HT_{2A} receptor with high affinity. While for MDL 100907 a K_i value of 0.2 nM⁴ and a K_D value of 0.56 nM (using [^3H]MDL 100907)⁵ were reported, for altanserin a K_i of 0.13 nM⁶ and a K_D of 0.3 nM⁷ were determined. Binding to other 5-HT receptor subtypes is very low for MDL 100907,⁵ and for altanserin moderate to low.⁷ A further difference between these two tracers is the binding to receptors outside the serotonergic system. Altanserin shows a relatively high affinity for D₂ (62 nM) and especially for adrenergic- α_1 receptors (4.55 nM),^{6,8} whereas the affinity of MDL 100907 to these receptors is insignificant.¹²

Another disadvantage of altanserin is the formation of at least four different metabolites in humans which lower the bioavailability and may cross the blood-brain-barrier.⁸ On the other hand, pharmacokinetic studies with MDL 100907 in rats and dogs indicate that the drug undergoes extensive first-pass metabolism which significantly reduces its bioavailability. The major metabolite of MDL 100907 in animals has been found to be 3'-O-demethylated MDL 100907 (MDL 105725), which also exhibits a high binding affinity to 5-HT_{2A} receptors (K_i = 0.45 – 2.2 nM).⁹ However, it was shown that the blood brain barrier (BBB) permeability of MDL 100907 is more than four times that of the metabolite MDL 105725, and that MDL 100907 does not undergo significant metabolism to MDL 105725 in the brain.⁹ Furthermore, ^{11}C -labelled MDL 100907, with the radiolabel at either the 2' or the 3' position, has been prepared and evaluated. Rat and baboon studies have been carried out with the 2' labelled compound while the 3' labelled compound has been evaluated in monkey and humans. Data from both animal and human studies indicated that [^{11}C]MDL 100907 labelled either at the 2' or 3' position is a useful radioligand for the *in vivo* studies using PET.^{4, 10, 11} If 3'-O-demethylation would play a major role, than differences should have occurred with the 2'-O-radiomethylated analogue.

Nevertheless, a major draw-back of [^{11}C]MDL 100907 is the short half-life of carbon-11 (20 min). This not only necessitates the availability of a cyclotron close to the PET scanner but also causes concern to reach a state of reversible binding during the PET scan.^{7, 10} These

problems can be avoided by the use of fluorine-18 with its half-life of 109.7 min. In summary [^{11}C]MDL 100907 is a very specific high affinity ligand for 5-HT_{2A} receptors, only hampered by the short half-life of C-11, while the binding of [^{18}F]altanserin lacks specificity.

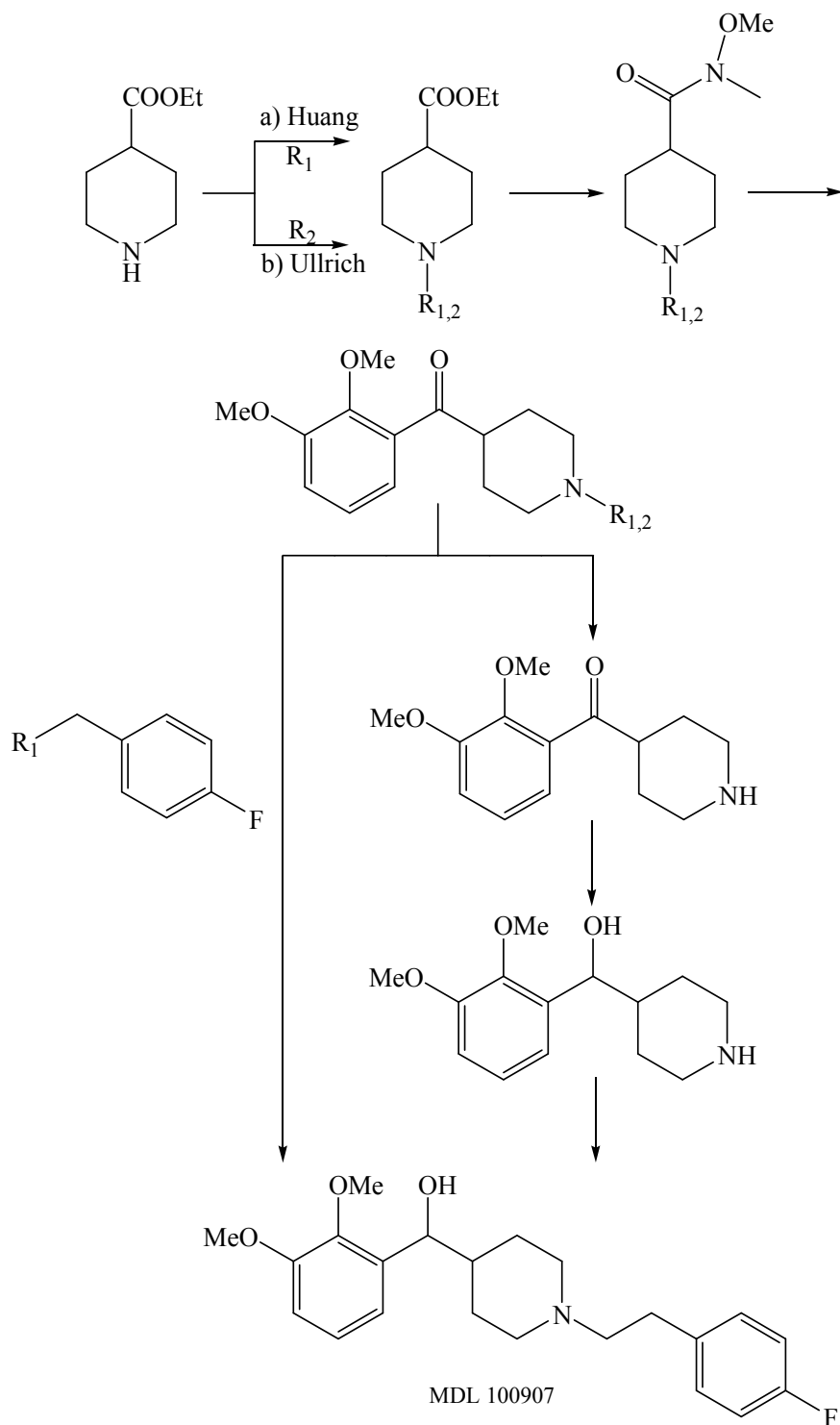
For combining the superior pharmacological and pharmacokinetic properties of MDL 100907 for PET imaging of 5-HT_{2A} receptors and the more suitable half-life of fluorine-18, the isotopically labelled compound (\pm)-[^{18}F]MDL 100907 was prepared by a 4 step radiosynthesis. From the known metabolism of MDL 100907 it might be expected that the 3'-O-demethylated metabolite [^{18}F]MDL 105725 will be formed *in vivo*. The 2'-labelled [^{11}C]MDL 100907 proved to be useful in rat and baboon even though [^{11}C]MDL 105725 probably occurs *in vivo*.¹¹ Therefore it appears worthwhile to find out if the metabolism of ^{18}F -labelled MDL 100907 will interfere in PET measurements of 5-HT_{2A} receptors in the brain. *In vitro* rat brain autoradiography was performed in order to confirm the binding of n.c.a. (\pm)-[^{18}F]MDL 100907 in analogy to the cerebral pattern of 5-HT_{2A} receptors. In this study, aiming at establishing a radiosynthesis of ^{18}F -labelled MDL 100907, only the racemic compound (\pm)-[^{18}F]MDL 100907 was prepared but of course the identical labelling procedure can also be performed with the optically resolved precursor to yield (+)-[^{18}F]MDL 100907.

Results and Discussion

Chemistry

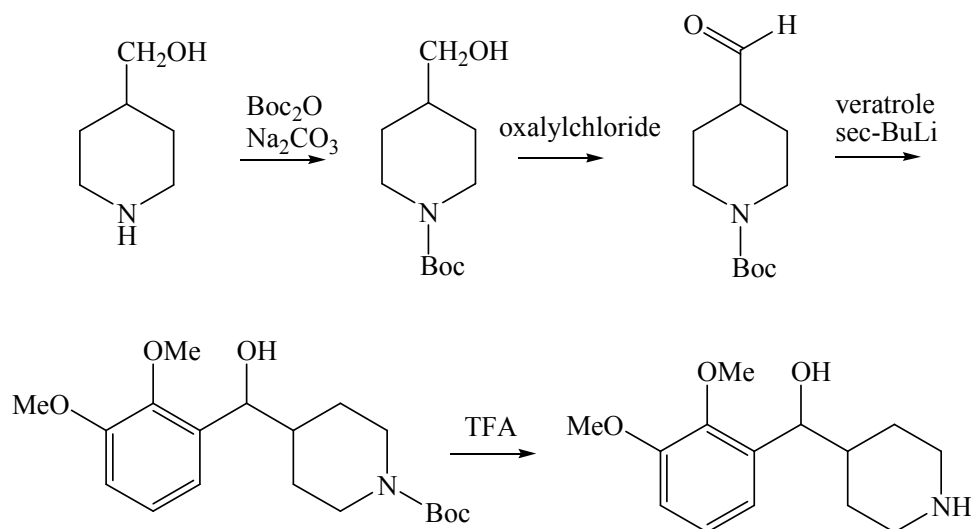
For the organic synthesis of MDL 100907 principally two different procedures are described in the literature^{13, 14, 15} (cf. Scheme 1). In the method by Huang et al.¹⁴ ethyl 1-(4-fluorophenethyl)piperidine-4-carboxylate (**1**) is initially synthesized by coupling of 2-(4-fluorophenyl)ethyl bromide to ethyl isonipecotate. Then **1** is subsequently coupled to 1,2-dimethoxybenzene and reduced to MDL 100907.^{13, 14} The method by Ullrich et al.¹⁵ changes the reaction sequence using 1-tert butyl 4-ethyl piperidine-1,4-dicarboxylate (**2**) for coupling to 1,2-dimethoxybenzene (veratrole). After reduction and deprotection of the resulting piperidine derivative, reaction with 2-(4-fluorophenyl)ethyl bromide was conducted yielding MDL 100907 (**9**). Even though the 6 step route of Ullrich et al.¹⁵ includes one more reaction step, it is better suited with respect to enantiomeric purity of MDL 100907. The intermediate

(±)-(2,3-dimethoxyphenyl)-(piperidin-4-yl)methanol (**8**) can optically be resolved¹⁵ and allows the introduction of a variety of N-substituents. Compound **8** was used as the labelling precursor in the work presented here. Both methods use an activated Weinreb amide (**3**, **4**) for coupling of the piperidine moiety to 1,2-dimethoxybenzene.



Scheme 1. Synthesis of MDL 100907 by Huang et al.¹⁴ (a) and Ullrich et al.¹⁵ (b)

In order to improve and shorten the method by Ullrich et al.¹⁵ a 5 step synthesis was developed where instead of the activated Weinreb amide **4** the aldehyde *tert*-butyl 4-formylpiperidine-1-carboxylate (**11**) was employed (cf. Scheme 2).



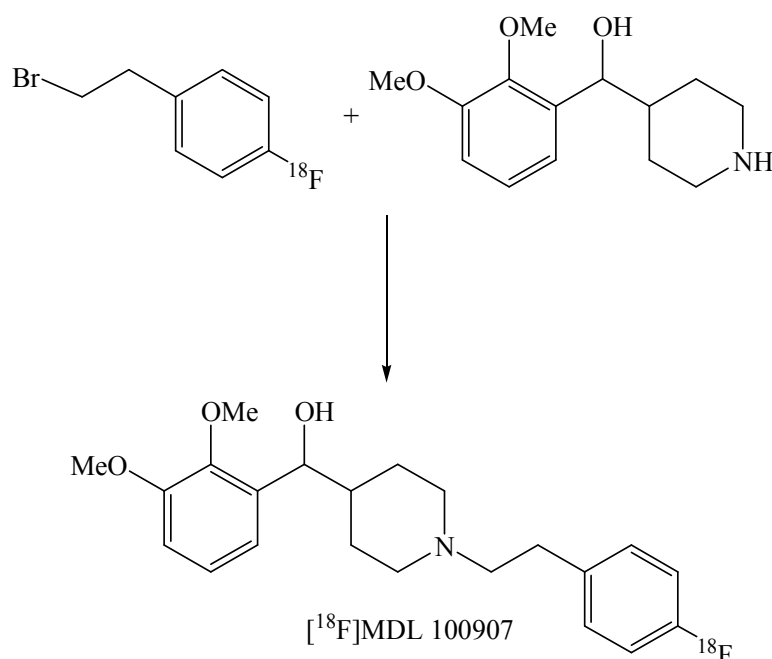
Scheme 2. Improved synthesis of (2,3-dimethoxyphenyl)(piperidine-4-yl)methanol (**8**)

For this purpose commercially available piperidin-4-yl-methanol was protected using di-*tert*-butyl dicarbonate. The resulting alcohol **10** was oxidized with oxalylchloride and DMSO in a Swern oxidation to get **11**. Subsequent reaction with 1,2-dimethoxybenzene, which was activated with *sec*-BuLi first, yielded *tert*-butyl 4-((2,3-dimethoxyphenyl)(hydroxy)methyl)piperidine-1-carboxylate (**12**). In contrast to the method by Ullrich et al. no reduction of the coupling product is necessary which saves one reaction step. Deprotection of **12** with TFA yields (\pm)-(2,3- dimethoxyphenyl)-(piperidin-4-yl)methanol (**8**) which can be alkylated with various phenylethyl bromides like 2-(4-fluorophenyl)ethyl bromide. In order to get (\pm)-MDL 100907 (**9**) **8** was deprotonated using NaHCO₃ and reacted with 2-(4-fluorophenyl)ethyl bromide as described by Ullrich et al.. Using this procedure the reaction route to **8** was abbreviated by one step and the average overall yield was optimized (54 % vs. 43 %¹⁵ or 48 % (own work)).

Radiochemistry

So far the synthesis of a suitable labelling precursor for the radiofluorination to no-carrier-added (n.c.a.) [¹⁸F]MDL 100907 ([¹⁸F]**9**) by direct nucleophilic substitution was not

successful. Therefore a more complex labelling procedure was chosen here. Using 1-(2-bromoethyl)-4- ^{18}F fluorobenzene (^{18}F **13**) as a secondary labelling precursor, the piperidine derivative (\pm)-(2,3-dimethoxyphenyl)(piperidine-4-yl)methanol (**8**) was alkylated yielding n.c.a. (\pm)- ^{18}F MDL 100907 (^{18}F **9**) (cf. Scheme 3).



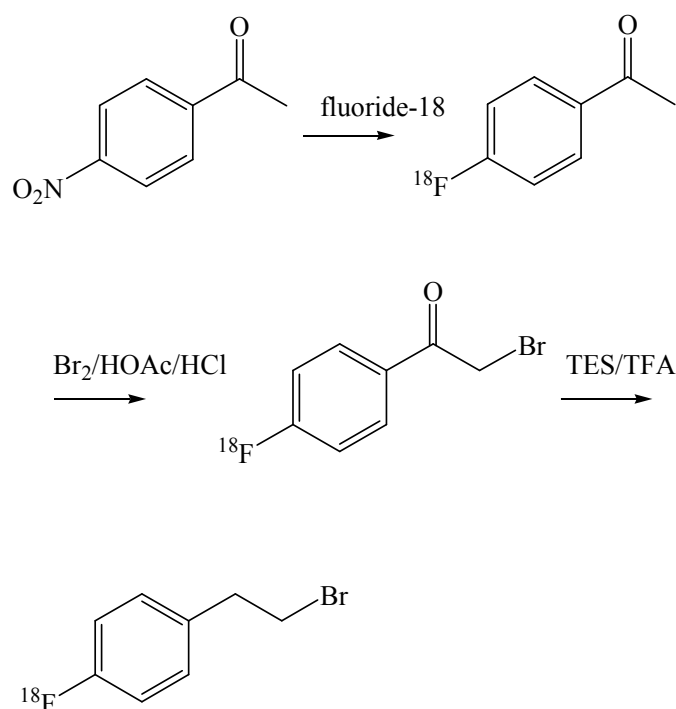
Scheme 3. Radiosynthesis of (\pm)- ^{18}F MDL 100907 (^{18}F **9**)

1-(2-Bromoethyl)-4- ^{18}F fluorobenzene (^{18}F **13**)

The preparation of 1-(2-bromoethyl)-4- ^{18}F fluorobenzene (^{18}F **13**) is described as a high yield three-step synthesis by Hwang et al.¹⁷ For the preparation of 2-bromo-4'- ^{18}F fluoroacetophenone (^{18}F **15**) basically two different methods are described in the literature.^{16, 17} Both of them use 4-nitroacetophenone as labelling precursor. The difference lies in the bromination reaction of 4- ^{18}F fluoroacetophenone (^{18}F **14**). While Hwang et al.¹⁷ use an acidic bromine solution, Dence et al.¹⁶ conduct this reaction step with polymer-bound perbromide. However, both reaction procedures could not be reproduced as described. This was also observed in a study by de Vries and coworkers¹⁸ who used the method by Dence et al.¹⁶ for the synthesis of 2-bromo-4'- ^{18}F fluoroacetophenone (^{18}F **15**). The labelling reaction was reproducible but despite considerable effort the bromination step failed or gave poor yields. Therefore they could only produce an overall radiochemical yield (RCY) for ^{18}F **15** of 3.9 ± 2.7 % instead of 65 %.¹⁶

After failure of the bromination reaction using the method by Dence et al.¹⁶ the principal reaction sequence of Hwang et al.¹⁷ was adopted here with some modifications of the procedure (cf. Scheme 4).

As a first step commercially available 4-nitroacetophenone was labelled with n.c.a. [¹⁸F]fluoride using Kryptofix® 222 and potassium carbonate. The labelling was conducted in DMF as solvent with conventional heating at 130 °C. 4-[¹⁸F]Fluoroacetophenone ([¹⁸F]14) was obtained with a RCY of 60 – 70 %. To remove the solvent and unreacted [¹⁸F]fluoride, solid phase extraction (SPE) was used followed by passing through a drying cartridge to remove water. Removal of water was essential for the next reaction step in order to achieve radical bromination in the side chain and to avoid side reactions.



Scheme 4. Radiosynthesis of 1-(2-bromoethyl)-4-[¹⁸F]fluorobenzene ([¹⁸F]13)

After removal of the solvent, bromination was carried out in chloroform/ethyl acetate, adding an acidic bromine solution (hydrochloric and acetic acid) at a temperature of 100 °C. Analysis

of the reaction mixture using reverse-phase HPLC showed two radioactive products. As described in the literature the desired 2-bromo-4'-[¹⁸F]fluoroacetophenone (**[¹⁸F]15**) as well as the dibrominated 2,2-dibromo-4'-[¹⁸F]fluoroacetophenone were formed.¹⁷ The RCY of **[¹⁸F]15** was 62 – 76 %, that of the side-product 23 – 37 %. An earlier report on a low fraction of < 5 % of dibrominated side-product using the same reaction conditions^{17, 19} could not be reproduced here. For the next reaction step the solvent as well as the remaining acids and traces of water had to be removed. This was accomplished by using an Alumina N cartridge followed by a drying cartridge. Relative to **[¹⁸F]14** the RCY of **[¹⁸F]15** after work up was 39 – 48 %.

For reduction of **[¹⁸F]15** to 1-(2-bromoethyl)-4-[¹⁸F]fluorobenzene (**[¹⁸F]13**), triethylsilane and TFA were used. The reaction temperature was varied between 90 °C and 100 °C. It was observed that the RCY at lower temperatures was higher and that formation of a side-product, which supposedly is 2-bromo-1-(4'-fluorophenyl)ethanol, was less. Very problematic with this reaction step was a loss of radioactivity, probably due to defluorination via formation of volatile triethylfluorosilane. HPLC analysis of the reaction mixture showed a RCY for 1-(2-bromoethyl)-4-[¹⁸F]fluorobenzene (**[¹⁸F]13**) between 52 and 86 %, depending on reaction temperature, while the side-product was formed in a RCY of 10 - 37 %. Furthermore, no **[¹⁸F]15** could be detected anymore. For further reaction **[¹⁸F]13** had to be isolated by semipreparative HPLC. In order to remove water, which is critical to achieve coupling of **[¹⁸F]13** to (±)-(2,3-dimethoxyphenyl)(piperidine-4-yl)methanol (**8**) (cf. Scheme 3), elution of purified **[¹⁸F]13** after solid phase extraction was conducted over a drying cartridge. **[¹⁸F]13** was isolated with a RCY of 13 – 26 % relative to **[¹⁸F]15**. The overall RCY of **[¹⁸F]13** relative to [¹⁸F]fluoride was 2.5 – 7 % with a radiochemical purity of > 99 % in a preparation time of 110 min.

(±)-[¹⁸F]MDL 100907 (**[¹⁸F]9**)

In order to get (±)-[¹⁸F]MDL 100907 (**[¹⁸F]9**), the piperidine derivative **8** was deprotonated using caesium carbonate and reacted with **[¹⁸F]13** (Scheme 3). In contrast to observations by Hwang et al.,¹⁷ who tried to couple **[¹⁸F]13** to piperidine under various conditions, the formation of the elimination product of **[¹⁸F]13**, 4-[¹⁸F]fluorostyrol, was moderate (< 15 %) under the conditions applied here. (±)-[¹⁸F]MDL 100907 (**[¹⁸F]9**) was isolated by

semipreparative HPLC with a RCY of 40 – 50 %, relative to [^{18}F]**13**. The radiochemical purity was > 99 % and the specific activity was at least 30 GBq/ μmol (end of synthesis). The preparation time of (\pm)-[^{18}F]MDL 100907 ([^{18}F]**9**) was 140 min and the overall RCY 1 – 2 % relative to [^{18}F]fluoride. There is still room for optimization of the reaction procedure concerning RCY as well as handling. This will become even more attractive if ongoing work on a preferred direct labelling approach is not successful.

***In vitro* Autoradiography**

For verifying the cerebral distribution of (\pm)-[^{18}F]MDL 100907 ([^{18}F]**9**) according to the location of 5-HT 2A receptors, *in vitro* autoradiography with cryosections of rat brain was conducted. High binding of (\pm)-[^{18}F]MDL 100907 ([^{18}F]**9**) was observed in the cortex with different intensities in various regions (cf. Figure 1a). Especially in the frontal part 5-HT $_{2A}$ receptors have been reported to be localized in the rat brain.²⁰ Moderately high binding was observed in striatum and low but still specific binding was measured in thalamus and cerebellum. This binding pattern is in good accordance with the distribution of 5-HT $_{2A}$ receptors in rat brain^{20, 21} and reflects the binding of [^3H]MDL 100907 previously described.²⁰ For blocking of (\pm)-[^{18}F]MDL 100907 ([^{18}F]**9**) binding ketanserin (10 μM) as well as spiperone (10 μM) were used (cf. Figure 1 b, c). With both an excellent displacement of (\pm)-[^{18}F]MDL 100907 ([^{18}F]**9**) was achieved, resulting in a non-specific binding of only about 6 % in frontal cortex with both blockers. In relation to the total binding (as average of the brain regions investigated) non-specific binding was only about 15 % with ketanserin and 10 % with spiperone. This reflects the reported pharmacological characteristics of [^3H]MDL 100907²⁰ as expected, due to authentic labelling of the compound with fluorine-18.

Experimental

General

The chemicals were analytical grade or better and were used without further purification (Sigma-Aldrich, Steinheim, Germany). Alumina N and Oasis HLB 1cc cartridges were purchased from Waters (Eschborn, Germany), LiChrolut RP-18e cartridges from Merck (Darmstadt, Germany). Analytical TLC was performed on aluminium-backed sheets (Silica gel 60 F254) and normal-phase column chromatography was performed using Silica gel 60, both from Merck (Darmstadt, Germany).

NMR spectra (1H-200 MHz) were obtained on a DPX Avance 200 spectrometer (Bruker, Rheinstetten, Germany). Chemical shifts are reported in parts per million, solvent peaks were referenced appropriately.

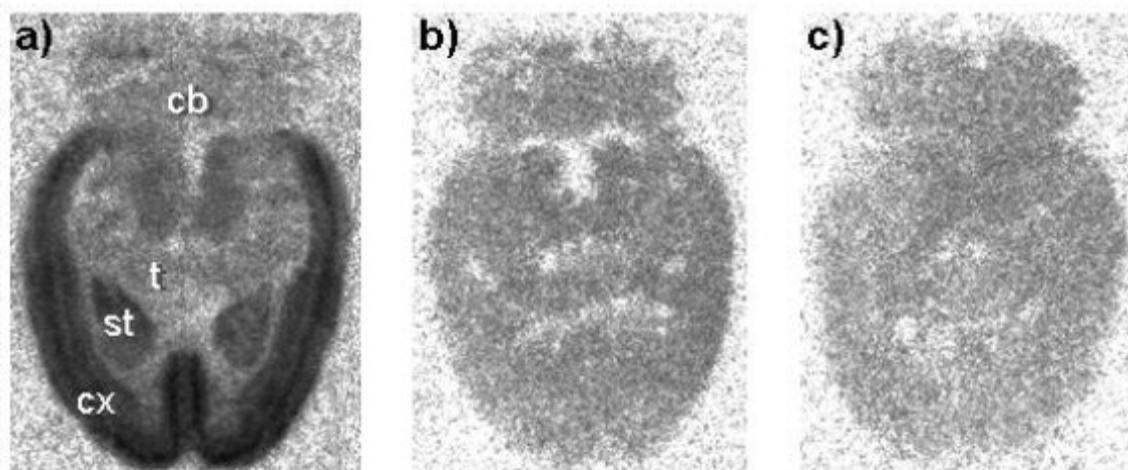


Figure 1. Autoradiography of [^{18}F]MDL 100907 ([^{18}F]9) distribution in horizontal rat brain sections; a) total binding, b) non-specific binding in the presence of ketanserin (10 μM), c) non-specific binding in the presence of spiperone (10 μM); cb: cerebellum, cx: cortex, st: striatum, t: thalamus

NMR spectra (1H-200 MHz) were obtained on a DPX Avance 200 spectrometer (Bruker, Rheinstetten, Germany). Chemical shifts are reported in parts per million, solvent peaks were referenced appropriately.

High performance liquid chromatography (HPLC) was performed on the following system from Dionex (Idstein, Germany): an Ultimate 3000 LPG-3400A HPLC pump, an Ultimate 3000 VWD-3100 UV/VIS-detector (272 nm), a UCI-50 chromatography interface, an injection valve P/N 8215. Radioactivity was detected with a Gabi Star NaI(Tl) radioactivity-detector from Raytest (Straubenhardt, Germany) and analysis of HPLC data accomplished with Chromeleon 6.80 software.

Reversed-phase HPLC was carried out using a Gemini 5 μ C18 110A column, for analytical separations with a dimension of 250 mm x 4.6 mm (flow 1 mL/min) and for semi-preparative applications 250 mm x 10 mm (flow 5 mL/min) from Phenomenex (Aschaffenburg, Germany). Analysis or isolation of [^{18}F]13, [^{18}F]14, and [^{18}F]15 was done by isocratic elution with acetonitrile and water 65:35 (v/v). For [^{18}F]MDL 100907 ([^{18}F]9) isocratic elution with

acetonitrile, water and TEA 50:50:0.1 (v/v/v) at a pH of 9.0 (phosphoric acid) was applied. For purpose of identification of all radioactive products the respective non-radioactive standard compounds were co-injected and co-eluted with the radioactive products.

Phosphor imager plates were scanned with a laser phosphor imager BAS 5000 (Fuji, Düsseldorf, Germany) utilizing software from the vendor (Version 3.14, Raytest, Straubenhardt, Germany). The resolution of a phosphor imager scan is 25 μm .

Radiochemical reactions were conducted in 5 mL conical vials (Reactival) from Wheaton Scientific (Millville, IL, USA) which were closed with a silicon septum.

Chemistry

tert-Butyl 4-(hydroxymethyl)piperidine-1-carboxylate (**10**)

Piperidin-4-yl-methanol (5.02 g, 43.4 mmol) and sodium carbonate (4.59 g, 43.2 mmol) were suspended in a mixture of water (29 mL) and THF (11 mL). di-*tert*-Butyl dicarbonate (10.45 g, 51.6 mmol) was added and the resulting mixture stirred at 95 °C for 2.5 h. After cooling to room temperature, water (100 mL) was added and the product extracted with ethyl acetate (3 x 50 mL). The combined organic phases were washed with brine (2 x 70 mL) and after drying over sodium sulfate the solvent was evaporated under reduced pressure. This yielded the pure product **10** (9.34 g, 43.4 mmol) in 100 %. ¹H NMR (DMSO-d₆): 3.98 (m, 2H, H_{2,6}), 3.34 (s, 2H, CH₂), 2.62 (m, 2H, H_{2,6}), 1.52 (m, 3H, H_{3,4,5}), 1.45 (s, 9H, Boc), 1.06 (m, 2H, H_{3,5}).

tert-Butyl 4-formylpiperidine-1-carboxylate (**11**)

Under an atmosphere of argon a solution of oxalylchloride (2 mL, 22.0 mmol) in absolute dichloromethane (50 mL) was cooled to – 50 °C. Absolute dimethylsulfoxide (3.5 mL, 44.0 mmol) in absolute dichloromethane (10 mL) was added dropwise. Then **10** (4.30 g, 20.0 mmol) was added. After stirring for 20 min at – 50 °C triethylamine (14 mL) was added and the suspension allowed to warm up to room temperature. The reaction was stopped by the addition of water (100 mL) after 2.5 h and the mixture extracted with dichloromethane (4 x 50 mL). The combined organic phases were washed with water (3 x 70 mL) and dried over sodium sulfate. The solvent was evaporated under reduced pressure to give **11** (4.27 g, 20.0 mmol) in 100 % yield. ¹H NMR (DMSO-d₆): 9.60 (s, 1H, CHO), 3.84 (m, 2H, H_{2,6}), 2.96 (m, 2H, H_{2,6}), 2.51 (m, 1H, H₄), 1.85 (m, 2H, H_{3,5}), 1.44 (s, 9H, Boc), 1.42 (m, 2H, H_{3,5}).

tert-Butyl 4-((2,3-dimethoxyphenyl)(hydroxy)methyl)piperidine-1-carboxylate (12)

Under an atmosphere of argon, 1,2-dimethoxybenzene (1.30 mL, 10.0 mmol) dissolved in absolute THF (25 mL) was cooled to $-50\text{ }^{\circ}\text{C}$ and *sec*-butyl lithium (1.3 M in *n*-hexane, 10 mL, 13.0 mmol) was added dropwise. The mixture was stirred at room temperature for 75 min before cooling again to $-50\text{ }^{\circ}\text{C}$. Then compound **11** (2.0 g, 9.4 mmol) dissolved in absolute THF (10 mL) was added and the mixture stirred at room temperature for 3 h. The reaction was quenched with water (50 mL) and extracted with diethyl ether (3 x 50 mL). The combined organic phases were washed with brine (2 x 70 mL), dried over sodium sulfate and the solvent was evaporated under reduced pressure. Purification by column chromatography (*n*-hexan:ethyl acetate, 2:1) gave **12** (2.0 g, 5.7 mmol) in 61 % yield. ^1H NMR (DMSO- d_6): 6.98 (m, 3H, ArH), 5.04 (d, 1H, OH), 4.63 (t, 1H, CHOH), 3.92 (s, 3H, OMe), 3.85 (s, 3H, OMe), 2.64 (m, 2H, P2,6), 1.75 (m, 2H, P2,4,6), 1.39 (s, 9H, Boc), 1.26 (m, 4H, P3,5).

(±)-(2,3-Dimethoxyphenyl)-(piperidin-4-yl)methanol (8)

At $0\text{ }^{\circ}\text{C}$ **12** (1.25 g, 3.65 mmol) was carefully dissolved in trifluoroacetic acid (12.5 mL, 161 mmol). The resulting solution was stirred at room temperature for 3 h. After addition of ethyl acetate (50 mL) and water (30 mL) the mixture was adjusted at pH 5 using sodium carbonate. The aqueous phase was extracted with ethyl acetate (3 x 50 mL) and the combined organic phases washed with brine (2 x 70 mL). After drying over sodium sulfate, the solvent was evaporated under reduced pressure to give **8** (0.9 g, 3.60 mmol) in 99 % yield. ^1H NMR (DMSO- d_6): 6.96 (m, 3H, ArH), 4.91 (d, 1H, OH), 4.58 (t, 1H, CHOH), 3.80 (s, 3H, OMe), 3.71 (s, 3H, OMe), 2.87 (m, 2H, P2,6), 2.34 (m, 2H, P2,6), 1.68 (m, 1H, P4), 1.51 (s, 1H, NH), 1.14 (m, 4H, P3,5).

Radiochemistry

N.c.a. [^{18}F]fluoride was produced via the $^{18}\text{O}(p,n)^{18}\text{F}$ nuclear reaction by the bombardment of an isotopically enriched [^{18}O]water target with 17 MeV protons at the JSW cyclotron BC 1710 (FZ Jülich).²² The [^{18}F]fluoride solution was azeotropically dried as described in the literature upon addition of Kryptofix® 222 and potassium carbonate for anion activation.²³

4-[¹⁸F]Fluoroacetophenone ([¹⁸F]14)

To the dry [K222][¹⁸F]F complex, 4-nitroacetophenone (2-3 mg, \approx 10 μ mol), dissolved in absolute DMF (0.5 mL), was added and the mixture stirred for 10 min at 130 °C which gave RCY of 60 – 70 %. After dilution with water (20 mL), [¹⁸F]14 was fixed on a conditioned Oasis HLB 1cc cartridge (Waters), washed with water (5 mL), dried with air and eluted with diethyl ether (4.5 mL) through a glass column (LiChrolut 65 x 10 mm, Merck) filled with 4-Å molecular sieves and sodium sulfate (170 mg). The solvent was evaporated under a stream of argon at 700 mbar.

2-Bromo-4'-[¹⁸F]fluoroacetophenone ([¹⁸F]15)

The residue of [¹⁸F]14 was taken up in chloroform/ethyl acetate (1:1, 1 mL) and an acidic solution of bromine (3.2 g Br₂ in 25 mL acetic acid and 1.25 mL concentrated hydrochloric acid; 0.1 mL) was added. The mixture was stirred at 100 °C for 6 min. In order to destroy the excess bromine at the end of the reaction, a 5 % aqueous solution of sodium bisulfite (1.5 mL) was added. After separating the layers, the organic phase was diluted with diethyl ether (3.5 mL) and passed over a conditioned Alumina N cartridge (Waters) followed by a glass column (LiChrolut 65 x 10 mm, Merck) filled with 4-Å molecular sieves and sodium sulfate (170 mg). The RCY of [¹⁸F]15 after work-up was 39 – 48 % relative to [¹⁸F]14. The solvent was evaporated under a stream of argon at 700 mbar.

1-(2-Bromoethyl)-4-[¹⁸F]fluorobenzene ([¹⁸F]13)

For the reduction of [¹⁸F]15, triethylsilane (0.05 mL) and TFA (0.5 mL) were added to the residue. The mixture was stirred at 90 – 95 °C for 15 min. After dilution with water (15 mL) it was passed over a conditioned Oasis HLB 1cc cartridge (Waters), washed with water (5 mL), dried with air and eluted with acetonitrile (1 mL). The solution was injected into a semipreparative reversed-phase HPLC. Elution occurred at $k' = 3.71$. The RCY of isolated [¹⁸F]13 was 13 – 26 % relative to [¹⁸F]15. After dilution with water (20 mL) the collected fraction was fixed on a conditioned Oasis HLB 1cc cartridge (Waters) again, washed with water (5 mL) and eluted with dry DMF (1 mL) through a glass column (LiChrolut 65 x 10 mm, Merck) filled with 4-Å molecular sieves and sodium sulfate (170 mg).

(±)-[¹⁸F]MDL 100907 ([¹⁸F]9)

The secondary labelling precursor [¹⁸F]13 (in 0.7 mL DMF) was added to a suspension of (±)-(2,3-dimethoxyphenyl)(piperidine-4-yl)methanol (**8**) (12.6 mg, 50 μmol), caesium carbonate (16.3 mg, 50 μmol) and potassium iodide (8.3 mg, 50 μmol) in dry DMF (50 μL) under an atmosphere of argon. The mixture was stirred at 85 °C for 8 min and after dilution with water (15 mL) passed through a conditioned LiChrolut RP18e cartridge (Merck). The cartridge was washed with water (5 mL) and eluted with acetonitrile (1 mL). The solution was injected into a semi-preparative reversed-phase HPLC. Elution occurred at $k' = 3.44$. The RCY of isolated [¹⁸F]9 was 40 – 50 % relative to [¹⁸F]13. After dilution with water (20 mL) the collected fraction was fixed on a conditioned Oasis HLB 1cc cartridge (Waters), washed with water (5 mL) and eluted with ethanol (0.7 mL).

***In vitro* autoradiography**

For autoradiography, frozen brains of Wistar rats were cut horizontally at -18 °C into 20 μm thick slices (Leica AG Microsystems, Germany), mounted onto gelatin-coated object glasses and stored at -80 °C until use. For the binding assays, the brain sections were thawed and dried at 23 °C and treated after a literature protocol²⁰ with some modifications. After preincubation for 10 min at 23 °C in 50 mM Tris-HCl, pH 7.4, the cryosections were incubated with 30 pM (±)-[¹⁸F]MDL 100907 ([¹⁸F]3) in buffer for 45 min at 23 °C (n = 6 cryosections). Adjacent sections were incubated in the presence of 10 μM ketanserin or spiperone. After treatment the sections were washed twice for 5 min in Tris-HCl, dipped in deionized water, dried and exposed to a phosphor imager plate (Fuji).

Conclusion

Combining the excellent *in vivo* properties of [¹¹C]MDL 100907 with the more suitable half-life of fluorine-18, made the radiosynthesis of (±)-[¹⁸F]MDL 100907 ([¹⁸F]9) attractive, even by a rather complex 4 step radiosynthesis. For this purpose 1-(2-bromoethyl)-4-[¹⁸F]fluorobenzene ([¹⁸F]13), synthesized as a secondary labelling precursor in 3 steps, could successfully be coupled to the piperidine-derivative **8**, to prepare (±)-[¹⁸F]MDL 100907 ([¹⁸F]9) with specific activities of at least 30 GBq/μmol in an overall RCY of 1 -2 % and a preparation time of 140 min. If on-going work on the principally more attractive direct

labelling approach to (\pm)-[^{18}F]MDL 100907 ([^{18}F]9) does not succeed, the reaction procedure described here will serve as a basis for optimization studies. Using optically resolved (+)-(2,3-dimethoxyphenyl)(piperidine-4-yl)methanol as labelling precursor in this approach will yield (+)-[^{18}F]MDL 100907. *In vitro* autoradiography using rat brain slices verified the excellent distribution of (\pm)-[^{18}F]MDL 100907 with high binding to 5-HT_{2A} receptors and very low non-specific binding of about 6 % in frontal cortex using ketanserin or spiperone for blocking. In further studies the *in vivo* formation of the 3'-O-demethylated metabolite [^{18}F]MDL 105725 has to be evaluated, especially whether it interferes with PET measurements of 5-HT_{2A} receptors in the brain. Thus, it appears of high interest to explore the potential of [^{18}F]MDL 100907 ([^{18}F]9) as a new ligand for PET studies of 5-HT_{2A} receptors.

Acknowledgement

The authors wish to thank Mrs. Wiebke Sihver for radiopharmacological evaluation studies, Marcus H. Holschbach for NMR measurements and Fabian Kügler for support in organic syntheses.

References and Notes

- [1] Naughton M, Mulrooney JB, Leonard BE. *Hum Psychopharmacol* 2000; **15**: 397-415.
- [2] Perry EK, Perry RH, Candy JM, Fairbairn AF, Blessed G, Dick DJ, Tomlinson BE. *Neurosci Lett* 1984; **51**: 353-357.
- [3] Dean B, Hayes W. *Schizophr Res* 1996; **21**: 133-139.
- [4] Lundkvist C, Halldin C, Ginovart N, Nyberg S, Swahn C-G, Carr AA, Brunner F, Farde L. *Life Sciences* 1996; **58**: 187-192.
- [5] Johnson MP, Siegel BW, Carr AA. *Naunyn-Schmiedeberg's Arch Pharmacol* 1996; **354**:205-209.
- [6] Leysen JE. In: *Drugs as Tools in Neurotransmitter Research*. Boulton AA, Baker GB, Juorio AV (Eds.). Clifton, New Jersey: Humana Press Neuromethods, 1989; 299-350.
- [7] Kristiansen H, Elfving B, Plenge P, Pinborg LH, Gillings N, Knudsen GM. *Synapse* 2005; **58**: 249-257.
- [8] Tan PZ, Baldwin RM, Van Dyck CH, Al-Tikriti M, Roth B, Khan N, Charney DS, Innis, RB. *Nucl Med Biol* 1999; **26**: 601-608.
- [9] Scott DO, Heath TG. *J Pharm Biomed Anal* 1998; **17**: 17-25.

-
- [10] Ito H, Nyberg S, Halldin C, Lundkvist C, Farde L. *J Nucl Med* 1998; **39**: 208-214.
- [11] Mathis CA, Mahmood K, Huang Y, Simpson NR, Gerdes JM, Price JC. *Med Chem Res* 1996; **6**: 1-10.
- [12] Hall H, Farde L, Halldin C, Lundkvist C, Sedvall G. *Synapse* 2000; **38**: 421-431.
- [13] Carr AA, Kane JM, Hay DA. *PCT Int Appl* 1991; WO 91/18602.
- [14] Huang Y, Mahmood K, Mathis CA. *J Labelled Cpd Radiopharm* 1999; **42**: 949-957.
- [15] Ullrich T, Rice KC. *Bioorg Med Chem* 2000; **8**: 2427-2432.
- [16] Dence CS., McCarthy TJ, Welch MJ. *Appl Radiat Isot* 1993; **44**: 981-983.
- [17] Hwang D-R, Dence CS., Gong J, Welch MJ. *Appl Radiat Isot* 1991; **42**: 1043-1047.
- [18] de Vries EFJ, Vroegh J, Elsinga PH, Vaalburg W. *Appl Radiat Isot* 2003; **58**: 469-476.
- [19] Banks WR, Hwang DR. *Appl Radiat Isot* 1994; **45**: 599-608.
- [20] López-Giménez JF, Mengod G, Palacios JM, Vilaró MT. *Naunyn-Schmiedeberg's Arch Pharmacol* 1997; **356**: 446-454.
- [21] Pazos A, Cortés R, Palacios JM. *Brain Res* 1985; **346**: 231-249.
- [22] Qaim SM, Clark JC, Crouzel C, Guillaume M, Helmecke HJ, Nebeling B, Pike VW, Stöcklin G. PET radionuclide production. In *Radiopharmaceuticals for PET*, Stöcklin G, Pike VW (eds). Kluwer Academic Publishers: Dordrecht, 1993; 15-26.
- [23] Ludwig T, Ermert J, Coenen HH. *Nucl Med Biol* 2002; **29**: 255-262.
- by Matthias M. Herth^{a,*}, Markus Piel^a, Fabian Debus^b, Ulrich Schmitt^b, Hartmut Lüddens^b and Frank Rösch^a

3.3 Preliminary in vivo and ex vivo evaluation of the 5-HT_{2A} imaging probe [¹⁸F]MH.MZ

^aInstitute of Nuclear Chemistry Johannes Gutenberg-University Mainz, Fritz-Strassmann-Weg 2, D-55128 Mainz, Germany

^bDepartment of Psychiatry and Psychotherapy Clinical Research Group, Untere Zahlbacher Straße 8, D-55131 Mainz, Germany

Abstract

Introduction: The 5-HT_{2A} receptor is one of the most interesting targets within the serotonergic system because it is involved in a number of important physiological processes and diseases.

Methods: [¹⁸F]MH.MZ, a 5-HT_{2A} antagonistic receptor ligand, is labelled by ¹⁸F-fluoroalkylation of the corresponding desmethyl analogue MDL 105725 with 2-[¹⁸F]fluoroethyltosylate ([¹⁸F]FETos). *In vitro* binding experiments were performed to test selectivity towards a broad spectrum of neuroreceptors by radioligand binding assays. Moreover, first μ PET experiments, *ex vivo* organ biodistribution, blood cell and protein binding and brain metabolism studies of [¹⁸F]MH.MZ were carried out in rats.

Results: [¹⁸F]MH.MZ showed a K_i of 3 nM towards the 5-HT_{2A} receptor and no appreciable affinity for a variety of receptors and transporters. *Ex vivo* biodistribution as well as μ PET showed highest brain uptake at ~ 5 min p.i. and steady state after ~ 30 min p.i.. While [¹⁸F]MH.MZ undergoes extensive first-pass metabolism which significantly reduces its bioavailability, it is insignificantly metabolised within the brain. The binding potential in the

rat frontal cortex is 1.45, whereas the cortex to cerebellum ratio was determined to be 2.7 after ~ 30 min.

Conclusion: Results from μ PET measurements of [^{18}F]MH.MZ are in no way inferior to data known for [^{11}C]MDL 100907 at least in rats. [^{18}F]MH.MZ appears to be a highly potent and selective serotonergic PET ligand in small animals.

Key Words

MDL 100907, altanserin, MH.MZ, PET, fluorine-18, 5-HT_{2A} receptor

1. Introduction

Serotonin is a neurotransmitter that has been linked to a number of physiological processes and diseases, including appetite, emotion, changes in mood, depression, Alzheimer's disease and the regulation of the sleep/wake cycle [1,2]. In particular, 5-HT_{2A} receptors have been implicated in the beneficial effects of some antidepressants as well as antipsychotics [3]. Most but not all hallucinogens, including LSD, function as agonists at 5-HT_{2A} receptors, while all clinically approved atypical antipsychotic drugs are potent 5-HT_{2A} receptor antagonists [3]. Therefore, *in vivo* studies of 5-HT_{2A} receptor occupancy would provide a significant advance in the understanding of the mentioned disorders and conditions.

Positron emission tomography (PET) is an appropriate tool to measure *in vivo* directly, non-invasively and repetitively the binding potential, the receptor availability, and uptake kinetics of radio tracers for neuroreceptors.

Successful radioligands studied in *in vivo* PET investigations to date for molecular imaging of the 5-HT_{2A} system are antagonistic ligands such as [^{11}C]MDL 100907 [4-6] and [^{18}F]altanserin [7-10]. It could be demonstrated that patients with mild cognitive impairment show a reduced 5-HT_{2A} receptor binding [9]. Furthermore, there is substantial evidence from

recently PET studies in humans to implicate dysfunction of the serotonergic transmitter system in the Alzheimer's disease (AD) [10]. For example, *in vivo* functional imaging studies have confirmed large reductions in 5-HT_{2A} receptor binding in mild to moderately demented AD-patients using PET [11-12]. Moreover, the implication of the 5-HT_{2A} receptor in the AD has also been reported by consistent post mortem findings. A reduction in the availability of the 5-HT_{2A} receptor subtype could be determined [13-16].

Currently, [¹⁸F]altanserin and [¹¹C]MDL 100907 are the most frequently used PET-tracers to probe for the 5-HT_{2A} receptor *in vivo* due to their high affinity and selectivity for the 5-HT_{2A} receptor (altanserin: K_i = 0.13 nM [7]; (R)-MDL 100907: K_i = 0.2 nM [4]). Binding to other 5-HT receptor subtypes is very low for [¹¹C]MDL 100907 [17], and moderate to low for [¹⁸F]altanserin [18]. A further difference between these two tracers is their binding to receptors others than the serotonergic system. Altanserin shows a relatively high affinity for D₂ receptors (62 nM) and adrenergic-α₁ receptors (4.55 nM) [18], whereas the binding potential of MDL 100907 to these receptors is insignificant [19]. Another drawback of [¹⁸F]altanserin is its rapid and extensive metabolism [18]. A disadvantage of [¹¹C]MDL 100907 is its slow kinetics combined with the short half-life of the β⁺-emitter ¹¹C. The main advantage of [¹⁸F]altanserin over [¹¹C]MDL 100907 is the possibility to perform equilibrium scans lasting several hours and to transport the tracer to other facilities based on the 110 minute half-life of ¹⁸F-fluorine.

In summary, [¹¹C]MDL 100907 is a very specific high affinity ligand for 5-HT_{2A} receptors with the disadvantages of the short half-live of C-11 and its slow kinetics [6]. The binding of [¹⁸F]altanserin lacks specificity and *in vivo* stability but due to its availability it is the most commonly used receptor ligand for 5-HT_{2A} imaging.

Consequently, recent attempts were tried to synthesize [^{18}F]MDL 100907 [20]. However, due to the very low radiochemical yield (RCY) of 2% this ligand is not suitable for *in vivo* studies. In contrast, we have reported the synthesis (Figure 1) [21], first *in vitro* and *ex vivo* evaluation studies of an ^{18}F -analog of MDL 100907, [^{18}F]MH.MZ (**1**), to create a ligand combining the better selectivity of MDL 100907 as compared to altanserin and the superior isotopic properties of ^{18}F -fluorine as compared to ^{11}C -carbon (concerning both half-life and spatial resolution of PET measurements). Thereby, the affinity of MH.MZ towards the 5-HT_{2A} receptor was determined to be $K_i = 3.00 \pm 0.10$ nM and thus 15 times lower than that of the parent compound MDL 100907 ($K_i = 0.2$ nM) [4]. Overall labelling yields are 30-50 %. These results indicate an improved clinical application profile and justified further examination of the potential of [^{18}F]MH.MZ for molecular imaging the 5-HT_{2A} receptor.

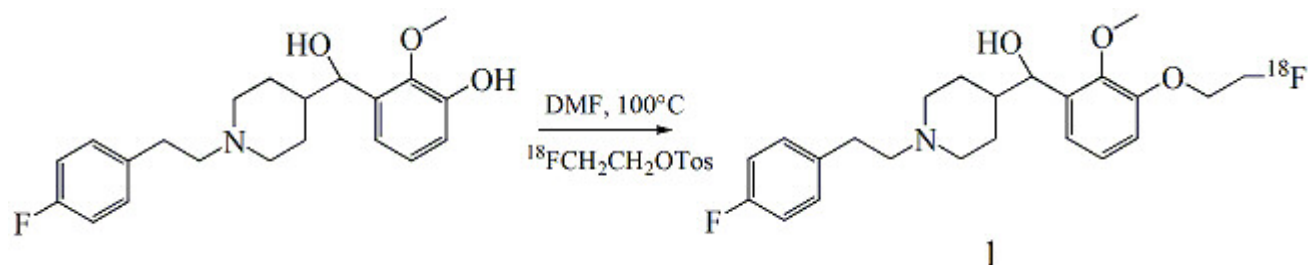


Figure 1: Radiosynthesis of [^{18}F]MH.MZ

2. Methods and Materials

2.1 Chemicals and Reagents

Chemicals were purchased from Acros, Fluka or Merck. Unless otherwise noted all chemicals were used without further purification.

2.1 Synthesis of the precursor MDL 105725 of [^{18}F]MH.MZ

MDL 105725 was synthesized as reported by Ullrich et al. [22].

2.3 Production of [^{18}F]MH.MZ

[^{18}F]FETos synthon synthesis: To an aqueous [^{18}F]fluoride solution (1400 - 1600 MBq) Kryptofix®222 (10 mg, 25 mmol), 12.5 mL potassium carbonate (1N) and 1mL acetonitrile were added. The mixture was dried in a stream of nitrogen at 80°C. The drying procedure was repeated three times until the reaction mixture was absolutely dry. The dried Kryptofix®222/[^{18}F]fluoride complex was then dissolved in 1mL acetonitrile and 4 mg (10 mmol) ethylene glycol-1,2-ditosylate were added and heated under stirring in a sealed vial for 3 min. Purification of the crude product was accomplished using HPLC (Lichrospher RP18-EC5, 250x10 mm; acetonitrile/water 50:50, flow rate: 5 ml/min, RT: 8 min). After diluting the HPLC fraction containing the 2-[^{18}F]fluoroethyltosylate with water, the product was loaded on a Phenomenex strata-X 33 μm Polymeric reversed Phase column, dried with nitrogen and eluted with 1mL of tempered (40-50 °C) DMSO.

Radiolabelling: [^{18}F]FETos diluted in 0.8 mL of dry DMSO was added to a solution of 3 mg MDL 105725 (7 mmol) dissolved in 0.2 mL dry DMSO and 1.5 μL 5N NaOH (7 mmol). The solution remained at 100 °C for 10 min and was quenched with 1 mL H₂O. Reactants and by-products were separated from [^{18}F]MH.MZ by semipreparative HPLC ($\mu\text{Bondapak C}_{18}$ 7.8 x 300 mm column, flow rate 8 mL/min, eluent: MeCN/0.05 phosphate-buffer, pH 7.4 adjusted with H₃PO₄ (40:60)). The retention time of [^{18}F]MH.MZ, [^{18}F]FETos and MDL 105725 were 9.8 min, 4.0 min and 4.9 min respectively. The collected product was diluted with water (4:1), passed through a conditioned strataX-cartridge (1 mL EtOH, 1 mL H₂O), washed with 10 mL H₂O and eluted with at least 1 mL EtOH. Finally, EtOH was removed *in vacuo* and [^{18}F]MH.MZ dissolved in 1 mL saline.

Determination of radiochemical purity and specific activity: The radiotracer preparation was visually inspected for clarity, absence of colour and particulates. Chemical and radiochemical purities were also assessed by TLC analyses and by analytical LUNA 250/ 4.6 mm 5 C₁₈(2): eluent: MeCN/buffer (0.05 M Na₂HPO₄ adjusted to pH = 6.7 with H₃PO₄), RT: [¹⁸F]F⁻ = 2.4 min; [¹⁸F]FETos = 22.0 min; [¹⁸F]MH.MZ = 11.3 min; MDL 105725 = 4.8 min; flow rate 1 mL/min; SiO₂-TLC: eluent: CHCl₃/MeOH/conc. NH₃, 8:1:0.2, R_f: [¹⁸F]MH.MZ: 0.36, [¹⁸F]FETos: 0.95 and R_f: [¹⁸F]fluoride ion: 0.0). Specific activity (A_s) of the radiotracer was calculated from three consecutive HPLC analyses (average) and determined as follows: The area of the UV absorbance peak corresponding to the radiolabelled product was measured (integrated) on the HPLC chromatogram and compared to a standard curve relating mass to UV absorbance.

2.4 Animals

Male 8 week mature catheterized Sprague-Dawley (SD) rats were obtained from Charles River Laboratories, France. In addition, Wistar rats were obtained from the animal husbandry of the Johannes Gutenberg University of Mainz were used for *ex vivo* distribution studies. All procedures were carried out in accordance with the European Communities Council Directive regarding care and use of animals for experimental procedures and were approved by local authorities of the state of Rheinland-Pfalz.

2.5 Binding assays

Binding assays were performed by the NIMH Psychoactive Drug Screening Program at the Department of Biochemistry, Case Western Reserve University, Cleveland, Ohio, USA (Bryan Roth, Director). Compound (1) was assayed for its affinities for a broad spectrum of

receptors and transporters in competitive binding experiments *in vitro* using cloned human receptors. Reported values of the inhibition coefficient (K_i) are mean \pm SD of four separate determinations.

2.6 *Ex vivo organ biodistribution*

Fully grown male Wistar rats (weight 250 - 310 g) were injected with \sim 10 MBq of [^{18}F]MH.MZ *via* tail vein. At 5, 15, 30 and 60 min post injection, animals were euthanized, blood and the indicated tissues removed. The radioactivity in brain, kidneys, liver, stomach and bones was determined. Data were corrected for decay and reported as mean % ID/ g tissue.

2.7 [^{18}F]MH.MZ metabolism studies in the brain

At 60 min p.i., Wistar rats (weight 250 - 310 g) were anesthetized with halothane and sacrificed. Blood samples for determination of the metabolism were centrifuged and the supernatant was mixed with MeCN 1:5. After an additional centrifugation step the supernatant was used for chromatography (Radio-TLC). Brains for determination of the metabolism were harvested, homogenized and mixed with MeOH and centrifuged. The supernatant was used for TLC. Blood and brain samples were analyzed *via* TLC ($\text{CHCl}_3/\text{MeOH}$ 5:2; R_f [^{18}F]FETos: 0.9, [^{18}F]MH.MZ: 0.7 and metabolite 0.1).

2.8 *Blood cell and protein binding of [^{18}F]MH.MZ*

The ratio of radioactivity concentration in blood cells versus protein and plasma water was determined in three Wistar rats. Four blood samples were obtained from 0 to 60 min (5, 10, 30, 60 minutes respectively) after intravenous injection of [^{18}F]MH.MZ. Whole blood was

centrifuged at 10,000 RPM for 5 min at 4°C to separate plasma and blood cells. Plasma and blood cell fractions were obtained, and the radioactivity was measured with an automatic γ -counter (2470 Wizard²; Perkin Elmer). Subsequently, plasma proteins were precipitated with MeCN (1:4), centrifuged at 10,000 RPM for 10 min at RT, and the radioactivity in supernatant (plasma water) and sediment was measured using the mentioned γ -counter. The percentage of radioactivity bound to plasma proteins was calculated thereafter.

2.9 μ PET experiments

μ PET imaging was performed with a Siemens/ Concorde Microsystems microPET Focus 120 small animal PET (μ PET) camera. Animals were 250 g 8 week old Sprague-Dawley rats bought catheterized with catheters in the femoral artery and vein. Animals were anesthetized with volatile anaesthetic isoflurane at a concentration of 1.8 %. The radiotracer was applied *via* i.v. injection into the femoral vein catheter (~ 10 MBq, $A_s = 50$ GBq/ μ mol) and blood samples were collected via the femoral artery catheter. After application of [¹⁸F]MH.MZ or collecting of blood samples, catheters were flushed with heparinised isotonic 0.9 % NaCl solution. Volumes of blood collected were re-injected as isotonic 0.9 % NaCl solution. Results were expressed as standardized uptake values (SUV) which is defined by: (activity concentration in Bq/mL) * (body weight in g) / (injected dose in Bq). Scans were carried out as dynamic scans over a time period of 60 min. Kinetic modelling and image quantification was done using the PMOD software package and a 4-parameter reference tissue model.

3. Results and Discussion

As previously reported, [^{18}F]MH.MZ could be obtained as an injectable solution in radiochemical yields of about 42% within a synthesis time of about 100 min in a purity of > 96% [21]. Thereby, high specific activities of ~ 50 GBq/ μmol with a batch activity of ~ 3 GBq were obtained.

The capability of the tracer related to its affinity and selectivity was examined by determining binding affinities (K_i) to a broad spectrum of receptors by radioligand binding assays through NIMH-psychoactive Drug Screening Program (PDSP). Results are summarized in Table 1. The new compound (**1**) has an excellent K_i of 3.0 nM for the 5-HT $_{2A}$ receptor. In contrast, K_i values for the other receptors and transporters are negligible (Table 1).

Ex vivo organ biodistribution of [^{18}F]MH.MZ was carried out in Wistar rats. Three adult male rats were used for each of four time points. Each animal was injected *via* tail vein. At 5, 15, 30 and 60 min post injection, animals were euthanized, blood and the indicated tissues removed.

The radioactivity in brain, kidneys, liver, stomach and bones was determined. Data were corrected for decay and reported as mean % ID/ g tissue (Table 2). [^{18}F]MH.MZ showed highest brain uptake (0.48 ± 0.16 % ID/g tissue) at 5 min p.i. and steady state appeared to be between ~ 30 and 60 min post injection (Figure 2). The highest % ID/g tissue could be detected in metabolising tissues. Maximum accumulation occurred in the liver at 5 min post injection, whereas the maximum accumulation in the kidneys was reached at ~ 15 min post injection. Blood showed highest uptake 15 min p.i and even after 60 min steady state is not reached. Due to Bonaventure et al. [23], the 5-HT $_{2A}$ receptor concentration in the spleen, the

stomach, the testis, the colon and the smooth muscle is about the same level at least in dogs. Therefore, we decided to harvest only the stomach. As no significant accumulation in the stomach could be detected, any additional tissues were harvested.

Table 1. *In vitro* binding affinities of MH.MZ toward human receptors and transporters

Target	K_i (nM)	Target	K_i (nM)
5-HT _{1A}	> 10.000	D1	899 ± 127
5-HT _{1B}	1846 ± 426	D2	> 10.000
5-HT _{1E}	> 10.000	D4	544 ± 41
5-HT _{2A}	3 ± 0	SERT	n.d
5-HT _{2B}	299 ± 27	DOR	> 10.000
5-HT _{2C}	71 ± 10	H1	n.d.
5-HT ₃	> 10.000	H2	3818 ± 142
5-HT _{5A}	> 10.000	H3	> 10.000
5-HT ₆	3890 ± 1921	H4	> 10.000
5-HT ₇	116 ± 14	DAT	> 10.000
KOR	> 10.000	MOR	> 10.000
M1	> 10.000	M2	> 10.000
M3	> 10.000	M4	> 10.000
M5	> 10.000	Beta3	> 10.000

Affinities were determined by PDSP; 5-HT: Serotonin; Beta; SERT: serotonin transporter; D: dopamine; DAT: dopamine transporter; DOR: delta opioid receptors; H: histamine; KOR: kappa opioid receptors; M: muscarinic; MOR: Opioid Receptor μ -splice variant

Table 2. Organ biodistribution of [^{18}F]MH.MZ in male Wistar rats. Radioactivity concentrations are expressed as percentage of the injected dose per gram tissue (% ID/g tissue). Results are mean \pm SD (n = 3).

Tissue	5 min	15 min	30 min	60 min
brain	0.48 \pm 0.16	0.17 \pm 0.03	0.08 \pm 0.01	0.08 \pm 0.01
blood	2.39 \pm 0.90	1.37 \pm 0.24	0.69 \pm 0.12	0.33 \pm 0.05
bones	0.08 \pm 0.04	0.04 \pm 0.02	0.05 \pm 0.01	0.06 \pm 0.01
stomach	0.32 \pm 0.12	0.44 \pm 0.16	0.37 \pm 0.05	0.34 \pm 0.08
kidneys	2.74 \pm 0.41	4.31 \pm 2.40	3.64 \pm 1.76	1.76 \pm 0.61
liver	5.52 \pm 0.94	4.31 \pm 0.50	2.98 \pm 0.28	1.62 \pm 0.29

Radioactivity concentrations are expressed as percentage of the injected dose per gram tissue (% ID/g tissue). Results are expressed as mean \pm SD (n = 3)

For analysing preliminary *in vivo* metabolism of [^{18}F]MH.MZ in brain and blood, samples were treated as described. Metabolite and intact tracer were analyzed by radio-TLC ($\text{CHCl}_3/\text{MeOH}$ 5:2). The tracer underwent fast metabolism [21]. Only one polar metabolite was found in plasma and the percentage of unmetabolized fractions was 43%, 32%, 16%, and 7% at 5, 10, 30, and 60 min, respectively.

In contrast, Figure 3 compares metabolized fractions of [^{18}F]MH.MZ in rat plasma and rat brain at 60 min post injection. Radio-TLC analyses showed non-metabolized [^{18}F]MH.MZ in rat brain samples whereas almost no intact [^{18}F]MH.MZ could be found in rat plasma.

Probably, the fluoroethoxy group is metabolized similar to the already published behaviour of the metabolism of [^{11}C]MDL 100907 [24]. The observed radioactive polar metabolite in figure 3 may not cross the blood-brain barrier (BBB) to a large extent because of its polarity.

Therefore, we expect that the radioactive metabolite is not able to interfere with the μ PET-imaging.

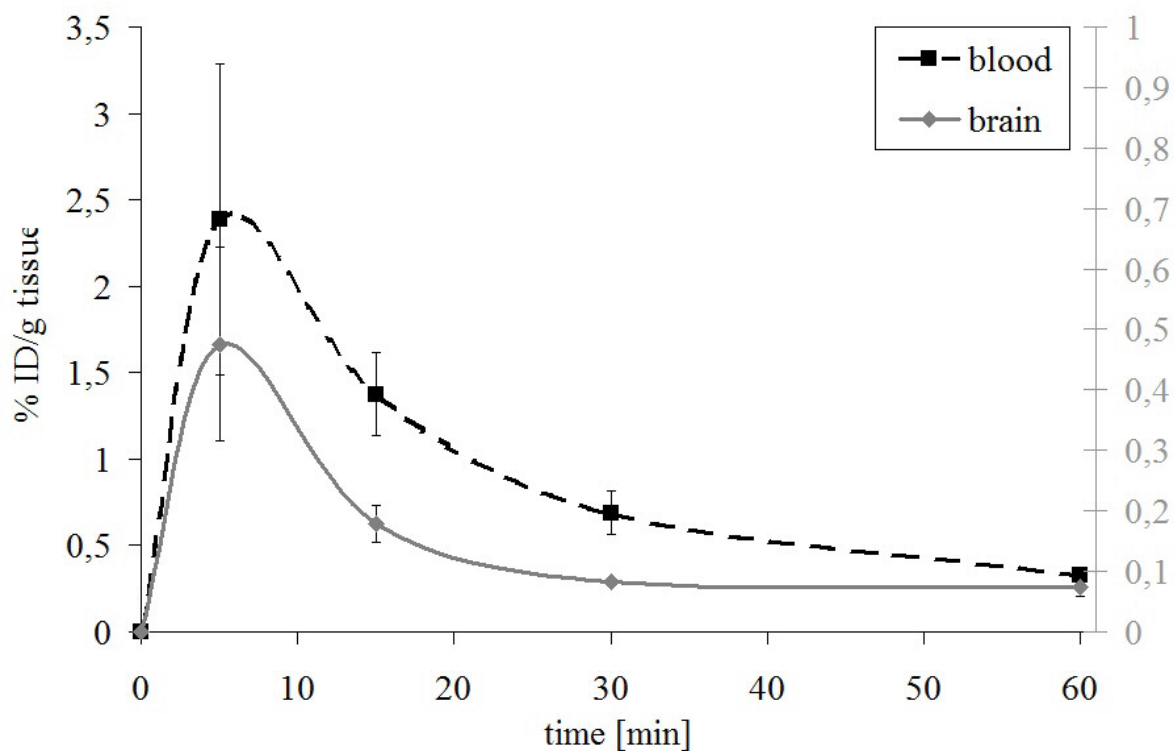


Figure 2: *Ex vivo* biodistribution of [^{18}F]MH.MZ in rat brain and blood at 5, 15, 30 and 60 min ($n = 3$ per time point; means \pm SD shown) following tail vein injection. Results are expressed as % ID / g tissue.

In addition, our reported time-activity-curves (TAC) confirm this hypothesis. No additional accumulation could be observed in the brain after 500 seconds, whereas the metabolite concentration still rises in the blood (Figure 4). Therefore, we believe, that the metabolite found is based on blood still located in vessels in the brain rather than beyond the BBB. However, this is mainly based on assumptions and it could very well be that the active metabolite is within the brain. This would be a considerable drawback of this tracer. Future

studies will be carried out to identify this metabolite, its biochemical behaviour and its possibility to enter the brain to prove usefulness as a human PET 5-HT_{2A} tracer.

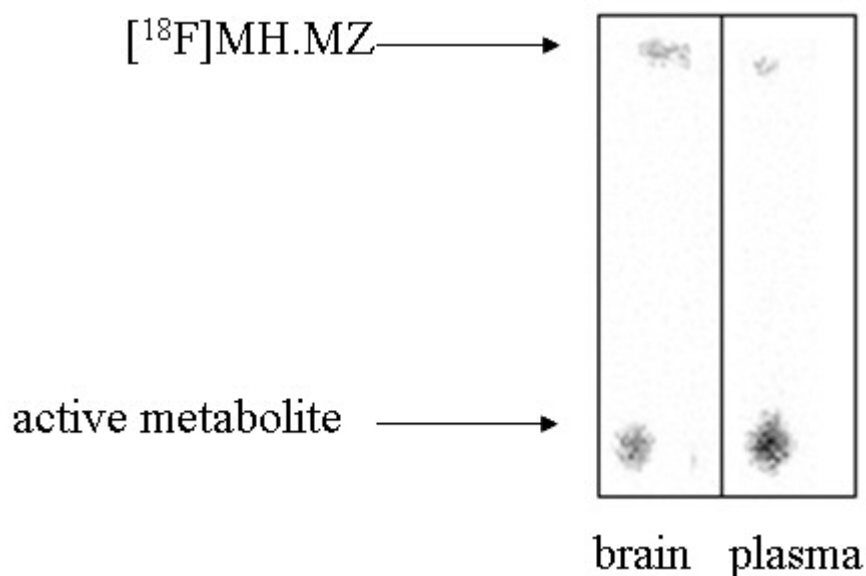


Figure 3: Comparison of metabolism in rat brain and plasma 60 min post injection. Unmetabolized tracer could be found in rat brain (**A**) whereas almost no intact tracer could be detected in plasma samples (**B**)

Moreover, protein binding and distribution of [¹⁸F]MH.MZ in rat blood were determined. After intravenous injection of [¹⁸F]MH.MZ into the study subjects (n = 4), free tracer is rapidly metabolised as previously reported [21]. The plasma-to-blood ratio of radioactivity was determined to be ~ 0.65 after 5 – 10 minutes and changed over 60 minutes to a value of ~ 0.85. This is exactly the timeframe used for PET imaging of [¹⁸F]MH.MZ in this manuscript. Approximately 40% of [¹⁸F]MH.MZ was bound to rat plasma proteins after 60 minutes, whereas only ~ 25% was bound after 10 minutes. The radioactivity bound to blood cells decreases over 60 minutes from about 30% to 25%. Figure 4 summarizes the radioactivity distribution in rat blood cells during a 60 minutes time frame.

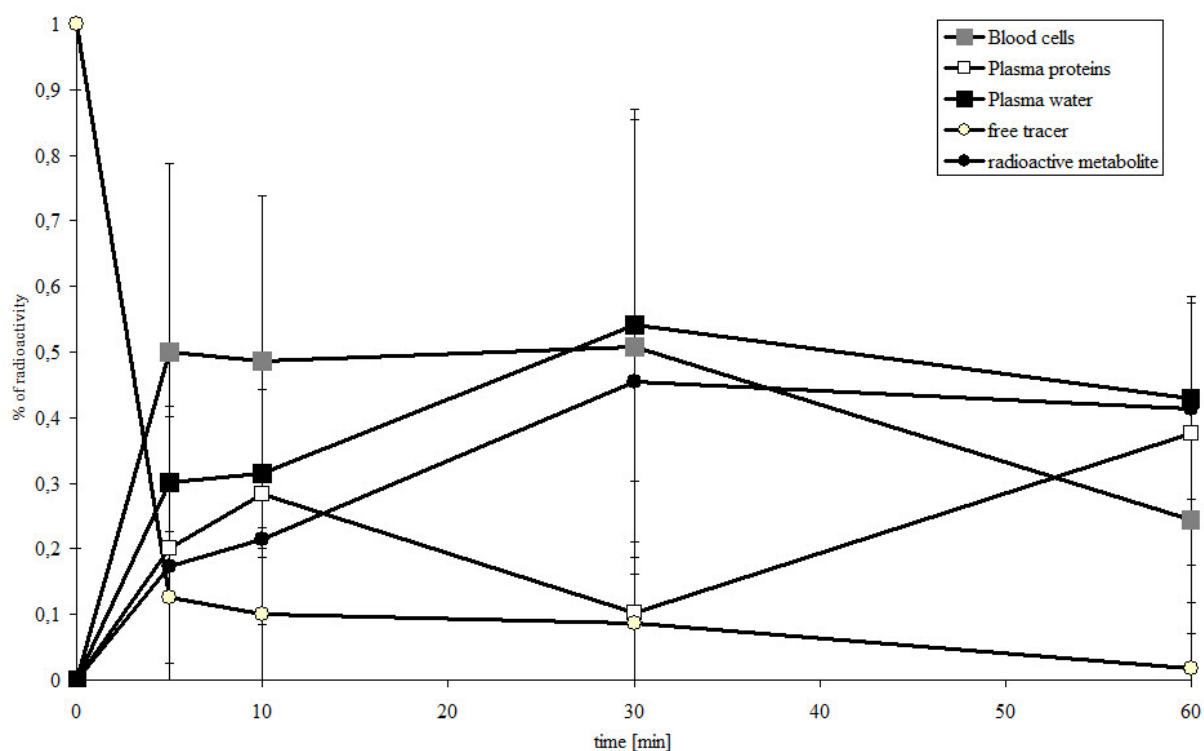


Figure 4: Distribution of radioactivity derived from $[^{18}\text{F}]\text{MH.MZ}$ in rat blood components

First μPET experiments ($n = 4$) were performed with a Siemens MicroPET Focus 120 camera in male 8 week mature catheterized Sprague-Dawley rats. Rats were anesthetized with isoflurane. The binding of $[^{18}\text{F}]\text{MH.MZ}$ is displayed in transversal (A), in sagittal (B) and in coronal orientation (C) in Figure 5. Images are displayed in false colour coding with white representing maximum and black representing minimum binding.

Images displayed in Fig. 5 represent summed images of a period of the last 20 minutes of the scan time. Highest specific uptake is visible in the frontal cortex. High nonspecific uptake was detected in the harderian glands and in the salivary and thyroid glands. Binding of

$[^{18}\text{F}]\text{MH.MZ}$ in the cerebellum is at background level. Thus, images represent a visualization of the system in equilibrium binding.

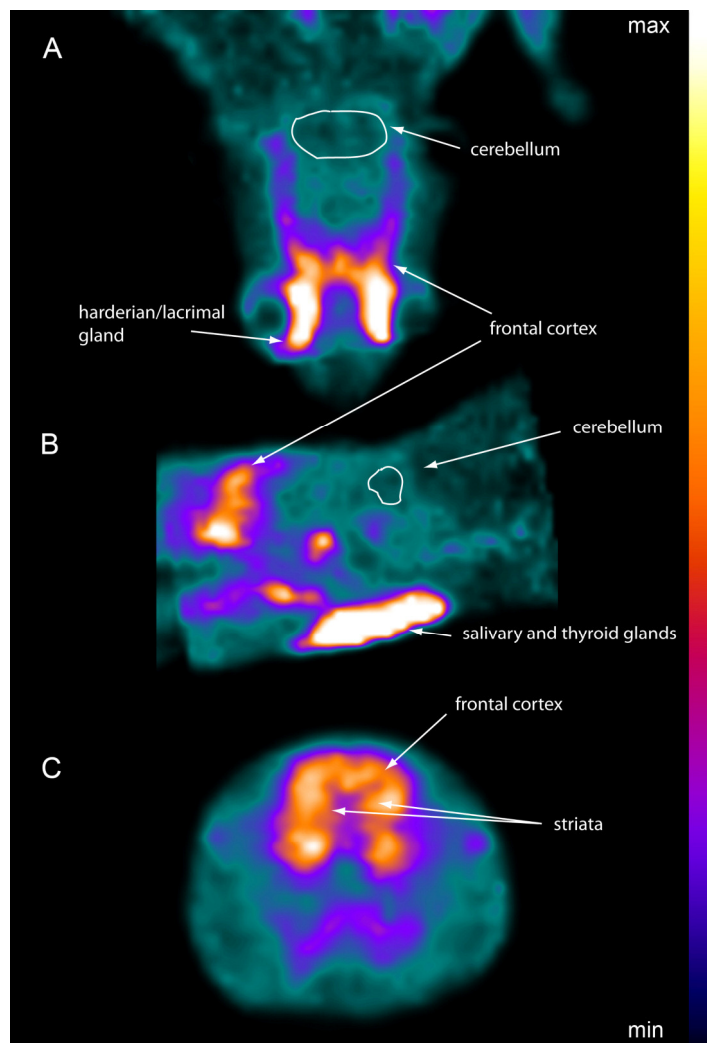


Figure 5: Representative μPET images of $[^{18}\text{F}]\text{MH.MZ}$ (n=1) with A) transversal, B) sagittal and C) coronal orientation.

This *in vivo* distribution is in very good agreement with the distribution recently shown in the autoradiographic images (Fig. 6) [21].

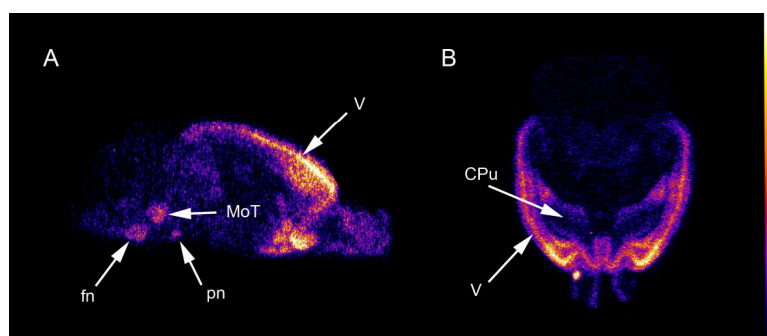


Figure 6: Images of an autoradiography of [^{18}F]MH.MZ binding at 14 μm thick rat brain sections; (A and B) total binding at a concentration of 5 nM with (A) lateral 0.9 mm and (B) coronal 5.8 mm from bregma. Major binding was detected in lamina V (V) of the frontal cortex, in the caudate-putamen (CPu), and three regions of the brain stem, the motor trigeminal nucleus (MoT), facial nucleus (fn), and the pontine nuclei (pn).

Uptake of [^{18}F]MH.MZ in near equilibrium state ($t > 2000$ sec) is more than 50% higher in cortical regions than in the cerebellum. The cortex to cerebellum ratio was determined to be 2.7 after ~ 40 min ($n=4$), which surprisingly resembles the primate ratios published by Lundkvist et al. [25] measured by [^{11}C]MDL 100907. This is much likely due to the decreased affinity of MH.MZ compared to MDL 100907. The binding potential (BP) was 1.45 ($n=4$) for the frontal cortex region using a four parameter reference tissue model and the PMOD software. Cerebellum uptake is employed instead of a plasma input curve.

Figure 7 shows a representative time-activity curve (TAC) of a total binding study of [^{18}F]MH.MZ which included four animals. Results are given as standardized uptake value (SUV).

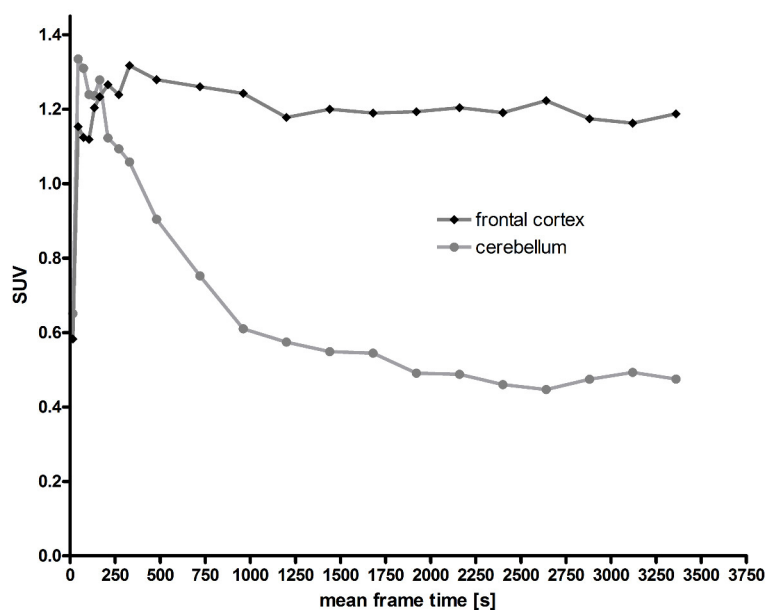


Figure 7: Representative time-activity curve (TAC) ($n=1$) of μ PET experiments with $[^{18}\text{F}]\text{MH.MZ}$ in SD rats. The graphs show results of a total binding study.

Equilibrium appears to be reached between 28 to 35 minutes post injection. The fact that the equilibrium state seems to be reached earlier than observed by Lundkvist et al. [25] is not too surprising given the faster metabolism of rodents as compared to primates. Once equilibrium binding is reached the specific binding remains very constant and might therefore even enable scans up to 2 hours.

4. Conclusion

In conclusion, $[^{18}\text{F}]\text{MH.MZ}$ appears to be a suitable new PET tracer for molecular imaging of the $5\text{-HT}_{2\text{A}}$ receptor system. It offers high affinity ($K_i = 3 \text{ nM}$) for the $5\text{-HT}_{2\text{A}}$ receptor and has any appreciable affinity for most of the tested receptors and transporters (Tab.1) thus representing excellent specificity. However, the affinity is 15 times lower than that of its parent MDL 100907. For rats, *ex vivo* biodistribution study as well as μ PET data showed

highest brain uptake at ~ 5 min p.i.. Equilibrium is reached at ~ 30 minutes post injection and stays on almost the same level for a relatively long time of about 1 h.

Non-metabolized [^{18}F]MH.MZ is present in rat brain samples in contrast to rat plasma after 60 minutes indicating that [^{18}F]MH.MZ is able to cross the blood-brain-barrier whereas metabolites were probably not accumulating in the brain. However, this has to be checked in more detail. For example, the metabolite and its biochemical behaviour should be identified, especially if the metabolite is able to cross the BBB. The characteristics observed for [^{18}F]MH.MZ meet the requirements for molecular imaging and quantitative data interpretation and might be evidently an improvement compared to [^{18}F]altanserin and be particularly relevant as [^{18}F]altanserin undergoes rapid and extensive metabolism forming ^{18}F -containing metabolites that cross the BBB. Results from small animal PET measurements of [^{18}F]MH.MZ are in no way inferior to data obtained with [^{11}C]MDL 100907. High uptake can be seen in the same brain regions. The BP of [^{18}F]MH.MZ for uptake in the rat frontal cortex is defined to be 1.45, whereas the cortex to cerebellum ratio was determined to be 2.7 at equilibrium (n=4). Nevertheless, the usefulness of [^{18}F]MH.MZ has to be tested in the primate brain because ratios may decrease by going from rat to primate brains.

All together, new auspicious results concerning the biological behaviour of [^{18}F]MH.MZ by both, *in vivo* and *ex vivo* experiments are reported. Compared to known tracers the data hint on a considerably improved 5-HT_{2A} imaging ligand at least in rats. Whether [^{18}F]MH.MZ is an improvement to the already used 5-HT_{2A} tracers in primates is dependent on the possibility of the metabolite to enter the brain. A toxicology study is planned and provided that it will result in a non-toxicity of the tracer, first human PET studies in healthy volunteers would be possible. Moreover, the polar metabolite will be determined and investigated in more detail.

5. Acknowledgments

The authors wish to thank Sabine Höhnemann and Vasko Kramer for the syntheses of [¹⁸F]FETos. They also thank Daniel Zils for technical assistance and excellent animal preparation as well as Matthias Schreckenberger (MD) for his support. Financial support by Friedrich-Naumann-Stiftung, the European Network of Excellence (EMIL) is gratefully acknowledged. K_i determinations were generously provided by the National Institute of Mental Health's Psychoactive Drug Screening Program, Contract # NO1MH32004 (NIMH PDSP). The NIMH PDSP is directed by Bryan L. Md, PhD at the University of North Carolina at Chapel Hill and Project Officer Jamie Driscoll at NIMH, Bethesda MD, USA.

6. References

- [1] Davis KL, Charney D, Coyle JT, Nemeroff C, Neuropsychopharmacology: The Fifth Generation of Progress, new York: Raven Press 2002.
- [2] Jones BE, Kryger MH, Roth T, Dement WC, Eds.; Principles and practice of sleep medicine, W.B. Saunders Company: Philadelphia 2000: 134-54.
- [3] Meltzer HY, Matsubara S, Lee JC. Classification of typical and atypical antipsychotic drugs on the basis of dopamine D-1, D-2 and serotonin₂ pK_i values. *J. Pharmacol. Exp. Ther.* 1989; 251: 238-46.
- [4] Ito H, Nyberg S, Halldin C, Lundkvist C, Farde L. PET Imaging of Central 5-HT_{2A} Receptors with Carbon-11-MDL 100,907. *J.Nuc.Med.* 1998; 39: 208-14
- [5] Bhagwagar Z, Hinz R, Taylor M, Fancy S, Cowen P, Grasby P. Increased 5-HT_{2A} Receptor Binding in Euthymic, Medication-Free Patients Recovered From Depression: A Positron Emission Study With [¹¹C]MDL 100,907. *Am J Psychiatry* 2006; 163:1580-87.

-
- [6] Watabe H, Channing MA, Der MG, Adams RH, Jagoda E, Herscovitch P, Eckelman WC, Carson RE. Kinetic Analysis of the 5-HT_{2A} Ligand [¹¹C]MDL 100,907. *J Cereb Blood Flow Metab* 2000; 20: 899-909.
- [7] Smith GS, Price JC, Lopresti BJ, Huang Y, Simpson N, Holt D, Mason NS, Meltzer CC, Sweet RA, Nichols T, Sashin D, Mathis CA. Test-retest variability of serotonin 5-HT_{2A} receptor binding measured with positron emission tomography and [¹⁸F]altanserin in the human brain. *Synapse* 1998; 30: 380-92.
- [8] Pinborg LH, Arfan H, Haugbol S, Kyvik KO, v. B. Hjelmberg J, Svarer C, Frokjaer VG, Paulson OB, Holm S, Knudsen GM. The 5-HT_{2A} receptor binding pattern in the human brain is strongly genetically determined. *NeuroImage* 2008; 40: 1175–80.
- [9] Hasselbalch SG, Madsen K, Svarer C, Pinborg LH, Holm S, Paulson OB, Waldemar G, Knudsen GM. Reduced 5-HT_{2A} receptor binding in patients with mild cognitive impairment. *Neurobiology of Aging* 2008; 29: 1830–38.
- [10] Meltzer CC, Smith G, DeKosky ST, Pollock BG, Mathis CA, Moore RY, Kupfer DJ, Reynolds, CFI. Serotonin in aging, late-life depression, and Alzheimer's disease: the emerging role of functional imaging. *Neuropsychopharmacology* 1998; 18: 407–30.
- [11] Meltzer CC, Price JC, Mathis CA, Greer PJ, Cantwell MN, Houck PR, Mulsant BH, Ben Eliezer D, Lopresti B, DeKosky ST, Reynolds CFI. PET imaging of serotonin type 2A receptors in late-life neuropsychiatric disorders. *Am. J. Psychiatry* 1999; 156: 1871–78.
- [12] Blin J, Baron JC, Dubois B, Crouzel C, Fiorelli M, Attar-Levy D, Pillon B, Fournier D, Vidailhet M, Agid Y. Loss of brain 5-HT₂ receptors in Alzheimer's disease. *In vivo* assessment with positron emission tomography and [¹⁸F]setoperone. *Brain* 1993; 116: 497- 510.

-
- [13] Bowen DM, Najlerahim A, Procter AW, Francis PT, Murphy E. Circumscribed changes of the cerebral cortex in neuropsychiatric disorders of later life. *Proc. Natl. Acad. Sci.* 1989; 86: 9504–8.
- [14] Cheng AV, Ferrier IN, Morris CM, Jabeen S, Sahgal A, McKeith IG, Edwardson JA, Perry RH, Perry EK. Cortical serotonin-5HT₂ receptor binding in Lewy body dementia. Alzheimer's and Parkinson's diseases. *J. Neurol. Sci.* 1991; 106: 50–55.
- [15] Lai MK, Tsang SW, Alder JT, Keene J, Hope T, Esiri MM, Francis PT, Chen CP. Loss of serotonin 5-HT_{2A} receptors in the postmortem temporal cortex correlates with rate of cognitive decline in Alzheimer's disease. *Psychopharmacology* 2005; 179: 673–77.
- [16] Reynolds GP, Arnold L, Rossor MN, Iversen LL, Mountjoy CQ, Roth M. Reduced binding of ketanserin to cortical 5-HT₂ receptors in senile dementia of the Alzheimer type. *Neurosci. Lett.* 1984; 44: 47–51.
- [17] Johnson MP, Siegel BW, Carr AA, [³H]MDL 100,907: a novel selective 5-HT_{2A} receptor ligand. *Naunyn Schmiedeberg's Arch Pharmacol* 1996; 354: 205–209.
- [18] Tan P, Baldwin RM, Fu T, Charney DS, Innis RB. Rapid Synthesis of F-18 and H- Dual labeled Altanserin, A metabolically Resistant PET ligand for 5-HT_{2A} Receptor. *J. Labelled Compd. Radiopharm.* 1999; 42: 457-67.
- [19] Hall H, Farde L, Halldin C, Lundkvist C, Sedvall G. Autoradiographic Localization of 5-HT_{2A} Receptors in the Human Brain Using [³H]M100907 and [¹¹C]M100907. *Synapse* 2000; 38; 421-31.
- [20] Mühlhausen U, Ermert J, Herth MM, Coenen HH. Synthesis, Radiofluorination and First Evaluation of (±)-[¹⁸F]MDL 100907 as Serotonin 5-HT_{2A} Receptor Antagonist for PET. *J. Labelled Compd. Radiopharm.* 2008; 52: 6-12

-
- [21] Herth MM, Debus F, Piel M, Palner M, Knudsen GM, Lüddens H, Rösch F. Total Synthesis and Evaluation of [^{18}F]MH.MZ. *Bioorg. Med. Chem. Lett.* 2008; 18: 1515-19.
- [22] Ullrich T, Ice KC. A Practical Synthesis of the Serotonin 5-HT_{2A} Receptor Antagonist MDL 100907, its Enantiomer and their 3-Phenolic Derivatives as Precursors for [^{11}C]Labeled PET Ligands. *Bioorg. Med. Chem.* 2000; 8: 2427-32.
- [23] Bonaventure P, Nepomuceno D, Miller K, Chen J, Kuei C, Kamme F, Tran D, Lovenberg TW, Liu C. Molecular and pharmacological characterization of serotonin 5-HT_{2A} and 5-HT_{2B} receptor subtypes in dog. *European Journal of Pharmacology* 2005; 513: 181-192.
- [24] Scott DO, Heath TG. Investigation of the CNS penetration of a potent 5-HT_{2A} receptor antagonist (MDL 100,907) and an active metabolite (MDL 105,725) using in vivo microdialysis sampling in the rat. *J. Pharm. Biomed. Anal.* 1998; 17: 17-25.
- [25] Lundkvist C, Halldin C, Ginovart N, Nyberg S, Swahn CG, Carr AA, Brunner F, Farde L. [^{11}C]MDL 100907, a radioligand for selective imaging of 5-HT_{2A} receptors with positron emission tomography. *Life Sci.* 1996; 58: 187-192

3.4 Synthesis and *in vitro* affinities of various MDL 100907 derivatives as potential ^{18}F -radioligands for 5-HT_{2A} receptor imaging with PET

by Matthias M. Herth,^{a, *} Vasko Kramer,^a Markus Piel,^a Mikael Palner,^b Patrick J. Riss,^a Gitte M. Knudsen^b and Frank Rösch^a

^aInstitute of Nuclear Chemistry Johannes Gutenberg-University Mainz, Fritz-Strassmann-Weg 2, 55128 Mainz, Germany

^bCenter for Integrated Molecular Brain Imaging and University of Copenhagen, Rigshospitalet, Blegdamsvej 9, DK-2100 Copenhagen Ø, Denmark

Abstract

Radiolabelled piperidine derivatives such as [^{11}C]MDL 100907 and [^{18}F]altanserin have played an important role in diagnosing malfunction in the serotonergic neurotransmission. A variety of novel piperidine MDL 100907 derivatives, possible to label with ^{18}F -fluorine, were synthesized to improve molecular imaging properties of [^{11}C]MDL 100907. Their *in vitro* affinities to a broad spectrum of neuroreceptors and their lipophilicities were determined and compared to the clinically used reference compounds MDL 100907 and altanserin. The novel compounds MA-1 (**53**) and (R)-MH.MZ (**56**) show K_i -values in the nanomolar range towards the 5-HT_{2A} receptor and insignificant binding to other 5-HT receptor subtypes or receptors. Interestingly, compounds MA-1 (**53**), MH.MZ (**55**) and (R)-MH.MZ (**56**) provide a receptor selectivity profile similar to MDL 100907. These compounds could possibly be preferable antagonistic ^{18}F -tracers for visualisation of the 5-HT_{2A} receptor status. Medium affine compounds (VK-1 (**32**), (**51**), (**52**), (**54**)) were synthesized and have K_i values between 30 and 120 nM. All promising compounds show logP values between 2 and 3, that is within the range of those for the established radiotracers altanserin and MDL 100907. The novel compounds

MA-1 (**53**) and (R)-MH.MZ (**56**) thus appear to be promising high affine and selective tracers of ^{18}F -labelled analogues for 5-HT_{2A} imaging with PET.

Key Words

MH.MZ, PET, MDL 100907, ^{18}F -fluorine

1. Introduction

Serotonin (5-hydroxytryptamine, 5-HT), its transporter and various receptors are of central interest in the field of medicinal chemistry.^{1,2,3} Seven major families of transmembrane receptors (5-HT₁₋₇) and one transporter (SERT) are known to control 5-HT function by three different structures (transporters, ligand-gated ion channels, and G-protein-coupled receptors).⁴ The role of 5-HT_{2A} receptors in the regulation of a number of processes of the central nervous system (CNS) such as mood, appetite, sexual behaviour, learning and memory and their dysfunctions such as psychosis, depression and anxiety has been well documented.^{5,6} In particular, the 5-HT_{2A} receptors have been implicated in the beneficial effects of some antidepressants as well as antipsychotics.⁷ All clinically approved atypical antipsychotic drugs are also potent 5-HT_{2A} receptor antagonists.^{8,9} Moreover, many hallucinogens including LSD function as agonists at 5-HT_{2A} receptors.⁷

Consequently, *in vivo* studies of 5-HT_{2A} receptor availability would significantly advance the understanding of the biological principles of mentioned disorders and contribute to the development of appropriate therapies. Positron emission tomography (PET) is an appropriate tool to measure *in vivo* directly, non-invasively and repetitively the relevant pharmacologic parameters of ligand-neuroreceptor interactions.

Supposed adequate radiolabelled neurotransmitter analogues are available for the molecular imaging of the 5-HT_{2A} receptor. To date, *in vivo* studies have been performed with several 5-HT_{2A} selective antagonists. Of these tracers, [^{11}C]MDL 100907 (**a**) and [^{18}F]altanserin (**b**) represent the radioligands of choice for *in vivo* 5-HT_{2A} PET imaging because of their high affinity and selectivity for the 5-HT_{2A} receptor. In addition to their high binding affinities to the 5-HT_{2A} receptor (altanserin: $K_i = 0.13$ nM; MDL 100907 $K_i = 0.36$ nM) their binding affinities are more than 30 fold lower for other relevant receptors such as 5-HT_{1A}, 5-HT_{2C}, α_1 , D₁ and D₂ (Table 1).¹⁰⁻¹⁴

Table 1: Affinities (K_i (nM)) of altanserin and MDL 100907¹⁰⁻¹⁴

	5-HT _{1A}	5-HT _{2A}	5-HT _{2c}	D ₂	α_1
Altanserin	1570	0.13	40	62	4.55
(R)-MDL 100907	> 10000	0.36	107	2250	128

In *in vitro* and in *in vivo* experiments, both tracers revealed high affinity, selectivity and a good ratio of specific to non-specific binding for 5-HT_{2A} receptors.^{15,16} However, table 1 indicates that the selectivity of [¹¹C]MDL 100907 for the 5-HT_{2A} receptor is slightly higher than that of [¹⁸F]altanserin.¹⁵ Tracer affinity and selectivity are of crucial importance for uptake kinetics in brain, and tracers with very high affinity and selectivity give new insights into the role of the status of the serotonergic system and antipsychotic drug action. For example, Mintun et al. measured *in vivo* with [¹⁸F]altanserin a decreased hippocampal 5-HT_{2A} receptor binding in major depressive patients.¹⁷

Concerning molecular imaging, the advantage of [¹⁸F]altanserin (**b**) over [¹¹C]MDL 100907 (**a**) is the possibility to perform equilibrium scans lasting several hours and to transport the tracer to other facilities based on the 110 min half-life of ¹⁸F-fluorine.

A drawback of [¹⁸F]altanserin is its rapid and extensive metabolism. Four metabolites are formed in humans that cross the blood-brain-barrier,¹³ whereas metabolites of [¹¹C]MDL 100907 do not enter the brain to any larger extent.¹⁸

The aim of this study was to synthesize a ligand combining the reported better selectivity and *in vivo* stability of MDL 100907 as compared to those of altanserin and the superior isotopic properties of an ¹⁸F-label as compared to those of an ¹¹C-label.

The promising results obtained in *ex vivo* and *in vivo* experiments^{19,20} encouraged us to study structure-activity relationships of MDL 100907 analogues in more detail aiming at even improving affinity and selectivity of new compounds. Unfortunately, no detailed structure-activity relationship has been reported yet for this class of compound.

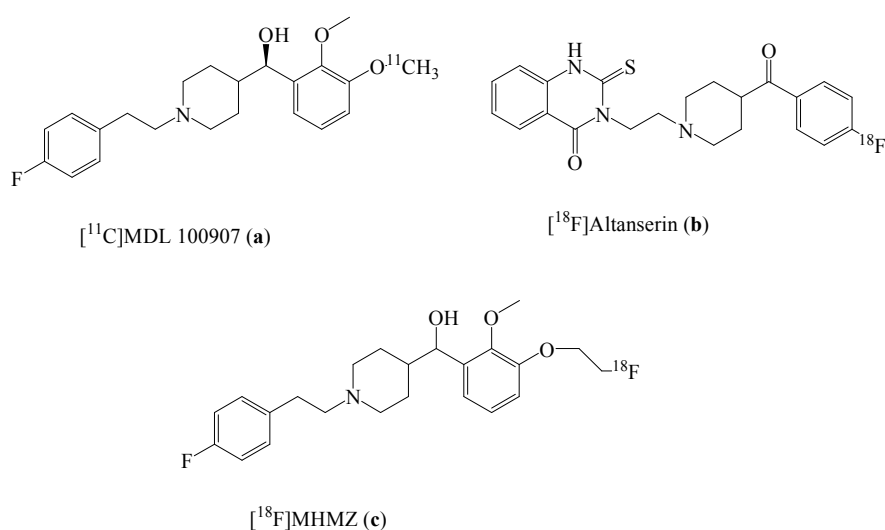


Figure 1: Structures of [¹¹C]MDL 100907 (a), [¹⁸F]altanserin (b) and [¹⁸F]MH.MZ (c)

Recently, we have reported the synthesis, first *in vitro*, *ex vivo* and *in vivo* evaluations of an ¹⁸F-analogue of MDL 100907, [¹⁸F]MH.MZ (c) (Figure 1).

A rudimental pharmacophore model has been published by Andersen et al.²¹ It describes the binding of various arylpiperidines at 5-HT₂ receptors. The model requires two aryl substituents, separated by distance a and located distances b and c from an amine moiety (Figure 2). Distances suggested by Anderson et al. for a, b and c are 5.1, 7.5 and 8.1 Å, respectively.

Heinrich et al.²² described an optimization of the structure and the discovery of a selective 5-HT_{2A} antagonist, but no attempts have been made to optimize these MDL 100907 analogues for *in vivo* PET - imaging.

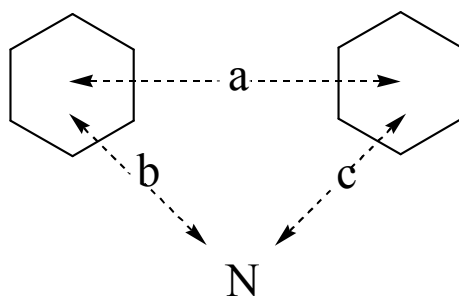


Figure 2: A general pharmacophore model to account for the binding of 5-HT₂ antagonists²¹

Herein, we report the syntheses of new MDL 100907 analogues to enlighten structure-activity relationships. In addition, some new derivatives may be considered as potential ^{18}F -radioligands for 5-HT_{2A} receptor PET imaging.

2. Results and Discussion

2.1 Chemistry

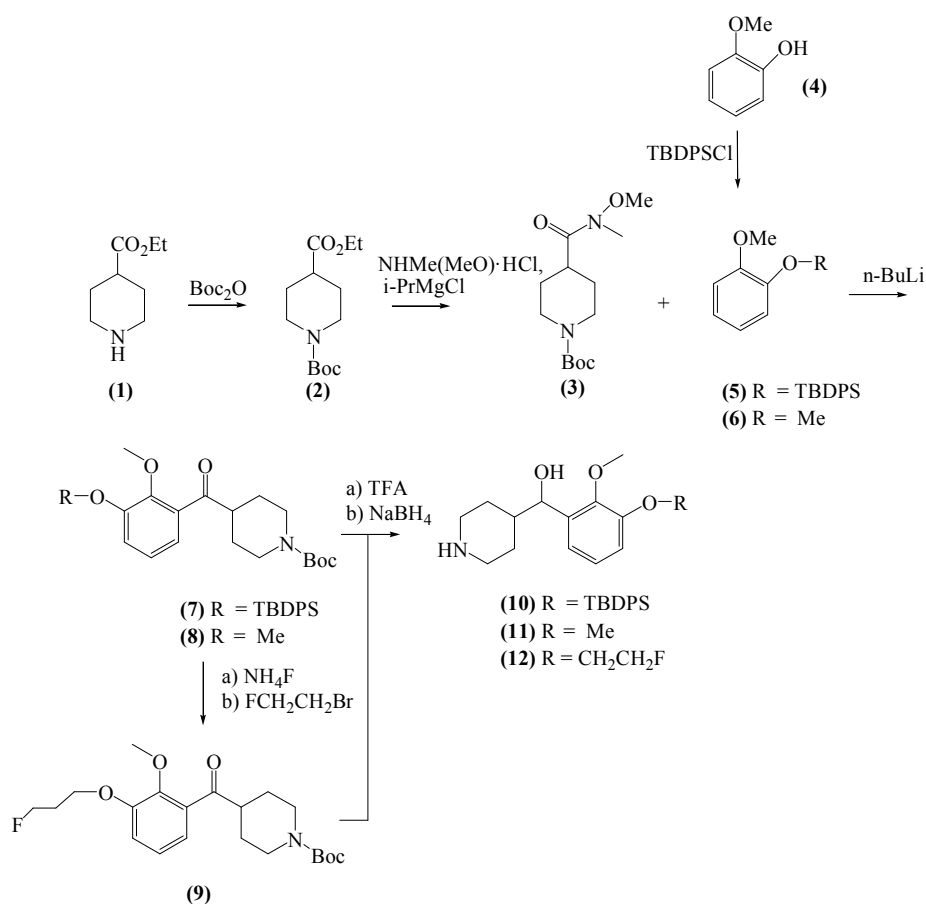
Organic synthesis of MDL 100907 has been described in the literature by Huang et al.¹⁶ and Ullrich and Ice.²³ Both methods depended upon the formation of a Weinreb amide, as a key intermediate, which is then reacted with ortho-lithiated veratrole derivatives to afford the ketone matrix of the MDL 100907 lead structure.

Huang et al.¹⁶ synthesized the racemic phenolic precursor molecule first, and subsequently separated the isomers by chiral derivatization with (S)-(+)- α -methoxyphenyl-acetic acid and flash chromatography. Whereas Ullrich and Ice²³ performed the optical resolution earlier, in particular before adding the p-fluorophenethyl substituent to the piperidine moiety. This strategy also allows introducing a variety of N-substituents.

We decided to follow a similar synthesis route, but in contrast to Ullrich et al.²³ the ketone bodies (**7**) and (**8**) were isolated (Scheme 1). Those compounds permit structure-affinity studies of the ketone group versus the racemic or enantioselective aliphatic secondary alcohol.

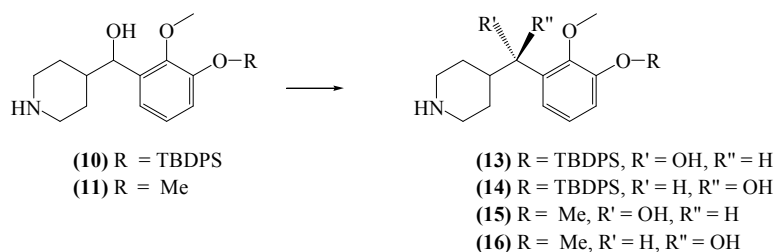
In addition, deprotection of the phenolic hydroxyl group is performed earlier to get versatile access to fluoroethylated reference compounds.

According to the literature,²³ ethylisonipecotate (**1**) was *t*-boc-protected and afterwards transformed to the corresponding Weinreb amide (**3**). Regioselective ortho-lithiated veratrole derivatives (**5/6**) were reacted with the mentioned amide (**3**) to afford the matrix ketone body (**7/8**). Either deprotection of the TBDPS-group with NH₄F followed by fluoroalkylation was performed or direct deprotection of the piperidine moiety with TFA ensued by reduction with NaBH₄ to the racemic alcohol was carried out. Compounds (**9**)-(12) were prepared in this way (Scheme 1).



Scheme 1: Synthesis of MDL 100907 key intermediates

The racemic alcohol could be separated by means of salt formation with (+)- and (-)-mandelic acid (Scheme 2) as reported by Ullrich and Ice.²³



Scheme 2: Optical resolution of (10) and (11)

The diastereomeric salts were isolated and recrystallized twice from methanol. Aqueous work up afforded the enantiomers in high purity, as determined via optical resolution (Table 2).

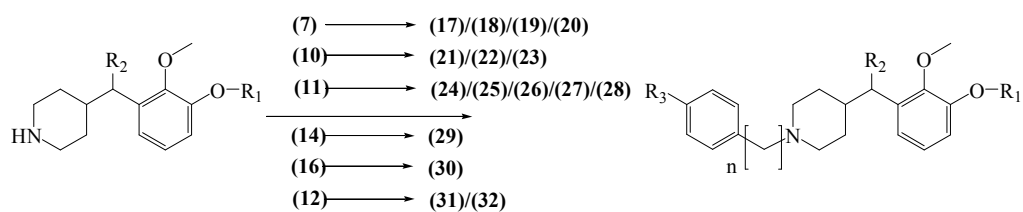
Table 2: Optical resolution of **(13)** – **(16)**

Cmpd#	[α] _D	
	this work	Ref. ²³
(13)	+46.86 (c 0.1, MeOH)	+ 45.5 (c 0.1, MeOH)
(14)	-53.34 (c 0.1, MeOH)	- 46.8 (c 0.1, MeOH)
(15)	- 6.32 (c 0.13; MeOH)	- 7.1 (c 0.1, MeOH)
(16)	+7.04 (c 0.12, MeOH)	+ 6.6 (c 0.1, MeOH)

Enantiomeric excess (ee) of compounds **(13)**-**(16)** was not examined via chiral HPLC. Instead, enantioselective reference compounds and precursors were tested on (ee) via chiral HPLC later on.

In addition, N-alkylation of piperidine derivatives was performed in DMF in yields of 60 – 90 % and provided compounds **(17)**-**(32)** that enable structure-activity studies of the p-substituent of the aromatic ring and of the chain length [(-CH₂)_n with n = 1,2] between the piperidine and phenyl moiety (Scheme 3). Longer chain lengths lead to a higher α_1 and D₂ affinity as reported by Schmidt et al.,²⁴ that is, n > 2 were not considered.

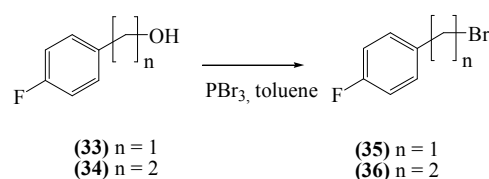
Commercially unavailable (2-bromoethyl)-4-fluorobenzene **(36)** and (1-bromomethyl)-4-fluorobenzene **(35)** were obtained by treatment of 4-fluorophenethyl alcohol **(34)** or (4-fluorophenyl) methanol **(33)** with PBr₃ (Scheme 4). The latter resulted in a heavy lachrymatory substance.



compd#	R ₁	R ₂	compd#	R ₁	R ₂	R ₃	n
7	TBDPS	= O	17	TBDPS	= O	- CH ₃	2
10	TBDPS	- OH	18	TBDPS	= O	- NO ₂	2
11	Me	- OH	19	TBDPS	= O	- OCH ₃	2
14	TBDPS	◀ OH	20	TBDPS	= O	- F	2
16	Me	◀ OH	21	TBDPS	- OH	- NO ₂	2
12	-[CH ₂] ₂ F	- OH	22	TBDPS	- OH	- OCH ₃	2
			23	TBDPS	- OH	- F	2
			24	Me	- OH	- F	1
			25	Me	- OH	- NO ₂	2
			26	Me	- OH	- OCH ₃	2
			27	Me	- OH	- CH ₃	2
			28	Me	- OH	- F	2
			29	TBDPS	◀ OH	- F	2
			30	Me	◀ OH	- F	2
			31	-[CH ₂] ₂ F	- OH	- H	2
			32 (VK-1)	-[CH ₂] ₂ F	- OH	- NO ₂	2

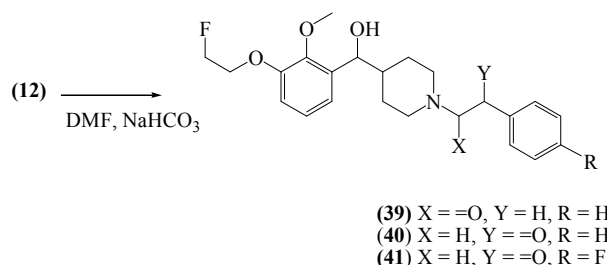
Scheme3: N-alkylation of piperidine derivatives

(general reaction conditions: alkylating agent, DMF, NaHCO₃, 85 °C, 90 min)



Scheme 4: Synthesis of bromo-alkyl-4-fluorobenzenes

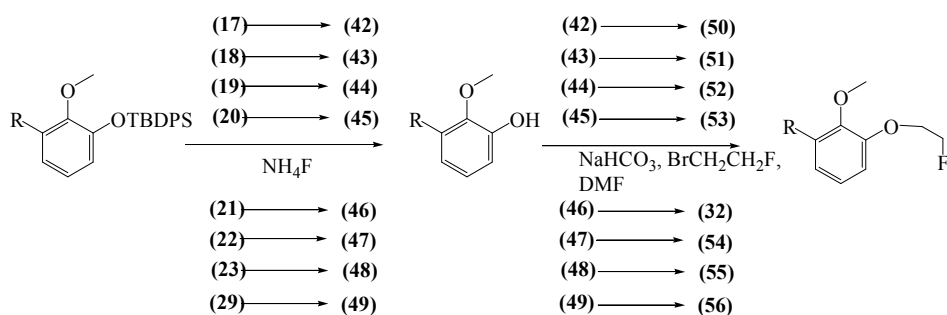
To determine the influence of a carbonyl group between the piperidine and the phenyl moiety, preparation of the three compounds **(39)**-**(41)** were tried to prepare via N-alkylation (Scheme 5).



Scheme 5: Synthesis to carbonyl derivatives of MDL 100907 via N-alkylation

In contrast to **(39)**, both ketone derivatives **(40)**-**(41)** were synthetically not accessible. Even Finkelstein-conditions, variation of solvent and temperature could not alter the synthetic behaviour. Modified reaction characteristics could possibly be due to the electronic withdrawing carbonyl group and could therefore lead to styrene derivatives. These reactive by-products could interact with themselves or other reactants thus forming a broad spectrum of compounds. However, protection of the carbonyl moiety by forming 2-(bromomethyl)-2-(4-fluorophenyl)-1,3-dioxolane **(37)**, and thus reducing the electronic withdrawing effect, could not overcome the problem. N-Alkylation to (3-(2-fluoroethoxy)-2-methoxyphenyl)(1-((2-(4-fluorophenyl)ethyl)-1,3-dioxolan-2-yl)methyl)piperidin-4-yl)methanol **(38)** was not accessible probably due to steric effects.

Deprotection of the phenolic hydroxy moiety with NH_4F or with K_2CO_3 overnight lead to high yields of $> 75\%$. Precursors **(42)**-**(49)** were prepared in such a way. In addition, reference compounds **(50)**-**(56)** were synthesized by fluoroalkylation with 1,2-bromofluoroethane (Scheme 6).

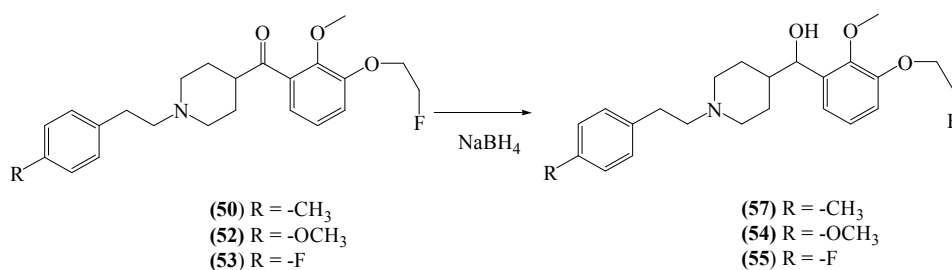


cmpd#	R	R ₁	R ₂	cmpd#	R	R ₁	R ₂
42		= O	-CH ₃	50		= O	-CH ₃
43		= O	-NO ₂	51		= O	-NO ₂
44		= O	- OCH ₃	52		= O	-OCH ₃
45		= O	-F	53 [MA-1]		= O	-F
46		-OH	-NO ₂	32 [VK-1]		-OH	-NO ₂
47		-OH	- OCH ₃	54		-OH	-OCH ₃
48		-OH	-F	55 [MH.MZ]		-OH	-F
49		◀ OH	-F	56 [(R)-MH.MZ]		◀ OH	-F

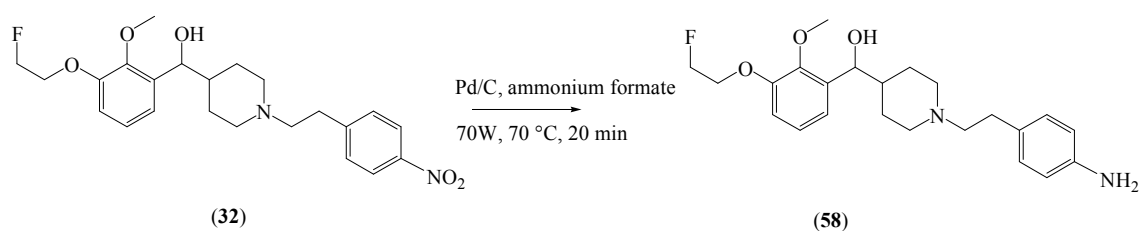
Scheme 6: Deprotection and fluoroalkylation of various MDL 100907 derivatives

Alternatively, MH.MZ (**55**) and (**54**) could be prepared by reduction of their carbonyl derivatives with NaBH₄. Similarly, compound (**57**) could also be obtained via that reaction route (Scheme 7).

Finally, an amine MDL 100907 derivative (**58**) was synthesized by reduction of the NO₂-compound (**32**) in a microwave oven (CEM LabMate) (Scheme 8).



Scheme 7: Reduction of carbonyl-compounds to their corresponding alcohol derivatives



Scheme 8: Synthesis of (58) by reduction of (32) in a microwave oven

Enantiomeric excess of (R)-MH.MZ (56) and (R)-MDL 100907 (30) was determined by chiral HPLC analysis (Figure 3). Purities of ee > 98 % were detected.

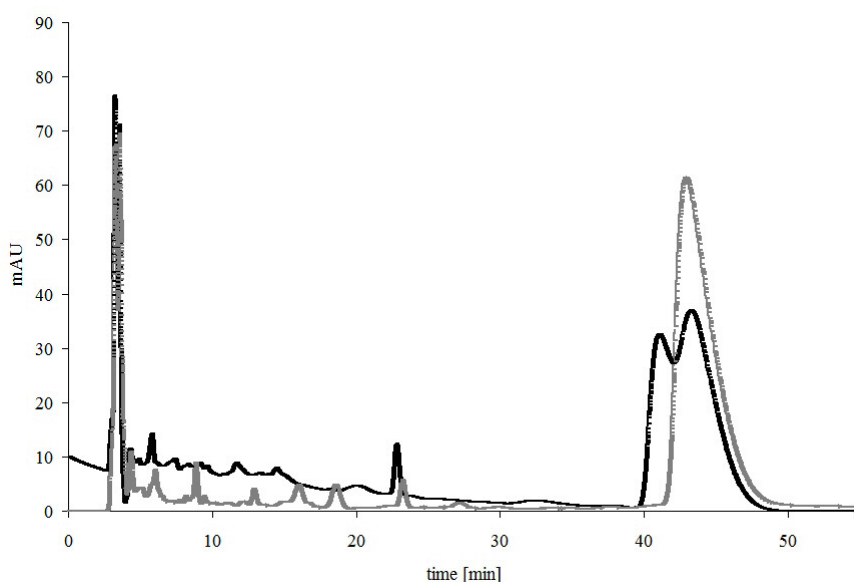


Figure 3: Chiral HPLC analyses of (R)-MH.MZ: The black line represents the racemate (MH.MZ); in contrast, the grey line shows the enantioselective pure compound (R)-MH.MZ

2.2 Lipophilicities

The lipophilicities of promising compounds were determined using the HPLC method according to Krass et al.²⁵ Soerensen buffer was used as eluent and logP values were calculated from retention times of the respective substances. The calculated logP values are displayed in table 3.

Table 3: Lipophilicities / logP values of altanserin, MDL 100907 and new MDL 100907 derivatives*

Reference compounds			Precursors	
Name	Cmpd#	LogP	Cmpd#	LogP
altanserin	-	2.15	(48)	2.27
(R)-MDL 100907	(30)	2.98	(46)	1.90
MDL 100907	(28)	2.98		
MH.MZ	(55)	2.80		
(R)-MH.MZ	(56)	2.80		
MA-1	(53)	3.08		
VK-1	(32)	2.37		
	(57)	3.40		
	(50)	3.64		
	(54)	2.72		
	(51)	2.71		
	(52)	3.02		
	(39)	1.57		
	(31)	2.92		

All new fluoroethylated reference compounds besides (39), (50) and (57) examined showed logP values between 2 and 3, ranging within those found for already established radiotracers such as altanserin and MDL 100907 (Table 3). Rowley et al. pointed out that a logP between 2 and 3 presents the ideal interval for small molecules for penetrating the blood-brain-barrier (BBB).²⁶ This fact gives rise to the assumption that the new compounds may have similarly good properties for molecular imaging.

As expected, logP values of precursors (46) and (48) are reduced by 0.4 compared to their corresponding reference compounds VK-1 (32) and MH.MZ (55) probably resulting in less

BBB penetrating ligands, which are formed by the metabolic cleavage of the ether. For compound (48), MDL 105725, this behaviour has already been observed.¹⁸ Comparison of ketone- versus hydroxyl moieties shows a 0.3 higher lipophilicity for carbonyl compounds, see, for example (53)-(55). MDL 100907 (28), MH.MZ (55) and MDL 105725 (48) indicate the expected descending order of lipophilicity. However, logP values of MDL 100907 (28) and MH.MZ (55) differ not much and therefore, similar lipophilicities should be expected. Influence of p-substitution of the aryl moiety was examined and showed the expected ascending tendency $-\text{NO}_2 < -\text{OMe} < -\text{F} < -\text{H} < -\text{Me}$.

In conclusion, almost all reference compounds besides (39), (50) and (57) demonstrated favourable lipophilicity and therefore should have good *in vivo* properties. In comparison, relevant labelling precursors, which could be possibly formed via metabolism of the parent, should penetrate the BBB less because of their reduced logP values.

2.3 Receptor characterization

2.3.1 Affinity towards the 5-HT_{2A} receptor

5-HT_{2A} receptor affinity was determined by a radioligand competition binding assay with GF-62 cells, a clonal cell line expressing high amounts (5-7 pmol/mg) of the 5-HT_{2A} receptor. The test tubes contained [³H]MDL (0.2 nM) and seven different concentrations of the test compounds (1 μM - 1 pM) in a total of 1 mL assay buffer. Ketanserin (1 μM) was added to determine non-specific binding. Binding affinities of the tested compounds are shown in table 4.

The tested compounds had affinities to the 5-HT_{2A} receptor in the nanomolar range, except (24) and (39). Both compounds are varied between the piperidine and phenyl ring. Shortening the chain length from n=2 to n=1 lead to a total loss of affinity towards the 5-HT_{2A} receptor and is therefore in accordance with the receptor model suggested by Andersen et al.²¹ It describes the ideal distance between the phenyl moieties to be 8.1 Å. Introducing an amide between the piperidine and phenyl ring reduced the affinity by a factor of 2000. This is probably due to the lower basic characteristic properties of the resulting compound than the

original tertiary amine structure.

Table 4: Affinities of tested ligands towards the 5-HT_{2A} receptor*

Name	Cmpd#	Ki [nM]	Cmpd#	Ki [nM]
altanserin	-	0.72 ± 0.19	(31)	1.63 ± 5.50
(R)-MDL 100907	(30)	0.38 ± 0.05	(39)	1987 ± 360
MDL 100907	(28)	2.10 ± 0.13	(45)	1.34 ± 0.48
MH.MZ	(55)	9.02 ± 2.11	(48)	1.24 ± 0.23
(R)-MH.MZ	(56)	0.72 ± 0.21	(49)	0.25 ± 0.06
MA-1	(53)	3.23 ± 0.18	(50)	4.56 ± 0.73
VK-1	(32)	26.0 ± 6.70	(51)	138 ± 20.0
	(24)	> 1000	(52)	153 ± 93.0
	(25)	90 ± 71.0	(54)	59 ± 54.0
	(26)	55 ± 12.0	(57)	1.83 ± 0.43
	(27)	0.31 ± 0.06	(58)	2.06 ± 0.96

Moreover, replacing the 3-methoxy- by a fluoroethoxy group slightly reduces the 5-HT_{2A} affinity but the remaining compound is still within the nanomolar range of the parent, for example (28)-(55), (30)-(56) and (27)-(57). However, 3-hydroxy derivatives (48)-(55) had a better affinity. In contrast, introducing a methoxy- or a nitro-moiety to the phenethyl group resulted in a reduced affinity by a factor of ~20 for methoxy- and by a factor of ~40 for nitro-derivatives, for example (28)-(25)-(26) or (53)-(52)-(51). One exception to the mentioned results was found by analyzing compounds (32) and (54). Indeed, replacing the fluorine atom of MH.MZ (55) by a nitro- or a methoxy group leads to a decreased affinity, but only by factor ~ 3 for the nitro- and by factor ~ 7 for the methoxy compound. Interestingly, reduction of affinity appears not so harsh and vice versa in that case compared with (28)-(25)-(26) and (53)-(52)-(51). Therefore, we speculate that (32) and (54) could fit differently in the binding pocket. Nevertheless, all compounds of these series show medium affinity towards the 5-HT_{2A} receptor. Besides, replacing the p-substituent of the phenethyl moiety by a methyl group, an amine or a single proton leads to a slightly increased affinity, for example (28)-(27) and (55)-(58)-(57). This may probably be due to the slightly different space required. Changing the racemic secondary hydroxy group to a ketone group [(28)-(53); (57)-(50)]

showed no dramatic effects but as expected, the enantioselective pure product (**56**) showed increased affinity than the carbonyl (**53**) and racemic compounds (**28**).

2.3.2 Selectivity of promising ligands

Promising 5-HT_{2A} affinity compounds (**32**) and (**50**)-(b57) were assayed for their selectivity for other 5-HT receptor subtypes (Table 5).

Table 5: Ligand affinities to 5-HT receptors

	K _i [nM] [*]								
	MA-1 (53)	(R)-MH.MZ (56)	MH.MZ (55)	(50)	(57)	(51)	VK-1 (32)	(52)	(54)
5-HT _{1A}	1681 ± 97	>10000	>10000	1883 ± 158	>10000	1723 ± 239	>10000	991 ± 135	>10000
5-HT _{1B}	2174 ± 336	884 ± 106	1846 ± 426	3359 ± 676	4886 ± 1081	>10000	>10000	>10000	>10000
5-HT _{1D}	713 ± 124	1062 ± 186	706 ± 109	n.d.	1440 ± 253	1835 ± 259	3418 ± 512	1436 ± 196	>10000
5-HT _{1E}	>10000	>10000	>10000	>10000	>10000	>10000	>10000	>10000	>10000
5-HT _{2A}	3.23 ± 0.18	0.72 ± 0.21	9.02 ± 2.11	4.56 ± 0.73	1.83 ± 0.43	118 ± 20.0	26.0 ± 6.70	153 ± 93.0	59 ± 54
5-HT _{2B}	960 ± 113	320 ± 27	299 ± 27	559 ± 58	466 ± 51	1052 ± 111	1844 ± 183	1972 ± 181	2751 ± 289
5-HT _{2C}	128 ± 14	53 ± 7	71 ± 10	497 ± 72	508 ± 70	>10000	>10000	9417 ± 2798	>10000
5-HT ₃	>10000	>10000	>10000	>10000	>10000	>10000	>10000	>10000	>10000
5-HT _{5A}	1584 ± 270	6814 ± 982	>10000	1684 ± 287	>10000	>10000	>10000	>10000	>10000
5-HT ₆	>10000	3842 ± 623	3890 ± 1921	>10000	>10000	>10000	>10000	>10000	>10000
5-HT ₇	210 ± 38	59 ± 11	116 ± 14	731 ± 117	498 ± 77	6241 ± 847	5170 ± 642	2862 ± 430	>10000

* K_i values in nM ± SEM are based on the means of 4 experiments; n.d. (not determined)

Besides a medium affinity of MH.MZ (**55**) towards the 5-HT₇ (K_i = 116 ± 14 nM), and the 5-HT_{2C} receptor (K_i = 71 ± 10 nM), all other tested receptors showed affinities in the μM range. Thus, MH.MZ (**55**) (5-HT_{2A}: K_i = 9.02 ± 2.11 nM) is a selective ligand for the 5-HT_{2A} receptor. Furthermore, the enantioselective derivative (R)-MH.MZ (**56**) even showed a better selectivity profile, whereas MA-1 (**53**) showed a good affinity towards the 5-HT_{2A} receptor (K_i = 3.23 ± 0.18 nM) and a medium affinity towards the 5-HT_{2C} receptor (K_i = 128 ± 14 nM). Moreover, the introduced carbonyl group within MA-1 (**53**) leads to a slightly affine compound of the 5-HT_{1A} receptor (K_i = 1681 ± 97 nM) compared to its structural related hydroxyl group derivatives MH.MZ (**55**) and (R)-MH.MZ (**56**). But still MA-1 (**53**) is a selective 5-HT_{2A} ligand. All other tested compounds (**32**), (**50**), (**51**), (**52**), (**54**) and (**57**) showed a similar behaviour regarding the 5-HT_{2A} selectivity.

Moreover, high 5-HT_{2A} affinity compounds (**50**), (**53**), (**56**), and (**57**) were also assayed for a broad spectrum of receptors and monoamine transporters in competitive binding experiments *in vitro* using cloned human receptors or transporters (Table 6). Interestingly, new compounds, (**50**), (**53**), (**56**), and (**57**), have no affinity to Beta1-3, H4, M1-M5, DOR, KOR receptors. Minor affinity towards the other tested receptors and transporters (D1-D5, H1-H2, DAT, SERT, MOR, sigma 2, alpha 1A-2B) is summarized in Table 6.

Table 6: Affinities to a broad spectrum of neuroreceptors and transporters of MDL 100907 derivatives

	K _i [nM] [*]				
	MA-1 (53)	(R)-MH.MZ (56)	MH.MZ (55)	(50)	(57)
D1	1410	3828	899	1930	1759
D2	3828	2686	>10000	>10000	>10000
D4	174	442	544	923	2708
D5	7398	7419	n.d.	n.d.	n.d.
Beta3	>10000	>10000	>10000	>10000	>10000
H1	944	509	374	665	439
H2	1757	2428	3178	827	1156
H3	>10000	>10000	>10000	9033	>10000
Sigma 2	86	923	n.d.	228	676
Alpha 1A	146	335	n.d.	n.d.	n.d.
Alpha 1B	550	500	325	n.d.	>10000
Alpha 2A	863	>10000	>10000	n.d.	>10000
Alpha 2C	333	n.d.	148	154	143
DAT	>10000	>10000	>10000	n.d.	>10000
SERT	3087	2207	3516	1009	2646
MOR	>10000	>10000	>10000	2009	>10000

* K_i values in nM ± SEM are based on the means of 4 experiments; n.d. (not determined)

3. Conclusion

A series of novel MDL 100907 derivatives containing a fluorine atom were synthesized and evaluated for their *in vitro* behaviour. Structure-Activity Relationships (SARs) studies suggested that the tested compounds had affinities to the 5-HT_{2A} receptor in the nanomolar range except (**24**) and (**39**), which are varied between the piperidine and phenyl ring. This is in accordance with the rudimental pharmacophore model that has been published by Andersen et al.²¹ Replacing the 3-methoxy by a fluoroethoxy group slightly reduces the 5-HT_{2A} affinity but still the affinity is within the nanomolar range of the parent, for example (**28**)-(55), (**30**)-(56) and (**27**)-(57). The 3-hydroxy derivatives (**48**)-(55) had a better affinity. In contrast, introducing a methoxy or a nitro moiety to the phenethyl group results in a reduction of

affinity to medium affine compounds ($K_i \sim 1 \mu\text{M}$). Besides, replacing the p-substituent of the phenethyl moiety by a methyl group, an amine or a single proton slightly increases the affinity, for example (28)-(27) and (55)-(58)-(57). This could be due to the slightly different space required. Changing the racemic secondary hydroxyl group to a ketone group [(28)-(53); (57)-(50)] causes no dramatic effects but as expected, the enantioselective pure product (56) enhances the affinity than the carbonyl (53) and the racemic compound (28). Furthermore, 5-HT_{2A} affine compounds (Table 5 and 6) were tested for selectivity. All tested ligands thereby showed a reasonable receptor profile and determined them as 5-HT_{2A} selective compounds. Except for (39), (50) and (57), all our fluoroethylated compounds had logP values between 2 and 3, that is within range of those of already established radiotracers such as altanserin and MDL 100907.

The novel compounds MA-1 (53) and (R)-MH.MZ (56) seem to be promising high affinity compounds for ¹⁸F-PET-tracer due to their K_i -values in the nanomolar range of 1–10 towards the 5-HT_{2A} receptor and their insignificant binding to other 5-HT receptor subtypes or receptors. Interestingly, compounds MA-1 (53), MH.MZ (55) and (R)-MH.MZ (56) showed a receptor selectivity profile similar to MDL 100907, which is slightly improved compared to that of altanserin. Therefore, the mentioned compounds could possibly be preferable antagonistic ¹⁸F-tracers for visualization of the 5-HT_{2A} status. Medium affine compounds (VK-1 (32), (51), (52) and (54)) have K_i values of 30 to 120 nM which are in the range of endogenous serotonin (according to PDSP). Challenging experiments with those compounds to measure changes in the endogenous serotonin level could be possible and allow a deeper insight in the serotonin system.

In extension to the *in vitro* data discussed concerning the SAR of the new fluorine containing MDL 100907 derivatives, ¹⁸F-fluoroethylation and small μPET studies are planned to exam the *in vivo* characteristics of the potential 5-HT_{2A} ligands. In particular, a comparison of [¹⁸F]MH.MZ to [¹⁸F]altanserin and other ¹⁸F-labelled MDL 100907 derivatives should be done.

4. Experimental

4.1 General

4.1.1 Chemicals, flash chromatographies and TLC

Chemicals were purchased from ABX, Acros, Aldrich, Fluka, Merck or Sigma. Unless otherwise noted all chemicals were used without further purification. Moisture sensitive reactions were carried out under an argon or nitrogen atmosphere using dry solvents over molecular sieve.

Chromatographic purifications were conducted on Silica gel 60 (0.040–0.063 mm, Acros) columns. TLCs were run on pre-coated plates of Silica gel 60F₂₅₄ (Merck).

4.1.2 Analytical HPLC

Systems were equipped with a Sykam S 1100 Solvent Delivery System, S 8110 Low Pressure Gradient Mixer, Rheodyne 9725i Inject Valve; Linear UVIS-205 Absorbance Detector; Axxiom Chromatography 900-200 Pyramid; Pyramid 2.07; loop: 20 μ L.

4.1.3 Spectroscopy

300 and 400 MHz NMR spectra were recorded on a Bruker 300 MHz-FT-NMR-spectrometer AC 300 or on a Bruker-Biospin DRX 400 MHz spectrometer. Chemical shifts were reported in parts per million (ppm). FD mass spectrometry was performed on a Finnigan MAT90-Spectrometer. Optical rotations were determined with a polarimeter Perkin-Elmer 241 using 10 cm, 1 mL cell.

4.1.4 Microwave

Syntheses were carried out in a commercially available microwave oven (CEM LabMate).

4.2 Chemistry

4.2.1 **4-(N-Methoxy-N-methyl-carboxamido)-1-piperidinecarboxylic acid *t*-butyl ester (3)**. 4-(N-Methoxy-N-methyl-carboxamido)-1-piperidinecarboxylic acid *t*-butyl ester (**3**) was synthesized as described by Carr et al.²⁷

4.2.2 ***t*-Butyldiphenylsilyl-guaiacol (5)**. *t*-Butyldiphenylsilyl-guaiacol (**5**) was synthesized as described by Mathis et al.²⁸

4.2.3 **4-(2-Methoxy-3-(*t*-butyldiphenylsilyloxy)-benzoyl)-1-piperidinecarboxylic acid *t*-butyl ester (7)** and **4-(2,3-Bismethoxy-benzoyl)-1-piperidinecarboxylic acid *t*-butyl ester (8)**. *n*-Butyllithium (64.5 mL of a 2.5 M solution in hexane, 161 mmol) was added to a stirred solution of *t*-butyldiphenylsilyl-guaiacol (**5**) or veratrole (**6**) (161 mmol) under nitrogen at 0 °C. The ice bath was removed and the solution was allowed to stir for 2 h. After cooling to -50 °C, 4-(N-methoxy-N-methyl-carboxamido)-1-piperidinecarboxylic acid *t*-butyl ester (**3**) (153 mmol) was added dropwise to the stirred solution, followed by warming to room temperature and stirring for 2 h. Saturated aqueous NH₄Cl was added; the layers were separated and the aqueous layer was extracted 3x with ether. The combined organic extracts were washed with brine, dried (Na₂SO₄), filtered and evaporated to afford the crude product. Chromatography of the residue gave the pure product.

4-(2-Methoxy-3-(*t*-butyldiphenylsilyloxy)-benzoyl)-1-piperidinecarboxylic acid *t*-butyl ester (7). 21 g (**5**) (58 mmol), *n*-BuLi (120 mmol), 15.9 g (**3**) (58 mmol) and 150 mL dry THF yielded 14.8 g of (**7**) (25.8 mmol; 44 %). *R*_f 0.43 (silica gel, 5:1 PE/EtOAc). ¹H-NMR: (300 MHz, CDCl₃) δ [ppm] = 7.702 (dd, 4H); 7.421-7.322 (m, 6H); 6.832 (t, 1H); 6.685 (t, 1H); 6.617 (dd, 1H); 4.053 (d, 2H); 3.901 (s, 3H); 3.176 (tt, 1H); 2.827 (dt, 2H); 1.764 (dd, 2H); 1.527 (dd, 2H); 1.444 (s, 9H); 1.113 (s, 9H) MS (FD) *m/z* (% rel Int.): 573.4 (100.0 [M]⁺); 574.4 (44.8 [M+1]⁺); 575.4 (14.2 [M+2]⁺)

4-(2,3-Bismethoxy-benzoyl)-1-piperidinecarboxylic acid *t*-butyl ester (8)

10.65 g veratrole (**6**) (58 mmol), *n*-BuLi (77 mmol), 20.63 g (**3**) (74.3 mmol), 200 mL dry THF yielded 18 g of (**8**) (51.72 mmol; 68 %). *R*_f 0.27 (silica gel, 4.5:1 PE/EtOAc). ¹H-NMR:

(300 MHz, CDCl₃) δ [ppm] = 7.087-6.922 (m, 3H); 4.095-4.048 (m, 2H); 3.861 (s, 3H); 3.832 (s, 3H); 3.241-3.167 (m, 1H); 2.839-2.747 (m, 2H); 1.843-1.789 (dd, 2H); 1.611-1.490 (m, 2H); 1.414 (s, 9H) **MS (FD) m/z (% rel Int.):** 349.4 (100.0 [M]⁺); 350.4 (20.69 [M+1]⁺)

4.2.4 General procedure for TBDPS-deprotection: A solution of TBDPS-protected substance (4 mmol) and NH₄F (9 mmol) in anhydrous MeOH (30 mL) was stirred for 15 min at 70 °C. After evaporation of the solvent, the residue was taken up in NH₄OH and extracted 3x with CHCl₃. The combined organic extracts were washed with brine, dried (Na₂SO₄), filtered and evaporated. Chromatography of the residue gave the pure product.

4-(3-Hydroxy-2-methoxy-benzoyl)-1-piperidinecarboxylic acid *t*-butyl ester (9a). 0.75 g (7) (1.31 mmol), 0.41 g NH₄F (5.54 mmol), 15 mL MeOH yielded 0.27 g of (9a) (0.8 mmol; 61 %). R_f 0.32 (silica gel, 1:1 PE/EtOAc). **¹H-NMR (300 MHz, CDCl₃) δ [ppm]** = 7.079-6.917 (m, 3H); 6.151 (bs, 1H); 4.065 (d, 2H); 3.779 (s, 3H); 3.211 (tt, 1H); 2.816 (t, 2H); 1.787 (dd, 2H); 1.639-1.496 (m, 2H); 1.427 (s, 9H) **MS (FD) m/z (% rel Int.):** 473.3 (100.0 [M]⁺); 474.3 (56.7 [M+1]⁺); 475.3 (12.5 [M+2]⁺)

4-(3-Hydroxy-2-methoxy-benzoyl)-1-(2-*p*-toluylethyl)-piperidine (42). 0.88 g (17) (1.49 mmol), 0.2 g NH₄F (2.64 mmol), 30 mL MeOH yielded 185 mg of (42) (0.52 mmol; 35 %). R_f 0.45 (silica gel, 8:1 CHCl₃/MeOH). **¹H-NMR (300 MHz, CDCl₃) δ [ppm]** = 7.173-6.882 (m, 7H); 3.789 (s, 3H); 3.200-3.154 (m, 1H); 3.077-3.038 (m, 2H); 2.889-2.852 (m, 3H); 2.436 (bs, 1H); 2.277 (s, 3H); 2.038-2.005 (m, 2H); 1.934-1.812 (m, 2H) **MS (FD) m/z (% rel Int.):** 354.3 (100.0 [M]⁺); 353.3 (98.37 [M-1]⁺); 475.3 (12.5 [M+2]⁺)

4-(3-Hydroxy-2-methoxy-benzoyl)-1-(2-*p*-nitrophenylethyl)-piperidine (43). 900 mg (18) (1.45 mol), 300 mg NH₄F (8 mmol), 16 mL dry MeOH yielded 475 mg of (43) (1.23 mmol; 86 %). R_f 0.55 (silica gel, 8:1 CHCl₃/MeOH). **¹H-NMR (300 MHz, CDCl₃) δ [ppm]** = 8.118 (dt, 2H); 7.320 (dt, 2H); 7.073-6.994 (m, 2H); 6.930 (dd, 1H); 3.905 (t, 1H); 3.784 (s, 3H); 3.095 (t, 1H); 2.998-2.864 (m, 4H); 2.635 (t, 2H); 2.204 (t, 2H); 1.884 (bd, 2H); 1.826-1.689 (m, 2H) **MS (FD) m/z (% rel Int.):** 384.2 (100.0 [M]⁺); 385.2 (66.1 [M+1]⁺); 386.2 (13.3 [M+2]⁺)

4-(3-Hydroxy-2-methoxy-benzoyl)-1-(2-p-methoxyphenylethyl)-piperidine (44). 591 mg (**19**) (0.88 mmol), 0.9 g NH₄F (24 mmol), 20 mL MeOH yielded 290 mg of (**44**) (0.78 mmol; 80 %). R_f 0.53 (silica gel, 8:1 CHCl₃/MeOH). ¹H-NMR (300 MHz, CDCl₃) δ [ppm] = 7.193-7.076 (m, 3H); 7.005 (t, 1H); 6.915 (dd, 1H); 6.801 (dt, 2H); 3.790 (s, 3H); 3.751 (s, 3H); 3.298 (bs, 1H); 3.092 (bs, 2H); 2.918 (dt, 4H); 2.884-2.594 (m, 2H); 2.174 (bs, 2H); 2.044-1.905 (m, 2H) **MS (FD) m/z (% rel Int.):** 369.2 (100.0 [M]⁺); 370.2 (62.1 [M+1]⁺); 371.2 (11.7 [M+2]⁺)

4-(3-Hydroxy-2-methoxy-benzoyl)-1-(2-p-fluorophenylethyl)-piperidine (45). 2.99 g (**20**) (5 mmol), 0.91 g NH₄F (12.43 mmol), 30 mL MeOH yielded 1.65 g of (**45**) (4.63 mmol; 92 %). R_f 0.64 (silica gel, 5:1 CHCl₃/MeOH). ¹H-NMR (300 MHz, CDCl₃) δ [ppm] = 7.144-6.906 (m, 7H); 3.785 (s, 3H); 3.108-2.967 (m, 3H); 2.814-2.759 (m, 2H); 2.611-2.557 (m, 2H); 2.192 (bs, 2H); 1.935-1.766 (m, 4H) **MS (FD) m/z (% rel Int.):** 358.2 (100.0 [M]⁺); 359.2 (17.19 [M+1]⁺)

(3-Hydroxy-2-methoxyphenyl)-(1-(2-p-nitrophenylethyl)-piperidine-4-yl)-methanol (46). 932 mg (**21**) (1.5 mmol), 300 mg NH₄F (8 mmol), 20 mL MeOH yielded 515 mg of (**46**) (1.33 mmol; 89%). R_f 0.52 (silica gel, 8:1 CHCl₃/MeOH). ¹H-NMR (300 MHz, CDCl₃) δ [ppm] = 9.202 (s, 1H); 8.111 (d, 2H); 7.490 (d, 2H); 6.889-6.679 (m, 2H); 4.891 (d, 1H); 4.552 (t, 1H); 3.684 (s, 3H); 3.333 (bs, 1H); 3.039-2.795 (m, 4H); 2.589-2.487 (m, 4H); 2.015-1.689 (m, 2H); 1.429 (bs, 1H); 1.330-1.119 (m, 2H) **MS (FD) m/z (% rel Int.):** 386.9 (100.0 [M]⁺); 387.9 (20.5 [M+1]⁺)

(3-Hydroxy-2-methoxyphenyl)-(1-(2-p-methoxyphenylethyl)-piperidine-4-yl)-methanol (47). 420 mg (**22**) (0.69 mmol), 600 mg NH₄F (16 mmol), 15 mL MeOH yielded 223 mg of (**47**) (0.6 mmol; 87 %). R_f 0.26 (silica gel, 8:1 CHCl₃/MeOH). ¹H-NMR (300 MHz, CDCl₃) δ [ppm] = 7.065 (dt, 2H); 6.985-6.752 (m, 5H); 4.635 (d, 1H); 3.788 (s, 3H); 3.743 (s, 3H); 3.177 (dd, 2H); 2.887 (d, 1H); 2.779 (dt, 4H); 2.221 (q, 1H); 2.108 (d, 2H); 1.709 (q, 1H); 1.535 (q, 1H); 1.318 (d, 1H) **MS (FD) m/z (% rel Int.):** 371.0 (100.0 [M]⁺); 372.0 (71.9 [M+1]⁺)

(3-Hydroxy-2-methoxyphenyl)-(1-(2-p-fluorophenylethyl)-piperidine-4-yl)-methanol

(48). 1 g **(23)** (1.82 mmol), 0.71 g NH₄F (9.6 mmol), 30 mL MeOH yielded 0.65 g of **(48)** (1.8 mmol; 95 %). R_f 0.64 (silica gel, 5:1 CHCl₃/MeOH). ¹H-NMR (300 MHz, CDCl₃) δ [ppm] = 7.083-7.181 (m, 2H); 6.811-7.073 (m, 5H); 4.649 (d, 1H); 3.810 (s, 3H); 3.063-3.175 (m, 1H); 2.884-3.004 (m, 1H); 2.768 (t, 2H); 2.542 (t, 2H); 1.855-2.147 (m, 3H); 1.624-1.797 (m, 1H); 1.197-1.586 (m, 3H) **MS (FD) m/z (% rel Int.):** 360.5 (100.0 [M]⁺); 359.5 (55.81 [M-1]⁺); 361.4 (14.00 [M+1]⁺); 358.5 (11.09 [M-2]⁺)

(R)-(3-Hydroxy-2-methoxyphenyl)-(1-(2-p-fluorophenylethyl)-piperidine-4-yl)-methanol

(49). 1 g **(29)** (1.82 mmol), 0.71 g NH₄F (9.6 mmol), 30 mL MeOH yielded 0.64 g of **(49)** (1.75 mmol; 93%). R_f 0.6 (silica gel, 5:1 CHCl₃/MeOH). ¹H-NMR (300 MHz, CDCl₃) δ [ppm] = 7.087-7.180 (m, 2H); 6.814-7.079 (m, 5H); 4.643 (d, 1H); 3.816 (s, 3H); 3.066-3.172 (m, 1H); 2.881-3.008 (m, 1H); 2.767 (t, 2H); 2.541 (t, 2H); 1.852-2.145 (m, 3H); 1.623-1.792 (m, 1H); 1.197-1.586 (m, 3H) **MS (FD) m/z (% rel Int.):** 360.5 (100.0 [M]⁺); 359.5 (52.98 [M-1]⁺); 361.4 (11.77 [M+1]⁺); 358.5 (11.34 [M-2]⁺) [α]_D = + 16.65 (c 0.1; MeOH)

4.2.5 Alkylating procedure for 1,2-bromofluoroethane: NaH (0.42 mmol) was gradually added to the corresponding phenolic derivatives (0.42 mmol) diluted in 20 mL of dry, cold DMSO (0 °C) and stirred for 30 min. To the resulted mixture 1,2-bromofluoroethane (0.42 mmol) was injected slowly and afterwards stirred for 20 h at 60 °C. After evaporation of the solvent, the residue was taken up in EtOAc, washed with H₂O and brine and finally extracted 3x with EtOAc. The combined organic extracts were dried (Na₂SO₄), filtered and evaporated. Chromatography of the residue gave the pure product.

4-(3-(2-Fluoroethoxy)-2-methoxybenzoyl)-1-piperidinecarboxylic acid *t*-butyl ester (9)

6.27 g **(9a)** (20 mmol), 481 mg NaH (20 mmol), 2.54 g 1,2-bromofluoroethane (20 mmol), 100 mL dry DMF yielded 7.77 g of **(9)** (20 mmol; 100 %). R_f 0.79 (silica gel, 20:1 CHCl₃/MeOH). ¹H-NMR (300 MHz, CDCl₃) δ [ppm] = 7.083-6.978 (m, 3H); 4.856 (t, 1H); 4.698 (t, 1H); 4.296 (t, 1H); 4.201 (t, 1H); 4.047 (br d, 2H); 3.882 (s, 3H); 3.215 (tt, 1H); 2.800 (t, 2H); 1.806 (dd, 2H); 1.623-1.478 (m, 2H); 1.423 (s, 9H) **MS (FD) m/z (% rel Int.):** 381.3 (100.0 [M]⁺); 382.3 (17.49 [M+1]⁺); 383.3 (1.57 [M+2]⁺)

(3-(2-Fluoroethoxy)-2-methoxyphenyl)-(1-(2-p-nitrophenylethyl)-piperidine-4-yl)-methanol (VK-1) (32). 415 mg (**46**) (1 mmol), 24 mg NaH (1 mmol), 0.13 g 1,2-bromofluoroethane (1 mmol), 10 mL dry DMF yielded 430 mg of (**32**) (0.93 mmol; 93 %). R_f 0.64 (silica gel, 8:1 CHCl₃/MeOH). ¹H-NMR (300 MHz, CDCl₃) δ [ppm] = 8.095-8.123 (d, 2H); 7.314-7.343 (d, 2H); 7.010 (t, 1H); 6.907 (d, 1H); 6.822 (d, 1H); 4.845 (q, 1H); 4.688 (q, 1H); 4.611 (d, 1H); 4.274 (t, 1H); 4.180 (t, 1H); 3.888 (s, 3H); 3.078 (d, 1H); 2.918 (t, 3H); 2.602 (t, 2H); 1.938-2.120 (m, 3H); 1.612-1.750 (m, 1H); 1.205-1.573 (m, 4H) **MS (FD) m/z (% rel Int.):** 432.0 (100.0 [M]⁺); 433.0 (45.8 [M+1]⁺); 434.0 (8.0 [M+2]⁺)

4-(3-(2-Fluoroethoxy)-2-methoxy-benzoyl)-1-(2-p-toluylethyl)-piperidine (50). 150 mg (**42**) (0.42 mmol), 10.1 mg NaH (0.42 mmol), 53.45 mg 1,2-bromofluoroethane (0.45 mmol), 20 mL dry DMF yielded 150 mg of (**50**) (0.38 mmol; 91 %). R_f 0.69 (silica gel, 12:1 CHCl₃/MeOH). ¹H-NMR (300 MHz, CDCl₃) δ [ppm] = 7.094-6.997 (m, 7H); 4.868-4.841 (m, 1H); 4.710-4.683 (m, 1H); 4.307-4.280 (m, 1H); 4.214-4.187 (m, 1H); 3.889 (s, 3H); 3.323 (bs, 1H); 3.097-2.694 (m, 7H); 2.349-2.164 (s, 5H); 2.071-1.900 (bs, 3H) **MS (FD) m/z (% rel Int.):** 399.3 (100.0 [M]⁺); 400.3 (29.86 [M+1]⁺)

4-(3-(2-Fluoroethoxy)-2-methoxy-benzoyl)-1-(2-p-nitrophenylethyl)-piperidine (51). 360 mg (**43**) (0.94 mmol), 23 mg NaH (0.94 mmol), 25 μ L 1,2-bromofluoroethane (0.94 mmol), 15 mL dry DMF yielded 203 mg of (**51**) (0.47 mmol; 50 %). R_f 0.86 (silica gel, 8:1 CHCl₃/MeOH). ¹H-NMR (300 MHz, CDCl₃) δ [ppm] = 8.094 (d, 2H); 7.317 (d, 2H); 7.082-7.007 (t, 3H); 4.857 (t, 1H); 4.699 (t, 1H); 4.296 (t, 1H); 4.203 (t, 1H); 3.882 (s, 3H); 3.077 (t, 1H); 2.971-2.849 (q, 2H); 2.918 (t, 2H); 2.587 (t, 2H); 2.120 (t, 2H); 1.871 (d, 2H); 1.727 (dt, 2H) **MS (FD) m/z (% rel Int.):** 429.9 (100.0 [M]⁺); 430.9 (2.64 [M+1]⁺)

4-(3-(2-Fluoroethoxy)-2-methoxy-benzoyl)-1-(2-p-methoxyphenylethyl)-piperidine (52). 20 mg (**44**) (0.54 mmol), 13 mg NaH (0.54 mmol), 14 μ L 1,2-bromofluoroethane (0.54 mmol), 15 mL dry DMF yielded 223 mg of (**52**) (0.53 mmol; 98 %). R_f 0.71 (silica gel, 8:1 CHCl₃/MeOH). ¹H-NMR (300 MHz, CDCl₃) δ [ppm] = 7.126-7.036 (m, 5H); 6.821 (d, 2H); 4.854 (t, 1H); 4.696 (t, 1H); 4.294 (t, 1H); 4.200 (t, 1H); 3.892 (s, 3H); 3.749 (s, 3H); 3.416 (s, 1H); 3.052 (m, 4H); 2.329 (m, 2H); 2.122 (m, 2H); 2.027 (s, 2H); 1.220 (s, 2H) **MS (FD) m/z (% rel Int.):** 415.2 (100.0 [M]⁺); 416.2 (35.5 [M+1]⁺); 417.3 (2.84 [M+2]⁺)

4-(3-(2-Fluoroethoxy)-2-methoxy-benzoyl)-1-(2-p-fluorophenylethyl)-piperidine (MA-1) (53). 0.6 g (45) (1.68 mmol), 44.25 mg NaH (1.68 mmol), 124 μ L 1,2-bromofluoroethane (1.68 mmol), 20 mL dry DMF yielded 420 mg of (53) (1.04 mmol; 63 %). R_f 0.8 (silica gel, 8:1 $\text{CHCl}_3/\text{MeOH}$). $^1\text{H-NMR}$ (300 MHz, CDCl_3) δ [ppm] = 7.155-6.908 (m, 7H); 4.872-4.845 (m, 1H); 4.712-4.687 (m, 1H); 4.312-4.285 (m, 1H); 3.885 (s, 3H); 3.128-3.078 (m, 1H); 3.032-2.931 (m, 2H); 2.823-2.771 (m, 2H); 2.611-2.539 (m, 2H); 2.021-1.929 (m, 2H); 1.840-1.686 (m, 2H) **MS (FD) m/z (% rel Int.):** 403.1 (100.0 $[\text{M}]^+$); 404.1 (26.75 $[\text{M}+1]^+$); 402.1 (26.17 $[\text{M}-1]^+$)

(3-(2-Fluoroethoxy)-2-methoxyphenyl)-(1-(2-p-methoxyphenylethyl)-piperidine-4-yl)-methanol (54). 150 mg (47) (0.4 mmol), 9.8 mg NaH (0.4 mmol), 11 μ L 1,2-bromofluoroethane (0.4 mmol), 15 mL dry DMF yielded 71 mg of (54) (0.17 mmol; 43 %). R_f 0.4 (silica gel, 8:1 $\text{CHCl}_3/\text{MeOH}$). $^1\text{H-NMR}$ (300 MHz, CDCl_3) δ [ppm] = 7.080 (d, 2H); 7.088 (t, 1H); 6.926 (dd, 1H); 6.809 (t, 3H); 4.840 (m, 1H); 4.688 (m, 1H); 4.634 (d, 1H); 4.161-4.283 (dt, 2H); 3.884 (s, 3H); 3.749 (s, 3H); 3.026-3.276 (dd, 2H); 2.635-2.864 (dt, 4H); 2.016-2.038 (m, 3H); 1.708 (m, 2H); 1.575 (t, 1H); 1.366 (d, 2H) **MS (FD) m/z (% rel Int.):** 417.2 (74.1 $[\text{M}]^+$); 418.2 (100.0 $[\text{M}+1]^+$); 419.3 (20.6 $[\text{M}+2]^+$)

(3-(2-Fluoroethoxy)-2-methoxyphenyl)-(1-(2-p-fluorophenylethyl)-piperidine-4-yl)-methanol (MH.MZ) (55). 0.2 g (48) (0.55 mmol), 20 mL DMF, 13.2 mg NaH (0.55 mmol), 70 mg 1,2-bromofluoroethane (0.041 mL, 0.55 mmol) yielded 90 mg of (55) (0.22 mmol; 40 %). R_f 0.36 ($\text{CHCl}_3/\text{MeOH}/\text{konz. NH}_3$ 9:1:0.2). $^1\text{H-NMR}$ (300 MHz, CDCl_3) δ [ppm] = 7.107-7.061 (m, 2H); 7.017-6.873 (m, 4H); 6.810-6.784 (d, 1H); 4.839-4.812 (m, 1H); 4.668-4.653 (m, 1H); 4.611-4.584 (d, 1H); 4.260-4.233 (m, 1H); 4.167-4.140 (m, 1H); 3.861 (s, 3H); 3.122-3.086 (d, 1H); 2.989-2.923 (d, 1H); 2.811-2.765 (m, 2H); 2.580-2.526 (m, 2H); 2.065-1.916 (m, 3H); 1.694-1.629 (m, 1H); 1.583-1.367 (m, 3H) **MS (FD) m/z (% rel Int.):** 405.2 (100.0 $[\text{M}]^+$); 406.2 (35.64 $[\text{M}+1]^+$)

(R)-(3-(2-Fluoroethoxy)-2-methoxyphenyl)-(1-(2-p-fluorophenylethyl)-piperidine-4-yl)-methanol ((R)-MH.MZ) (56). 0.1 g (49) (0.275 mmol), 20 mL DMF, 6.6 mg NaH (0.275 mmol), 35 mg 1,2-bromofluoroethane (0.020 mL, 0.275 mmol) yielded 56 mg of (56) (0.15 mmol; 52%). R_f 0.36 ($\text{CHCl}_3/\text{MeOH}/\text{konz. NH}_3$ 9:1:0.2). $^1\text{H-NMR}$ (300 MHz, CDCl_3) δ

[ppm] = 7.107-7.061 (m, 2H); 7.017-6.873 (m, 4H); 6.810-6.784 (d, 1H); 4.839-4.812 (m, 1H); 4.668-4.653 (m, 1H); 4.611-4.584 (d, 1H), 4.260-4.233 (m, 1H); 4.167-4.140 (m, 1H); 3.861 (s, 3H); 3.122-3.086 (d, 1H); 2.989-2.923 (d, 1H); 2.811-2.765 (m, 2H); 2.580-2.526 (m, 2H); 2.065-1.916 (m, 3H); 1.694-1.629 (m, 1H); 1.583-1.367 (m, 3H) **MS (FD) m/z (% rel Int.):** 405.5 (100.0 [M]⁺); 406.5 (57.17 [M+1]⁺) **[α]_D** = +6.84 (c 0.16; CHCl₃)

4.2.6 General procedure for boc-deprotection: Ketones (**7**), (**8**) and (**9**) (70 mmol) were carefully and gradually dissolved in trifluoroacetic acid (160 mL). After 2 h of stirring at room temperature, the solutions was diluted with 500 mL of ether and carefully neutralized with NH₄OH and ice bath cooling. The layers were separated and the aqueous layer were extracted 3x with ether. The combined organic extracts were washed with water, dried (Na₂SO₄), filtered and evaporated to afford a viscous oil. Chromatography of the residues gave the pure products.

4-(2-Methoxy-3-(*t*-butyldiphenylsilyloxy)-benzoyl)-piperidine (10a**).** 5.2 g (**7**) (9.1 mmol), 100 mL TFA yielded 3.23 g of (**10a**) (6.8 mmol; 75 %). R_f 0.33 (CHCl₃/MeOH 5:1). **¹H-NMR (300 MHz, CDCl₃) δ [ppm]** = 7.727-7.670 (m, 4H); 7.466-7.319 (m, 6H); 6.881 (dt, 1H); 6.751-6.631 (m, 2H); 6.417 (bs, 1H); 3.908 (s, 3H); 3.383 (bs, 2H); 3.083 (bd, 2H); 2.098 (bs, 2H); 2.029-1.839 (m, 2H); 1.114 (s, 9H) **MS (FD) m/z (% rel Int.):** 473.3 (100.0 [M]⁺); 474.3 (56.7 [M+1]⁺); 475.3 (12.5 [M+2]⁺)

4-(2,3-Bismethoxy-benzoyl)-piperidine (11a**).** 18 g (**8**) (51 mmol), 120 mL TFA yielded 7.7 g of (**11a**) (31 mmol; 62 %). R_f 0.57 (CHCl₃/MeOH 5:1). **¹H-NMR: (300 MHz, DMSO-*d*₆) δ [ppm]** = 7.077-6.917 (m, 3H); 3.851 (s, 3H); 3.823 (s, 3H); 3.235-3.068 (m, 3H); 2.897 (bs, 2H); 1.903-1.788 (d, 2H); 1.621-1.489 (m, 2H) **MS (FD) m/z (% rel Int.):** 249.4 (100.0 [M]⁺); 250.4 (23.31 [M+1]⁺)

4-(3-(2-Fluoroethoxy)-2-methoxybenzoyl)-piperidine (12a**).** 7.68 g (**9**) (20 mmol), 100 mL TFA yielded 5.15 g of (**12a**) (18.3 mmol; 92 %). R_f 0.15 (CHCl₃/MeOH 10:1). **¹H-NMR (300 MHz, CDCl₃) δ [ppm]** = 7.075-6.964 (m, 3H); 4.852 (t, 1H); 4.694 (t, 1H); 4.294 (t, 1H); 4.198 (t, 1H); 3.879 (s, 3H); 3.197 (tt, 1H); 3.100 (dt, 2H); 2.659 (td, 2H); 2.538 (bs, 1H); 1.834 (dd, 2H); 1.622-1.480 (m, 2H) **MS (FD) m/z (% rel Int.):** 281.1 (100.0 [M]⁺);

282.1 (16.6 [M+1]⁺); 283.1 (1.56 [M+2]⁺)

4.2.7 General procedure for reduction of carbonyl compounds via NaBH₄: 30 mmol of the corresponding hydroxyl derivative was dissolved in 150 mL dry MeOH. Under nitrogen atmosphere 55 mmol NaBH₄ was added gradually at 25-30 °C, and the solution was stirred until no more gas evolved, generally overnight. After evaporation of the solvent, the residue was taken up in NH₄OH and extracted 3x with CHCl₃. The combined organic extracts were washed with brine, dried (Na₂SO₄), filtered and evaporated to afford pure product.

(2-Methoxy-3-(*t*-butyldiphenylsilyloxy)-phenyl)-(piperidine-4-yl)-methanol (10). 4.22 g (10a) (8.9 mmol), 800 mg NaBH₄ (21 mmol), 40 mL MeOH yielded 3.45 g of (10) (7.3 mmol; 81 %). R_f 0.36 (CHCl₃/MeOH 8:1). ¹H-NMR (300 MHz, CDCl₃) δ [ppm] = 7.756-7.676 (m, 4H); 7.450-7.286 (m, 6H); 6.767 (dd, 1H); 6.614 (t, 1H); 6.408 (dd, 1H); 4.595 (d, 1H); 3.964 (s, 3H); 3.059 (dd, 2H); 2.616-2.435 (m, 2H); 2.314-1.956 (m, 2H); 1.720 (bs, 1H); 1.352-1.136 (m, 4H); 1.102 (s, 9H) MS (FD) m/z (% rel Int.): 475.2 (100.0 [M]⁺); 476.2 (64.6 [M+1]⁺); 477.2 (18.6 [M+2]⁺)

(2,3-Dimethoxyphenyl)-(piperidine-4-yl)-methanol (11). 7.7 g (11a) (31 mmol), 2.3 g NaBH₄ (62 mmol), 200 mL dry MeOH yielded 6.7 g of (11) (27 mmol; 87 %). R_f 0.39 (CHCl₃/MeOH 8:1). ¹H-NMR (300 MHz, CDCl₃) δ [ppm] = 7.042-6.990 (t, 1H); 6.877-6.790 (q, 2H); 4.595-4.568 (d, 1H); 3.834 (s, 6H); 3.104-3.062 (d, 1H); 2.984-2.942 (d, 1H); 2.566-2.405 (m, 2H); 2.242 (bs, 2H); 2.030-1.999 (d, 1H); 1.788-1.658 (m, 1H); 1.333-1.091 (m, 3H) MS (FD) m/z (% rel Int.): 251.4 (100.0 [M]⁺); 252.4 (16.48 [M+1]⁺)

(3-(2-Fluoroethoxy)-2-methoxy-phenyl)-(piperidine-4-yl)-methanol (12). 4.24 g (12a) (15.1 mmol), 1.15 g NaBH₄ (30.2 mmol), 70 mL dry MeOH yielded 2.4 g of (12) (8.4 mmol; 56 %). R_f 0.2 (CHCl₃/MeOH 8:1). ¹H-NMR: (300 MHz, DMSO-d₆) δ [ppm] = 7.027-6.873 (m, 3H); 4.913 (bs, 1H); 4.832 (t, 1H); 4.671 (t, 1H); 4.570 (dd, 1H); 4.270 (t, 1H); 4.170 (t, 1H); 3.720 (s, 3H); 3.328 (bs, 2H); 2.906-2.782 (m, 2H); 2.334-2.220 (m, 2H); 1.663 (d, 1H); 1.482 (bs, 1H); 1.094 (q, 2H) MS (FD) m/z (% rel Int.): 283.0 (100.0 [M]⁺); 284.0 (19.1 [M+1]⁺)

(3-(2-Fluoroethoxy)-2-methoxyphenyl)-(1-(2-p-fluorophenylethyl)-piperidine-4-yl)-methanol (MH.MZ) (55). 168 mg (**53**) (0.42 mmol), 100 mg NaBH₄ (2.6 mmol), 20 mL MeOH yielded 158 mg of (**55**) (0.38 mmol; 93 %). R_f 0.36 (CHCl₃/MeOH/conz. NH₃ 9:1:0.2). ¹H-NMR (300 MHz, CDCl₃) δ [ppm] = 7.107-7.061 (m, 2H); 7.017-6.873 (m, 4H); 6.810-6.784 (d, 1H); 4.839-4.812 (m, 1H); 4.668-4.653 (m, 1H); 4.611-4.584 (d, 1H), 4.260-4.233 (m, 1H); 4.167-4.140 (m, 1H); 3.861 (s, 3H); 3.122-3.086 (d, 1H); 2.989-2.923 (d, 1H); 2.811-2.765 (m, 2H); 2.580-2.526 (m, 2H); 2.065-1.916 (m, 3H); 1.694-1.629 (m, 1H); 1.583-1.367 (m, 3H) MS (FD) m/z (% rel Int.): 405.5 (100.0 [M]⁺); 406.5 (57.17 [M+1]⁺)

(3-(2-Fluoroethoxy)-2-methoxyphenyl)-(1-(2-p-toluyphenylethyl)-piperidine-4-yl)-methanol (57). 90 mg (**50**) (0.15 mmol), 11.5 mg NaBH₄ (0.3 mmol), 6 mL dry MeOH yielded 31 mg of (**57**) (0.08 mmol; 52 %). ¹H-NMR (300 MHz, CDCl₃) δ [ppm] = 7.135-6.815 (m, 7H); 4.860-4.832 (m, 1H); 4.709-4.673 (m, 2H); 4.283-4.255 (m, 1H); 4.189-4.162 (m, 1H); 3.888 (s, 3H); 3.674-3.618 (d, 1H); 3.550-3.511 (d, 1H); 3.164 (bs, 2H); 3.083 (bs, 2H); 2.239-1.985 (m, 6H); 1.894 (m, 1H) MS (FD) m/z (% rel Int.): 401.2 (100.0 [M]⁺); 402.3 (46.56 [M+1]⁺)

(2-Methoxy-3-(*t*-butyldiphenylsilyloxy)-phenyl)-(1-(2-p-methoxyphenylethyl)-piperidine-4-yl)-me-thanol (22). 600 mg (**19**) (0.99 mmol), 150 mg NaBH₄ (4 mmol), 20 mL dry MeOH yielded 520 mg of (**22**) (0.86 mmol; 87%). R_f 0.54 (CHCl₃/MeOH 8:1). ¹H-NMR (300 MHz, CDCl₃) δ [ppm] = 7.718-7.646 (m, 4H); 7.412-7.270 (m, 6H); 7.131 (d, 2H); 6.816 (q, 3H); 6.615 (t, 1H); 6.433 (d, 1H); 4.695 (d, 1H); 3.946 (s, 3H); 3.753 (s, 3H); 3.523 (s, 1H); 3.242-3.012 (m, 4H); 2.662-2.4305 (m, 2H); 2.285-2.052 (m, 2H); 1.911-1.671 (m, 2H); 1.422-1.176 (m, 3H); 1.093 (s, 9H) MS (FD) m/z (% rel Int.): 607.4 (100.0 [M]⁺); 608.4 (54.8 [M+1]⁺); 609.4 (16.5 [M+2]⁺)

4.2.8 Optical resolution

Optical resolution of (10)/(11): Optical resolution was carried out as described by Ullrich and Ice.²³ NMR and mass spectral data for both enantiomers are identical with (**10**). Enantiomeric purity was determined via chiral HPLC separation.

4.2.9 General procedure for N-alkylation:

Method A): A suspension of the appropriate amine (21.4 mmol), NaHCO₃ (32.1 mmol), and the corresponding bromo-derivative (21.4 mmol) in anhydrous DMF (100 mL) was stirred for 90 min at 85 °C. After evaporation of the solvent, the residue was taken up in NH₄OH and extracted 3x with EtOAc. The combined organic extracts were washed 3x with brine, dried (Na₂SO₄), and evaporated.

Method B [Finkelstein conditions]): Conducted as *Method A*), but beside mentioned raw materials NaI (21.4 mmol) was added.

4-(2-Methoxy-3-(*t*-butyldiphenylsilyloxy)-benzoyl)-1-(2-*p*-toluylethyl)-piperidine (17). (*Method A*) 1.41 g (**7**) (2.98 mmol), 0.60 g 1-(2-bromoethyl)-4-methyl-benzene (2.98 mmol), 10 mL DMF, 0.37 g NaHCO₃ (4.47 mmol) yielded 0.88 g of (**17**) (1.49 mmol; 50 %) as colourless crystalline. R_f 0.53 (silica gel, 8:1 CHCl₃/MeOH). ¹H-NMR (300 MHz, CDCl₃) δ [ppm] = 7.731-7.695 (m, 4H); 7.473-7.302 (m, 6H); 6.923-7.281(m, 7H); 3.793 (s, 3H); 3.146-3.275 (m, 1H); 3.046-2.858 (m, 2H); 2.744-2.633 (m, 2H); 2.381-2.559 (m, 1H); 2.3 (s, 3H), 1.992-2.182 (m, 2H); 1.800-1.933 (m, 2H); 1.211 (s, 9H) MS (FD) m/z (% rel Int.): MS (FD) m/z (% rel Int.): 591.5 (100.0 [M]⁺); 592.5 (22.8 [M+1]⁺)

4-(2-Methoxy-3-(*t*-butyldiphenylsilyloxy)-benzoyl)-1-(2-*p*-nitrophenylethyl)-piperidine (18). (*Method A*) 2.4 g (**10a**) (5 mmol), 0.65 g NaHCO₃ (7.5 mmol), 1.5 g *p*-nitrophenethylbromide (5 mmol), 25 mL dry DMF yielded 1 g of (**18**) (1.6 mmol; 32 %). R_f 0.9 (CHCl₃/MeOH 8:1). ¹H-NMR (300 MHz, CDCl₃) δ [ppm] = 8.195-8.121 (q, 2H); 7.712-7.695 (m, 4H); 7.458-7.317 (m, 8H); 6.888 (dd, 1H); 6.738-6.635 (m, 2H); 3.784 (s, 3H); 3.095 (tt, 1H); 2.998-2.864 (m, 4H); 2.635 (t, 2H); 2.204 (t, 2H); 1.884 (bd, 2H); 1.826-1.689 (m, 2H); 1.106 (s, 9H) MS (FD) m/z (% rel Int.): 622.4 (100.0 [M]⁺); 623.4 (50.1 [M+1]⁺); 624.4 (9.3 [M+2]⁺)

4-(2-Methoxy-3-(*t*-butyldiphenylsilyloxy)-benzoyl)-1-(2-*p*-methoxyphenylethyl)-piperidine (19). (*Method A*) 2.4 g (**10a**) (5 mmol), 0.65 g NaHCO₃ (7.5 mmol), 1.5 g *p*-methoxyphenethylbromide (5 mmol), 25 mL dry DMF yielded 1.28 g of (**19**) (2.1 mmol; 42 %). R_f 0.83 (CHCl₃/MeOH 8:1). ¹H-NMR (300 MHz, CDCl₃) δ [ppm] = 7.709-7.653 (m, 4H); 7.457-7.302 (m, 6H); 7.116 (q, 2H); 6.885 (m, 1H); 6.862-6.803 (m, 4H); 4.431 (d, 1H);

3.858 (s, 3H); 3.761 (s, 3H); 3.623 (bs, 1H); 3.382 (bd, 2H); 3.235-3.023 (m, 4H); 3.003-2.885 (m, 2H); 2.729-2.534 (m, 2H); 2.374-2.150 (m, 1H); 2.141 (s, 9H) **MS (FD) m/z (% rel Int.)**: 607.4 (100.0 [M]⁺); 608.4 (54.8 [M+1]⁺); 609.4 (16.5 [M+2]⁺)

4-(2-Methoxy-3-(*t*-butyldiphenylsilyloxy)-benzoyl)-1-(2-*p*-fluorophenylethyl)-piperidine (20). (*Method B*) 4.91 g (**10a**) (8.14 mmol), 0.64 g NaHCO₃ (9 mmol), 1.02 g *p*-fluorophenethylbromide (8.14 mmol), NaI (8.14 mmol), 50 mL dry DMF yielded 2.99 g of (**20**) (5.02 mmol; 61 %). R_f 0.5 (EtOAc). ¹H-NMR (300 MHz, CDCl₃) δ [ppm] = 7.719-7.663 (m, 4H); 7.457-7.302 (m, 6H); 7.114-7.055 (m, 2H); 6.962-6.921 (m, 2H); 6.806-6.748 (dd, 1H), 6.666-6.405 (t, 2H); 3.995 (s, 3H); 3.131-2.983 (m, 2H), 2.87 (m, 3H); 2.201 (m, 2H); 1.955-1.735 (m, 4H); 1.211 (s, 9H) **MS (FD) m/z (% rel Int.)**: 595.5 (100.0 [M]⁺); 596.5 (72.30 [M+1]⁺); 597.5 (21.48 [M+2]⁺); 594.5 (18.92 [M-1]⁺)

(2-Methoxy-3-(*t*-butyldiphenylsilyloxy)-phenyl)-(1-(2-*p*-nitrophenylethyl)-piperidine-4-yl)-methanol (21). (*Method A*) 1.33 g (**10**) (2.8 mmol), 0.93 g NaHCO₃ (4.2 mmol), 0.84 g *p*-nitrophenethylbromide (2.8 mmol), 25 mL dry DMF yielded 1 g of (**21**) (1.57 mmol; 56 %). R_f 0.65 (CHCl₃/MeOH 8:1). ¹H-NMR (300 MHz, CDCl₃) δ [ppm] = 8.121 (d, 2H); 7.704 (dt, 5H); 7.454-7.304 (m, 10H); 3.970 (s, 3H); 3.895 (s, 1H); 3.071 (d, 1H); 2.965-2.765 (m, 4H); 2.594 (t, 2H); 2.124-1.889 (m, 3H); 1.509-1.185 (m, 3H); 1.101 (s, 9H) **MS (FD) m/z (% rel Int.)**: 624.3 (100.0 [M]⁺); 625.3 (44.7 [M+1]⁺); 626.3 (8.7 [M+2]⁺)

(2-Methoxy-3-(*t*-butyldiphenylsilyloxy)-phenyl)-(1-(2-*p*-methoxyphenylethyl)-piperidine-4-yl)-methanol (22). (*Method A*) 2 g (**10**) (4.2 mmol), 0.4 g 4-methoxyphenethylbromide (4.2 mmol), 20 mL dry DMF, 0.53 g NaHCO₃ (6.3 mmol) yielded 0.38 g of (**22**) (0.63 mmol; 15 %). R_f 0.45 (CH₂Cl/MeOH 8:1). ¹H-NMR (300 MHz, CDCl₃) δ [ppm] = 7.732-7.681 (m, 4H); 7.416-7.301 (m, 6H); 7.095-6.996 (m, 3H); 6.893-6.776 (m, 4H); 4.648-4.622 (d, 1H); 3.839 (s, 3H); 3.187-3.152 (d, 1H); 3.055-3.014 (d, 1H); 2.818-2.744 (m, 2H); 2.637-2.583 (m, 2H); 2.131-1.963 (m, 3H); 1.756-1.429 (m, 1H); 1.345-1.281 (m, 3H) **MS (FD) m/z (% rel Int.)**: 609.5 (100.0 [M]⁺), 610.5 (30.12 [M-1]⁺)

(2-Methoxy-3-(*t*-butyldiphenylsilyloxy)-phenyl)-(1-(2-*p*-fluorophenylethyl)-piperidine-4-yl)-methanol (23). (*Method B*) 2 g (**10**) (4.2 mmol), 0.85 g *p*-fluorophenethylbromide (4.2

mmol), NaI (4.2 mmol) 15 mL dry DMF, 0.53 g NaHCO₃ (6.3 mmol) yielded 2.52 g (4.6 mmol; 100 %) of **(23)**. ¹H-NMR (300 MHz, CDCl₃) δ [ppm] = 7.732-7.681 (m, 4H); 7.416-7.301 (m, 6H); 7.156-7.110 (m, 2H); 6.969-6.911 (t, 2H); 6.787-6.762 (d, 1H); 6.642-6.589 (d, 1H); 6.418-6.391 (d, 1H); 4.622-4.595 (d, 1H); 3.968 (s, 3H); 3.113-3.077 (d, 1H); 2.975-2.932 (d, 1H); 2.806-2.752 (m, 2H); 2.571-2.517 (m, 2H); 2.101-1.924 (m, 3H); 1.650-1.639 (m, 1H); 1.554-1.215 (m, 3H); 1.102 (s, 9H) MS (FD) m/z (% rel Int.): 597.6 (100.0 [M]⁺); 598.6 (77.39 [M+1]⁺); 599.6 (24.91 [M+2]⁺); 595.6 (24.91 [M-1]⁺)

(2,3-Dimethoxyphenyl)-(1-(p-fluorobenzyl)-piperidine-4-yl)-methanol (24). (*Method A*) 100 mg **(11)** (0.38 mmol), 72 mg 1-bromomethyl-4-fluorobenzene (0.38 mmol), 10 mL dry DMF, 40 mg NaHCO₃ (0.56 mmol) yielded 82 mg of **(24)** (0.22 mmol; 58 %) R_f 0.48 (CH₂Cl/MeOH 8:1). ¹H-NMR (300 MHz, CDCl₃) δ [ppm] = 7.300-7.240 (m, 2H); 7.739-6.937 (m, 3H); 6.859-6.798 (m, 2H); 4.616-4.589 (d, 1H); 3.836 (s, 6H); 3.481 (bs, 2 H); 2.983-2.945 (d, 1H); 2.861-2.817 (d, 1H); 2.345-2.326 (bs, 1H); 2.050-1.868 (m, 3H); 1.683-1.596 (m, 1H); 1.579-1.310 (m, 2H) MS (FD) m/z (% rel Int.): 359.2 (100.0 [M]⁺); 360.23 (26.57 [M+1]⁺)

(2,3-Dimethoxyphenyl)-(1-(2-p-nitrophenylethyl)-piperidine-4-yl)-methanol (25). (*Method A*) 1.5 g **(11)** (5.95 mmol), 1.35 g 2-(4-nitrophen)-1-bromethane (5.95 mmol), 50 mL DMF, 0.75g NaHCO₃ (8.93 mmol) yielded 2.41 g of **(25)** (5.91 mmol; 99%) as a orange oil. R_f 0.62 (CHCl₃/MeOH 5:1 + 5% formic acid). ¹H-NMR (300 MHz, CDCl₃) δ [ppm] = 8.173-8.081 (d, 2H); 7.323-7.294 (d, 2H); 7.046-6.993 (t, 1H); 6.878-6.803 (q, 2H); 4.621-4.594 (d, 1H); 3.836 (s, 6H); 3.049-2.982 (d, 1H); 2.923-2.836 (m, 3H); 2.614-2.483 (m, 2H); 2.066-1.854 (m, 3H); 1.649 (bs, 1H); 1.466-1.179 (m, 3H) MS (FD) m/z (% rel Int.): 400.5 (100.0 [M]⁺), 401.5 (27.80 [M-1]⁺)

(2,3-Dimethoxyphenyl)-(1-(2-p-methoxyphenylethyl)-piperidine-4-yl)-methanol (26). (*Method A*) 50 mg **(11)** (0.19 mmol), 18 mg 4-methylphenethylbromide (0.19 mmol), 10 mL dry DMF, 20 mg NaHCO₃ (0.28 mmol) yielded 18 mg of **(26)** (0.05 mmol; 26 %). R_f 0.50 (CH₂Cl/MeOH 8:1). ¹H-NMR (300 MHz, CDCl₃) δ [ppm] = 7.095-6.996 (m, 3H); 6.893-6.776 (m, 4H); 4.648-4.622 (d, 1H); 3.839 (s, 3H); 3.749 (s, 3H); 3.187-3.152 (d, 1H); 3.055-3.014 (d, 1H); 2.818-2.744 (m, 2H); 2.637-2.583 (m, 2H); 2.131-1.963 (m, 3H); 1.756-1.429 (m, 1H); 1.345-1.281 (m, 3H) MS (FD) m/z (% rel Int.): 385.1 (100.0 [M]⁺), 384.1 (91.67

[M-1]⁺)

(2,3-Dimethoxyphenyl)-(1-(2-p-toluylethyl)-piperidine-4-yl)-methanol (27). (*Method B*) 50 mg (**11**) (0.19 mmol), 38 mg 4-methylphenethylbromide (0.19 mmol), NaI (0.19 mmol), 10 mL dry DMF, 20 mg NaHCO₃ (0.28 mmol) yielded 42 mg of (**27**) (0.11 mmol; 58 %). R_f 0.4 (CH₃Cl/MeOH 8:1). ¹H-NMR (300 MHz, CDCl₃) δ [ppm] = 7.128-6.993 (m, 5H); 6.890-6.805 (m, 2H); 4.638-4.612 (d, 1H); 3.839 (s, 6H); 3.159-3.115 (d, 1H); 3.014-2.978 (d, 1H); 2.804-2.748 (m, 2H); 2.610-2.556 (m, 2H); 2.280 (s, 3H); 2.084-1.908 (m, 3H); 1.711-1.597 (m, 1H); 1.322-1.232 (m, 3H) MS (FD) m/z (% rel Int.): 369.1 (100.0 [M]⁺), 370.15 (77.30 [M+1]⁺) [α]_D = -12.49 (c 0.12; MeOH)

(2,3-Dimethoxyphenyl)-(1-(2-p-fluorophenylethyl)-piperidine-4-yl)-methanol (28). (*Method A*) 0.7 g (**11**) (2.78 mmol), 0.56 g (**36**) (2.78 mmol), 50 mL DMF, 0.35 g NaHCO₃ (4.17 mmol) yielded 786 mg of (**28**) (2.33 mmol; 84%) as a colourless powder. R_f 0.24 (CHCl₃/MeOH 10:1). ¹H-NMR: (300 MHz, CDCl₃) δ [ppm] = 7.128- 6.801 (m, 7H); 4.633-4.606 (d, 1H); 3.840 (s, 3H); 3.086-3.046 (d, 1 H); 2.946-2.914 (d, 1H); 2.791-2.686 (m, 2H); 2.538-2.455 (m, 2H); 2.061-1.864 (m, 3H); 1.715-1.600 (m, 1H), 1.549-1.232 (m, 3H) MS (FD) m/z (% rel Int.): 373.5 (100.0 [M]⁺); 374.5 (37.03 [M+1]⁺)

(R)-(2-Methoxy-3-(*t*-butyldiphenylsilyloxy)-phenyl)-(1-(2-p-fluorophenylethyl)-piperidine-4-yl)-methanol (29). (*Method A*) 2 g (**14**) (4.2 mmol), 0.85 g p-fluorophenethylbromide (4.2 mmol), 15 mL dry DMF, 0.53 g NaHCO₃ (6.3 mmol) yielded 2.3 g (4.2 mmol; 91 %) of (**29**). ¹H-NMR (300 MHz, CDCl₃) δ [ppm] = 7.732-7.681 (m, 4H); 7.416-7.301 (m, 6H); 7.156-7.110 (m, 2H); 6.969-6.911 (t, 2H); 6.787-6.762 (d, 1H); 6.642-6.589 87, 1H); 6.418-6.391 (d, 1H); 4.622-4.595 (d, 1H); 3.968 (s, 3H); 3.113-3.077 (d, 1H); 2.975-2.932 (d, 1H); 2.806-2.752 (m, 2H); 2.571-2.517 (m, 2H); 2.101-1.924 (m, 3H); 1.650-1.639 (m, 1H); 1.554-1.215 (m, 3H); 1.102 (s, 9H) MS (FD) m/z (% rel Int.): 597.5 (100.0 [M]⁺); 598.5 (68.22 [M+1]⁺); 595.5 (17.39 [M-1]⁺) [α]_D = -12.07 (c 0.9; CHCl₃)

(R)-(2,3-Dimethoxyphenyl)-(1-(2-p-fluorophenylethyl)-piperidine-4-yl)-methanol((R) MDL 100907) (30). (*Method A*) 0.7 g (**15**) (2.78 mmol), 0.56 g (**36**) (2.78 mmol), 50 mL DMF, 0.35 g NaHCO₃ (4.17 mmol) yielded 786 mg of (**30**) (2.33 mmol; 84%) as a colourless

powder. **¹H-NMR: (300 MHz, CDCl₃) δ [ppm]** = 7.128- 6.801 (m, 7H); 4.633-4.606 (d, 1H); 3.840 (s, 3H); 3.086-3.046 (d, 1 H); 2.946-2.914 (d, 1H); 2.791-2.686 (m, 2H); 2.538-2.455 (m, 2H); 2.061-1.864 (m, 3H); 1.715-1.600 (m, 1H), 1.549-1.232 (m, 3H) **MS (FD) m/z (% rel Int.):** 373.5 (100.0 [M]⁺); 374.5 (37.03 [M+1]⁺) [α]_D = + 15.67 (c 0.06; MeOH)

(3-(2-Fluoroethoxy)-2-methoxyphenyl)-(1-(2-phenylethyl)-piperidine-4-yl)-methanol

(31). (*Method A*) 200 mg (**12**) (0.71 mmol), 90 mg NaHCO₃ (1.1 mmol), 130 mg phenethylbromide (0.71 mmol), 10 mL dry DMF yielded 246 mg of **(31)** (0.64 mmol; 90 %). R_f 0.43 (CHCl₃/MeOH 8:1). **¹H-NMR: (300 MHz, CDCl₃) δ [ppm]** =7.270 – 7.131 (m, 5H); 7.006 (t, 1 H); 6.922 (dd, 1H); 6.812 (dd, 1 H); 4.839 (t, 1 H); 4.686 (t, 1H); 4.599 (d, 1H); 4.268 (t, 1H); 4.174 (t, 1H); 3.883 (s, 3H); 3.067 (d, 1H); 2.825 (s, 1H); 2.795-2.498 (dt, 4H); 2.074-1.983 (m, 2H); 1.961-1.835 (m, 2H); 1.531-1.357 (m, 2H); 1.300-1.200 (m, 2H) **MS (FD) m/z (% rel Int.):** 387.2 (100.0 [M]⁺); 388.2 (36.0 [M+1]⁺); 389.3 (8.0 [M+2]⁺)

(3-(2-Fluoroethoxy)-2-methoxyphenyl)-(1-(2-p-nitrophenylethyl)-piperidin-4-yl)-

methanol (VK-1) (32). (*Method A*) 200 mg (**12**) (0.71 mmol), 90 mg NaHCO₃ (1.1 mmol), 130 mg p-nitrophenethylbromide (0.71 mmol), 10 mL dry DMF yielded 276 mg of **(32)** (0,65 mmol; 91 %). R_f 0.64 (silica gel, 8:1 CHCl₃/MeOH). **¹H-NMR (300 MHz, CDCl₃), δ [ppm]** = 8.095-8.123 (d, 2H); 7.314-7.343 (d, 2H); 7.010 (t, 1H); 6.907 (d, 1H); 6.822 (d, 1H); 4.845 (q, 1H); 4.688 (q, 1H); 4.611 (d, 1H); 4.274 (t, 1H); 4.180 (t, 1H); 3.888 (s, 3H); 3.078 (d, 1H); 2.918 (t, 3H); 2.602 (t, 2H); 1.938-2.120 (m, 3H); 1.612-1.750 (m, 1H); 1.205-1.573 (m, 4H) **MS (FD) m/z (% rel Int.):** 432.0 (100.0 [M]⁺); 433.0 (45.8 [M+1]⁺); 434.0 (8.0 [M+2]⁺)

4-(3-(2-Fluoroethoxy)-2-methoxybenzoyl)-1-(2-p-fluorophenylethyl)-piperidine (MA-1)

(53). (*Method A*) 400 mg (**12a**) (1.42 mmol), 180 mg NaHCO₃ (2.2 mmol), 287 mg p-fluorophenethylbromide (1.42 mmol), 15 mL dry DMF yielded 466 mg of **(53)** (1.15 mmol; 81 %). R_f 0.66 (CHCl₃/MeOH 8:1). **¹H-NMR: (300 MHz, CDCl₃) δ [ppm]** = 7.148-7.077 (m, 2H); 7.031-6.903 (m, 5H); 4.857 (t, 1H); 4.699 (t, 1H); 4.296 (t, 1H); 4.203 (t, 1H); 3.883 (s, 3H); 3.077 (tt, 1H); 2.953 (dt, 2H); 2.644 (dt, 4H); 2.109 (t, 2H); 1.918 (d, 2H); 1.799-1.658 (m, 2H) **MS (FD) m/z (% rel Int.):** 402.8 (100.0 [M]⁺); 403.8 (25.8 [M+1]⁺); 404.8 (3.1 [M+2]⁺)

4.2.10 General procedure for the bromination of p-fluorophenylalkyl alcohols: To a stirred solution of the corresponding p-fluorophenylalkyl alcohol (0.4 mol) dissolved in 40 mL toluene 0.3 mol PBr₃ was slowly added, heated to 100 °C and then cooled, treated with ice water and washed with saturated Na₂CO₃ solution and water. The aqueous phase was extracted with toluene (3x 250 mL), the organic extracts dried over Na₂SO₄ and the solvent evaporated under reduced pressure. The products were obtained via distillation.

p-Fluorophenylmethyl bromide (35). The crude product was purified via distillation (85 °C, 20 mbar) to yield 55.16 g (0.29 mol; 75 %) of (35) as a colourless oil. ¹H-NMR: (300 MHz, CDCl₃) δ [ppm] = 7.413-7.382 (m, 2H); 7.034 (m, 2H); 4.555 (s, 2H) MS (FD) m/z (% rel Int.): 189.9 (100.0 [M]⁺); 187.9 (33.96 [M-2]⁺)

2-p-Fluorophenylethyl bromide (36). The crude product was purified via distillation (105 °C, 15-20 mbar) to yield 45.68 g (0.22 mol; 81 %) of (36) as a colourless oil. ¹H-NMR: (300 MHz, CDCl₃) δ [ppm] = 7.114 (t, 2H); 7.034 (t, 2H); 3.567 (t, 2H); 3.188 (t, 2H) MS (FD) m/z (% rel Int.): 202.0 (100.0 [M]⁺); 204.0 (63.77 [M+2]⁺)

4.2.11 2-Bromoethyl-2-(4-fluorophenyl)-(1,3)dioxolane (37). 4 g 2-bromo-4-fluoroacetophenone (18 mmol), 8.92 g ethylenglycol (144 mmol) and 0.76 p-toluenesulfonic acid (4 mmol) were dissolved in 50 mL benzene and refluxed for 16 h. After evaporating the solvent, the residue was taken up with CH₂Cl₂, washed with K₂CO₃ and then extracted with CH₂Cl₂, and dried with MgSO₄. The solvent was reduced to afford 2.2 g of a yellowish oil (16.1 mmol; 89%). ¹H-NMR (300 MHz, CDCl₃) δ [ppm] = 7.484-7.429 (m, 2H); 7.036-6.970 (m, 2H); 4.172-4.092 (m, 2H); 3.877-3.802 (m, 2H); 3.596 (s, 2H) MS (FD) m/z (% rel Int.): 167.6 (100.0 [M]⁺); 168.6 (6.37 [M+1]⁺); 260.4 (9.95 [M+3]⁺)

4.2.12 (3-(2-Fluoroethoxy)-2-methoxyphenyl)-(1-(2-p-aminophenylethyl)piperidine-4-yl)-methanol (58). 350 mg (32) (0.81 mmol) were dissolved in 5 mL isopropanol. 500 mg Pd/C and 204.2 mg ammonium formate (3.24 mmol) were added and then heated to 70 °C for 20 min (70 W) in a microwave. Afterwards the mixture was filtered, the solvent reduced, the residue taken up with 1 M HCl and 3x extracted with EtOAc. Organic layers were dried (Na₂SO₄) and the solvent removed to yield 248 mg of (58) (0.62 mmol; 76 %) as colourless

crystals. R_f 0.33 (CHCl₃/MeOH 8:1). **¹H-NMR (300 MHz, CDCl₃) δ [ppm]** = 7.030-6.890 (m, 4H); 6.817 (d, 1H); 6.586 (d, 2H); 4.840 (t, 1H); 4.688 (t, 1H); 4.608 (d, 1H); 4.267 (t, 1H); 4.173 (t, 1H); 3.885 (s, 3H); 3.528 (bs, 2H); 2.983 (dd, 2H); 2.565 (dt, 4H); 2.021 (t, 1H); 1.941-1.816 (m, 2H); 1.719-1.579 (m, 1H); 1.517-1.324 (m, 2H); 1.260 (d, 2H) **MS (FD) m/z (% rel Int.)**: 402.3 (100.0 [M]⁺); 403.3 (46.1 [M+1]⁺); 404.3 (7.2 [M+2]⁺)

4.2.13 (3-(2-Fluoroethoxy)-2-methoxyphenyl)-(1-phenylacetyl-piperidine-4-yl)-methanol (39). To 200 mg (**12**) (0.71 mmol) dissolved in 10 mL of dry THF 100 μ L of phenacetylchloride (0.84 mmol) was added while cooling to 0 °C. The resulting mixture was then stirred for 2 h and afterwards the solvent evaporated. The residue was taken up with EtOAc, washed with water, extracted 3x with EtOAc and finally dried (Na₂SO₄). The solvent was removed to give the crude product which is purified via chromatography yielding 180 mg of (**39**) (0.45 mmol; 64 %). R_f 0.71 (CHCl₃/MeOH 8:1). **¹H-NMR: (300 MHz, CDCl₃) δ [ppm]** = 7.325-7.158 (m, 5H); 7.000 (t, 1H); 6.887-6.787 (m, 2H); 4.841 (t, 1H); 4.684 (t, 1H); 4.552 (d, 1H); 4.267 (t, 1H); 4.173 (t, 1H); 3.956-3.671 (m, 2H); 3.874 (s, 3H); 3.692 (d, 2H); 2.960-2.740 (m, 1H); 2.566-2.361 (m, 1H); 2.044.1.722 (m, 3H); 1.367-0.948 (m, 3H) **MS (FD) m/z (% rel Int.)**: 401.2 (100.0 [M]⁺); 402.2 (23.3 [M+1]⁺); 403.2 (3.1 [M+2]⁺)

4.3 Lipophilicity

Lipophilicities were determined using the HPLC system described above with a Lichrospher 100 RP 18 EC-5 μ (250 x 7.8 mm) and a 20 μ L loop. Soerensen buffer was used as eluent with a flow rate of 4 mL/min. Retention times for all tested compounds and for reference substances (ascorbic acid, benzaldehyd, anisol, toluene, 4-bromoanisol, 4-iodoanisol) of known logP were assessed and enabled the calculation of the capacity factor k. A plot of these reference values against their known logP values gave a reference curve which was used to calculate logP values for synthesized compounds.

4.4 *In vitro* pharmacological evaluation

4.4.1 Binding assays

(A) *In vitro* radioligand competition binding assay of ^{18}F -tracers on high 5-HT_{2A} expressing GF-62 cells

Cell membrane homogenate. NIH3T3 cells, derived from mouse fibroblasts, were stably transfected with the rat 5-HT_{2A} receptor cDNA before isolation of GF-62, a clonal cell line expressing higher amounts (5-7 pmol/mg) of the 5-HT_{2A} receptor. Cells were homogenized in buffer (5 mM Tris-Base, 5 mM EDTA, pH 7.4, 4 °C) and incubated for 10 min at 4 °C. Centrifuged for 10 min (33.000 x G) at 2-4 °C and the pellet was suspended in assay buffer 4 mg/mL wet weight (50 mM Tris-base, 120 mM NaCl, 50 mM KCl, 1% bovine serum albumin, 0.1% ascorbic acid, pH 7.4, 37 °C) added 50 µL/mL protease inhibitor cocktail was added (4-(2-aminoethyl) benzenesulfonyl fluoride (AEBSF), aprotinin, leupeptin, bestatin, pepstatin A, E-64), aliquoted in NUNC tubes and stored at -80 °C until use.

Radioligand binding assay. Competition binding experiments were carried out in test tubes containing [^3H]MDL (0.2 nM), seven different concentrations of the test compound (1 µM - 1 pM) and 10-20 µg GF-62 clonal cells in a total of 1 mL assay buffer (50 mM Tris-Base, 120 mM NaCl, 50 mM KCl, 1% bovine serum albumin, 0.1% ascorbic acid, pH 7.4, 37 °C). Ketanserin (1 µM) was used to determine non-specific binding. Incubation was carried out for 1 h at 37 °C and terminated by rapid filtration over glass fibre GF/C filters presoaked in 1% polyethyleneimine, using a Brandel cell harvester. Filters were washed with 300 mL cold assay buffer (tritrated to pH 7.4 at 4 °C). Filters were placed in scintillation vials and 2.5 mL Ultima Gold scintillation fluid was added. The scintillation cocktails were placed in cold and dark overnight and counted for 4 min in a Tri-Carb 2900TR Liquid Scintillation Analyser from Packard. K_i and error values were calculated with Graphpad Prism 5.

(B) *In vitro* radioligand binding assays through NIMH-Psychoactive Drug Screening Programme (PDSP)

Binding assays were performed by the NIMH Psychoactive Drug Screening Program at the Department of Biochemistry, Case Western Reserve University, Cleveland, Ohio, USA (Bryan Roth, Director). Compounds (32), (50)-(53) and (55)-(57) were assayed for their affinities for a broad spectrum of receptors and transporters in competitive binding

experiments *in vitro* using cloned human receptors. Reported values of the inhibition coefficient (K_i) are mean \pm SD of four separate determinations.

5. Acknowledgements

Financial support by Friedrich-Naumann-Stiftung and the European Network of Excellence (EMIL) are gratefully acknowledged. Mikael Palner was supported by an unlimited grant by Cimbi, SUND, DRC. We also like to thank the VCI (Verband der chemischen Industrie e.V.) for the donation of solvents.

6. References

1. Fischer, W. *Pharm. Unserer Zeit* **1991**, 20, 21
2. Barch, D.M. *Psychopharmacology* **2004**, 174, 126
3. Ohuoha, D.C.; Hyde, T.M.; Kleinman, J.F. *Psychopharmacology* **1993**, 112, 5
4. Hoyer, D.; Martin, G.R. *Behav. Brain Res.* **1996**, 73, 263
5. Glennon, R.; Dukat, M. *ID Res. Alert* **1997**, 2, 107
6. Kennett, G.A. *Curr. Res. Serotonin* **1998**, 3, 1
7. Meltzer, H.Y.; Matsubara, S.; Lee, J.C. *J. Pharmacol. Exp. Ther.* **1989**, 238
8. Remington, G.; Kapur, S. *Psychopharmacology* **2000**, 148, 3
9. Zhang, W.; Bymaster, F.P. *Psychopharmacology* **1999**, 141, 291
10. Ito, H.; Nyberg, S.; Halldin, C.; Lundkvist, C.; Farde, L. *J. Nuc.Med.* **1998**, 39, 208
11. Smith, G.S.; Price, J.C.; Lopresti, B.J.; Huang, Y.; Simpson, N.; Holt, D.; Mason, N.S.; Meltzer, C.C.; Sweet, R.A.; Nichols, T.; Sashin, D.; Mathis, C.A. *Synapse* **1998**, 30, 380
12. Johnson, M.P.; Siegel, B.W.; Carr, A.A. *Naunyn Schmiedebergs Arch Pharmacol* **1996**, 354, 205
13. Tan, P.; Baldwin, R.M.; Fu, T.; Charney, D.S.; Innis, R.B. *J. Labelled Compd. Radiopharm.* **1999**, 42, 457
14. Hall, H.; Farde, L.; Halldin, C.; Lundkvist, C.; Sedvall, G. *Synapse* **2000**, 38, 421
15. Meltzer, C. C.; Smith, G.; DeKosky, S. T.; Pollock, B. G.; Mathis, A. M.; Moore, R. Y.; Kupfer, D. J.; Reynolds, C.F. *Neuropsychopharm* **1998**, 18, 407
16. Huang, Y.; Mahmood, K.; Mathis, C. A. *J. Labelled Compd. Radiopharm.* **1999**, 42,

949

17. Mintun, M. A., Sheline, Y.I., Moerlein, S. M., Vlassenko, A.G., Yiyun Huang, Y., Snyder, A. Z. *Biol Psychiatry* **2004**, 55,217
18. Scot, D.; Heath, T. G. *J. Pharm. Biomed. Anal.* **1998**, 17, 17
19. Herth, M.M.; Debus, F.; Piel, M.; Palner, M. Knudsen, G.M.; Lüddens, H.; Rösch, F. *Bioorg. Med. Chem. Lett.* **2008**, 18, 1515
20. Herth, M.M.; Piel, M.; Debus, P.; Schmitt, U.; Lüddens. H.; Rösch, F. *J. Nucl. Med.&Biology.* **2008**, (accepted).
21. Andersen, K.; Liljefors, T.; Gundertofe, K.; Perregaard, J.; Bogeso, K.P. *J. Med. Chem.* **1994**, 37, 950
22. Heinrich, T., Böttcher, H., Prücher, H., Gottschlich, R., Ackermann, K-A., van Amsterdam, C. *Chem. Med. Chem.* **2006**, 1, 245
23. Ullrich, T.; Ice, K.C. *Bioorg. Med. Chem.* **2000**, 8, 2427
24. Schmidt, C.J.; Kehne, J.H.; Carr, A.A. *CNS Drug Reviews* **1997**, 3, 49
25. Krass, J.D.; Jastorff, B.; Genieser, H.G. *Anal. Chem.* **1997**, 69, 2575
26. Rowley, M.; Kulagowski, J.J.; Watt, A.P.; Rathbone, D.; Stevenson, G.I.; Carling, R.W.; Baker, R.; Marshall, G.R.; Kemp, J.A.; Foster, A.C.; Grimwood, S.; Hargreaves, R.; Hurley, C.; Saywell, K.L.; Tricklebank, M.D.; Leeson, P.D. *J. Med. Chem.* **1997**, 40, 4053
27. Carr, A. A.; Kane, J. M.; Hay, D. A.; Schmidt, C. J. PCT WO 91/18602 **1996**; *Chem. Abstr.* **1996**, 116, 106031
28. Mathis, C. A.; Mahmood, K.; Huang, Y.; Simpson, N. R.; Gerdes, J. M.; Price, J. C. *Med. Chem. Res.* **1996**, 6, 1

3.5 Determination of structure-activity relationships of MDL 100907, altanserin and SR 46349B

by Vasko Kramer,^{a,*†} Matthias M. Herth,^{a,†} Mikael Palner,^b Gitte M. Knudsen,^b and Frank Rösch^a

^a Institute of Nuclear Chemistry, University of Mainz, Fritz-Strassmann-Weg 2, 55128 Mainz, Germany

^b Center for Integrated Molecular Brain Imaging, Rigshospitalet, Blegdamsvej 9, DK-2100 Copenhagen Ø, Denmark

[†] Both authors are equally contributed

Abstract

MH.MZ, MDL 100907 and altanserin are structurally similar 4-benzoyl-piperidine derivatives and are well accommodated to receptor interaction models.¹ We combined structural elements of different high affine and selective 5-HT_{2A} antagonists, as MH.MZ, altanserin and SR 46349B, to improve the binding properties of new compounds. Three new derivatives were synthesised with a 4-benzoyl-piperidine moiety as lead structure. The *in vitro* affinity of the novel compounds was determined by a [³H]MDL 100907 competition binding assay. The combination of MH.MZ and SR 46349B resulted in a compound (**8**) with a moderate affinity toward the 5-HT_{2A} receptor ($K_i = 57$ nM). The remarkably reduced affinity of other compounds (**4a**) and (**4b**) ($K_i = 411$ nM and 360 nM respectively) indicates that MH.MZ can only bind to the 5-HT_{2A} receptor with the p-fluorophenylethyl residue in a sterically restricted hydrophobic binding pocket. By varying size and hydrophobic properties of the substituent in the para position of the phenylethyl residue, it should be possible to improve the binding characteristics of the established compounds.

Serotonin (5-hydroxytryptamine (5-HT)) is a neurotransmitter that has been implicated in almost every conceivable physiologic or behavioural function as affect, aggression, appetite, cognition, endocrine function, gastrointestinal function, motor function, neurotrophism, sex, sleep, and vascular function.¹ Moreover, most drugs that are currently used for the treatment of psychiatric disorders (e.g., Alzheimer's disease, depression, mania, schizophrenia, autism, obsessive compulsive, alcoholism, disorder, anxiety disorders) are thought to act, at least partially, through serotonergic mechanisms.² Most if not all clinically approved atypical antipsychotic drugs are potent 5-HT_{2A} receptor antagonists.^{3,4}

In particular, it was shown by [¹⁸F]altanserin and Positron-Emission-Tomography (PET) that 5-HT_{2A} receptor binding in patients with mild cognitive impairment is reduced and that hippocampal 5-HT_{2A} receptor availability is decreased in major depressive patients.⁵

To date, high affine and selective 5-HT_{2A} receptor antagonists are well known, such as MDL 100907, MH.MZ, altanserin and SR 46349B (Fig 1).^{6,7} MH.MZ, MDL 100907 and altanserin are structural similar 4-benzoyl-piperidine derivatives, whereas SR 46349B contains no piperidine but a dimethylaminoethyl oxime ether moiety.

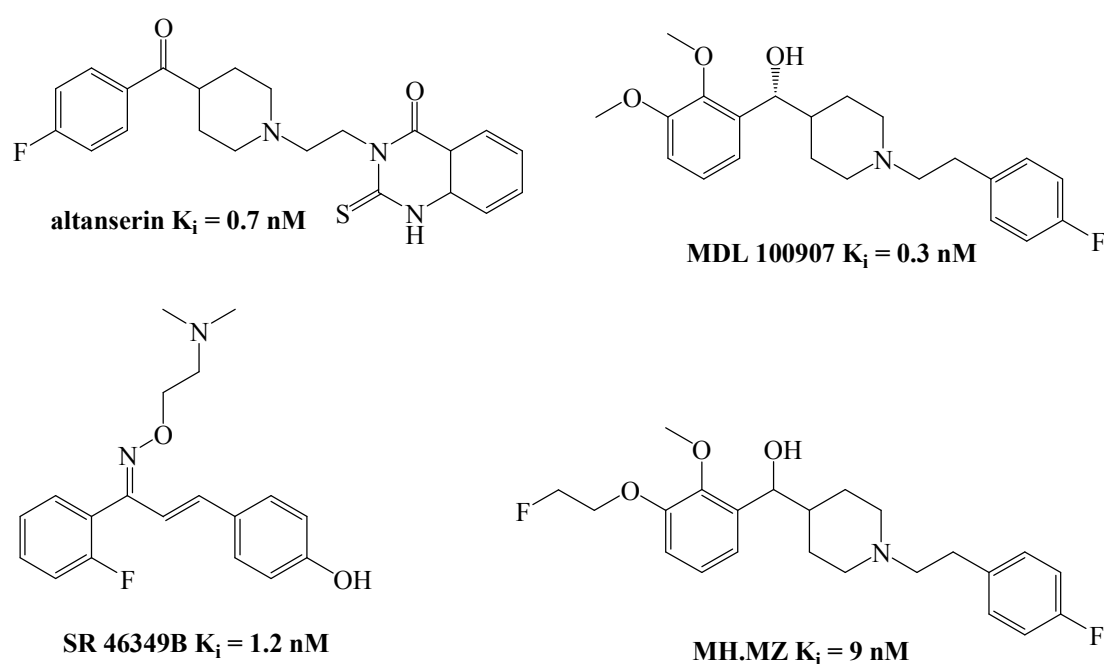


Figure 1: Structure and affinities of selective 5-HT_{2A} antagonists

Especially MH.MZ, MDL 100907 and altanserin are in accordance regarding their structural body with a rudimental pharmacophore model published by Anderson et al..¹ Two aryl substituents, separated by distance a, located distance b and c from an amine moiety (Figure

2) are required in this model for effective 5-HT_{2A} receptor ligands. Distances suggested by Anderson et al. for a, b and c are 5.1, 7.5 and 8.1 Å, respectively.

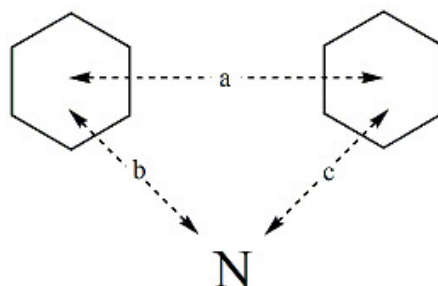


Figure 2: A general pharmacophore model to account for the binding of 5-HT_{2A} antagonists¹

Recently, Herth et al. described ¹⁸F-labelable MDL 100907 derivatives, MHMZ and MA-1, retaining the favourable characteristics of the parent compound (Table 1).^{6,8,9}

The purpose of this study is to combine structural elements of MH.MZ, MDL 100907, altanserin and SR 46349B to study their structure-activity relationship (SAR) and to investigate possible improvements of the compounds structures achieving improved binding characteristics.

For 3-(2-(4-(3-(2-fluoroethoxy)-2-methoxybenzo-yl)-piperidin-1-yl)-ethyl)-2-thioxo-2,3-dihydro-1H-quinazolin-4-on (**4a**) the p-fluorophenyl ring of altanserin was replaced by the 3-fluoroethoxy-2-methoxyphenyl ring of MH.MZ. 3-(2-(4-(3-(2-Fluoroethoxy)-2-methoxy- α -hydroxybenzyl)-piperidin-1-yl)-ethyl)-2-thioxo-2,3-dihydro-1H-quinazolin-4-on (**4b**) contains a quinazolinone ring instead of the p-fluorophenyl substituent of MH.MZ. Moreover, the influence of the ketone, the secondary hydroxyl or the dimethylaminoethyl oxime ether moiety of SR 46349B toward the affinity profile of these compounds is determined (Figure 3).

Organic syntheses of key intermediates (**1a**) and (**1b**) were carried out similar to a route described by Ullrich et al..¹⁰ Synthesis of the quinazolinone derivatives was achieved by a route similar to that reported by Tan et al..¹¹ Therefore, reaction with boc-protected bromoethylamine, deprotection and ringclosure with methyl-2-isothiocyanatobenzoate¹² resulted in compounds (**6a**) and (**6b**) (Figure 4).

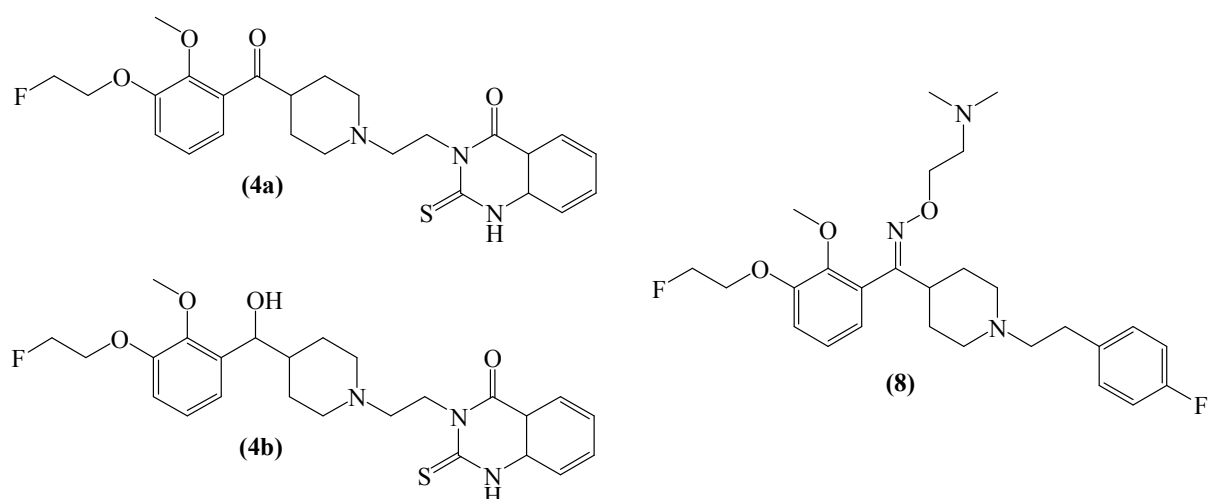


Figure 3: Restudied structural combinations of altanserine, MDL 100907 and SR 46349B

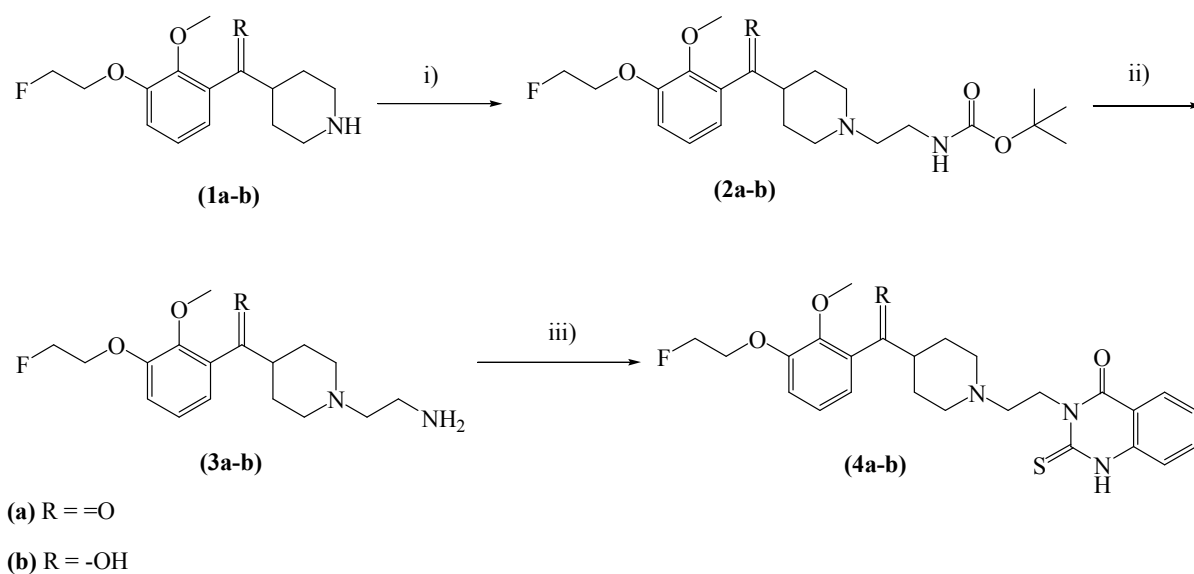


Figure 4: Synthesis of **(4a)** and **(4b)**: reagents and conditions: i) tert-butyl-2-bromethylcarbamate, KI, K₂CO₃, DMF, rt, 51-77 %; ii) TFA, rt, 83-95 %; iii) methyl-2-isothiocyanatobenzoate, THF, rt, 30-32 %

The 4-(3-(2-fluoroethoxy)-2-methoxybenzyl)-piperidine moiety of MH.MZ and the dimethylaminoethyl oxime ether residue of SR 46349B were combined following a condensation reaction of ketone **MA-1** and amine **(7)**.¹³ The necessary educts were produced as reported by Herth et al.⁶ and Villani et al.¹⁴, respectively. Figure 5 illustrates the synthetic route to **(8)**.

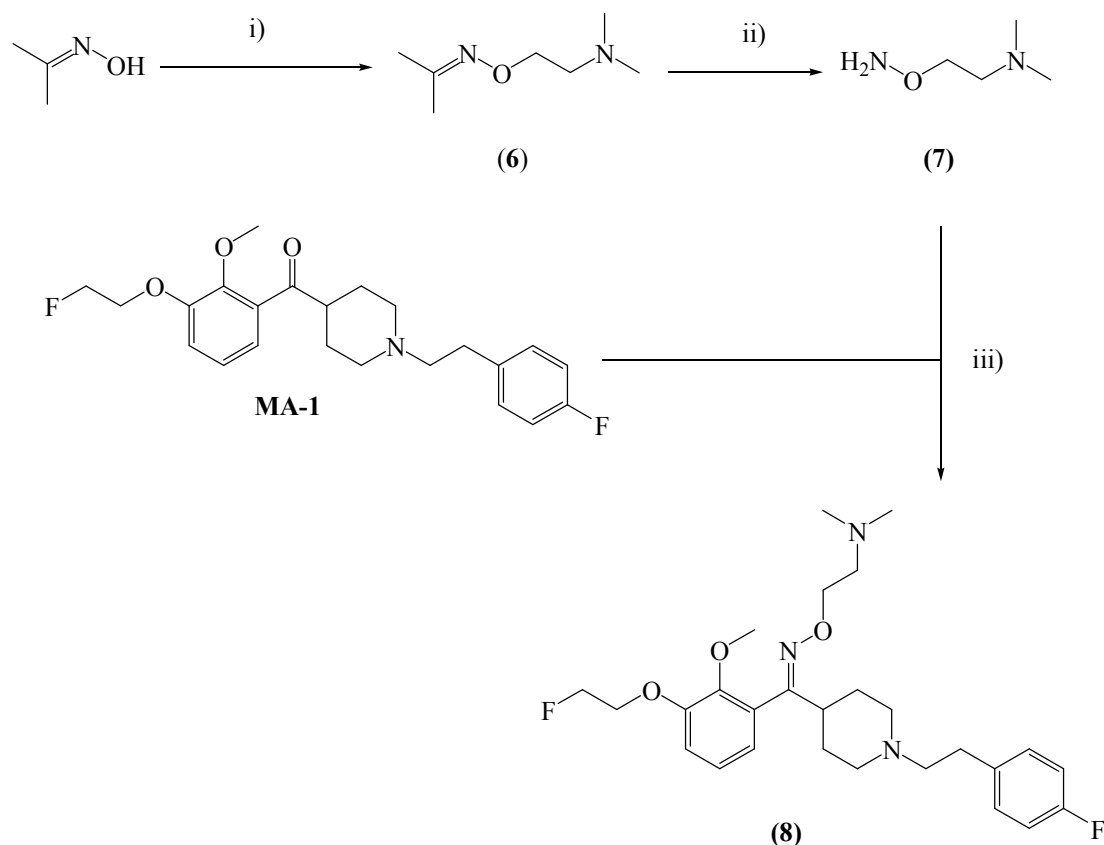


Figure 5: Synthesis of (8): reagents and conditions: i) dimethylamino-ethylchloride hydrochloride, K_2CO_3 ; benzene, reflux, 54 %; ii) hydrochloric acid 10 %, reflux, 74 %; iii) 1.25 M hydrochloric acid in ethanol, reflux, 23 %

5-HT_{2A} receptor affinity (K_i), was determined by a radioligand competition binding assay with GF-62 cells, a clonal cell line expressing high amounts (5-7 pmol/mg) of the 5-HT_{2A} receptor. The test tubes contained [³H]MDL 100907 (0.3 nM) and seven different concentrations of the test compounds (1 μ M - 1 pM) in a total of 1 mL assay buffer. Ketanserin (1 μ M) was added to determine non-specific binding. Binding affinities of the tested and reference compounds are summarized in table 1.¹⁵

The combination of structural elements of MH.MZ and SR 46349B led to the medium affine compound E-dimethylaminoethoxy-[3-(2-fluoroethoxy)-2-methoxy-phenyl]-1-[2-(p-fluorophenyl)-ethyl]-pipe-ridin-4-yl-methanoxim (8). It has a ~6 fold lower K_i -value (57 nM) compared to MH.MZ. This is probably due to the additional space required by the dimethylaminoethyl oxime residue. The affinity of (4a) and (4b) to the human 5-HT_{2A} receptor is 411 nM and 390 nM, respectively.

Table 1: Affinities toward human 5-HT_{2A} receptor of various antagonists (n = 4)^{5,16}

compound	K _i [nM]
altanserin	0.74 ± 0.88
MDL 100907	0.3 ± 0.1
MH.MZ	9.02 ± 2.11
SR 46349B	1.2
(4a)	411 ± 347
(4b)	390 ± 60
(8)	57 ± 18

The binding properties in the receptor-altanserin-complex are described in a 3D-QSAR study published by Dezi et al.¹⁷ Therein, altanserin binds to the 5-HT_{2A} receptor with the p-fluorobenzoyl moiety in a hydrophobic binding pocket. This result is in good agreement with experimental data from previously published mutagenesis experiments.^{18,19} The size of the binding pocket is restricted by the aminoacids Trp6.48, Phe6.51 and Phe6.52 from which Phe6.52 participates in π - π -interactions with the aromatic ring of the ligands.¹⁹

The remarkably reduced affinity of compound **(4a)** and **(4b)** indicates that the additional space required by the fluoroethoxy group and the methoxy group is not tolerated by the receptor binding pocket. We suggest that the benzyl alcohol of MH.MZ and the benzoyl ring of altanserin cannot bind to the same site at the 5-HT_{2A} receptor. Two different binding modes might be possible for antagonists with a 4-benzoylpiperidin lead structure. MH.MZ may bind to the 5-HT_{2A} receptor with the p-fluorophenylethyl residue at the same hydrophobic binding pocket as the benzoyl ring of altanserin. This result totally reflects the slightly reduced affinity for compounds with larger substituents at the phenylring of MH.MZ.⁵ By varying size and hydrophobic properties of the substituent it should be possible to improve the binding characteristics of MH.MZ.

The lipophilicities of the reference compounds were determined using the HPLC method according to Krass et al.²⁰ Soerensen buffer was used as eluent and log P values were calculated from retention times of the respective substances.²¹ The calculated log P values are

displayed in table 2.

The lipophilicities of altanserin, MDL 100907 and MH.MZ are in the range of Log P = 2-3 and indicate a good penetration of the blood brain barrier. The increased lipophilicity of **(8)** can be explained by the dimethylaminoethyl oxime residue. Compounds **(4a)** and **(4b)** in contrast are more hydrophilic because of the two additional aromatic ether functions. These derivatives are more polar and may not be able to cross the blood brain barrier.

Table 2: Lipophilicities / logP values of altanserin, MDL 100907 and new MDL 100907 derivatives (n = 3)

compound	Log P-values
altanserin	2.15 ± 0.01
MDL 100907	2.98 ± 0.01
MH.MZ	2.80 ± 0.01
(4a)	1.65 ± 0.02
(4b)	1.31 ± 0.01
(8)	3.80 ± 0.01

In conclusion, three new 4-(2-fluoroethoxybenzoyl)-piperidine compounds were synthesized in good chemical yields. The affinity to the 5-HT_{2A} receptor was determined in a [³H]MDL 100907 binding assay. The combination of MH.MZ and SR 46349B represents a compound **(8)** with a moderate affinity toward the 5-HT_{2A} receptor (K_i = 57 nM). The affinity of **(4a)** and **(4b)** in contrast is reduced significantly. This indicates that MH.MZ binds to the 5-HT_{2A} receptor with the p-fluorophenylethyl residue in a sterically restricted hydrophobic binding pocket. Therefore, it should be possible to improve the binding characteristics of MH.MZ by variation of the substituent in the para position. Small lipophilic residues such as a methyl group or a hydrogen may lead to higher affinities, whereas larger substituents lead to medium affine compounds.

Acknowledgments

Financial support by Friedrich-Naumann-Stiftung and the European Network of Excellence (EMIL) is gratefully acknowledged. We also like to thank the VCI (Verband der chemischen Industrie e.V.) for the donation of solvents. Financial support by Friedrich-Naumann-Stiftung and the Deutsche Forschungsgemeinschaft (DFG) is gratefully acknowledged.

References and Notes:

1. Andersen, K.; Liljefors, T.; Gundertofe, K.; Perregaard, J.; Bogeso, K.P. *J. Med. Chem.* 1994, 37, 950-962
2. Davis, K.L.; Charney, D.; Coyle, J.T.; Nerneroff, C., *Neuropsychopharmacology: The Fifth Generation of Progress*, New York: Raven Press, 2002
3. Meltzer, H.Y.; Matsubara, S.; Lee, J.C., *J. Pharmacol. Exp. Ther.*, 1989, 238-246
4. Akash, K.G.; Balarama, K.S.; Paulose, C.S., *Cell. Mol. Neurobiol.*, 2008, 28, 1017-1025
5. Hasselbach, S.G.; Madsen, K.; Svarer, C.; Pinborg, L.H.; Holm, S.; Paulson, O.B.; Waldemar, G.; Knudsen, G.M.; *Neurobiology of Aging*, 2008, 29, 1830-1838
6. Herth, M.M.; Kramer, V.; Piel, M.; Palner, M.; Riss, P.J.; Knudsen, G.M.; Rösch, F. *Bioorg. Med. Chem.* 2009 (accepted)
7. Rinaldi-Carmona, M.; Christian Congy, C.; Pointeau, P.; Vidal, H.; Breliere, JC; Le Fur, G. *J. Pharmacolgy and Experimental Therapeutics* 1992, 262, 759-768
8. Herth, M.M.; Debus, F.; Piel, M.; Palner, M. Knudsen, G.M.; Lüddens, H.; Rösch, F., *Bioorg. Med. Chem. Lett.*, 2008, 18, 1515-1519
9. Herth, M.M.; Piel, M.; Debus, P.; Schmitt, U.; Lüddens. H.; Rösch, F. *Nucl. Med. Biol.* 2009, (accepted)
10. Ullrich, T.; Ice, K.C.; *Bioorg. Med. Chem.* 2000, 8, 2427-2432
11. Tan, P.Z.; Baldwin, M.B.; Fu, T.; Charney, D.S.; Innis, R.B.; *J. Lab. Comp. Radiopharmaceuticals*, 1999, 42, 457-467
12. Note: 3-(2-(4-(3-(2-Fluoroethoxy)-2-methoxybenzo-yl)-piperidin-1-yl)-ethyl)-2-thioxo-2,3-dihydro-1H-quinazolin-4-on (**4a**) and 3-(2-(4-(3-(2-Fluoroethoxy)-2-methoxy- α -hydroxybenzyl)-piperidin-1-yl)-ethyl)-2-thioxo-2,3-dihydro-1H-quinazolin-4-on (**4b**): (0,61 mmol) (**3a**) or (**3b**) and (2 mmol) methyl-2-isothiocyanatobenzoate were dissolved in 10 mL dry methanole and stirred 2 h at room temperature. Evaporation of the solvent and CC (ethylacetate) gave the product as colorless crystals

- (3a)**: (0.18 mmol; 30 %) ¹H-NMR (300 MHz, DMSO-d₆) δ [ppm] = 12.908 (bs, 1H); 7.939 (d, 1H); 7.722 (t, 1H); 7.399-7.292 (m, 2H); 7.206 (d, 1H); 7.100 (t, 1H); 6.952 (d, 1H); 4.851 (t, 1H); 4.695 (t, 1H); 4.510 (t, 2H); 4.338 (t, 1H); 4.238 (t, 1H); 3.802 (s, 3H); 3.321 (s, 1H); 3.025-2.881 (m, 3H); 2.601 (t, 2H); 2.107 (t, 2H); 1.709 (d, 2H); 1.541-1.377 (m, 2H); MS (FD) m/z (% rel Int.): 485.4 (100 [M]⁺); 486.4 (69.5 [M+1]⁺); 487.4 (24.3 [M+2]⁺);
- (3b)**: (0.19 mmol; 32 %) ¹H-NMR: (300 MHz, DMSO-d₆) δ [ppm] = 12.875 (bs, 1H); 7.932 (d, 1H); 7.717 (t, 1H); 7.391-7.275 (m, 2H); 7.031-6.872 (m, 3H); 4.938 (d, 1H); 4.832 (t, 1H); 4.675 (t, 1H); 4.582 (t, 1H); 4.487 (t, 2H); 4.272 (t, 1H); 4.172 (t, 1H); 3.722 (s, 3H); 3.320 (bs, 1H); 3.001-2.829 (m, 2H); 2.548 (t, 2H); 1.879 (q, 2H); 1.781 (d, 1H); 1.411 (bs, 1H); 1.314-1.130 (m, 2H); MS (FD) m/z (% rel Int.): 487.4 (43.6 [M]⁺); 488.4 (100 [M+1]⁺); 489.4 (25.9 [M+2]⁺)
13. Note: E-Dimethylaminoethoxy-[3-(2-fluoroethoxy) -2- methoxy-phenyl] -1- [2-(p-fluoro-phenyl)-ethyl]-pipe-ridin-4-yl-methanoxim (**8**): 2 mmol **MA-1** and 2 mmol dimethylaminoethoxy-amine (**7**) were dissolved in ethanol containing 1.25 M HCl and heated under reflux for 20 h. After evaporation of the solvent and extraction with chloroform the residue was taken up in conc. ammonia solution. Extraction with chloroform, evaporation and CC (chloroform/methanol 5:1) gave the product as colorless crystals (0.5 mmol; 25 %). ¹H-NMR (300 MHz, CDCl₃) δ [ppm] = 7.148-7.072 (m, 3H); 7.026-6.829 (m, 4H); 6.581 (dd, 1H); 4.841 (t, 1H); 4.683 (t, 1H); 4.274 (t, 1H); 4.181 (t, 1H); 4.142 (t, 2H); 3.806 (s, 3H); 3.048-2.951 (m, 3H); 2.771-2.688 (m, 2H); 2.628 (t, 2H); 2.580-2.483 (m, 2H); 2.240 (s, 6H); 2.085 (q, 2H); 1.909-1.792 (m, 2H); 1.778-1.596 (m, 2H); MS (FD) m/z (% rel Int.): 490.5 (100 [M+1]⁺); 491.5 (27.9 [M+2]⁺)
14. Villani, F.J.; Tavares, R.F.; Ellis, C.A.; J. Pharm. Sci., 1969, 58, 138
15. Competition binding experiments were carried out in test tubes containing [³H]MDL 100907 (0.2 nM), seven different concentrations of the test compound (1 μM - 1 pM) and 10-20 μg GF-62 clonal cells in a total of 1 mL assay buffer (50 mM Tris-Base, 120 mM NaCl, 50 mM KCl, 1% bovine serum albumine, 0.1% ascorbic acid, pH 7.4, 37 °C). Ketanserin (1 μM) was used to determine non-specific binding. Incubation was carried out for 1 h at 37 °C and terminated by rapid filtration over glass fibre GF/C filters presoaked in 1% polyethyleneimine, using a Brandel cell harvester. Filters were washed with 300 mL cold assay buffer (titrated to pH 7.4 at 4 °C). Filters were placed in scintillation vials and 2.5 mL Ultima Gold scintillation fluid were added. The

scintillation cocktails were placed in cold and dark overnight and counted for 4 min in a Tri-Carb 2900TR Liquid Scintillation Analyser from Packard. K_i and error values were calculated with Graphpad Prism 5.

16. Rinaldi-Carmona, M.; Congy, C.; Santucci, V.; Simiand, J.; Gautret, B.; Naliat, G.; Labeeuw, B.; Le Fur, G.; Soubrie, P.; Breliere, J.C.; *J. Pharmacol. Exp. Ther.*, 1992, 262, 759-768
17. Dezi, C.; Brea, J.; Ravina, E.; Masaguer, C.F.; Loza, M.I.; Sanz, F.; Pastor, M.; *J. Med. Chem.*, 2007, 50, 3242-3255
18. Braden, M.R.; Parrish, J.C.; Naylor, J.C.; Nichols, D.E.; *Mol. Pharmacol.*, 2006, 70, 1956-1964
19. Choudhary, M.S.; Craigo, S.; Roth, B.L.; *Mol. Pharmacol.*, 1993, 43, 755-761
20. Krass, J.D.; Jastorff, B.; Genieser, H.G. *Anal. Chem.*, 1997, 69, 2575-2581
21. Lipophilicities were determined using the HPLC system described above with a LiChrospher 100 RP 18 EC-5 μ (250 x 7.8 mm) and a 20 μ L loop. Soerensen buffer was used as eluent with a flow rate of 4 mL/min. Retention times for all tested compounds and for reference substances (ascorbic acid, benzaldehyd, anisol, toluene, 4-bromoanisol, 4-iodoanisol) of known logP were assessed and enabled the calculation of the capacity factor k. A plot of these reference values against their known logP values gave a reference curve which was used to calculate logP values for synthesized compounds.

3.6 ^{18}F -Labeling and evaluation of novel MDL 100907 derivatives as potential 5-HT_{2A} antagonists for molecular imaging

by Fabian Debus,^{b,*†} Matthias M. Herth,^{a,†} Hans-Georg Buchholz,^c Nicole Bausbacher,^c Vasko Kramer,^a Dorothea Moderegger,^a Hartmut Lüddens,^b Frank Rösch^a

^aInstitute of Nuclear Chemistry, Johannes Gutenberg University-Mainz, Fritz-Strassmann-Weg 2, 55128 Mainz, Germany

^bDepartment of Psychiatry, Clinical Research Group, Johannes Gutenberg University-Mainz, Untere Zahlbacher Straße 8, 55131 Mainz, Germany

^cDepartment of Nuclear Medicine, Johannes Gutenberg University-Mainz, Langenbeckstraße. 1, 55131 Mainz, Germany

Abstract

Introduction: The serotonergic, especially the 5-HT_{2A} receptor, is involved in various diseases and conditions. It is a very interesting target for medicinal applications.

Methods: Two novel 5-HT_{2A} antagonistic tracers, namely [^{18}F]DD-1 and the enantiomeric pure (R)-[^{18}F]MH.MZ were radiolabelled by ^{18}F -fluoroalkylation of the corresponding desmethyl analogue. *In vitro* binding autoradiography on rat brain slices was performed to test the affinity and selectivity of these tracers. Moreover, first μPET experiments of (R)-[^{18}F]MH.MZ were carried out in SD rats.

Results: [^{18}F]DD-1 ($K_i = 3.23 \text{ nM}$) and (R)-[^{18}F]MH.MZ ($K_i = 0.72 \text{ nM}$) were ^{18}F -fluoroalkylated by the secondary synthon [^{18}F]FETos in a radiochemical yield (RCY) of > 70%. The final formulation for both tracers took no longer than 100 min with an overall RCY of ~ 40%. It provided [^{18}F]tracers with a purity > 96% and a typical specific activity of 25 – 35 GBq/ μmol . Autoradiographic images of (R)-[^{18}F]MH.MZ (**5**) and [^{18}F]DD-1 (**4**) showed excellent visualization and selectivity of the 5-HT_{2A} receptor for (R)-[^{18}F]MH.MZ and less specific binding for [^{18}F]DD-1. The BP of (R)-[^{18}F]MH.MZ was determined to be 2.6 in the frontal cortex and 2.2 in the cortex (n=4), whereas the cortex to cerebellum ratio was determined to be 3.2 at equilibrium (n=4). Cortex to cerebellum ratios of (R)-[^{18}F]MH.MZ

were almost twice as much as compared with the racemic [^{18}F]MH.MZ. Thereby, equal levels of specific activities were used. High uptake could be demonstrated in cortex regions.

Conclusion: Labeling of both novel tracers was carried out in high RCY. Autoradiography revealed (R)-[^{18}F]MH.MZ as a very selective and affine 5-HT_{2A} tracer, whereas [^{18}F]DD-1 showed no reasonable distribution pattern on autoradiographic sections. Moreover, results from μPET scans of (R)-[^{18}F]MH.MZ hint on improved molecular imaging characteristics compared with those of [^{18}F]MH.MZ. Therefore, (R)-[^{18}F]MH.MZ appears to be a highly potent and selective serotonergic PET ligand in small animals.

1. Introduction

Several diseases and physiological processes, including appetite, emotion, changes in mood, depression, Alzheimer's disease and the regulation of the sleep/wake cycle are involved in the serotonergic system.^{1,2,3} In particular, all clinically approved atypical antipsychotic drugs are potent 5-HT_{2A} receptor antagonists.⁴ Therefore, *in vivo* positron emission tomography (PET) studies of the 5-HT_{2A} receptor occupancy and availability would provide a significant advance in the understanding of the mentioned disorders and conditions. PET is an appropriate tool to measure non-invasively and repetitively various parameters as the binding potential, the receptor availability, and uptake kinetics of radio tracers for neuroreceptors *in vivo*. Novel ^{18}F -labeled 5-HT_{2A} antagonists would provide a significant advance in the field of molecular imaging of the serotonergic system, as, clinically used ligands to study the 5-HT_{2A} receptor as [^{18}F]altanserin or [^{11}C]MDL 100907 have notable disadvantages. [^{11}C]MDL 100907 is a very specific high affinity ligand for 5-HT_{2A} receptors with limitations due to its slow kinetics and its short half-life of C-11.^{5,6,7} The binding of [^{18}F]altanserin lacks specificity and *in vivo* stability.^{8,9}

Recently, we have reported the syntheses and first *in vitro* and *in vivo* evaluation of [^{18}F]MH.MZ (**1**), an ^{18}F -analog of MDL 100907 (Figure 1).^{9,10} The novel labeling reaction route could possibly be a superior compared to that of [^{18}F]altanserin. *In vivo* as *in vitro* studies defined [^{18}F]MH.MZ as a potent tracer to image the 5-HT_{2A} receptor status via PET at least in rats.¹⁰

Encouraged of these results, a new series of MDL 100907 derivatives was synthesized aiming for even more selective reference ligands.¹¹

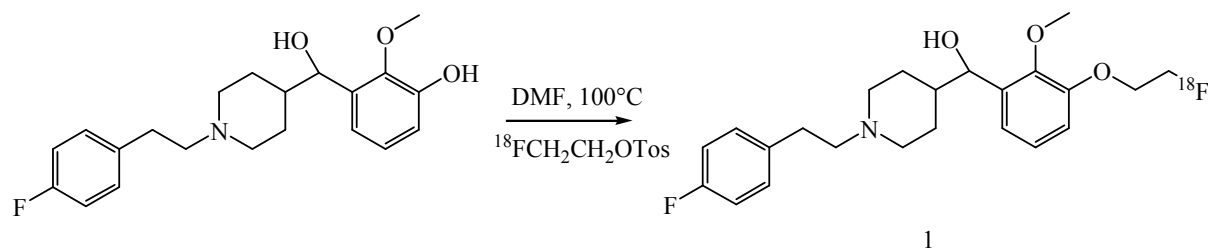


Figure 1: Radiosynthesis of [^{18}F]MH.MZ

Due to carried out *in vitro* experiments 2 novel and potent compounds (DD-1 and (R)-MH.MZ) displayed in figure 2 showed promising characteristics as high affinity and selectivity ligands (Figure 2).¹¹

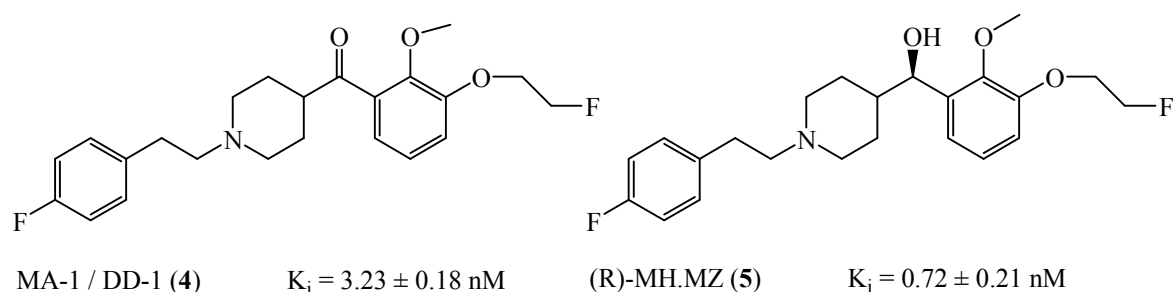


Figure 2: Structures of new potent, selective [^{18}F]antagonists of the 5-HT_{2A} receptor.¹¹

These results justified further experiments like *in vitro* autoradiography and *in vivo* μPET experiments to proof the applicability of these two novel ligands. The represent manuscript reports on the labeling of DD-1 and (R)-MH.MZ with F-18 and their evaluation as potential new and improved 5-HT_{2A} imaging agents in rats.

2. Methods and Materials

2.1 Chemicals and Reagents

Chemicals were purchased from Acros, Fluka or Merck. Unless otherwise noted all chemicals were used without further purification.

2.2 HPLC

Analytical HPLC: A HPLC system was used equipped with a Sykam S 1100 solvent delivery system, S 8110 low pressure gradient mixer, Rheodyne 9725i inject valve; linear UVIS-205 absorbance detector; Axxiom Chromatography 900-200 Pyramid; Pyramid 2.07; loop: 20 μ L)

Semipräparative HPLC: HPLC-system equipped with a Dionex P 680A pump, software Dionex Chromeleon vers., a Raytest 6.6 NaI scintillation counter (Gabi) and a linear UVD170U (254 nm) absorbance detector.

2.3 Hardware

Imager: Autoradiographic images were analyzed via an Imager FLA 7000 Fujifilm. Radioactive spots were detected using a Canberra Packard Instant Imager.

μ PET: PET studies were performed with a Siemens MicroPET Focus 120 camera.

2.4 Animals

Male 8 week mature catheterized Sprague-Dawley (SD) rats were obtained from the animal husbandry of the Johannes Gutenberg University of Mainz, Germany, were used for *ex vivo* distribution as well as for PET studies. All procedures were carried out in accordance with the European Communities Council Directive regarding care and use of animals for experimental procedures and were approved by local authorities of the state of Rhineland-Palatine.

2.5 Preparation of rat brain sections

Rats were narcotized with CO₂ and subsequently decapitated by a rodent guillotine. Brains were carefully removed from the skull, shortly rinsed in ice cold 50 mM Tris/Citrate pH 7.4 buffer to remove hairs and blood. The brains were then frozen on a pre-cooled -80 °C cold steel plate. Brains were either stored in parafilm or aluminum foil at -80 °C or transferred to a Leica cryostate and kept in parafilm at -24 °C for 30 min. After warming up to -24 °C brains were frozen onto object carrier with tissue tack freezing medium in the desired orientation for either sagittal, coronal or transversal sectioning. Sections were cut at 14 μ m thickness, knife angle of 5° and an object temperature of -13 °C. Sections were melted onto super frosted glass slides (Menzel), air dried and were either used immediately or stored at -80 °C until further use.

2.6 Radiochemistry

Preparation of the K^[18F]F–K₂₂₂-complex

Aqueous [¹⁸F]fluoride was passed through an anion exchange resin Sep-Pak[®] Light Waters Accell_{TM} Plus QMA cartridge initially in the chloride form, then washed with aq 1 M K₂CO₃ (10 mL) and rinsed with water (20 mL) and CH₃CN (10 mL) by helium pressure (1.5 – 2 bar). The [¹⁸F]fluoride ion was then eluted from the resin using an aqueous solution of K₂CO₃ (1.0 mL of a 15 μL/mL solution) and 15 mg Kryptofix[®]₂₂₂ (K₂₂₂: 4,7,13,16,21,24-hexaoxa-1,10diazabicyclo[8.8.8]hexa-cosane). The resulting solution was then gently concentrated to dryness at 90 °C under a nitrogen stream for 15 min to give no-carrier-added K^[18F]F–K₂₂₂ complex as a white semi-solid residue.

Radiosynthesis of [¹⁸F]FETos

To an aqueous [¹⁸F]fluoride solution (1400- 1600 MBq) were added Kryptofix[®]₂₂₂ (10 mg, 25 mmol), 12.5 mL potassium carbonate (1 N) and 1 mL acetonitrile. The mixture was dried in a stream of nitrogen at 80 °C. The drying procedure was repeated three times until the reaction mixture was absolutely dry. The dried K^[18F]F–K₂₂₂ complex was then dissolved in 1 mL acetonitrile and 4 mg (10 mmol) ethylenglycol-1,2-ditosylate were added and heated under stirring in a sealed vial for 3 min. Purification of the crude product was accomplished using HPLC (Lichrospher RP18-EC5,250x10 mm; acetonitrile/water 50:50, flow rate: 5 ml/min, rt: 8 min). After diluting the HPLC fraction containing the 2 [¹⁸F]fluoroethyltosylate with water, the product was loaded on a Phenomenex strata-X 33μm Polymeric reversed phase column, dried with nitrogen and eluted with 1 mL of tempered (40-50 °C) DMSO.

General procedure of the synthesis of [¹⁸F]FE1-MDL 100907 derivatives

[¹⁸F]FETos trapped on a Phenomenex strata-X 33μm polymeric reversed phase column was directly rinsed with 1 ml of tempered (40-50 °C) DMSO into a vial with 3 mg precursor (7 mmol) and 1.5 μL 5 N NaOH (7 mmol). The tube was placed in a heating block and stirred during the reaction time. The reaction vessel was then cooled to room temperature using an ice-water bath and quenched with 1 mL H₂O. The remaining radioactivity was measured, which was 90–95% of the initial radioactivity. The resulting reaction mixture was analyzed by radio-TLC. The reaction yield was calculated from the TLC-radiochromatogram and defined as the ratio of radioactivity area of the ¹⁸F-labeled compound over total fluorine-18.

(R)-[¹⁸F]MHMZ: SiO₂-TLC, eluent: CHCl₃/MeOH/conz. NH₃, 8:1:0.2, (R)-[¹⁸F]MHMZ: R_f = 0.36, [¹⁸F]FETos: R_f=0.95, [¹⁸F]fluoride ion: R_f = 0.0.

[¹⁸F]DD-1: SiO₂-TLC: eluent: CHCl₃/MeOH, 20:1, [¹⁸F]DD-1: R_f = 0.72, [¹⁸F]FETos R_f = 0.97, [¹⁸F]fluoride ion: R_f = 0.0).

Formulation

Formulation of the labelled product for evaluation studies was effected as follows: Reactants and by-products were separated from ¹⁸F-tracers by semipreparative HPLC (μBondapak C₁₈ 7.8 x 300 mm column, RT, flow rate 8 mL/min).

(R)-[¹⁸F]MHMZ: 0.05 M Na₂HPO₄ (pH 7.4 H₃PO₄)/ MeCN, 60:40, [¹⁸F]F⁻=1.8 min; [¹⁸F]FETos=4 min; (R)-[¹⁸F]MHMZ=9.76 min; MDL 105725=4.85 min.

[¹⁸F]DD-1: 0.25 M NH₄Ac-buffer (pH 5.6 acetic acid)/MeCN, 75:25, RT: [¹⁸F]F⁻=2.5 min; [¹⁸F]FETos=11.54 min; [¹⁸F]DD-1=21.73 min; (45)=7.23 min.

The collected fraction containing the ¹⁸F-labeled compound with water (4:1), passed through a conditioned strataX-cartridge (1 mL EtOH, 1 mL H₂O) and washed with 10 mL H₂O. The ¹⁸F-labeled compound was eluted with at least 1 mL of EtOH. Less than 8% of the total radioactivity was left on the cartridge. Finally, EtOH was removed *in vacuo* and the ¹⁸F-labeled tracer solved in 1 mL saline.

Quality control

The radiotracer preparation was visually inspected for clarity, absence of colour and particulates. Chemical and radiochemical purities were also assessed on an aliquot by TLC analyses (see 4.4.3) and by analytical HPLC (ET 250/8/4 Nucleosil® 5 C₁₈).

(R)-[¹⁸F]MHMZ: see above.

[¹⁸F]DD-1: NH₄Ac-buffer (pH 5.6)/MeCN, 60:40 flow rate 1 mL/min, RT: [¹⁸F]F⁻=2.4 min; [¹⁸F]FETos=16.34 min; [¹⁸F]DD-1=24.63 min; (45)=11.40. Specific activity (A_s) of the radiotracer was calculated from three consecutive HPLC analyses (average) and determined as follows: The area of the UV absorbance peak of the ¹⁸F-analogue of the ¹⁸F-labeled tracer was integrated on the HPLC chromatogram and compared to a standard curve relating mass to UV absorbance.

2.6 *In vitro* autoradiography of rat brain slices with [¹⁸F]DD-1 and (R)-[¹⁸F]MH.MZ

Autoradiography experiments were carried out at room temperature in reaction buffer (50 mM Tris/HCl buffer, pH 7.4, containing 120 mM NaCl, and 5 mM KCl) with ¹⁸F-labeled

compounds on ice. Sections were washed 2 x 2 min in reaction buffer containing 0.01% Triton X-100 and 1 x 2 min in reaction buffer, shortly dipped into deionized water, and quickly dried in a stream of cold air. Sections were exposed to Fuji phosphor screen for 3 h. Screens were read out with a Fuji FLA-7000 scanner. ^{18}F -quantification was done after calibration by a standard curve which was obtained by a dilution series of an ^{18}F -solution. Calibration was repeated for each fresh radiotracer synthesis. Calibration, quantification and data evaluation was done with Multi Gauge, Fujifilm image analysis software.

2.7 *In vivo* PET studies of (R)-[^{18}F]MH.MZ

Positron emission tomography scans were performed with a Siemens/Concorde Microsystems microPET Focus 120 small animal PET (μPET) scanner. 8 week old male Sprague-Dawley rats (weight: 220g-325g) were obtained from the animal husbandry of the Johannes Gutenberg University of Mainz. Animals were anaesthetised with a combination of xylazine (Rompun®) (2%) and ketamine (Ketavet®) (10%) by i.p. injection of 1.1 mL/kg. Rats were placed in supine position on the scanner bed and fixed with adhesive strips. Listmode acquisition was started with the tracer injection of 15-25 MBq.(specific activity: xxx GBq/ μmol) The ^{18}F -labeled tracers were applied via i.v. injection into the jugular vein catheter. Then, catheters were flushed with 0.25 ml isotonic 0.9 % NaCl solution.

After the dynamic recordings a transmission scan for attenuation correction was carried out using a ^{57}Co point source. Listmode acquisition was histogrammed into 25 frames. The frame duration increased progressively from 20s to 5min resulting in a total scanning time of 90 min. Finally, images were reconstructed with scatter and attenuation correction using a 3D maximum a posteriori (MAP) algorithm with 18 iterations and regularization parameter of 0.002.

Images were scaled as standardized uptake values (SUV) which is defined by: (activity concentration in Bq/mL) * body weight in g/ (injected dose in Bq). Kinetic modeling and image quantification was carried out using the PMOD software package. First, the images were transformed into standardized views according to the paxinos orientation. A volume-of-interests (VOI) template comprising frontal cortex, cortex and cerebellum were defined on an transaxial slices using an integral image between 60 min and 90 min p.i. reflecting specific binding of the tracer. Time-activity-curves (TAC) were derived from dynamic. Assuming negligible receptor density the cerebellum was used as reference region. Binding potential (BP) was calculated using the TAC and the simplified reference tissue model.

3. Results and Discussion

3.1 Radiochemistry

Precursors and reference compounds were synthesized as previously described.¹¹ Radioactive labeling was carried out similar to the reported synthesis of [¹⁸F]MH.MZ.^{9,10} Thereby, necessary [¹⁸F]FETos synthon production was performed in an automated module according to Bauman et al.¹² and used for [¹⁸F]fluoroalkylation resulting in (R)-[¹⁸F]MH.MZ and [¹⁸F]DD-1 (Figure 3).

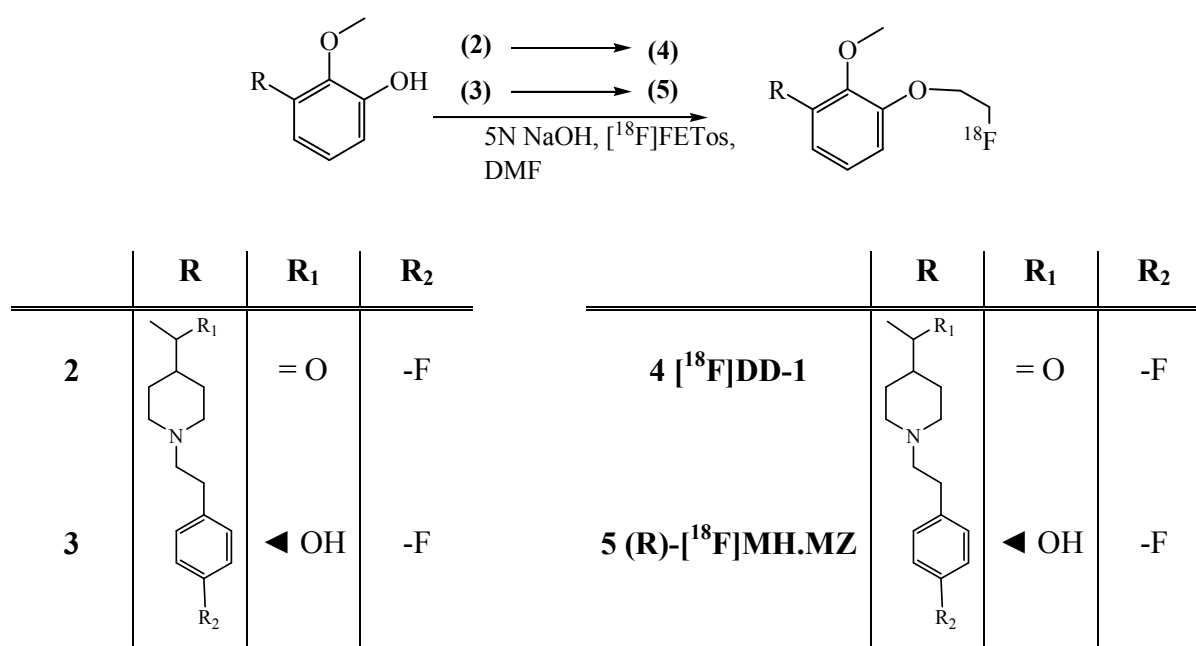


Figure 3: Syntheses of [¹⁸F]DD-1 and (R)-[¹⁸F]MH.MZ

[¹⁸F]Fluoroalkylation of the precursor (**2**) was optimized only due to temperature variations resulting in radiochemical yields > 70%. Labeling kinetics were compared with those reported for [¹⁸F]MH.MZ, whereas the [¹⁸F]alkylation of the enantioselective precursor (R)-MDL 105725 (**3**) was carried out using exactly the same reaction conditions as for its racemic analog. Used parameters enable radiochemical yields of about 80%. Final reaction conditions were 100 °C, 15 min reaction time, 7 mmol precursor, 7 mmol 5 N NaOH and dry DMSO (Figure 4).

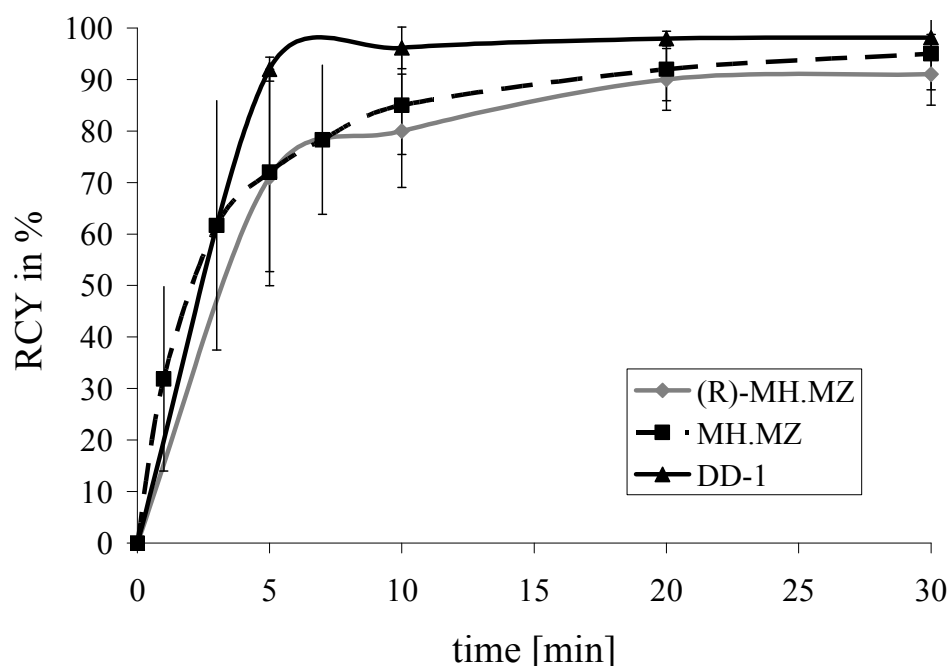


Figure 4: ^{18}F -Fluoroalkylation of 7 mmol precursor at 100 °C using DMF and 7 mmol 5 N NaOH yielding [^{18}F]MH.MZ, [^{18}F]DD-1 and (R)-[^{18}F]MH.MZ

The final formulation of the injectable solution including a semipreparative HPLC took no longer than 100 min for all compounds and provided ^{18}F -labeled tracers with a purity > 96%. Typical specific activities (A_s) are between 35-45 GBq/ μmol . Thereby, amounts of ~ 3 GBq of [^{18}F]fluorine were used as starting radioactivity.

The new ^{18}F -labeled compounds could be obtained as an injectable solution in an overall radiochemical yield of about 40% referred to the starting activity of ^{18}F -fluoride. This is very similar to the radiosynthesis of [^{18}F]altanserin, which takes 75 to 100 min and results in a radiochemical yield of 30-50%.¹³

3.2 *In vitro* Autoradiography

Autoradiographic images obtained with (R)-[^{18}F]MH.MZ (**5**) and [^{18}F]DD-1 (**4**) showed accumulation of radioactivity in known 5-HT_{2A} receptor regions in rat brain slices at equal A_s of 30 GBq/ μmol (Figure 5).

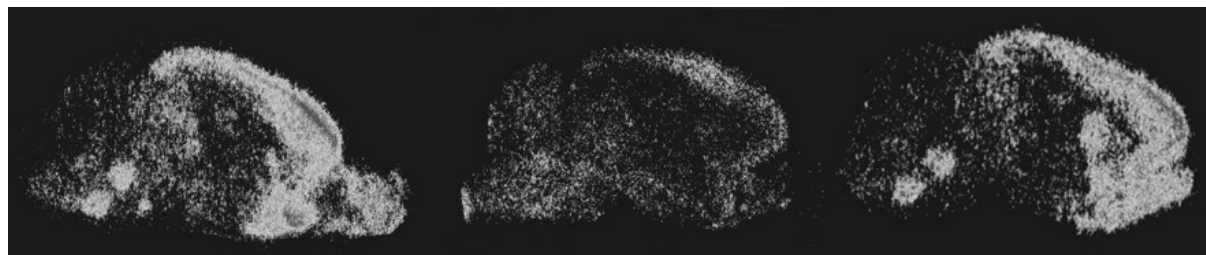


Figure 5: Images of an autoradiography of [^{18}F]MH.MZ (left), (R)-[^{18}F]MH.MZ (right) and [^{18}F]DD-1 (middle) showing high specific binding for the MH.MZ analogues and less binding and specificity for [^{18}F]DD-1 at 14 μm thick rat brain sections.

Excellent visualization was obtained by (R)-[^{18}F]MH.MZ. These data are in accordance with the known distribution of [^3H]MDL 100907¹⁴ and [^{18}F]MH.MZ⁹ in the rat brain.

Due to the higher 5-HT_{2A} binding of (R)-MH.MZ ($K_i = 0.72$ nM) compared to MH.MZ ($K_i = 3.0$ nM) this enantioselective tracer should be more valuable in PET experiments concerning the possibly improved binding potential (BP) and the regional cortex to cerebellum ratio within the brain.

Visualisation by [^{18}F]DD-1 showed less specific binding (Figure 5). Indeed, reduced binding characteristics is expected due to its decreased affinity compared to (R)-[^{18}F]MH.MZ (Table 1), but unexpected for [^{18}F]DD-1 compared to its [^{18}F]MH.MZ analogue (Table 1). In addition, selectivity of [^{18}F]DD-1 showed no intense alteration compared to that of MHMZ.¹¹ Therefore, the observed properties are most probably due to the increased lipophilicity of [^{18}F]DD-1 (MH.MZ: $\text{LogP} = 2.80 \pm 0.06$, DD-1: $\text{LogP} = 3.08 \pm 0.1$).¹¹

Competition autoradiography experiments (Figure 6) were conducted with the new enantioselective tracer to prove its potential as PET imaging agent. Thereby, 1 nM of (R)-[^{18}F]MH.MZ and 10 μM of ketanserin, fallypride, WAY 100635 and prazosin were used in these competition assays. High specificity of (R)-[^{18}F]MH.MZ toward 5-HT_{2A} receptors was obtained as expected because of the affinity and selectivity determined by radioligand binding assays through NIMH-psychoactive Drug Screening Program (PDSP).¹¹

Total displacement could be observed with ketanserin as a known 5-HT_{2A} receptor ligand, whereas no displacement could be detected with WAY 100635, a 5-HT_{1A} antagonist, and

prazosin, a α_1 ligand. Another displacement could only be detected with fallypride. However, co-incubation of fallypride led to a displacement of $25 \pm 8\%$ ($n=4$) of total binding in the frontal cortex as well as in the caudate-putamen, which does not imply that [^{18}F]MH.MZ recognizes D_2/D_3 receptors but might rather be explained by the known cross affinity of fallypride to 5-HT $_2$ receptors (Figure 6).¹⁶ These results are very similar to the observed of the racemic analogue, [^{18}F]MH.MZ.⁹

Binding parameters of (R)-[^{18}F]MH.MZ of cortex to cerebellum ratios of the rat brain obtained with autoradiography assays at equal levels of specific activities at sagittal sections are displayed in table 1 and compared with the binding parameters of [^{18}F]MH.MZ.⁹ Binding in the cerebellum was at the level of non-specific binding so levels of binding in different brain regions are also given relative to that brain area. However, as a matter of fact (R)-[^{18}F]MH.MZ showed region to cerebellum ratios almost twice as high as compared with [^{18}F]MH.MZ. Results of [^{18}F]DD-1 were not evaluated due to its unfavorable distribution pattern.

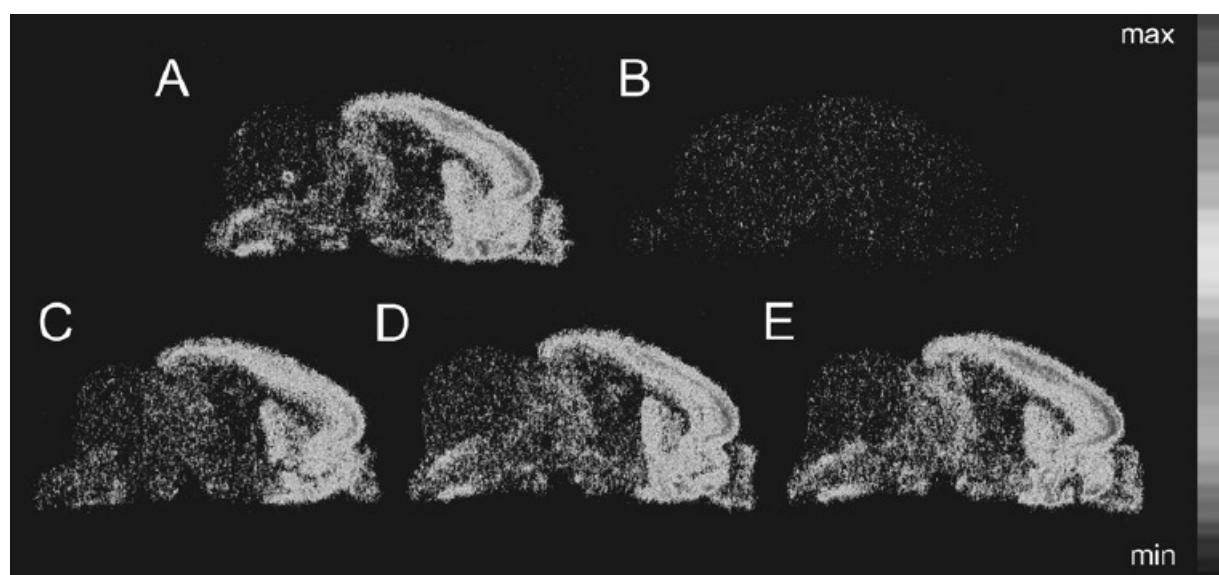


Figure 6: Sagittal autoradiographies on 14 μm rat brain sections with (R)-[^{18}F]MHMZ at a concentration of 1 nM ($K_i = 0.72$ nM for 5-HT $_{2A}$). **A** total binding, **B** non-specific binding measured in the presence of 10 μM ketanserin, **C** co-incubation with 10 μM fallypride, **D** co-incubation with 10 μM WAY 100635, **E** co-incubation with 10 μM prazosin.

Table 1: Binding parameters obtained with (R)-[¹⁸F]MH.MZ and [¹⁸F]MH.MZ from binding experiments at 14 μ m sagittal sections of the rat brain (means \pm SEM)

		(R)-[¹⁸ F]MH.MZ	[¹⁸ F]MH.MZ
	n	region/cerebellum	region/cerebellum
Lamina V	4	91.8 \pm 0.5	59.5 \pm 2.8
Frontal cortex	4	57.5 \pm 3.2	31.4 \pm 1.3

In conclusion, the results suggest that the non-specific binding associated with these radiotracers is low for [¹⁸F]MH.MZ and (R)-[¹⁸F]MH.MZ and moderate to low for [¹⁸F]DD-1 (Figure 4). [¹⁸F]MH.MZ and (R)-[¹⁸F]MH.MZ could possibly be useful as ¹⁸F-labeled tracers for imaging the 5-HT_{2A} receptor *in vivo* by PET experiments. Especially, (R)-[¹⁸F]MH.MZ could improve binding characteristics such as BP or regional distribution expressed as cortex to cerebellum ratios due to its higher affinity.

3.3 *In vivo* PET-experiments

Due to the relative moderate binding characteristics of [¹⁸F]DD-1, we decided only to perform PET scans with (R)-[¹⁸F]MH.MZ expecting better *in vivo* results compared to its racemic derivative [¹⁸F]MH.MZ. Dynamic images were analyzed with pixel-wise modeling computer software (PMOD; Zurich, Switzerland). For illustrative purposes an integral image between 60 and 90 min. after tracer injection is displayed in figure 7, whereby the last 30min of the dynamics reflects the specific binding of (R)-[¹⁸F]MH.MZ. Images are shown in horizontal orientation with a slice thickness of 0.8 cm. False colour coded images in A) display of horizontal slices through the rat brain from top (1) to bottom (12), whereas B) shows a representative horizontal slice through the cortex, the frontal cortex and the cerebellum area .

These PET images clearly visualizes the binding of (R)-[¹⁸F]MH.MZ in the frontal cortex known to posses high availability of 5-HT_{2A} receptors, whereas the cerebellum, which is devoid of 5-HT_{2A} receptors, is at background level.¹⁴ Results are very similar to those obtained by its racemic analogue [¹⁸F]MH.MZ.⁹

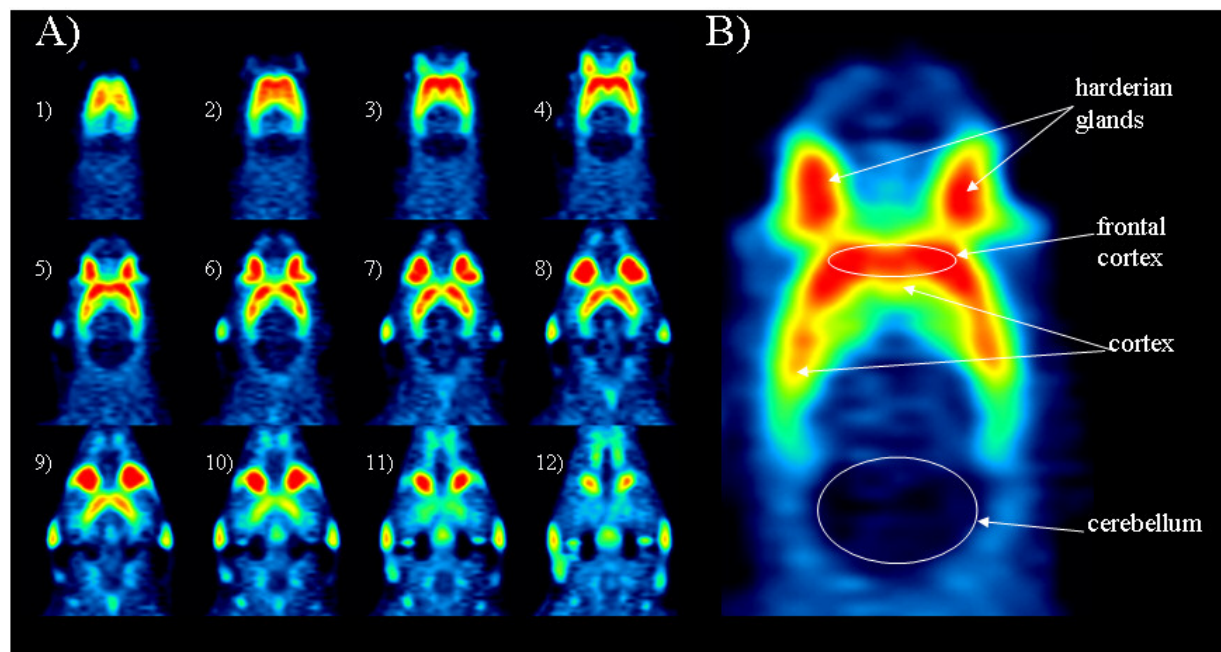


Figure 7: μ PET images of (R)-[¹⁸F]MH.MZ binding in horizontal orientation. A) horizontal slices from top (1) to bottom (12) B) representative horizontal slicethrough the cortex, the frontal cortex and the cerebellum showing highest specific binding in the frontal cortex and a high nonspecific binding in the hardierian glands. Uptake in the cerebellum was at background level.

Figure 8 shows a representative time-activity-curve (TAC) of a total binding study of (R)-[¹⁸F]MH.MZ which included four animals. Results are given as standardized uptake value (SUV) ((% injected dose \times Bq/mL) \times animal weight in g). Uptake of (R)-[¹⁸F]MH.MZ between 60 and 90 min is more than 150% higher in cortical regions than in the cerebellum, whereas the uptake of [¹⁸F]MH.MZ is only 50 % higher in these regions.⁹ The binding potential (BP) of (R)-[¹⁸F]MH.MZ was determined to be 2.6 for the frontal cortex region and to be 2.2 for the cortex (n=4) using a four parameter simple reference tissue model and the PMOD software, whereas the BP for its racemic derivative [¹⁸F]MH.MZ was only determined to be 1.45 in the frontal cortex.⁹ Cerebellum uptake is used as a reference region and is employed instead of a plasma input curve. The time-activity curve shows the uptake in the frontal cortex, the cortex as well as the cerebellum (cereb).

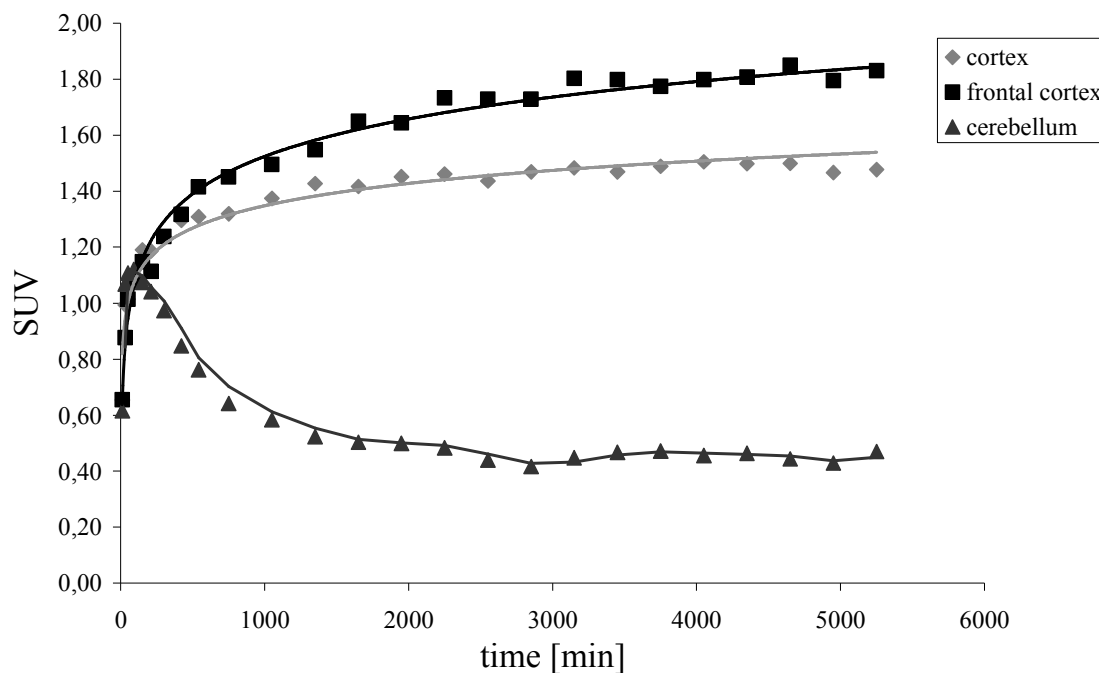


Figure 8: Representative time-activity-curve (TAC) of μ PET experiments of (R)- $[^{18}\text{F}]$ MH.MZ in SD rats. The graph shows results of a total binding study. Results are given as SUV ((% injected dose x Bq/mL) x animal weight in g).

The region to cerebellum ratios between 60-90 min are displayed in table 2. An improved ratio of 3.3 was found for (R)- $[^{18}\text{F}]$ MH.MZ compared to the value of 2.7 for its racemic analogue $[^{18}\text{F}]$ MH.MZ. The ratio for the frontal cortex is also improved to be 3.9. According to the time-activity curves (TAC) displayed in figure 8, equilibrium appears to be reached between 28 to 35 minutes post injection and the specific binding remains very constant over 60 min. This is identical with the observed one of $[^{18}\text{F}]$ MH.MZ.

Table 2: Region to cerebellum ratios of (R)- $[^{18}\text{F}]$ MH.MZ in rat brains (n=4)

Region	Region to cerebellum ratio
Cortex	3.3 ± 0.2
Frontal cortex	3.9 ± 0.1

4. Conclusion

In conclusion, two new 5-HT_{2A} affine tracers, [¹⁸F]DD-1 ($K_i = 3.23$ nM) and (R)-[¹⁸F]MH.MZ ($K_i = 0.72$ nM), were ¹⁸F-fluoroalkylated by the secondary synthon [¹⁸F]FETos in radiochemical yields of > 70%. The final formulation of the injectable solution including [¹⁸F]FETos synthesis took no longer than 100 min for the two compounds. The overall RCY was about 40%. It provided ¹⁸F-labeled compounds with a purity > 96% and a typical specific activity of 35 – 40 GBq/μmol with a starting radioactivity of ~ 3 GBq of [¹⁸F]fluorine.

Autoradiographic images of (R)-[¹⁸F]MH.MZ (**5**) and [¹⁸F]DD-1 (**4**) showed excellent visualization of the 5-HT_{2A} receptor for (R)-[¹⁸F]MH.MZ and less specific binding for [¹⁸F]DD-1 in rat brain slices. This is reasonable for (R)-[¹⁸F]MH.MZ due to its increased affinity, but unexpected for [¹⁸F]DD-1. The reduced binding for [¹⁸F]DD-1 may be explained because to its decreased affinity compared to (R)-[¹⁸F]MH.MZ, but it is unexpected for [¹⁸F]DD-1 due to its affinity compared with the racemic derivative [¹⁸F]MH.MZ. In addition, selectivity of [¹⁸F]DD-1 showed no intense alteration compared to that of MHMZ. Therefore, the observed properties are most probably due to the increased lipophilicity of [¹⁸F]DD-1.

Competition autoradiography experiments were conducted with the new enantioselective tracer and to prove its selective binding characteristics. Cortex to cerebellum ratios of (R)-[¹⁸F]MH.MZ were almost twice as much as compared with [¹⁸F]MH.MZ. Thereby, equal levels of specific activities were used.

Results from μPET scans of (R)-[¹⁸F]MH.MZ hint on significantly improved molecular imaging characteristics compared with those of [¹⁸F]MH.MZ due to the higher 5-HT_{2A} binding of (R)-MH.MZ ($K_i = 0.72$ nM) compared to MH.MZ ($K_i = 3.0$ nM). High uptake could be demonstrated in cortex regions. The binding potential of (R)-[¹⁸F]MH.MZ was determined to be 2.2 in the cortex and 2.6 in the frontal cortex (n=4), whereas the cortex to cerebellum ratio was determined to be 3.3 at equilibrium in the cortex and in the frontal cortex 3.9 (60 – 90 min, n=4). All values represent an important improvement compared to those obtained by [¹⁸F]MH.MZ.⁹

Therefore, the enantioselective derivative (R)-[¹⁸F]MH.MZ is probably the more valuable tracer for molecular imaging of the 5-HT_{2A} receptor system by PET.

5. Acknowledgments

The authors wish to thank Sabine Höhnemann for the syntheses of [¹⁸F]FETos, Daniel Zils for excellent animal preparation, Dr. Markus Piel as well as Matthias Schreckenberger (MD) for his support. Financial support by Friedrich-Naumann-Stiftung and the European Network of Excellence (EMIL) is gratefully acknowledged.

6. References and Notes:

1. Smith GS, Price JC, Lopresti BJ, Huang Y, Simpson N, Holt D, Mason NS, Meltzer CC, Sweet RA, Nichols T, Sashin D, Mathis CA. Test–retest variability of serotonin 5-HT_{2A} receptor binding measured with positron emission tomography and [¹⁸F]altanserin in the human brain. *Synapse* 1998; 30: 380-392.
2. Naughton M, Mulrooney JB, Leonard BE. A review of the role of serotonin receptors in psychiatric disorders. *Hum Psychopharmacol* 2000; 15: 397–415.
3. Davis KL, Charney D, Coyle JT, Nerneroff C. *Neuropsychopharmacology: the fifth generation of progress*. New York: Raven Press; 2002.
4. Jones BE, Kryger MH, Roth T, Dement WC, Eds.; *Principles and practice of sleep medicine*, W.B. Saunders Company: Philadelphia 2000; 134-154
5. Hall H, Farde L, Halldin C, Lundkvist C, Sedvall, G. Autoradiographic localization of 5-HT_{2A} receptors in the human brain using [³H]M100907 and [¹¹C]M100907. *Synapse* 2000; 38: 421-431.
6. Watabe H, Channing MA, Der MG, Adams HR, Jagoda E, Herscovitch P, Eckelman WC, Carson RE. Kinetic analysis of the 5-HT_{2A} ligand [¹¹C]MDL 100,907. *J Cereb Blood Flow Metab.* 2000; 20: 899–909.
7. Ito H, Nyberg S, Halldin C, Lundkvist C, Farde L. PET imaging of central 5-HT_{2A} receptors with carbon-11-MDL 100,907. *J.Nuc.Med.* 1998; 39: 208-214.
8. Tan P, Baldwin RM, Fu T, Charney DS, Innis RB. Rapid synthesis of F-18 and H-dual labeled altanserin, a metabolically resistant PET ligand for 5-HT_{2A} receptor. *J. Labelled Compd. Radiopharm.* 1999; 42: 457-467.
9. Herth MM, Debus F, Piel M, Palner M, Knudsen GM, Lüddens H, Rösch F. Total synthesis and evaluation of [¹⁸F]MH.MZ. *Bioorg. Med. Chem. Lett.* 2008; 18: 1515-1519.
10. Herth MM, Piel M, Debus F, Schmitt U, Lüddens H, Rösch F. Preliminary in vivo and ex vivo evaluation of the 5-HT_{2A} imaging probe [¹⁸F]MH.MZ. 2009; (accepted)

11. Herth MM, Kramer V, Piel M, Palner M, Riss PJ, Knudsen GM, Rösch F. Synthesis and *in vitro* Affinities of Various MDL 100907 Derivatives as Potential ¹⁸F-Radioligands for 5-HT_{2A} Receptor Imaging with PET. 2009; (submitted)
12. Bauman A, Piel M, Schirmacher R, Rösch F. Efficient alkali iodide promoted ¹⁸F-fluoro ethylations with 2-[¹⁸F]fluoroethyl tosylate and 1-bromo-2-[¹⁸F]fluoroethane. *Tetrahedron Lett.* 2003; 44: 9165-9167.
13. Lemaire C, Cantineau R, Guillaume M, Plenevaux A, Christiaens L. Fluorine- 18-Altanserin: A Radioligand for the Study of Serotonin Receptors with PET: Radiolabeling and In Vivo Biologic Behavior in Rats. *J. Nucl. Med.* 1991; 32: 2266-2272.
14. Lopez-Gimenez JF, Mengod D, Palacios JM, Vilario MT. Selective visualization of rat brain 5-HT_{2A} receptors by autoradiography with [³H]MDL 100,907. *Naunyn-Schmiedeberg's Arch. Pharmacol.* 1997; 356: 446-454.
15. Lundkvist C, Halldin C, Ginovart N, Swahn CG, Carr AA, Brunner F, Farde L. [¹¹C]MDL 100907, a radioligand for selective imaging of 5-HT(2A) receptors with positron emission tomography. *Life Sci.* 1996; 58: 187-192.
16. Stark D, Piel M, Hübner H, Gmeiner P, Gründer G, Rösch F. In vitro affinities of various halogenated benzamide derivatives as potential radioligands for non-invasive quantification of D₂-like dopamine receptors *Biorg. Med. Chem.* 2007; 15: 6819-6829.

3.7 Analysis of P-glycoprotein influence on the brain-uptake of a 5-HT_{2A} ligand: [¹⁸F]MH.MZ

by Ulrich Schmitt,^a Dianne E. Lee,^b Matthias Herth,^c Marcus Piel,^c Hans-Georg Buchholz,^d Frank Rösch,^c Christoph Hiemke,^a Hartmut Lüddens^{a,#} and Fabian Debus^{a,#}

^aDepartment of Psychiatry, Clinical Research Group, Johannes Gutenberg University-Mainz, Untere Zahlbacher Straße 8, D-55131 Mainz, Germany

^bBrookhaven National Laboratory, Upton, New York 11973, USA;

^cInstitute of Nuclear Chemistry, University of Mainz, Fritz-Strassmann-Weg 2, D-55128 Mainz, Germany

^dDepartment of Nuclear Medicine, University of Mainz, Langenbeckstraße. 1, D-55131 Mainz, Germany

Abstract

The serotonergic system, especially the 5-HT_{2A} receptor, is involved in various diseases and conditions. Therefore, we have recently developed a new ¹⁸F-5-HT_{2A} receptor ligand using an analogue, MDL 100907, as a basis for molecular imaging via PET. This tracer, [¹⁸F]MH.MZ, has shown to be an adequate tool to visualize the 5-HT_{2A} receptors *in vivo*. However, [¹⁸F]altanserin, similar in chemical structure, has recently been shown to be a substrate of efflux transporters, namely P-glycoprotein (P-gp), of the blood-brain-barrier, thus limiting its availability in the CNS. Therefore, the aim of this study was to determine whether P-gp influences the distribution ratio of [¹⁸F]MH.MZ, in the frontal cortex compared to cerebellum. The approach was based on transgenic P-gp k.o. mice which were compared to wild type mice under several conditions. Thereby, an *ex vivo* pharmacokinetic, and brain accumulation study as well as an *in vivo* in a microPET investigation were carried out. All analysis carried out showed that [¹⁸F]MH.MZ entered the brain and was sensitive to P-gp transport. Detailed analyses clearly indicated the necessity investigating the functional role of transport mechanisms at the blood-brain-barrier, presently P-gp, including its sub-regional distribution not only for drug treatment but also for diagnostic purposes using PET.

Introduction

Serotonin (5-hydroxytryptamine, 5-HT) is one of the oldest neurotransmitters in terms of evolution and has been implicated in the aetiology of numerous disease states, including depression, anxiety, social phobia, schizophrenia, and obsessive-compulsive disorder and panic disorders (Benkelfat, 1993; Dubovski, 1995; Murphy et al., 1998). 5-HT produces its effects through a variety of membrane-bound receptors. The 5-HT₂ receptor subtype is widely distributed in peripheral and central tissues. Centrally, these receptors are located in the cortex, claustrum and basal ganglia. Its activation stimulates hormone secretion, e.g. ACTH, corticosterone, oxytocin, rennin and prolactin (Murphy et al., 1998; van de Kar et al., 2001). 5-HT antagonists have been implicated for the treatment of schizophrenia (Breier, 1995). The so called atypical antipsychotics, such as clozapine, olanzapine, quetiapine, risperidone and most recently paliperidone, its active metabolite, adhere to the concept that the combination of dopamine D₂ and 5-HT_{2A} receptor antagonism may best explain the antipsychotic activity (Lieberman et al., 1998; Horachek et al., 2006).

The development of specific radiotracers enabled non invasive *in vivo* studies of receptor occupancy by Positron Emission Tomography (PET) which improved substantially the understanding of the mechanisms underlying the antipsychotic effects of dopamine and 5-HT receptor antagonists (Talvik et al., 2004). However, these studies referred primarily to the dopaminergic site of activity, of the used drugs (Talvik et al., 2003). Moreover, a number of 5-HT neurotransmitter analogues were synthesized as radiopharmaceuticals for imaging the 5-HT_{2A} receptor and thus brought about a better understanding of the involvement of the serotonergic systems in these conditions (Mamo et al., 2007; Erritzoe et al., 2008).

To date *in vivo* studies have been performed with several 5-HT_{2A} selective antagonists for PET such as [¹¹C]MDL 100907, or [¹⁸F]altanserin. Based on the advantage of the high affinity and selectivity of the compound MDL 100907 we recently developed an ¹⁸F-analogue of MDL 100907, [¹⁸F]MH.MZ with a K value of 3.0 nM). We believe that the resultant PET-tracer for 5-HT_{2A} receptors is superior, at least in rats (van de Kar et al., 2001; Kristiansen et al., 2005; Herth et al., 2008,2009). However, [¹⁸F]altanserin similar in structure (Figure 1), has recently been shown to be a substrate of efflux transporters, namely P-glycoprotein (P-gp), of the blood-brain-barrier limiting its availability in the CNS (Palner et al., 2007). *Ex vivo* as well as *in vivo* studies in rats showed that altanserin has a limited brain uptake. Consequently, its binding potential (BP) is highly variable. Rats pre-treated with cyclosporine A (CsA), a P-gp inhibitor, exhibited a 52 % higher total brain uptake of [¹⁸F]altanserin and a

6.46 fold increase in the BP of the frontal cortex compared to untreated controls (Palner et al., 2007).

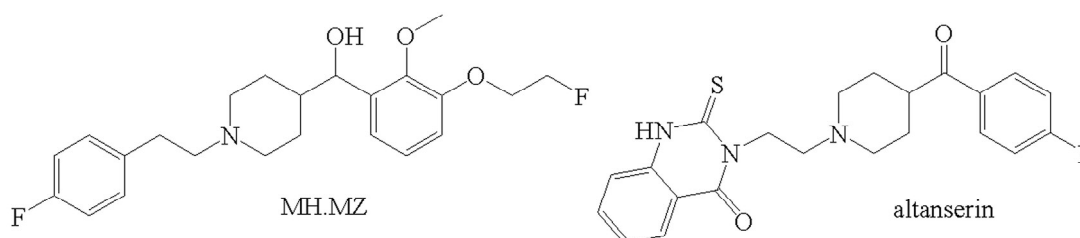


Figure 1: Chemical structures of the two 5-HT_{2A} antagonists MH.MZ and altanserin

PET studies on rodents have also shown the influence of P-gp on the pharmacokinetics and brain uptake of the two 5-HT_{1A} receptor ligands, [¹⁸F]MPPF and [¹¹C]WAY 100635 (Passchier et al., 2000). The specific brain uptake of [¹⁸F]MPPF is 5 to 10 higher than that of [¹¹C]WAY 100635. After CsA application, [¹⁸F]MPPF uptake in the rat brain increased to that level of the ¹¹C-derivative. Cerebral uptake of [¹¹C]WAY 100635 was also increased by P-gp modulation, but lower than that observed for [¹⁸F]MPPF (2-3 fold) (Elsinga et al., 2005).

For PET imaging studies, brain delivery remains a significant challenge in the optimal design of PET ligands. Therefore, it is imperative that the development of new radioligands for PET be evaluated for substrate specificity of carriers like P-gp and if, whether the BP is altered.

P-gp belongs to the superfamily of ATP-binding cassette transport proteins in the blood-brain-barrier, its function is an efflux pump limiting the access of xenobiotics into the CNS (Mizuno et al., 2003). This efflux pump has been shown to oppose passive diffusion of many drugs including antipsychotics and antidepressants (Uhr et al., 2003; Doran et al., 2005; Kirschbaum et al., 2008). Kirschbaum and co-workers (2008) have shown that substrate properties of risperidone for P-gp had not only pharmacokinetic but also pharmacodynamic consequences.

The present studies used molecular imaging with microPET, complemented by *ex vivo* studies, to measure [¹⁸F]MH.MZ uptake in the frontal cortex and cerebellum in wild-type and k.o. mice to examine the alterations in its kinetic profile with respect to P-gp substrate properties of the compound.

Methods

Preparation of MH.MZ and [¹⁸F]MH.MZ:

[¹⁸F]MH.MZ as well as the cold substance MH.MZ were synthesised according to Herth et al., (2008; 2009).

Synthesis of MH.MZ: MH.MZ was derived from MDL 105725 by fluoroalkylation. The synthesis of MDL 105725 has already been described by Ullrich et al. (2000) and Huang et al., (1999). The synthetic route to MDL 105725 is dependent on the transformation of an ester to a ketone via an amide intermediate. Finally, MH.MZ was synthesized via a fluoroalkylation of the precursor MDL 105725 in dry DMF by addition of equimolar sodium hydride and 1-bromo-2-fluoroethane in a yield of 40%.

Synthesis of [¹⁸F]MH.MZ: [¹⁸F]FETos diluted in 0.8 mL of dry DMSO was added to a solution of 3 mg MDL 105725 (7 mmol) dissolved in 0.2 mL dry DMSO and 1.5 μL 5N NaOH (7 mmol). The solution remained at 100 °C for 10 min and was quenched with 1 mL H₂O. [¹⁸F]MH.MZ was separated from reactants and by-products by semipreparative HPLC (μBondapak C₁₈ 7.8 x 300 mm column, flow rate 8 mL/min, eluent: MeCN/0.05 phosphate-buffer {pH 7.4 adjusted with H₃PO₄} (40:60)]. The retention times of [¹⁸F]MH.MZ, [¹⁸F]FETos and MDL 105725 were 9.76 min, 3.97 min and 4.85 min respectively. The collected product was diluted with water (4:1), passed through a conditioned strataX-cartridge (1 mL EtOH, 1 mL H₂O), washed with 10 mL H₂O and eluted with at least 1 mL EtOH. Finally, EtOH was removed *in vacuo* and [¹⁸F]MH.MZ solved in 1 mL saline.

Animals:

Male *mdr1a/1b* (-/-, -/-) double-knockout mice (P-gp k.o.; FVB/N background, Taconic, Germantown, NY) and male wild type controls (also FVB/N) were used. Animals had access to food and water *ad libitum*. Temperature and humidity were kept at 22 ± 2° C and 60% respectively. All animals were maintained on a 12/12 light/dark cycle. Handling occurred only during the light cycle. Animal procedures were in strict accordance with the National Institutes of Health guide for the care and use of all laboratory animals and were approved by the local animal care and use committee.

In vitro analysis:

a) Plasma and brain concentrations of MH.MZ were analysed in accordance to Kirschbaum et al. (2008) and Waldschmitt et al. (2009). In brief, P-gp knockout and wild type mice (n = 5 per

group) were injected i.p. with either 20 mg/kg MH.MZ or 20 mg/kg of MDL 105725. After 1h and 3h, animals were killed by decapitation under isoflurane (Forene®, Abbott GmbH & Co. KG, Wiesbaden, Germany) anaesthesia. Trunk blood was collected immediately and the brain was dissected. Serum, obtained by centrifugation of blood at 3000 x g for 10 min, was stored at -20°C or analysed immediately by high performance liquid chromatography (HPLC). One half of the brain was frozen on dry ice and stored at -20°C, the other half was weighed and homogenized in four volumes of methanol (HPLC-grade; Merck, Darmstadt, Germany) for MH.MZ and MDL 105725 analysis. Homogenates were centrifuged at 13000 x g and the supernatant was frozen at -20°C or analyzed directly by HPLC.

Serum or methanolic brain extracts were injected directly into the HPLC system with column switching and analyzed by established methods using peak heights for quantification. MH.MZ and MDL 105725 concentrations were measured using a Lichrospher column (60 RP-Select B, 125 x 4 mm, 5 µm particle size; MZ-Analysentechnik, Mainz, Germany) as analytical column. The analytical eluent contained 32.63% acetonitrile and di-potassium-hydrogenphosphate (Merck, Darmstadt, Germany) adjusted to pH 3.35. Sample clean up was done on a CN 20 µm PerfectBond pre-column (10 x 4 mm, MZ-Analysentechnik) using deionized water containing 8% (v/v) acetonitrile. Absorption was measured by spectrophotometric detection at a wavelength of 210 nm. Retention times were 8 and 11 min for MH.MZ and MDL105725, respectively, at a flow rate of 1mL min⁻¹.

b) Accumulation of [¹⁸F]MH.MZ in brains of P-gp k.o. and FVB wild type mice was analyzed 60 min post injection. Mice were anesthetized with halothane and sacrificed by decapitation. Blood samples for determination of the metabolism were centrifuged and the supernatant was mixed with MeCN 1:5 (v/v). After an additional centrifugation step the supernatant was used for chromatography (radio-TLC). Brains for determination of the metabolism were harvested, homogenized and mixed with MeOH and centrifuged. The supernatant was used for radio-TLC. Blood and brain samples were analyzed *via* radio-TLC (CHCl₃/MeOH 5:2 (v/v); R_f: [¹⁸F]FETos 0.9; [¹⁸F]MH.MZ 0.7; metabolite 0.1).

***In vivo* imaging studies:**

microPET imaging was performed with a Siemens/Concorde Microsystems microPET Focus 120 small animal PET (microPET) camera. The radiotracer [¹⁸F]MH.MZ was synthesized and applied i.p. (~ 12 MBq; A = 50 GBq/µmol) (Schiffer et al., 2007) to P-gp k.o. (n=3) and wild type (n=3) mice. Following a 45 min awake uptake period, mice were anesthetized with chloralhydrate (7%) by i.p. injection of 6 mL/kg and a 10 min static PET scan ensued.

Dynamic PET studies showed that equilibrium is reached within this time frame and the BP remains stable. Images were reconstructed without scatter and attenuation correction using a 3D maximum a posteriori (MAP) algorithm with 18 iterations and regularization parameter of 0.005, as previously described (Lee et al 2006). Tomographic images were analyzed with pixel-wise modeling computer software (PMOD; Zurich, Switzerland). Based on a digital mouse brain atlas, a region of interest (ROI) template was created including ROIs for frontal cortex and cerebellum. microPET images of the P-gp k.o. group were realigned and co-registered to create a mean [^{18}F]MH.MZ image using Statistical Parametric Mapping 2 (SPM). Then, image sets of both groups were realigned to the mean image using affine transformation of SPM2. Statistics were derived from the ROI template applied to each transformed image set of the P-gp k.o. and wild type group. ROI data were normalized for whole brain uptake and compared between groups (P-gp k.o. vs. wild type) using $P \leq 0.05$ significance threshold. Results were expressed as standardized uptake values (SUV) which are defined by (activity concentration in Bq/mL) * (body weight in g) / (injected dose in Bq).

Statistics

For statistical analysis of effects of genotype on the pharmacokinetics for each time point and substance student's t-test was used. P values < 0.05 were considered statistically significant. Area under the data (AUD), which is the area under the curve between 0 h and 3h after injection, was calculated using the trapezoid rule. Statistical analysis of microPET data was done by multiple analysis of variance (MANOVA) with post-hoc t-test. All statistical analyses were performed using SPSS version 12.0G for Windows (SPSS Inc., Chicago, IL).

Results

Ex vivo studies

To study the regional uptake of MH.MZ in the brain and whether P-gp expression-dependent differences occurred, serum and brain levels of MH.MZ and MDL 105725 were measured 1h and 3h after drug administration. *In vivo* distribution data revealed significantly different brain concentrations of MH.MZ between wild type and P-gp k.o. mice (Figure 2). MH.MZ levels were 6.2-fold (1 h) and 3.7-fold (3 h) higher in brains of P-gp k.o. mice (both $p < 0.05$). MDL 105725 levels in these mice exceeded brain concentrations in wild type mice 3.7-fold (1 h) and to 5.5-fold (3 h) (both $p < 0.05$) (Figure 2). Serum levels of MH.MZ showed a 1.7-fold (1h, $p < 0.05$) increase and no difference after 3h (n.s.). MDL 105725 was only slightly increased after 1h 1.1 fold (n.s.) and decreased after 3 h 0.7 fold (n.s.) (Figure 2). The area under the

data (AUD) calculations revealed that MH.MZ brain concentrations in P-gp k.o. mice attained 512% of the level measured in wild type mice while MDL 105725 brain levels in P-gp deficient mice represented 483% of wild type mice brain concentrations. Further, serum levels of P-gp k.o. mice attained 138% of the level measured in wild type mice while the MDL 105725 serum levels in P-gp k.o. mice represented only 89% of wild type mice serum concentrations (Table 1).

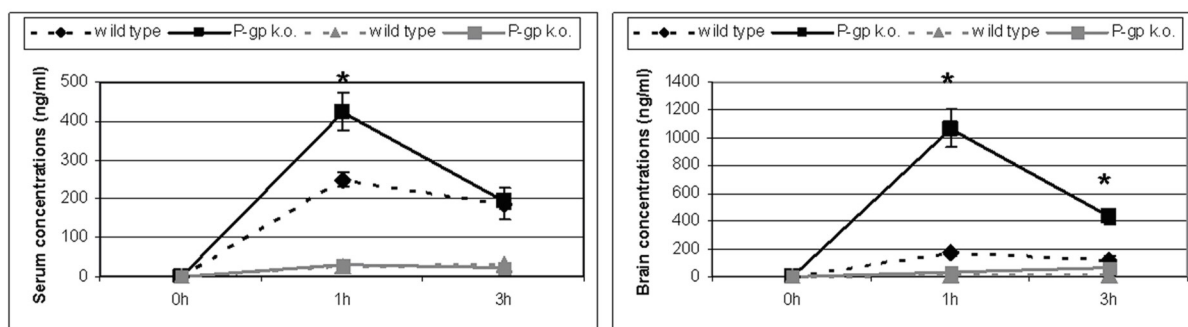


Figure 2: Serum and brain concentration-time profiles for MH.MZ (black symbols/lines) and MDL 105725 (gray symbols/lines) in FVB wild type (dashed line) and P-gp k.o. mice (solid line) following i.p. injection. Data points represent mean + SEM values. Asterisk indicate significant concentration differences of MH.MZ between genotypes (student t-test; $p < 0.05$); for significant differences in MDL 105725 concentrations see results section.

Table 1: AUD (Area under the data) values (ng/mL/3h) in P-gp k.o. and FVB wild type mice for the time period 0 to 3 h after i.p. injection.

Drug	Brain		Serum	
	P-gp k.o.	wild type	P-gp k.o.	wild type
MH.MZ	3952.40	771.90	1637.50	1186.99
MDL 105725	268.30	55.50	139.00	156.99

Relative amounts of MH.MZ and MDL 105725 in the brains of P-gp k.o. mice were 3 fold higher after 1h with respect to brains of wild type mice. After 3h MH.MZ was still 3 fold higher, while the metabolite MDL 105725 was 7.5 fold higher in P-gp k.o. mice (Figure 3).

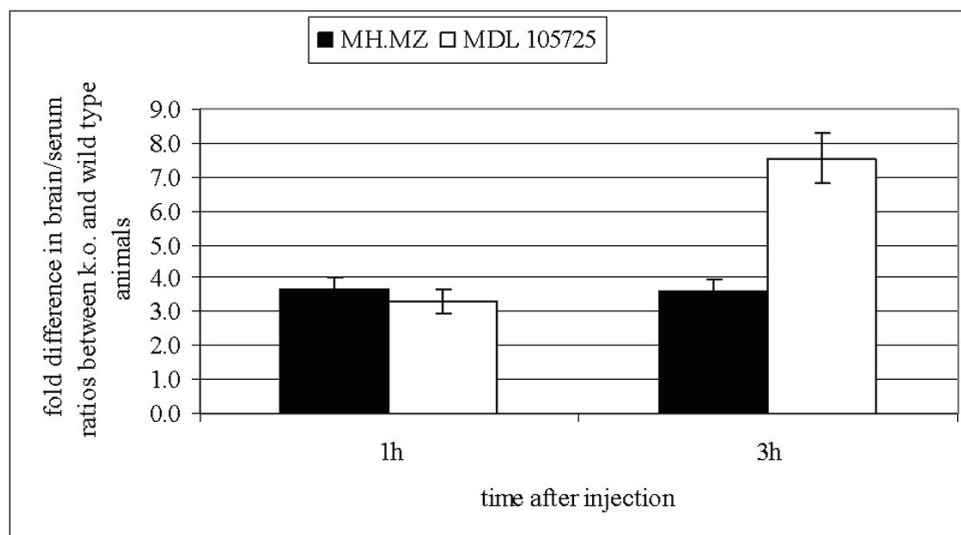


Figure 3: Difference in magnitude of brain/serum ratios between FVB wild type and P-gp k.o. mice.

The accumulation of [^{18}F]MH.MZ was also measured *ex vivo* 1h post injection in P-gp k.o. animals. In accordance with the results reported above for the unlabeled compound, the accumulation of [^{18}F]MH.MZ was significantly increased compared to wild type mice (Figure 4).

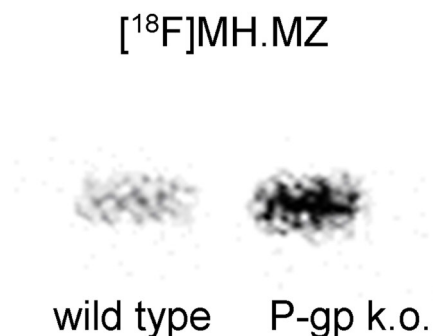


Figure 4: Brain accumulation of [^{18}F]MH.MZ in P-gp k.o. and FVB wild type mice visualized 60 minutes post injection by radio-TLC

***In vivo* imaging**

With respect to the afore reported globally increased uptake of [^{18}F]MH.MZ in the brains of P-gp k.o. vs. those of wild type mice, the *in vivo* studies of [^{18}F]MH.MZ by microPET were consistent with the *ex vivo* results (Figure 5).

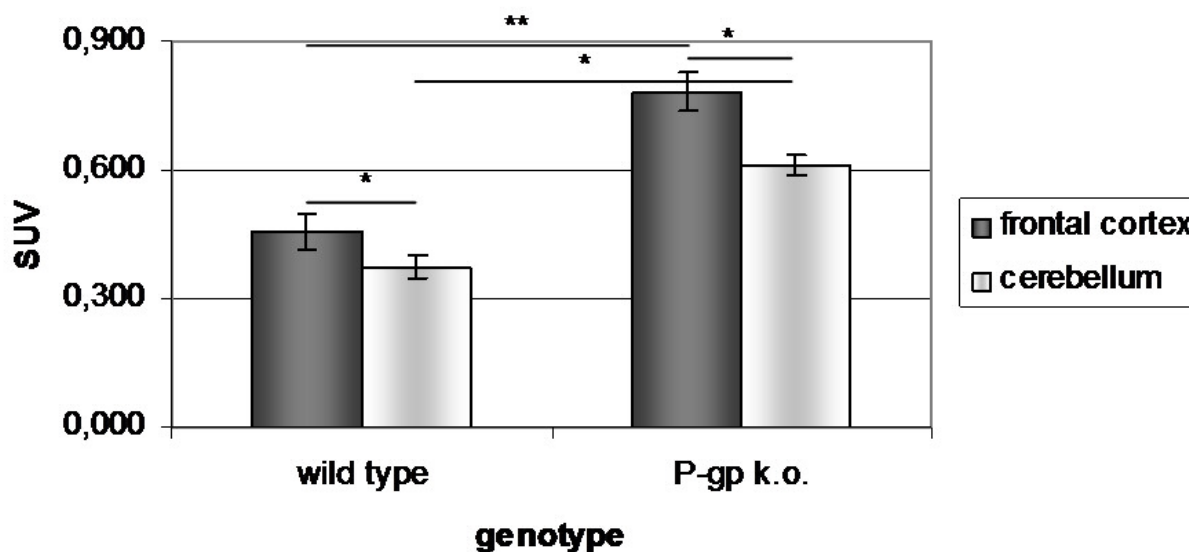


Figure 5: Comparison of brain accumulation expressed as standardized uptake values (SUV) of $[^{18}\text{F}]\text{MH.MZ}$ in P-gp k.o. and FVB wild type mice in the frontal cortex and the cerebellum. Asterisk indicate significant SUV differences with * $p < 0.05$ and ** $p < 0.01$ post hoc t-test following MANOVA.

$[^{18}\text{F}]\text{MH.MZ}$ entered the brains of the mice with a significant difference between brain regions and the two genotypes (Figures 5 and 6). ROI results showed a higher accumulation in the frontal cortex compared to the cerebellum, both in wild type and P-gp k.o. animals. MANOVA indicated significant main effects on Factor A *genotype* $F_{(1;4)} = 32,403$ $P \leq 0.01$ and Factor B brain region (treated as repeated measure) $F_{(1;4)} = 84,794$ $P \leq 0.001$ as well as a significant AxB interaction $F_{(1;4)} = 9.621$ $P \leq 0.05$ (Figure 5). However, frontal cortex to cerebellum ratios of wild type and P-gp k.o. animals did not differ significantly (Figure 7). Nevertheless, PET results in addition showed a significant increase of $[^{18}\text{F}]\text{MH.MZ}$ in P-gp k.o. mice compared to wild type in both brain areas investigated (Figures 5 and 6).

Discussion

Pharmacokinetic peculiarities of individual patients due to variations in absorption, distribution, metabolism or elimination of drugs alter the efficacy of drug treatment (Uhr et al., 2008). One contributing factor is the passage through the blood-brain-barrier, which is regulated by various efflux transport proteins. P-glycoprotein, a member of the ATP-binding cassette superfamily (ABC family) plays an important role as an efflux pump in the blood-brain-barrier for many drugs (Potschka and Löscher 2001; Uhr et al., 2003; Doran et al., 2005; Kirschbaum et al., 2008). The passage through the blood-brain-barrier is important not only

with respect to drug-treatment but also to the use of PET-tracers as a diagnostic tool. Poor penetration of these radiolabelled compounds limits their effectiveness in a comparable way (Coutyn et al., 2004, Elsinga et al., 2005, Ishiwata et al., 2007, Palner et al., 2007). *Ex vivo* studies in support of advancing *in vivo* P-gp evaluation have already demonstrated that PET tracer uptake in brain can be quantified after modulation of P-gp. For example, increased brain uptake of P-gp substrates, [^{11}C]verapamil [^{11}C]carvediol, occurred in the presence of P-gp inhibitors (Hendrikse et al., 1999a/b, Bart et al., 2003).

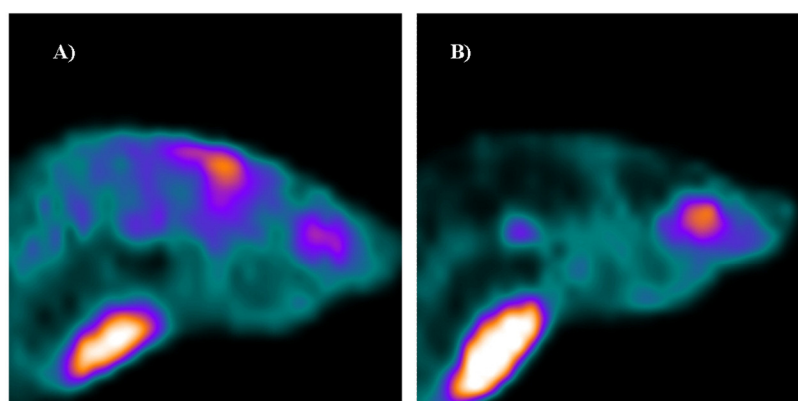


Figure 6: [^{18}F]MH.MZ μPET scan of a A) P-gp k.o. and B) FVB wild type mouse brain. Images derive from a 10 min. static scan 45 min. after i.p. injection of ~ 12 MBq. The imaging was performed with the Focus 120 microPET scanner.

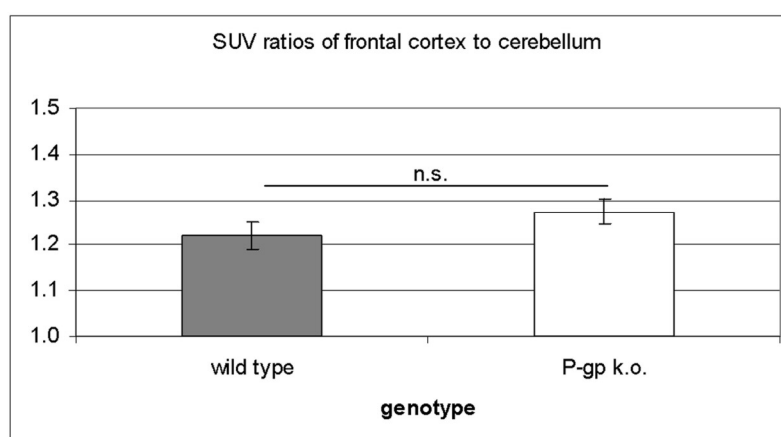


Figure 7: Frontal cortex/cerebellum ratios of standardized uptake values (SUV) for P-gp k.o. and FVB wild type mice

We recently developed a ^{18}F -analog of MDL 100907, [^{18}F]MH.MZ resulting in a superior PET-tracer of the 5-HT $_2\text{A}$ receptor, at least in rats (Herth et al., 2008,2009). However, its similarity in structure (Figure 1) to [^{18}F]altanserin which has recently been shown to be a

substrate of P-gp (Palner et al., 2007; Svyänen et al., 2009), increased the likelihood that MH.MZ might also be a P-gp substrate.

Thus present studies were carried out to evaluate whether MH.MZ is a substrate of P-gp and whether those characteristics had an influence on its potential use in humans. Lacan et al. (2008) recently brought an additional fact into consideration, which is the heterogeneous brain distribution of P-gp that might influence quantification by simplified reference tissue method (SRTM) using cerebellum as a non-specific reference region for modelling. Although the distribution of P-gp content through out rat or mouse brain has by far not been comprehensively analysed, regional differences were supported by several studies including PET analyses (Matsuoka et al., 1999; Liow et al., 2007; van Vliet et al., 2007).

Both, our *ex vivo* and *in vivo* results show that MH.MZ as well as [¹⁸F]MH.MZ enter the brain in a P-gp dependent manner. By pharmacokinetic analysis in P-gp k.o. mice treated with 20 mg/kg of MH.MZ, a time dependent increase up to 7 fold in brain to plasma concentration ratio was observed compared to wild type mice. The increase was additionally found in the metabolite MDL 105725 concentration. Our *in vivo* data in parallel revealed a significantly higher uptake of the radiolabeled tracer, [¹⁸F]MH.MZ, in P-gp k.o. compared to wild type animals in both brain regions analysed. Here, the uptake profile in both in wild type and in P-gp k.o. mice was higher within the frontal cortex known to possess higher amounts of 5-HT_{2A} receptors compared to the cerebellum which is supposed to be devoid of 5-HT_{2A} receptors (Hall et al., 2000). However, Eastwood and colleagues reported 5-HT_{2A} receptor availability in the cerebellum at least in humans (Eastwood et al., 2001). Previous mentioned results and those of Lacan et al. (2008) however, questions the cerebellum as an adequate reference region (Lacan et al., 2008). Therefore, two factors could be responsible for the limited frontal cortex/cerebellum ratio of [¹⁸F]MH.MZ seen in the present investigation despite a high affinity and selectivity of the compound (Herth et al., 2008,2009). Ratios for both genotypes were in the range of 1.25 and at least statistically not different (P>0.2). However, if arguing with statistical means, 2-way ANOVA with Factor A *genotype* and Factor B *brain region* (treated as repeated measure) indicated a statistically significant AxB interaction. With respect to the finding of Lacan et al. (2008), showing a higher P-gp effect in cerebellum of rats, cortex/cerebellum ratio in P-gp k.o. was supposed to be smaller compared to wild-type. The opposite was seen in the present investigation. Although, the increase in the cortex as well as in the cerebellum might support a specific binding of [¹⁸F]MH.MZ also in the cerebellum, which is in line with Eastwood et al. (2001). Collectively, our results suggest a

prominent role of P-gp with respect to PET tracer uptake and interpretation of receptor densities dependent on kinetic models.

In summary, we demonstrated *ex vivo* as well as *in vivo* that MH.MZ enters the brain, but brain uptake is dependent on P-gp as brain to plasma concentration ratios and brain uptake in small animal PET were higher in P-gp k.o. transgenic mice compared to wild-type mice. We anticipate that the enhanced brain levels of [¹⁸F]MH.MZ are a direct measure of the parent radioligand and inactivity of radio-metabolites.

Our results gave evidence for a functional role of transport mechanisms at the blood-brain-barrier, presently P-gp, and its sub-regional distribution. These results not only benefit the development of drug therapy but also for using molecular imaging, e.g. PET as a diagnostic tool.

References

- Bart J, Willemsen AT, Groen HJ, van der Graaf WT, Wegman TD, Vaalburg W, de Vries EG, and Hendrikse NH (2003) Quantitative assessment of P-glycoprotein function in the rat blood-brain barrier by distribution volume of [¹¹C]verapamil measured with PET. *Neuroimage* **20**: 1775-82.
- Benkelfat C (1993) Serotonergic mechanisms in psychiatric disorders: new research tools, new ideas. *Int Clin Psychopharmacol* **8**: 53-56.
- Breier A. (1995) Serotonin, schizophrenia and antipsychotic drug action. *Schizophr Res* **14**: 187-202.
- Courtyn J, Cornelissen B, Oltenfreiter R, Vandecapelle M, Slegers G, and Strijckmans K (2004) Synthesis and assessment of [¹¹C]acetylhomotaurine as an imaging agent for the study of the pharmacodynamic properties of acamprosate by positron emission tomography. *Nucl Med Biol* **31**: 649-654.
- Doran A, Obach RS, Smith BJ, Hosea NA, Becker S, Callegari E, Chen C, Chen X, Choo E, Cianfrogna J, Cox LM, Gibbs JP, Gibbs MA, Hatch H, Hop CE, Kasman IN, Laperle J, Liu J, Liu X, Logman M, Maclin D, Nedza FM, Nelson F, Olson E, Rahematpura S, Raunig D, Rogers S, Schmidt K, Spracklin DK, Szewc M, Troutman M, Tseng E, Tu M, Van Deusen JW, Venkatakrishnan K, Walens G, Wang EQ, Wong D, Yasgar AS, and Zhang C (2005) The impact of P-glycoprotein on the disposition of drugs targeted for indications of the central nervous system: evaluation using the MDR1A/1B knockout mouse model. *Drug Metab Dispos* **33**: 165-174.

- Dubovsky SL and Thomas MJ (1995) Serotonergic mechanisms and current and future psychiatric practice. *Clin Psychiatry* **56**: 38-48.
- Eastwood SL, Burnet PW, and Gittins R, Baker K, Harrison PJ (2001) Expression of serotonin 5-HT_{2A} receptors in the human cerebellum and alterations in schizophrenia. *Synapse* **42**: 104-114.
- Elsinga PH, Hendrikse NH, Bart J, van Waarde A, and Vaalburg W (2005) Positron emission tomography studies on binding of central nervous system drugs and P-glycoprotein function in the rodent brain. *Mol. Imaging Biol* **7**: 37-44.
- Erritzoe D, Rasmussen H, Kristiansen KT, Frokjaer VG, Haugbol S, Pinborg L, Baaré W, Svarer C, Madsen J, Lublin H, Knudsen GM, and Glenthoj BY (2008) Cortical and subcortical 5-HT_{2A} receptor binding in neuroleptic-naive first-episode schizophrenic patients. *Neuropsychopharmacology* **33**: 2435-2441.
- Hall H, Farde L, Halldin C, Lundkvist C, and Sedvall G (2000) Autoradiographic localization of 5-HT_{2A} receptors in the human brain using [³H]M100907 and [¹¹C]M100907. *Synapse* **38**: 421-31.
- Hendrikse NH, Franssen EJ, van der Graaf WT, Vaalburg W, and de Vries EG (1999a) Visualization of multidrug resistance in vivo *Eur J Nucl Med* **26**: 283-293.
- Hendrikse NH, de Vries EG, Eriks-Fluks L, van der Graaf WT, Hospers GA, Willemsen AT, Vaalburg W, and Franssen EJ (1999b) A new in vivo method to study P-glycoprotein transport in tumors and the blood-brain barrier. *Cancer Res* **59**: 2411-2416.
- Herth MM, Debus F, Piel M, Palner M, Knudsen GM, Lüddens H, and Rösch F (2008) Total synthesis and evaluation of [¹⁸F]MHMZ. *Bioorg Med Chem Lett* **18**: 1515-1519.
- Herth MM, Piel M, Debus F, Schmitt U, Lüddens H, and Rösch F (2009) preliminary in vivo and ex vivo evaluation of [¹⁸F]MH.MZ. *Nucl Med and Biol* (accepted)
- Horacek J, Bubenikova-Valesova V, Kopecek M, Palenicek T, Dockery C, Mohr P, and Höschl C (2006) Mechanism of action of atypical antipsychotic drugs and the neurobiology of schizophrenia. *CNS Drugs* **20**: 389-409.
- Huang Y, Mahmood K, and Mathis CA (1999) An efficient synthesis of the precursor of [¹¹C]MDL 100907 labelled in two specific positions. *J. Labelled Compd. Radiopharm* **42**: 949-957.
- Ishiwata K, Kawamura K, Yanai K, and Hendrikse NH (2007) In vivo evaluation of P-glycoprotein modulation of 8 PET radioligands used clinically. *J Nucl Med* **48**: 81-87.

- Kirschbaum KM, Henken S, Hiemke C, and Schmitt U (2008) Pharmacodynamic consequences of P-glycoprotein-dependent pharmacokinetics of risperidone and haloperidol in mice. *Behav Brain Res* **188**: 298-303.
- Kristiansen H, Elfving B, Plenge P, Pinborg LH, Gillings N, and Knudsen GM (2005) Binding characteristics of the 5-HT^{2A} receptor antagonists altanserin and MDL 100907. *Synapse* **58**: 249-257.
- Laćan G, Plenevaux A, Rubins DJ, Way BM, Defraiteur C, Lemaire C, Aerts J, Luxen A, Cherry SR, and Melega WP (2008) Cyclosporine, a P-glycoprotein modulator, increases [18F]MPPF uptake in rat brain and peripheral tissues: microPET and ex vivo studies. *Eur J Nucl Med Mol Imaging* **35**: 2256-2266.
- Lee DE, Schottlander D, Alexoff DL, and Vaska P (2006) Quantitative Comparison in Estimation of Binding Potential from Dynamic Rat Brain Images using 3-D MAP and 2-D FBP Reconstruction. IEEE Nuclear Science Symposium Conference Record, 2006
- Lieberman JA, Mailman RB, Duncan G, Sikich L, Chakos M, Nichols DE, and Kraus JE (1998) Serotonergic basis of antipsychotic drug effects in schizophrenia. *Biol Psychiatry* **44**: 1099-117.
- Liow JS, Lu S, McCarron JA, Hong J, Musachio JL, Pike VW, Innis RB, and Zoghbi SS (2007) Effect of a P-glycoprotein inhibitor, Cyclosporin A, on the disposition in rodent brain and blood of the 5-HT_{1A} receptor radioligand, [11C](R)-(-)-RWAY. *Synapse* **61**: 96-105.
- Mamo D, Graff A, Mizrahi R, Shammi CM, Romeyer F, and Kapur S (2007) Differential effects of aripiprazole on D₂, 5-HT₂, and 5-HT_{1A} receptor occupancy in patients with schizophrenia: a triple tracer PET study. *Am J Psychiatry* **164**: 1411-1417.
- Matsuoka Y, Okazaki M, Kitamura Y, and Taniguchi T (1999) Developmental expression of P-glycoprotein (multidrug resistance gene product) in the rat brain. *J Neurobiol* **39**: 383-392.
- Mizuno M, Niwa T, Yotsumoto Y, and Sugiyama Y (2003) Impact of drug transporter studies on drug discovery and development. *Pharmacol Rev* **55**: 425-461.
- Murphy DL, Andrews AM, Wichems CH, Li Q, Tohda M, and Greenberg B (1998) Brain serotonin neurotransmission: an overview and update with an emphasis on serotonin subsystem heterogeneity, multiple receptors, interactions with other neurotransmitter systems, and consequent implications for understanding the actions of serotonergic drugs. *J Clin Psychiatry* **59**: 4-12.

- Palner M, Syvänen S, Kristoffersen US, Gillings N, Kjaer A, and Knudsen GM (2007) The effect of a P-glycoprotein inhibitor on rat brain uptake and binding of [¹⁸F]altanserin: a micro PET study. *Abstract Brain and Mind Forum*
- Passchier J, van Waarde A, Pieterman RM, Elsinga PH, Pruijm J, Hendrikse HN, Willemsen AT, and Vaalburg W (2000) Quantitative imaging of 5-HT_{1A} receptor binding in healthy volunteers with [(18)f]p-MPPF. *Nucl Med Biol* **27**: 473-476.
- Potschka H and Löscher W (2001) In vivo evidence for P-glycoprotein-mediated transport of phenytoin at the blood-brain barrier of rats. *Epilepsia* **42**: 1231-1240.
- Schiffer WK, Mirrione MM, and Dewey SL (2007) Optimizing experimental protocols for quantitative behavioral imaging with ¹⁸F-FDG in rodents. *J Nucl Med* **48**: 277-287.
- Syvänen S, Lindhe O, Palner M, Kornum BR, Rahman O, Långström B, Knudsen GM, and Hammarlund-Udenaes M. (2009) Species differences in blood-brain barrier transport of three positron emission tomography radioligands with emphasis on P-glycoprotein transport. *Drug Metab Dispos* **37**: 635-643.
- Talvik M, Nordström AL, Larsen NE, Jucaite A, Cervenka S, Halldin C, and Farde L (2004) A cross-validation study on the relationship between central D₂ receptor occupancy and serum perphenazine concentration. *Psychopharmacology* **175**: 148-153.
- Talvik M, Nordström AL, Olsson H, Halldin C, and Farde L (2003) Decreased thalamic D₂/D₃ receptor binding in drug-naive patients with schizophrenia: a PET study with [¹¹C]FLB 457. *Int J Neuropsychopharmacol* **6**: 361-370.
- Uhr M, Grauer MT, and Holsboer F (2003) Differential enhancement of antidepressant penetration into the brain in mice with abcb1ab (mdr1ab) P-glycoprotein gene disruption. *Biol Psychiatry* **54**: 840-846.
- Uhr M, Tontsch A, Namendorf C, Ripke S, Lucae S, Ising M, Dose T, Ebinger M, Rosenhagen M, Kohli M, Kloiber S, Salyakina D, Bettecken T, Specht M, Pütz B, Binder EB, Müller-Myhsok B, and Holsboer F (2008) Polymorphisms in the drug transporter gene ABCB1 predict antidepressant treatment response in depression. *Neuron* **57**: 203-209.
- Ullrich T and Rice KC (2000) A practical synthesis of the serotonin 5-HT_{2A} receptor antagonist MDL 100907, its enantiomer and their 3-phenolic derivatives as precursors for [¹¹C]labeled PET ligands. *Bioorg Med Chem* **8**: 2427-2432.
- Van de Kar LD, Javed A, Zhang Y, Serres F, Raap DK, and Gray TS (2001) 5-HT_{2A} receptors stimulate ACTH, corticosterone, oxytocin, renin, and prolactin release and activate hypothalamic CRF and oxytocin-expressing cells. *J Neurosci* **21**: 3572-3579.

van Vliet EA, van Schaik R, Edelbroek PM, Voskuyl RA, Redeker S, Aronica E, Wadman WJ, and Gorter JA (2007) Region-specific overexpression of P-glycoprotein at the blood-brain barrier affects brain uptake of phenytoin in epileptic rats. *J Pharmacol Exp Ther* **322**: 141-147.

Waldschmitt C, Pfuhlmann B, and Hiemke C (2009) Analysis of multiple antidepressants and antipsychotic drugs including active metabolites in serum of psychiatric patients by LC with column switching and spectrophotometric detection. *Chromatographia* doi: 10.1365/s10337-009-1003-5

3.8 Synthesis of novel WAY 100635 derivatives containing a norbornene group and radiofluorination of [¹⁸F]AH1.MZ, as a serotonin 5-HT_{1A} receptor antagonist for molecular imaging

by Matthias M. Herth, Vasko Kramer and Frank Rösch

Institute of Nuclear Chemistry, University of Mainz, Fritz-Strassmann-Weg 2, D-55128
Mainz, Germany

Abstract

5-HT_{1A} receptors are involved in a variety of psychiatric disorders and in vivo molecular imaging of the 5-HT_{1A} status represents an important approach to analyze and treat these disorders. We report herein the synthesis of three new fluoroethylated 5-HT_{1A} ligands (AH1.MZ, AH2.MZ and AH3.MZ) as arylpiperazine derivatives containing a norbornene group. AH1.MZ (K_i = 4.2 nM) and AH2.MZ (K_i = 30 nM) showed reasonable *in vitro* affinities to the 5-HT_{1A} receptor, whereas AH3.MZ appeared to be non-affine toward the 5-HT_{1A} receptor. The receptor profile of AH1.MZ and AH2.MZ showed selectivity within the 5-HT system. ¹⁸F-labelling via [¹⁸F]FETos to [¹⁸F]AH1.MZ was carried out in radiochemical yields of >70%. The final formulation of injectable solutions including [¹⁸F]FETos synthon synthesis, radiosynthesis and semipreparative high-performance liquid chromatography (HPLC) separation took no longer than 130 min and provided [¹⁸F]AH1.MZ with a purity of >98% as indicated by analytical HPLC analyses.

Key Words

radiofluorination; WAY 100635; [¹⁸F]AH1.MZ; 5-HT_{1A} antagonist; PET

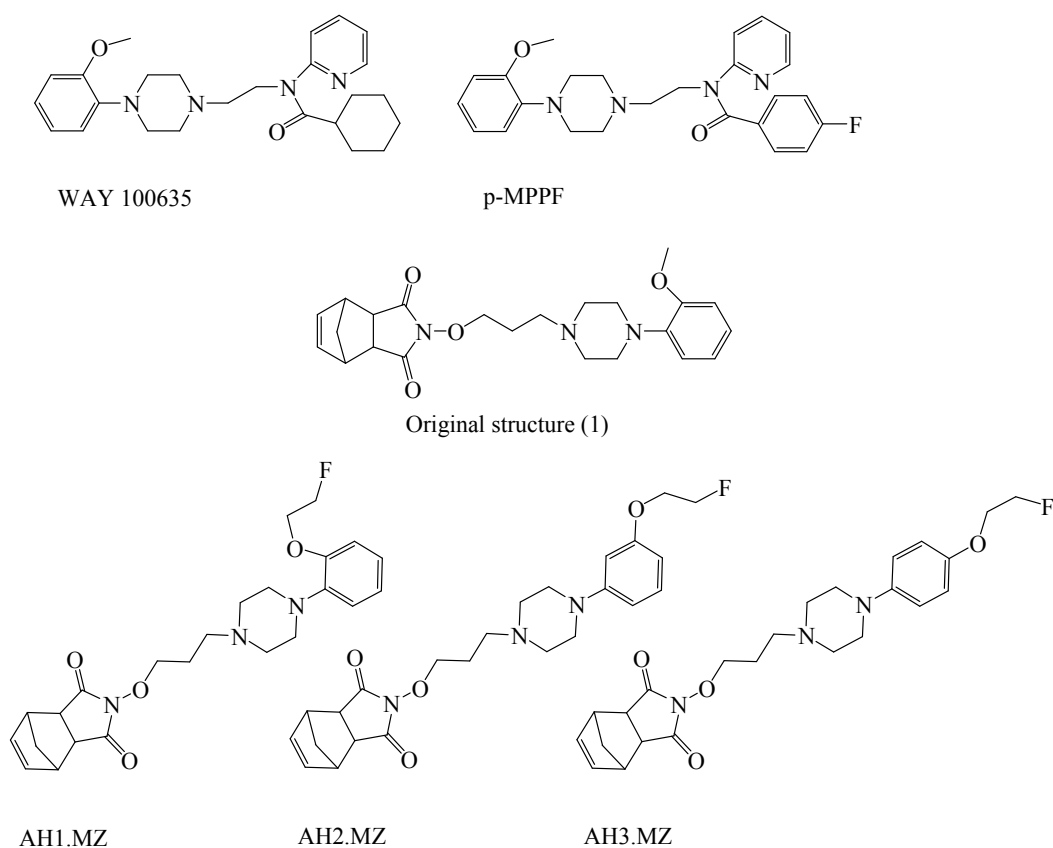
Introduction

Serotonin (5-hydroxytryptamine, 5-HT) is an important neurotransmitter that is involved in physiological and pathophysiological processes in both the peripheral and the central nervous systems. Therefore, the 5-HT system is one of the most important targets for medicinal chemistry.¹⁻⁴ Alterations in serotonin neurotransmission have been implicated in a number of human disorders such as migraine, schizophrenia, depression and anxiety as well as in normal human functions such as learning, sleep, sexual activity and appetite. Especially, it is the 5-HT_{1A} receptor that may be involved in these various physiological processes.⁵⁻¹⁰ A major task in the clinical routine is depression, because it affects an estimated 121 million people worldwide¹¹ while the molecular basis for depression is not fully being understood. However, deficits in the activity of serotonin mediated neurons in the brain are clearly central to the disease.¹² *In vivo* studies to quantitatively determine 5-HT_{1A} receptor availability would provide a significant advance in the understanding of the mentioned disorders and conditions. Positron emission tomography (PET) is an appropriate tool to measure *in vivo* directly, non-invasively and repetitively the binding potential, the receptor availability, uptake kinetics of radio tracers for neuroreceptors as well as to evaluate the efficacy of drugs directed to these molecular targets.

A number of neurotransmitter analogs labelled with β^+ - emitter containing radioligands were synthesized as radiopharmaceuticals for imaging the 5-HT_{1A} receptor. To date, *in vivo* studies have been performed with several 5-HT_{1A} selective antagonists such as [¹¹C]WAY 10063513 and [¹⁸F]p-MPPF.¹⁴ The chemical structures of WAY 100635 and p-MPPF are presented in Scheme 1.

Fiorino et al. synthesized new arylpiperazines containing a norbornene group as 5-HT_{1A} receptor antagonists and reported their outstanding *in vitro* selectivity for the 5-HT_{1A} receptor.¹⁵ 4-[3-[4-(*o*-Methoxyphenyl)piperazin-1-yl]propoxy]-4-aza-tricyclo- [5.2.1.0^{2,6}]dec-8-ene-3,5-dione (1) showed even affinity in the subnanomolar range for 5-HT_{1A} receptors and moderate to no affinity for other relevant receptors (Table 1).

Therefore, we decided to slightly modify promising ligands by replacing a methoxy- by a fluoroethoxy group for labelling purposes, to alter the position of the fluoroethoxy group within the phenylic ring (Scheme 1) and to determine the affinities of the new compounds toward several 5-HT receptors. In addition, we report the optimized labelling and purification procedure of the promising candidate [¹⁸F]AH1.MZ.



Scheme 1. Structures of novel compounds (2)–(4) compared with the original (1) and chemical structures of WAY 100635 and p-MPPF.

Table 1. Affinities of (1) for 5-HT_{1A}, 5-HT_{2A}, 5-HT_{2C}, D₁, D₂, α₁ and α₂ receptors

	5-HT _{1A}	5-HT _{2A}	5-HT _{2c}	D ₁	D ₂	α ₁	α ₂
(1)	0.021	> 10 ⁴	> 10 ⁴	> 10 ⁴	> 10 ⁴	75.3	3650

* K_i values in nM are based on the means of 4 experiments

Results and discussion

Chemistry

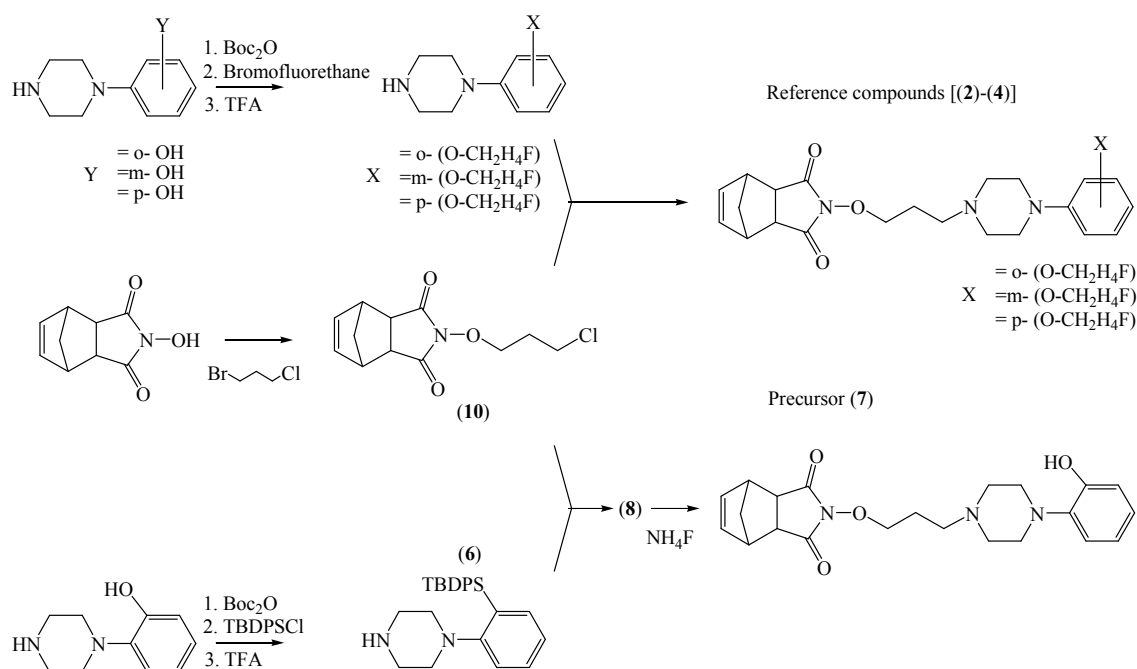
Organic synthesis of WAY 100635 derivatives containing a norbornene group has been described by Fiorino et al.¹⁵. Owing to the necessary structural replacement of a methoxy- by a fluoroethoxy group for labelling purposes, a similar synthesis route was applied, but hydroxyphenylpiperazines were used as starting materials for both precursors and reference compounds. The synthesis strategy, shown in Scheme 2, employs a protection/deprotection

approach of the secondary amine and the phenolic hydroxy group followed by alkylation of the key intermediates (5) or (6) performed in MeCN in the presence of K_2CO_3 and NaI under reflux. By means of Finkelstein exchange, alkylation yields were improved by the increased leaving tendency of iodine. However, (10) was synthesized by the starting heterocycle endo-N-hydroxy-5-norbornene-2,3-dicarboximide with 1-bromo-3-chloropropane in the presence of NaOH in absolute ethanol as reported by Fiorino et al.¹⁵

Receptor characterization

The potential of new fluoroethylated derivatives related to their affinity and selectivity was examined by determining affinities (K_i 's) to 5-HT receptors by radioligand binding assays through NIMH Psychoactive Drug Screening Program (PDSP). The results are summarized in Table 2.

AH1.MZ (2) ($K_i = 4.2$ nM) and AH2.MZ (3) ($K_i = 30$ nM) reveal a low to moderate nanomolar affinity to the 5-HT_{1A} receptor, whereas AH3.MZ (4) shows no affinity toward the 5-HT_{1A} receptors. Medium receptor affinity toward 5-HT_{2B} ($K_i = 144$ nM) could be detected for the o-fluoroethylated compound (2), whereas the m-substituted ligand (3) lost this affinity.



Scheme 2. General synthesis strategy.

However, AH1.MZ and AH2.MZ showed a reasonable *in vitro* affinity profile, with high to moderate affinity to the 5-HT_{1A} receptor and selectivity to other 5-HT receptors. The outstanding affinity and selectivity of the reference compound 4-[3-[4-(o-

methoxyphenyl)piperazin-1-yl]propoxy]-4-aza-tricyclo- [5.2.1.0^{2,6}]dec-8-ene-3,5-dione (1) is lost by introducing a fluoroethyl group (Table 2).

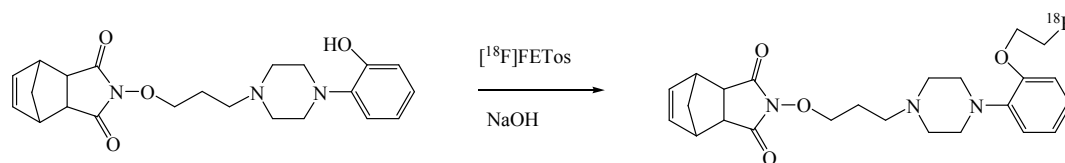
Table 2. Affinities of novel compounds (1) – (4) to 5-HT neuroreceptors

	Original structure(1) [†]	AH1.MZ (2)	AH2.MZ (3)	AH3.MZ (4)
5-HT _{1A}	0.021	4.2 ± 0	30 ± 6	> 10.000
5-HT _{1B}	-	343 ± 57	> 10.000	> 10.000
5-HT _{1D}	-	> 10.000	n.d.	n.d.
5-HT _{1E}	-	382 ± 59	1738 ± 238	> 10.000
5-HT _{2A}	> 10 ⁴	599 ± 60	4406 ± 794	2229 ± 490
5-HT _{2B}	-	144 ± 9	1150 ± 140	3570 ± 333
5-HT _{2C}	> 10 ⁴	> 10.000	> 10.000	> 10.000
5-HT ₃	-	> 10.000	n.d.	n.d.
5-HT _{5A}	-	1767 ± 279	> 10.000	> 10.000
5-HT ₆	-	> 10.000	> 10.000	> 10.000
5-HT ₇	-	n.d.	552 ± 53	> 10.000

* K_i values in nM ± SEM of human receptors are based on the means of 4 experiments; n.d. (not determined); [†] K_i values reported by Fiorino et al.

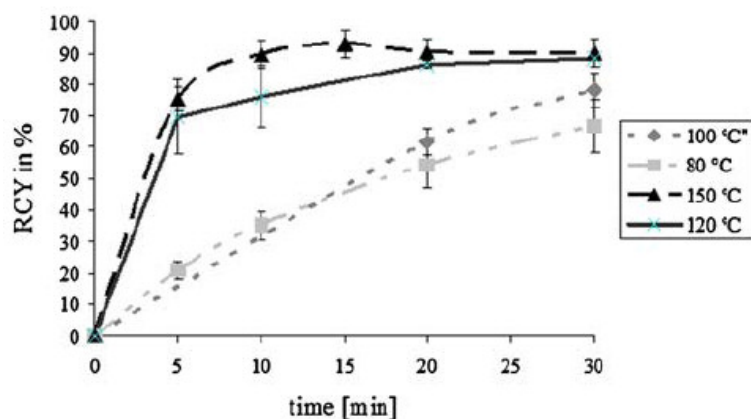
Radiochemistry

The ¹⁸F-labelling of the precursor (7) was carried out similar to that reported in Herth et al.¹⁶ The necessary [¹⁸F]FETos synthon production was performed in an automated module according to Bauman et al.¹⁷ and used for [¹⁸F]fluoroalkylation (Scheme 3).



Scheme 3. Radiosynthesis of [¹⁸F]AH1.MZ.

The [¹⁸F]fluoroalkylation of the precursor (7) was optimized only due to temperature variation resulting in radiochemical yields of >70% (Figure 1). Final reaction conditions were 120°C, 7 mmol of precursor (7) and 7 mmol of 5 N NaOH dissolved in 1mL of dry DMSO with a reaction time of 20 min.

**Figure 1.**

[¹⁸F]fluoroalkylation of 7mmol of precursor (7) to [¹⁸F]AH1.MZ at different reaction temperatures using DMSO and 7 mmol of 5 N NaOH.

The final formulation of injectable solutions including [¹⁸F]FETos synthon synthesis, radiosynthesis and a semi-preparative high-performance liquid chromatography (HPLC) separation (μ Bondapak C18 7.8x300mm column, flow rate 8 mL/ min, eluent: MeCN/0.25M NH₄Ac buffer, pH 4.3 adjusted with acetic acid (25/75)) took no longer than 130 min and provided [¹⁸F]AH1.MZ with a radiochemical purity of >98% as indicated by analytical HPLC analyses (ET 250/8/4 Nucleosil 5 C18, flow rate 1 mL/min, eluent: MeCN/0.05 Na₂HPO₄ buffer, pH 7.4 adjusted with H₃PO₄ (40:60)). Thereby, amounts of ~3 GBq of [¹⁸F]fluorine were used as starting radioactivity. A typical specific activity of 5 GBq/mmol could be observed for these low-scale activities.

In conclusion, a new ¹⁸F-labelled compound could be obtained as an injectable solution in overall radiochemical yields of about 25% within 130 min.

Experimental

General

Chemicals were purchased from ABX, Acros, Aldrich, Fluka, Merck or Sigma and were used without further purification. Moisture sensitive reactions were carried out under an argon or a nitrogen atmosphere using dry solvents over molecular sieve. Flash chromatographies were conducted on silica gel 60 (0.040–0.063 mm, Acros) columns. TLCs were run on pre-coated plates of silica gel 60F₂₅₄ (Merck). HPLC was performed on the following systems:

Analytical HPLC: System equipped with a Sykam S 1100 Solvent Delivery System, S 8110 Low Pressure Gradient Mixer, Rheodyne 9725i Inject Valve, Linear UVIS-205 Absorbance Detector, Axxiom Chromatography 900-200 Pyramid, Pyramid 2.07, loop: 20 mL).

Semi-preparative HPLC: HPLC system equipped with a Dionex P 680A pump, software Dionex Chromeleon vers., a Raytest 6.6 NaI scintillation counter (Gabi) and a Linear UVD170U (254 nm) absorbance detector. Reversed-phase HPLC was carried out for

analytical separations using an ET 250/8/4 Nucleosil 5 C18 column and for semi-preparative applications a μ Bondapak C18 7.8x300mm column was used.

Three hundred and 400 MHz NMR spectra were recorded on a Bruker 300 MHz-FT-NMRSpectrometer AC 300 or a Bruker-Biospin DRX 400 MHz spectrometer. Chemical shifts were reported in parts per million (ppm). FD mass spectrometry (MS) was performed on a Finnigan MAT90-Spectrometer.

Radio-TLC plates were scanned and detected using a Canberra Packard Instant Imager.

Chemistry

4-(3-Chloropropoxy)-4-aza-tricyclo-[5.2.1.0_{2,6}]dec-8-ene-3,5-dione (**10**)

4-(3-Chloropropoxy)-4-aza-tricyclo-[5.2.1.0_{2,6}]dec-8-ene-3,5-dione (**10**) was synthesized as described by Fiorino et al.¹⁵

General procedure for boc-protection

To a solution of 15.7 mmol of N-hydroxyphenylpiperazine and 27 mmol of NaHCO₃ dissolved in 50 mL of THF/H₂O/dioxane (1:1:1), 18.8 mmol of Boc₂O was added and stirred overnight. Later, the solution was diluted with H₂O, extracted with CH₂Cl₂, dried over Na₂SO₄ and concentrated. Purification by column chromatography (PE:EtOAc 7:3) gave the final pure product.

Tert-butyl 4-(2-hydroxyphenyl)piperazine-1-carboxylate (11a): A total of 2.8 g of N-2-hydroxyphenylpiperazine (15.7 mmol), 2.3 g of NaHCO₃ (27 mmol) and 4.1 g of Boc₂O (18.8 mmol) yielded 2.43 g (8.9 mmol, 57%) of the pure product. ¹H-NMR (300 MHz, CDCl₃), δ [ppm] = 7.135–7.054 (m, 2H), 6.959–6.928 (m, 1H), 6.875–6.19 (m, 1H), 3.597–3.566 (t, 4H), 2.837–2.805 (t, 4H), 1.470 (s, 9H). MS (FD) m/z (% rel. int.): 278.2 (100.0 [M]⁺), 279.2 (17.27 [M+1]⁺). R_f = 0.6 (PE/EtOAc 7:3).

Tert-butyl 4-(3-hydroxyphenyl)piperazine-1-carboxylate (11b): A total of 5 g of N-3-hydroxyphenylpiperazine (28.04 mmol), 4.11 g of NaHCO₃ (48 mmol) and 7.32 g of Boc₂O (33.6 mmol) yielded 6.98 g (25.05 mmol, 89%) of the pure product. ¹H-NMR (300 MHz, CDCl₃), δ [ppm] = 7.129–7.074 (t, 1H), 6.524–6.401 (m, 3H), 3.606–3.572 (t, 4H), 3.123–3.088 (t, 4H), 1.465 (s, 9H). MS (FD) m/z (% rel. int.): 278.1 (100.0 [M]⁺), 279.1 (10.78 [M+1]⁺). R_f = 0.52 (PE/EtOAc 7:3).

Tert-butyl 4-(4-hydroxyphenyl)piperazine-1-carboxylate (11c): A total of 2.8 g of N-4-hydroxyphenylpiperazine (15.7 mmol), 2.3 g of NaHCO₃ (27 mmol) and 4.1 g of Boc₂O (18.8

mmol) yielded 4.01 g (14.4 mmol, 92%) of the pure product. $^1\text{H-NMR}$ (300 MHz, CDCl_3), δ [ppm] = 7.101–6.784 (m, 4H), 3.702–3.669 (t, 4H), 3.111–3.054 (t, 4H), 1.459 (s, 9H). MS (FD) m/z (% rel. int.): 278.1 (100.0 $[\text{M}]^+$), 279.1 (15.56 $[\text{M}+1]^+$). R_f = 0.35 (PE/EtOAc 7:3).

Alkylating procedure for 1,2-bromofluoroethane

NaH (7.19 mmol) was gradually added to the corresponding phenolic derivatives (7.19 mmol) dissolved in 50 mL of dry, cold DMF (0°C) and stirred for 30 min. To the resulting mixture 1,2-bromofluoroethane (7.19 mol) was added slowly and later stirred for 20 h at 60°C. After evaporation of the solvent, the residue was taken up in EtOAc, washed with H_2O and finally extracted 3x with EtOAc. The combined organic extracts were dried (Na_2SO_4), filtered and evaporated. Chromatography of the residue gave the pure product.

Tert-butyl 4-(2-(2-fluoroethoxy)phenyl)piperazine-1-carboxylate (12a): A total of 2 g of tert-butyl 4-(2-hydroxyphenyl)piperazine-1-carboxylate (7.19mmol), 189.4 mg of NaH (7.19mmol) and 916 mg of 1,2-bromofluoroethane (0.52mL; 7.19mmol) yielded 2.04 g (5.8mmol, 86%) of the pure product. $^1\text{H-NMR}$ (300MHz, CDCl_3), δ [ppm] = 6.968–6.842 (m, 4H), 4.852–4.825 (m, 1H), 4.694–4.667 (m, 1H), 4.304–4.276 (m, 1H), 4.209–4.182 (m, 1H), 3.591 (bs, 4H), 3.029 (bs, 4H), 1.459 (s, 9H). MS (FD) m/z (% rel. int.): 324.2 (100.0 $[\text{M}]^+$), 325.2 (11.16 $[\text{M}+1]^+$). R_f = 0.54 (PE/EtOAc 7:3).

Tert-butyl 4-(2-(3-fluoroethoxy)phenyl)piperazine-1-carboxylate (12b): A total of 2 g of tert-butyl 4-(3-hydroxyphenyl)piperazine-1-carboxylate (7.19 mmol), 189.4 mg of NaH (7.19 mmol) and 916 mg of 1,2-bromofluoroethane (0.52 mL; 7.19 mmol) yielded 1.92 g (5.5 mmol, 81%) of the pure product. $^1\text{H-NMR}$ (300 MHz, CDCl_3), δ [ppm] = 7.189–7.135 (t, 1H), 6.566–6.403 (m, 3H), 4.815–4.788 (m, 1H), 4.657–4.630 (m, 1H), 4.241–4.212 (m, 1H), 4.148–4.119 (m, 1H), 3.562–3.528 (t, 4H), 3.128–3.094 (t, 4H), 1.461 (s, 9H). MS (FD) m/z (% rel. int.): 323.9 (100.0 $[\text{M}]^+$), 324.9 (17.82 $[\text{M}+1]^+$). R_f = 0.7 (PE/EtOAc 7:3).

Tert-butyl 4-(2-(4-fluoroethoxy)phenyl)piperazine-1-carboxylate (12c): A total of 2 g of tert-butyl 4-(4-hydroxyphenyl)piperazine-1-carboxylate (7.19 mmol), 189.4 mg of NaH (7.19mmol) and 916 mg of 1,2-bromofluoroethane (0.52 mL; 7.19 mmol) yielded 1.55 g (4.79 mmol, 67%) of the pure product. $^1\text{H-NMR}$ (300 MHz, CDCl_3), δ [ppm] = 6.942–6.810 (m, 4H), 4.801–4.772 (m, 1H), 4.643–4.614 (m, 1H), 4.210–4.182 (m, 1H), 4.117–4.089 (m, 1H), 3.573–3.540 (t, 4H), 3.012–2.979 (t, 4H), 1.460 (s, 9H). MS (FD) m/z (% rel. int.): 323.9 (100.0 $[\text{M}]^+$), 324.9 (17.23 $[\text{M}+1]^+$). R_f = 0.76 (PE/EtOAc 7:3).

General procedure for TBDPS-protection

Tert-butyldiphenylsilyl chloride was added to a solution of the corresponding phenolic derivative, imidazole, and 30 mL of THF at 0°C. This solution was stirred at 0°C for 30 min, then stirred at 40°C for 1 h, cooled, diluted with brine and extracted with CH₂Cl₂. Standard workup gave crude silyl ether, which was purified by silica gel column chromatography.

4-[2-(Tert-butyl-diphenyl-silanyloxy)-phenyl]-piperazine-1-carboxylic acid tert-butylester (9a): A total of 2.27 g of tert-butyldiphenylsilyl chloride (8.27 mmol), 2.30 g of 4-(2-hydroxyphenyl)piperazine-1-carboxylate (8.27 mmol) and 1.11 g of imidazole (16.2 mmol) yielded 1.33 g (2.57 mmol, 31.2%) of the pure product. ¹H-NMR (300 MHz, CDCl₃), δ [ppm] = 7.716–7.694 (d, 4H), 7.432–7.320 (m, 6H), 6.994–6.412 (m, 4H), 3.573 (bs, 4H), 3.043 (bs, 4H), 1.472 (s, 9H), 1.088 (s, 9H). MS (FD) m/z (% rel. int.): 516.2 (100.0 [M]⁺), 517.2 (42.08 [M+1]⁺). R_f = 0.65 (PE/EtOAc 4:1).

4-[4-(Tert-butyl-diphenyl-silanyloxy)-phenyl]-piperazine-1-carboxylic acid tert-butylester (9b): A total of 2.27 g of tertbutyldiphenylsilyl chloride (8.27 mmol), 2.30 g of 4-(4-hydroxyphenyl) piperazine-1-carboxylate (8.27 mmol) and 1.11 g of imidazole (16.2 mmol) yielded 1.1 g (2.12 mmol, 25%) of the pure product. ¹H-NMR (300 MHz, CDCl₃), δ [ppm] = 7.657–7.631 (d, 4H), 7.466–7.384 (m, 6H), 6.723–6.593 (dd, 4H), 2.955–2.889 (m, 8H), 1.471 (s, 9H), 1.008 (s, 9H). MS (FD) m/z (% rel. int.): 415.9 (100.0 [M]⁺), 416.9 (31.68 [M+1]⁺). R_f = 0.62 (CHCl₃/MeOH 5:1).

General procedure for boc-deprotection

The starting material (2.4 mmol) was carefully and gradually dissolved in trifluoroacetic acid (TFA) (10 mL). After 2 h of stirring at room temperature, the solutions were diluted with 30 mL of ether and carefully neutralized with NH₄OH and ice bath cooling. The layers were separated and the aqueous layer was extracted 3x with ether. The combined organic extracts were washed with water, dried (Na₂SO₄), filtered and evaporated to afford a viscous oil. Silica gel column chromatography of the residues gave the pure products.

1-(2-(2-Fluoroethoxy)phenyl)piperazine (5a): A total of 1 g of tert-butyl 4-(2-(2-fluoroethoxy)phenyl)piperazine-1-carboxylate (2.4 mmol) and 10mL of TFA yielded 435mg (1.55 mmol, 64%) of the pure product. ¹H-NMR (300 MHz, CDCl₃), δ [ppm] = 7.073–6.856 (m, 4H), 4.861–4.819 (m, 1H), 4.702–4.661 (m, 1H), 4.313–4.246 (m, 1H), 4.235–4.142 (m, 1H), 3.374 (bs, 8H). MS (FD) m/z (% rel. int.): 223.5 (100.0 [M]⁺), 224.5 (13.32 [M+1]⁺). R_f = 0.92 (CH₃Cl/MeOH 8:1).

1-(2-(3-Fluoroethoxy)phenyl)piperazine (5b): A total of 1 g of tert-butyl 4-(2-(2-fluoroethoxy)phenyl)piperazine-1-carboxylate (2.4mmol) and 10mL of TFA yielded 653 mg (2.31mmol, 95%) of the pure product. ¹H-NMR (300MHz, CDCl₃), d [ppm] = 7.183–7.128 (t, 1H), 6.656–6.354 (m, 3H), 4.812–4.4.784 (m, 1H), 4.654–4.626 (m, 1H), 4.237–4.179 (m, 1H), 4.144–4.117 (m, 1H), 3.342 (bs, 1H), 3.181–3.148 (t, 4H), 3.060–3.027 (t, 4H). MS (FD) m/z (% rel. int.): 223.6 (100.0 [M]⁺), 224.6 (10.02 [M+1]⁺).

1-(2-(4-Fluoroethoxy)phenyl)piperazine (5c): A total of 1 g of tert-butyl 4-(2-(2-fluoroethoxy)phenyl)piperazine-1-carboxylate (2.4 mmol) and 10 mL of TFA yielded 676 mg (2.39 mmol, 99%) of the pure product. ¹H-NMR (300 MHz, CDCl₃), d [ppm] = 6.898–6.830 (m, 4H), 4.851–4.739 (m, 1H), 4.640–4.612 (m, 1H), 4.229–4.162 (m, 1H), 4.115–4.086 (m, 1H), 3.039 (s, 8H), 2.306 (bs, 1H). MS (FD) m/z (% rel. int.): 224.1 (100.0 [M]⁺), 225.1 (1.12 [M+1]⁺).

1-[2-(Tert-butyl-diphenyl-silanyloxy)-phenyl]-piperazine (6a): A total of 1.19 g of 4-[2-(tert-butyl-diphenyl-silanyloxy)-phenyl]-piperazine-1-carboxylic acid tert-butylester (2.31 mmol) and 8.7 mL of TFA yielded 0.91 g (2.2 mmol, 94%) of the pure product. ¹H-NMR (300 MHz, CDCl₃), d [ppm] = 7.660–7.629 (d, 4H), 7.466–7.389 (m, 6H), 6.727–6.691 (m, 2H), 6.619–6.593 (m, 2H), 3.213 (bs, 8H), 1.049 (s, 9H). MS (FD) m/z (% rel. int.): 416.2 (100.0 [M]⁺), 417.2 (32.98 [M+1]⁺).

General procedure for N-alkylation

A 4-(3-chloropropoxy)-4-aza-tricyclo-[5.2.1.0^{2,6}]dec-8-ene-3,5- dione (10) (0.006 mol) and NaI (0.009 mol) were stirred in 50 mL of dry MeCN under reflux for 30 min. Then, the appropriate arylpiperazine (0.03 mol) and anhydrous K₂CO₃ (0.009 mol) were added. The reaction mixture was stirred under reflux for 24 h. After cooling, the mixture was filtered, concentrated to dryness and the residue was dissolved in water (50 mL). The solution was extracted several times with CH₂Cl₂. The combined organic layers were dried over anhydrous Na₂SO₄, and the solvent was removed under vacuum. The crude mixtures were purified by silica gel column chromatography.

4-(3-(4-[2-(Tert-butyl-diphenyl-silanyloxy)-phenyl]-piperazin-1-yl)-propoxy)-4-aza-tricyclo-[5.2.1.0^{2,6}]dec-8-ene-3,5-dion (8): A total of 2.16 g of 4-(3-chloropropoxy)-4-aza-tricyclo-[5.2.1.0^{2,6}]dec-8-ene-3,5-dione (8.47mmol), 1.125 g of NaI (7.5 mmol), 0.91 g of 1-[2-(tert-butyl-diphenyl-silanyloxy)-phenyl]-piperazine (2.31mmol) and 5.4 g of K₂CO₃ (7.5mmol) yielded 1.33 g (2.1mmol, 90%) of the pure product. ¹H-NMR (300 MHz, CDCl₃), d [ppm] = 7.725–7.693 (m, 4H), 7.423–7.304 (m, 6H), 6.941–6.909 (dd, 1H), 6.826–6.771

(m, 1H), 6.598–6.545 (t, 1H), 6.454–6.427 (d, 1H), 6.158–6.152 (m, 2H), 4.073–4.005 (t, 2H), 3.413 (bs, 3H), 3.251–3.105 (m, 6H), 2.693 (bs, 4H), 2.003–1.885 (m, 2H), 1.768–1.732 (d, 1H), 1.508–1.477 (d, 2H), 1.077 (s, 9H). MS (FD) m/z (% rel. int.): 635.9 (100.0 $[M]^+$), 635.9 (62.64 $[M+1]^+$). R_f = 0.45 ($\text{CHCl}_3/\text{MeOH}$ 8:2).

4-(3-(4-[2-(2-Fluoroethoxy)-phenyl]-piperazin-1-yl)-propoxy)-4-aza-tricyclo[5.2.1.0^{2,6}]

dec-8-ene-3,5-dion (2): A total of 1.53 g of 4-(3-chloropropoxy)-4-aza-tricyclo[5.2.1.0^{2,6}]dec-8-ene-3,5-dione (6.01 mmol), 0.79 g of NaI (5.32 mmol), 0.356 g of 1-(2-(2-fluoroethoxy)phenyl)piperazine (1.64 mmol) and 3.83 g of K_2CO_3 (5.32 mmol) yielded 260 mg (0.58 mmol, 38%) of the pure product. $^1\text{H-NMR}$ (300 MHz, CDCl_3), δ [ppm] = 6.999–6.815 (m, 4H), 6.162–6.123 (t, 2H), 4.838–4.810 (t, 1H), 4.679–4.651 (t, 1H), 4.277–4.249 (t, 1H), 4.182–4.155 (t, 1H), 4.063–4.025 (t, 2H), 3.395 (s, 2H), 3.297 (bs, 4H), 3.192 (s, 2H), 2.951–2.873 (m, 6H), 2.082 (bs, 2H), 1.754–1.723 (d, 1H), 1.495–1.460 (d, 1H). MS (FD) m/z (% rel. int.): 443.3 (100.0 $[M]^+$), 444.3 (26.04 $[M+1]^+$). R_f = 0.4 ($\text{CHCl}_3/\text{MeOH}$ 12:2).

4-(3-(4-[2-(3-Fluoroethoxy)-phenyl]-piperazin-1-yl)-propoxy)-4-aza-tricyclo[5.2.1.0^{2,6}]

dec 8-ene-3,5-dion (3): A total of 1.53 g of 4-(3-chloropropoxy)-4-aza-tricyclo[5.2.1.0^{2,6}]dec-8-ene-3,5-dione (6.01 mmol), 0.79 g of NaI (5.32 mmol), 0.356 g of 1-(2-(3-fluoroethoxy)phenyl)piperazine (1.64 mmol) and 3.83 g of K_2CO_3 (5.32 mmol) yielded 460 mg (1.02 mmol, 52%) of the pure product. $^1\text{H-NMR}$ (300 MHz, CDCl_3), δ [ppm] = 7.190–7.035 (m, 1H), 6.585–6.339 (m, 3H), 6.227–6.058 (s, 2H), 4.791–4.776 (t, 1H), 4.647–4.618 (t, 1H), 4.228–4.171 (t, 1H), 4.135–4.107 (t, 1H), 4.029–3.986 (m, 2H), 3.399 (bs, 2H), 3.157 (bs, 6H), 2.566 (bs, 6H), 1.897–1.806 (m, 2H), 1.752–1.722 (d, 1H), 1.490–1.461 (d, 1H). MS (FD) m/z (% rel. int.): 443.0 (100.0 $[M]^+$), 444.0 (33.19 $[M+1]^+$). R_f = 0.44 ($\text{CHCl}_3/\text{MeOH}$ 8:1).

4-(3-(4-[2-(4-Fluoroethoxy)-phenyl]-piperazin-1-yl)-propoxy)-4-aza-tricyclo[5.2.1.0^{2,6}]

dec-8-ene-3,5-dion (4): A total of 1.53 g of 4-(3-chloropropoxy)-4-aza-tricyclo[5.2.1.0^{2,6}]dec-8-ene-3,5-dione (6.01 mmol), 0.79 g of NaI (5.32 mmol), 0.356 g of 1-(2-(4-fluoroethoxy)phenyl)piperazine (1.64 mmol) and 3.83 g of K_2CO_3 (5.32 mmol) yielded 200 mg (0.44 mmol, 27%) of the pure product. $^1\text{H-NMR}$ (300 MHz, CDCl_3), δ [ppm] = 6.883–6.815 (m, 4H), 6.141 (s, 2H), 4.792–4.764 (t, 1H), 4.633–4.606 (t, 1H), 4.199–4.171 (t, 1H), 4.106–4.078 (t, 1H), 4.033–3.991 (t, 2H), 3.403 (bs, 2H), 3.159 (bs, 3H), 3.087–3.055 (t, 4H), 2.614–2.531 (m, 6H), 1.909–1.818 (m, 2H), 1.755–1.726 (d, 1H), 1.496–1.466 (d, 1H). MS (FD) m/z (% rel. int.): 442.9 (100.0 $[M]^+$), 443.9 (43.73 $[M+1]^+$). R_f = 0.52 ($\text{CHCl}_3/\text{MeOH}$ 8:1), 0.6 (EtOH).

4-(3-[4-(2-Hydroxy-phenyl)-piperazin-1-yl]-propoxy)-4-aza-tricyclo[5.2.1.0^{2,6}]dec-8-ene-3,5-dion (7): A solution of 0.68 g of 4-(3-[4-(2-(tert-butyl-diphenyl-silanyloxy)-phenyl]-piperazin-1-yl)propoxy)-4-aza-tricyclo[5.2.1.0^{2,6}]dec-8-ene-3,5-dion (1.14mmol) and 0.21 g of NH₄F (2.8 mmol) in anhydrous MeOH (30 mL) was stirred for 2 h at 70°C. After evaporation of the solvent, the residue was taken up in NH₄OH and extracted 3x with CHCl₃. The combined organic extracts were washed with brine, dried with Na₂SO₄ and evaporated. Chromatography (CHCl₃/MeOH 10:1) of the residue yielded 380 mg (0.96mmol, 84 %) of the pure product. ¹H-NMR (300MHz, CDCl₃), δ [ppm] = 7.154–7.124 (dd, 1H), 7.073–7.018 (m, 1H), 6.937–6.900 (dd, 1H), 6.855–6.793 (m, 1H), 6.154–6.141 (t, 2H), 4.041–3.998 (t, 2H), 3.408 (bs, 2H), 3.175–3.162 (m, 2H), 2.893–2.863 (t, 4H), 2.617 (m, 6H), 1.912–1.820 (m, 2H), 1.762–1.732 (d, 1H), 1.500–1.471 (d, 1H). MS (FD) m/z (% rel. int.): 396.8 (100.0 [M]⁺), 397.8 (40.03 [M+1]⁺). R_f = 0.67 (CHCl₃/MeOH 5:1).

Radiochemistry

[¹⁸F]FETos synthesis

To a dried Kryptofix®2.2.2./[¹⁸F]fluoride complex, 4 mg of ethyleneglycol- 1,2-ditosylate in 1mL of acetonitrile was added and heated under stirring in a sealed vial for 3 min. Purification of the crude product was accomplished using HPLC (Lichrosphere RP18-EC5, 250x10mm, acetonitrile/water 50:50, flow rate 5 mL/min, R_f: 8 min). After diluting the HPLC fraction containing the [¹⁸F]FETos with water (HPLC fraction/water 1:4), the product was loaded on a C18-Sepac cartridge, dried with a nitrogen stream and eluted with 1.2 mL of DMSO. The whole preparation time was about 40 min and the overall radiochemical yield was between 60 and 80%.¹⁷

Radiolabelling of [¹⁸F]AH1.MZ

[¹⁸F]FETos diluted in 0.8 mL of dry DMSO was added to a solution of 3 mg of 4-f3-[4-(2-hydroxy-phenyl)-piperazin-1-yl]-propoxyg-4-aza-tricyclo[5.2.1.0^{2,6}]dec-8-ene-3,5-dion (7) (7mmol) and 1.5 mL of 5N NaOH (7mmol) dissolved in 0.2mL of dry DMSO. The solution remained at 120°C for 20 min and was quenched with 1mL of H₂O. Reactants and by-products were separated from [¹⁸F]AH1.MZ by semi-preparative HPLC (μBondapak C18 7.8x300mm column, flow rate 8mL/min, eluent: MeCN/NH₄Ac buffer, pH 4.3 adjusted with acetic acid (25/75)). The retention times of [¹⁸F]AH1.MZ, [¹⁸F]FETos and 4-(3-[4-(2-hydroxy-phenyl)-piperazin-1-yl]-propoxy-4-aza-tricyclo[5.2.1.0^{2,6}]dec-8-ene-3,5-dion (7) were 5.02, 13.4 and 9.72 min, respectively. The collected product was diluted with water

(4:1), passed through a conditioned strataX-cartridge (1mL of EtOH, 1mL of H₂O), washed with 10 mL of H₂O and eluted with at least 1mL of EtOH. Finally, EtOH was removed in vacuo and [¹⁸F]AH1.MZ was dissolved in 1 mL of saline.

In vitro receptor and monoamine transporter binding

Binding assays were performed by the NIMH PDSP at the Department of Biochemistry, Case Western Reserve University, Cleveland, OH, USA (Bryan Roth, Director). Compounds AH1.MZ (2), AH2.MZ (3) and AH3.MZ (4) were assayed for their affinities for the 5-HT receptor family. Competitive binding experiments were performed in vitro using cloned human receptors. Reported values of the inhibition coefficient (K_i) are mean±SD of four separate determinations.

Conclusion

Fiorino et al.¹⁵ reported about an outstanding high affine (K_i = 0.021 nM) and selective compound, 4-[3-[4-(o-methoxyphenyl)- piperazin-1-yl]propoxy]-4-azatricyclo-[5.2.1.0_{2,6}]dec-8-ene-3,5-dione, for the 5-HT_{1A} receptor subtype. By replacing the methoxy- by a fluoroethoxy group of the parent compound, three different reference compounds (2)–(4) were obtained enabling a labelling strategy with [¹⁸F]FETos. In vitro evaluation of these ligands showed high to moderate affinities to the 5-HT_{1A} receptor of AH1.MZ (K_i = 4.2 nM) and of AH2.MZ (K_i = 30 nM), but not any affinity toward the 5-HT_{1A} receptor of the p-substituted fluoroethylated compound (AH3.MZ) (K_i >10.000 nM). The receptor profile of AH1.MZ and AH2.MZ demonstrates selectivity within the 5-HT system. However, the outstanding affinity and selectivity of the literature reference compound 4-[3-[4-(o-methoxyphenyl)piperazin-1-yl]propoxy]- 4-aza tricyclo-[5.2.1.0_{2,6}]dec-8-ene-3,5-dione (1) is mainly lost by introducing a fluoroethyl group. Nevertheless, compound AH1.MZ may provide potential for molecular imaging of the 5-HT_{1A} receptor system. Because of this potential, ¹⁸F-labelling via [¹⁸F]FETos to [¹⁸F]AH1.MZ was carried out and optimized. Radiochemical yields were >70%. The final formulation of injectable solutions including [¹⁸F]FETos synthon synthesis, radiosynthesis and a semi-preparative HPLC separation took no longer than 130 min and provided [¹⁸F]AH1.MZ with a purity >98%.

In the near future, a broad receptor screening, *in vitro* autoradiography and *in vivo* PET experiments are planned to verify the potential for non-invasive molecular imaging of [¹⁸F]AH1.MZ as an ¹⁸F-tracer for the 5-HT_{1A} system.

Acknowledgement

The authors wish to thank Sabine Höhnemann for the syntheses of [¹⁸F]FETos. Financial support by Friedrich-Naumann-Stiftung and by the European Network of Excellence (EMIL) is gratefully acknowledged. K_i determinations were generously provided by the National Institute of Mental Health's Psychoactive Drug Screening Program, Contract / NO1MH32004 (NIMH PDSP). The NIMH PDSP is directed by Bryan L. Md, PhD, at the University of North Carolina at Chapel Hill and Project Officer Jamie Driscoll at NIMH, Bethesda, MD, USA.

References

- [1] H. G. Baumgarten, M. Gother, Handbook of Experimental Pharmaceuticals, Vol. 129, Springer, Berlin, 1997.
- [2] G. R. Martin, R. M. Eglen, D. Hoyer, M. W. Hamblin, F. Yocca, N. Y. Ann. Acad. Sci. **1998**, 861, 31-37
- [3] N. M. Barnes, T. Sharp, Neuropharmacology 1999, 38, 1083–1152.
- [4] D. Hoyer, J. P. Hannon, G. R. Martin, Pharmacol. Biochem. Behav. 2002, 71, 533–554.
- [5] S. Hillver, L. Bjork, Y. Li, B. Svensson, S. Ross, N. Ande'n, U. J. Hacksell, Med. Chem. 1990, 33, 1541–1544.
- [6] J. P. Gardner, C. A. Fornal, B. L. Jacobs, Neuropsychopharmacology 1997, 17, 72–81.
- [7] R. A. Glennon, Neurosci. Biobehav. Rev. 1990, 14, 35–47.
- [8] W. Kostowski, A. Plaznik, T. Archer, New Trends Exp. Clin. Psychiatry 1989, 5, 91–116.
- [9] E. Seifritz, M. S. Stahl, J. C. Gillin, Brain Res. 1997, 759, 84–91.
- [10] P. R. Saxena, Pharmacol. Ther. 1995, 66, 339–368.
- [11] World Health Organization, WHO Fact Sheet Number 265, The World Health Organization, Geneva, Switzerland, 2001.
- [12] M. J. Fava, Clin. Psychiatry 2003, 64, 30–34.
- [13] C. A. Mathis, N. R. Simpson, K. Mahmood, P. E. Kinahan, M. A. Mintun, Life Sci. 1994, 55, 403–407.
- [14] A. Plenevaux, D. Weissmann, J. Aerts, C. Lemaire, C. Brihaye, C. Degueldre, D. Le Bars, D. Comar, J. F. Pujol, A. Luxen, J. Neurochem. 2000, 75, 803–811.

-
- [15] F. Fiorino, E. Perissutti, B. Severino, V. Santagada, D. Cirillo, S. Terracciano, P. Massarelli, G. Bruni, E. Collavoli, C. Renner, G. Caliendo, *J. Med. Chem.* 2005, 48, 5495–5503.
- [16] M. M. Herth, F. Debus, M. Piel, M. Palner, G. M. Knudsen, H. Lüddens, F. Rösch, *Bioorg. Med. Chem. Lett.* 2008, 18, 1515–1519.
- [17] A. Bauman, M. Piel, R. Schirmacher F. Rösch, *Tetrahedron Lett.* 2003, 44, 9165–9167

4 Conclusion

This thesis describes the successful development and evaluation of ^{18}F -labelled 5-HT_{2A} and 5-HT_{1A} antagonists. MDL 100907 derivatives which combine the better selectivity of MDL 100907 and the more valuable isotopic characteristics used in [^{18}F]altanserin were studied systematically. High affinity and medium affinity ^{18}F -labeled tracers were synthesized and their potential value tested *in vitro*, *ex vivo* and *in vivo*. Promising results hint on improved molecular imaging of the 5-HT_{2A} receptor system, especially for [^{18}F]MH.MZ and (R)-[^{18}F]MH.MZ. Moreover, a P-gp dependency of [^{18}F]MH.MZ could be determined. A SAR study showed that altanserin and MDL 100907 probably bind to the same binding pocket but in different orientations, whereas SR 46349B does not bind to this pocket. [^{18}F]VK-1, a medium affinity but 5-HT_{2A} selective compound, could lead to the possibility to determine the influence of changed endogenous level of serotonin on the receptor.

The second aim to synthesize a high selective, ^{18}F -labeled 5-HT_{1A} antagonist could also be achieved. *In vitro* evaluation studies determined [^{18}F]AH1.MZ and [^{18}F]AH2.MZ to be promising tracers for the 5-HT_{1A} receptor status.

Figure 1 shows the interaction of the novel ^{18}F -labelled tracers within the synaptic cleft.

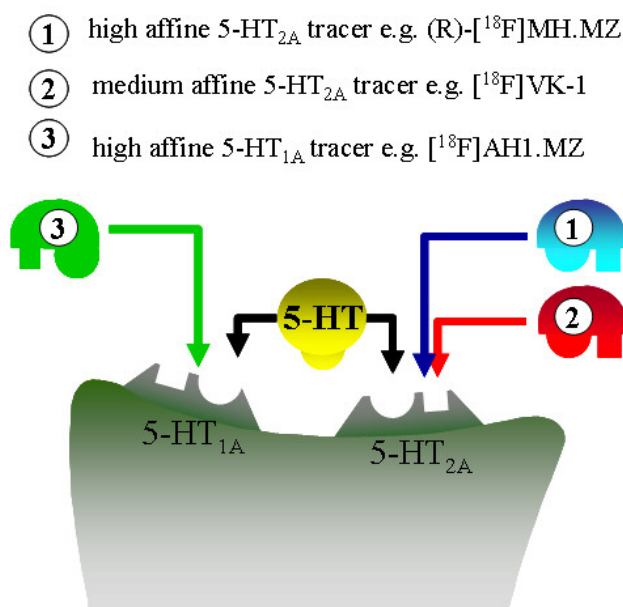


Figure 1: Interaction of ^{18}F -labelled imaging agents which are presented in this thesis.

In the following, a more detailed overview of the results obtained in this thesis will be given.

5-HT_{2A}:

A number of neurotransmitter analogues labelled with β^+ -emitter containing radioligands are available as radiopharmaceuticals for PET imaging of the 5-HT_{2A} receptor. Within those ligands, [¹⁸F]altanserin represents the radioligand of choice for *in vivo* 5-HT_{2A} PET imaging because of its high affinity and selectivity. Nevertheless, the selectivity of [¹¹C]MDL 100907 for the 5-HT_{2A} receptor is slightly higher than that of [¹⁸F]altanserin. The advantage of [¹⁸F]altanserin over [¹¹C]MDL 100907 is the possibility to perform equilibrium scans lasting several hours and to transport the tracer to other facilities based on the 110 min half-life of ¹⁸F-fluorine. A drawback of [¹⁸F]altanserin is its rapid and extensive metabolism, whereas metabolites of [¹¹C]MDL 100907 do not enter the brain to any larger extent.

In this thesis, a series of novel MDL 100907 derivatives (Figure 2) acting as 5-HT_{2A} antagonists containing a fluorine atom were synthesized and evaluated. These compounds should combine the better selectivity of MDL 100907 derivatives and the better isotopic characteristics of ¹⁸F-fluorine.

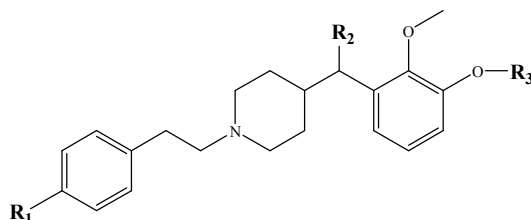


Figure 2: General chemical structure of MDL 100907 derivatives investigated for substituents R₁, R₂, R₃ (see Table 1)

Structure-Activity Relationships (SAR) studies suggested that almost all tested compounds had affinities toward the 5-HT_{2A} receptor in the nanomolar range, except compounds (**24**) and (**39**) varied between the piperidine and phenyl ring (Table 1).

This is in accordance with the rudimental pharmacophore model that has been published by Andersen et al.¹ Replacing the 3-methoxy by a fluoroethoxy group slightly reduces the 5-HT_{2A} affinity but keeps the affinity within the nanomolar range of the parent, e.g. (**28**)-(55), (**30**)-(56), (**27**)-(57). The 3-hydroxy derivatives (**48**)-(55) had a better affinity.

Table 1: Affinities and their lipophilicity of tested ligands toward the 5-HT_{2A} receptor

Name	Cmpd#	K _i [nM]	Log P	R ₁	R ₂	R ₃
(R)-MDL 100907	(30)	0.38 ± 0.05	2.98	-F	◀ OH -	-(CH ₂) ₂ F
MDL 100907	(28)	2.10 ± 0.13	2.98	-F	-OH	-(CH ₂) ₂ F
MH.MZ	(55)	9.02 ± 2.11	2.80	-F	-OH	-(CH ₂) ₂ F
(R)-MH.MZ	(56)	0.72 ± 0.21	2.80	-F	◀ OH	-(CH ₂) ₂ F
MA-1	(53)	3.23 ± 0.18	3.08	-F	=O	-(CH ₂) ₂ F
VK-1	(32)	26.0 ± 6.70	2.37	-NO ₂	-OH	-(CH ₂) ₂ F
	(25)	90 ± 71.0	n.d.	-NO ₂	-OH	Me
	(26)	55 ± 12.0	n.d.	-OCH ₃	-OH	Me
	(27)	0.31 ± 0.06	n.d.	-CH ₃	-OH	Me
	(31)	1.63 ± 5.50	2.92	-H	-OH	-(CH ₂) ₂ F
	(45)	1.34 ± 0.48	n.d.	-F	=O	-OH
	(48)	1.24 ± 0.23	2.27	-F	-OH	-OH
	(49)	0.25 ± 0.06	n.d.	-F	◀ OH	-OH
	(50)	4.56 ± 0.73	3.64	-CH ₃	=O	-(CH ₂) ₂ F
	(51)	138 ± 20.0	2.71	-NO ₂	=O	-(CH ₂) ₂ F
	(52)	153 ± 93.0	3.02	-OCH ₃	=O	-(CH ₂) ₂ F
	(54)	59 ± 54.0	2.72	-OCH ₃	-OH	-(CH ₂) ₂ F
	(57)	1.83 ± 0.43	3.40	-CH ₃	-OH	-(CH ₂) ₂ F
	(58)	2.06 ± 0.96	n.d.	-NH ₂	-OH	-(CH ₂) ₂ F

In contrast, introducing a methoxy or a nitro moiety to the phenethyl group results in a reduction of the affinity down to medium affine compounds ($K_i \sim 1 \mu\text{M}$). Besides, replacing the p-substituent of the phenethyl moiety by a methyl group, an amine or a single proton, slightly increases the affinity, e.g. (28)-(27), (55)-(58)-(57). This could be due to the different space required. Changing the racemic secondary hydroxyl group to a ketone group [(28)-(53); (57)-(50)] causes no major effects. Finally, as expected the enantioselective pure product (56) enhances the affinity compared to the carbonyl (53) and the racemic compound (28).

The new 5-HT_{2A} affine compounds were tested for selectivity (see 3.3). All tested ligands showed thereby a reasonable receptor profile which determined them as 5-HT_{2A} selective compounds.

Except for (39), (50), (57), all fluoroethylated compounds had logP values between 2 and 3, i.e. within range of those of already established radiotracers such as altanserin and MDL 100907.

The novel compounds MA-1 (53), MH.MZ (55) and (R)-MH.MZ (56) (Figure 3) seem to be promising compounds for ^{18}F -PET-tracers due to their K_i -values in the nanomolar range of 1–10 toward the 5-HT_{2A} receptor and their insignificant binding to other 5-HT receptor subtypes or receptors. Interestingly, these derivatives showed a receptor selectivity profile similar to MDL 100907, which is slightly improved compared to that of altanserin. Therefore, mentioned compounds could possibly be preferable antagonistic ^{18}F -tracers for visualization of the 5-HT_{2A} status. Medium affine compounds (VK-1 (32), (51), (52), (54) (Figure 3)) have K_i 's of 30 to 120 nM which is in the range of endogenous serotonin. Challenge experiments with those compounds to measure changes in the endogenous serotonin level may be more relevant and could allow a deeper insight in interactions inside serotonergic synapse. Figure 3 shows the most important derivatives synthesized in this thesis.

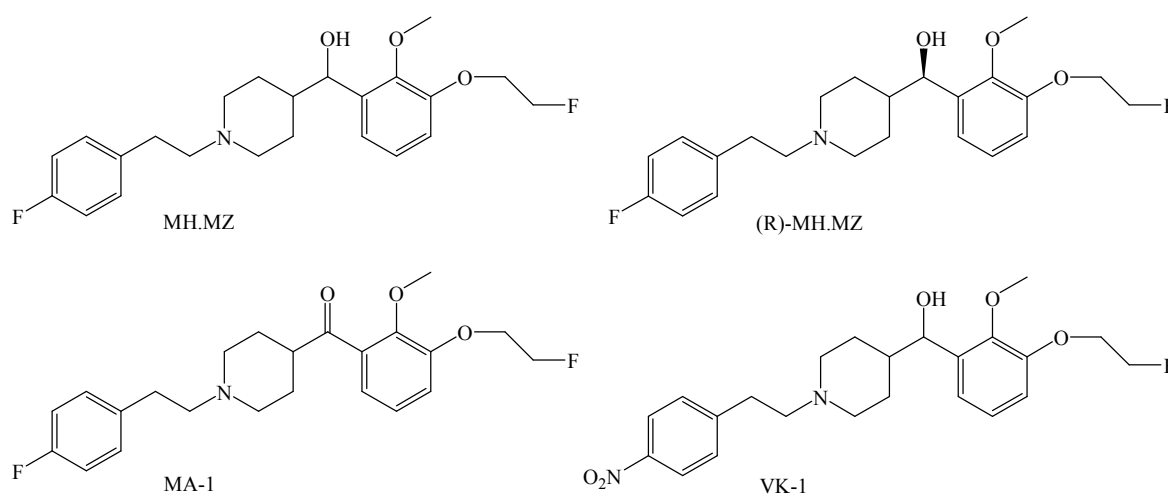


Figure 3: Chemical structures of most promising novel MDL 100907 derivatives considered for ^{18}F -labeling

Due to these promising results, MA-1 (53), MH.MZ (55) and (R)-MH.MZ (56) were radiolabelled using the secondary labelling precursor 2- ^{18}F fluoroethyltosylate (^{18}F FETos) in yields over 80% (Figure 4) and in a specific activity between 10-50 GBq/ μmol with a starting activity of 3 GBq.

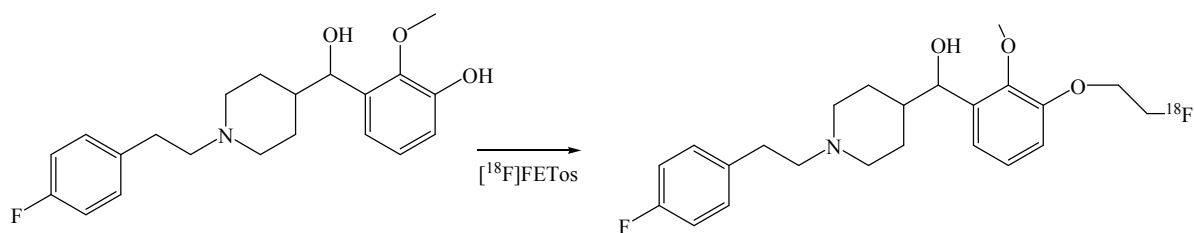


Figure 4: General ^{18}F -labeling of MDL 100907 derivatives

Overall radiochemical yields including ^{18}F FETos synthon synthesis, ^{18}F fluoroalkylation and preparing the injectable solution of these ^{18}F -tracers were 30-40 % within a synthesis time of ~ 100 min.

First autoradiographic studies showed excellent *in vitro* binding of ^{18}F MH.MZ and (R)- ^{18}F MH.MZ with high specificity for 5-HT_{2A} receptors and very low non-specific binding, whereas ^{18}F MA-1 showed less specific binding (Figure 5). Its reduced binding characteristics are expected due to its decreased affinity compared to (R)- ^{18}F MH.MZ ($K_i = 0.72$ nM). However, it is unexpected for ^{18}F MA-1 ($K_i = 3.0$ nM) compared to its racemic ^{18}F MH.MZ ($K_i = 9.0$ nM) analogue. In addition, selectivity of ^{18}F MA-1 showed no intense alteration compared to MH.MZ. Therefore, the observed properties are most probably due to the increased lipophilicity of ^{18}F MA-1 resulting in a higher unspecific binding.

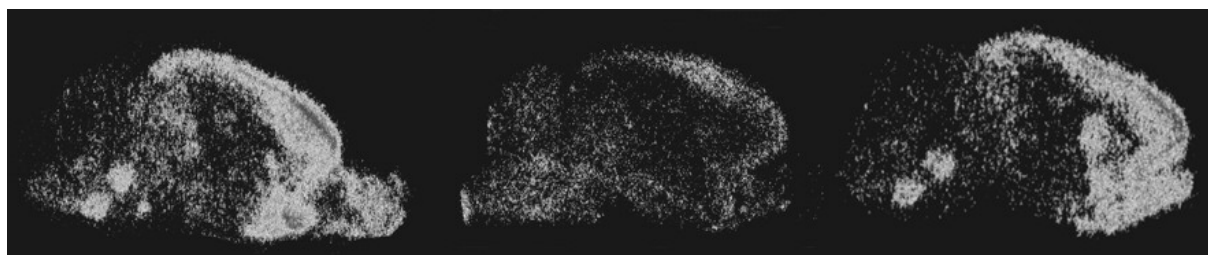


Figure 5: Autoradiographic images of ^{18}F MH.MZ (left), (R)- ^{18}F MH.MZ (right) and ^{18}F MA-1 (middle) showed high specific binding for the MH.MZ analogues and less for ^{18}F MA-1

Furthermore, the metabolism of ^{18}F MH.MZ was tested. It undergoes fast metabolism resulting in one very polar active metabolite. However, non-metabolized ^{18}F MH.MZ is present in rat brain samples in contrast to rat plasma after 60 minutes indicating that ^{18}F MH.MZ is able to cross the blood-brain-barrier whereas metabolites are probably not accumulating in the brain. However, this has to be checked in more detail. For example, the

metabolite and its biochemical behaviour should be identified, especially if the metabolite is able to cross the BBB.

These promising results for [^{18}F]MH.MZ and (R)- [^{18}F]MH.MZ lead to first *in vitro* and *in vivo* μPET experiments. For rats, *ex vivo* biodistribution study of [^{18}F]MH.MZ as well as μPET data of both derivatives showed highest brain uptake at ~ 5 min p.i.. Equilibrium is reached at ~ 30 min post injection and stays on almost the same level for a relatively long period of about 1 h. The characteristics observed for [^{18}F]MH.MZ and (R)-[^{18}F]MH.MZ meet the requirements for molecular imaging and quantitative data interpretation and might be evidently an improvement compared to [^{18}F]altanserin, particularly related to [^{18}F]altanserin's rapid and extensive metabolism forming ^{18}F -containing metabolites that cross the BBB. Results from small animal PET measurements of [^{18}F]MH.MZ and (R)-[^{18}F]MH.MZ are in no way inferior to data obtained with [^{11}C]MDL 100907.

Figure 6 compares the time-activity-curves of both tracers and shows a representative summed μPET image (60 – 90 min) of (R)-[^{18}F]MH.MZ. High uptake can be seen in the same cortex brain regions. The binding potential of [^{18}F]MH.MZ in the rat frontal cortex is 1.45 and for (R)-[^{18}F]MH.MZ 2.6 (n=4). The cortex to cerebellum ratio was determined to be 2.7 (n=4) for [^{18}F]MH.MZ and for (R)-[^{18}F]MH.MZ 3.3 (n=4) at equilibrium.

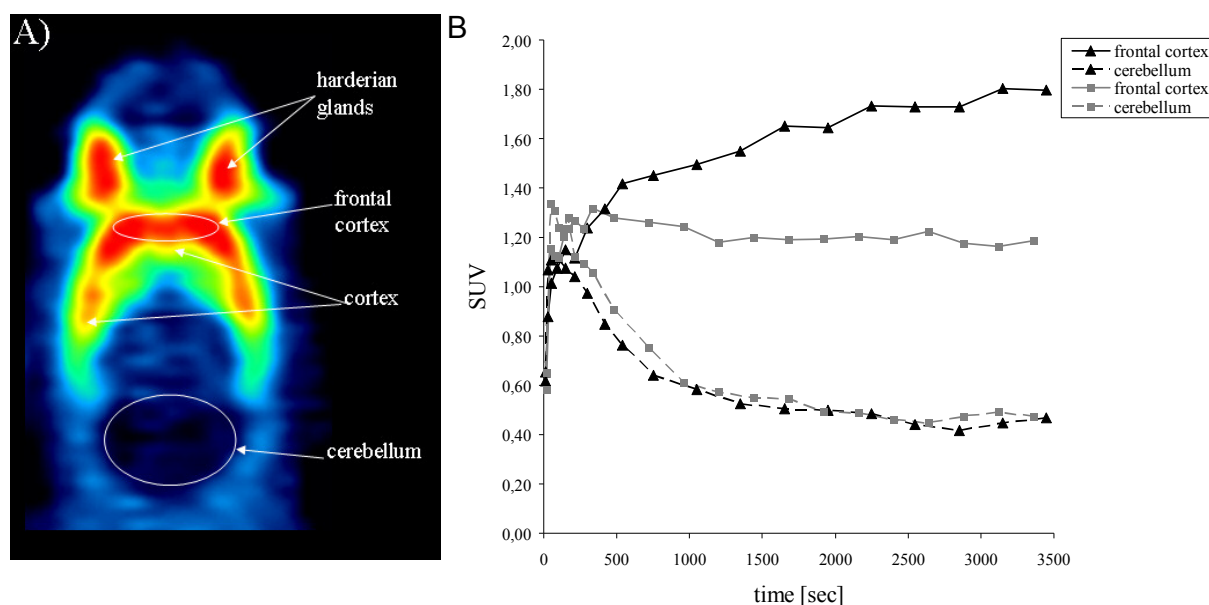


Figure 6: A representative summed μPET image (60 – 90 min) of (R)-[^{18}F]MH.MZ (A) and a comparison of the time-activity curves (TAC's) of [^{18}F]MH.MZ (grey) and (R)-[^{18}F]MH.MZ (black) (B).

Consequently, (R)-[¹⁸F]MH.MZ is the more potent ligand for molecular imaging the 5-HT_{2A} receptor regarding the BP and the cortex to cerebellum ratio.

The possible influence of P-gp on the overall brain uptake and specificity, on the distribution ratio of [¹⁸F]MH.MZ in the frontal cortex compared to cerebellum was determined due to the fact that [¹⁸F]altanserin, a compound similar in structure, has recently been shown to be a substrate of this efflux transporter. The approach was based on transgenic P-gp k.o. mice which were compared to wild type mice under several conditions: *ex vivo* in a pharmacokinetic and brain accumulation study and *in vivo* in a μ PET analysis. All analysis carried out showed that MH.MZ entered the brain but is sensitive to P-gp transport. However, detailed analysis clearly indicated the necessity investigating the functional role of transport mechanisms at the blood-brain barrier, presently P-gp, including its sub-regional distribution not only for drug treatment but also for diagnostic purposes using PET. This is rationalized e.g. due to the fact that Lacan et al.² recently brought the fact into consideration, that the heterogeneous brain distribution of P-gp might influence quantification by simplified reference tissue method (SRTM) using cerebellum as a non-specific reference region for modelling. However, the cortex to cerebellum ratio of [¹⁸F]MH.MZ was not altered by P-gp suggesting any influence of heterogeneous brain distribution of P-gp in rats (Figure 7).

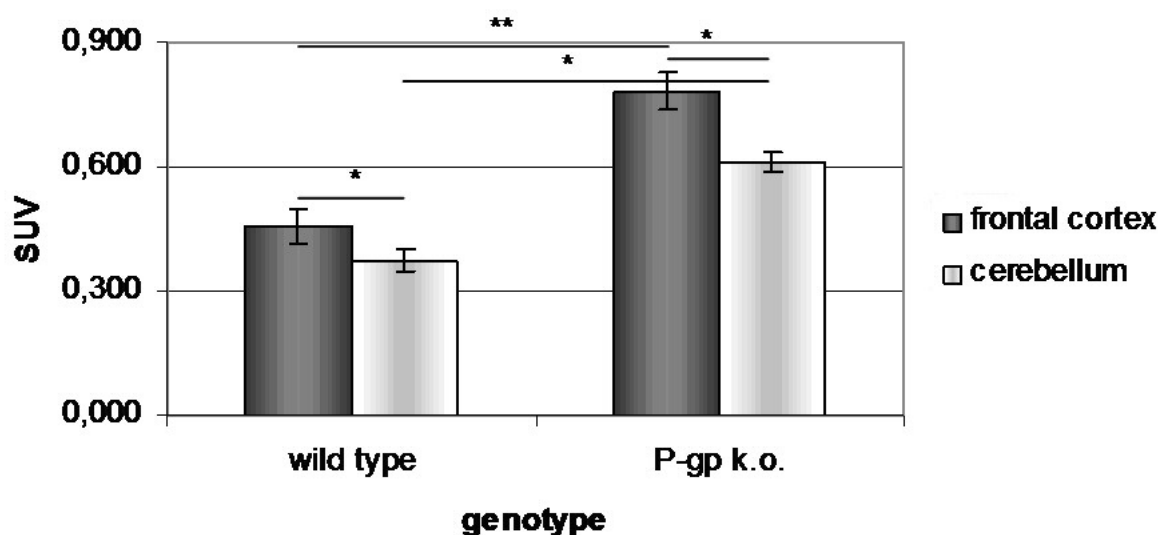


Figure 7: Accumulation of [¹⁸F]MH.MZ in wild type and P-gp k.o. mice showing an increased uptake in P-gp k.o. compared to wild type mice but no altered cortex to cerebellum ratio.

A different labelling approach of MDL 100907 derivatives was also carried out trying to substitute the already in its structure existing fluorine by ^{18}F -fluorine. [^{18}F]MDL 100907 was radiofluorinated in 4 steps using 1-(2-bromoethyl)-4- ^{18}F fluorobenzene as a secondary labelling precursor. The complex reaction required an overall reaction time of 140 min and (\pm)- ^{18}F]MDL 100907 was obtained with a specific activity of at least 30 GBq/ μmol (EOS) and an overall radiochemical yield of 1 to 2 % (Figure 8).

In order to verify its binding to 5-HT_{2A} receptors, *in vitro* rat brain autoradiography was conducted showing the typical distribution of 5-HT_{2A} receptors and a very low nonspecific binding of about 6 % in frontal cortex, using ketanserin or spiperone for blocking.

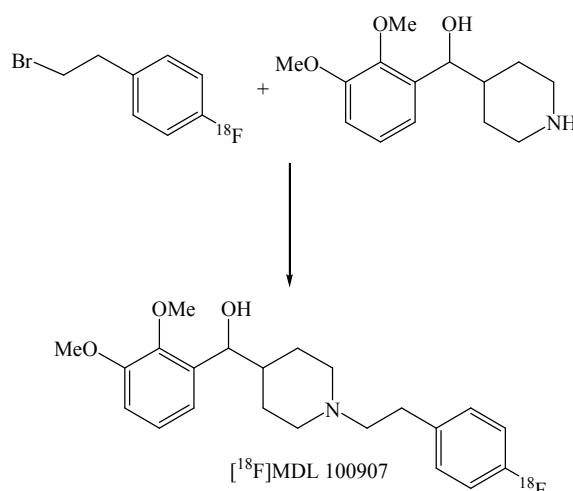


Figure 8: Radiosynthesis of (\pm)- ^{18}F]MDL 100907

A comparison of [^{18}F]MH.MZ and [^{18}F]MDL 100908 shows a similar distribution pattern (Figure 9). However, due to the very low radiochemical yields of 2%, the ^{18}F -labeled MH.MZ derivatives represent the more valuable tracers regarding imaging the 5-HT_{2A} receptor in PET experiments.

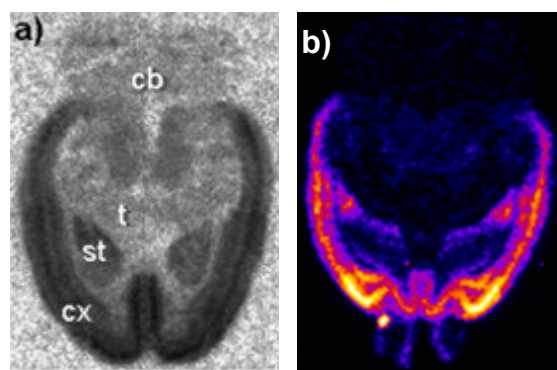


Figure 9: Autoradiographies of [^{18}F]MDL 100907 (a) and [^{18}F]MH.MZ (b). Distribution in horizontal rat brain sections; cb: cerebellum, cx: cortex, st: striatum, t: thalamus

In order to understand the mode of binding of MH.MZ to the 5-HT_{2A} G-protein, three moieties of used 5-HT_{2A} receptor ligands, namely MDL 100907, altanserin, SR46349B, were synthesized and evaluated. Figure 10 shows the chemical structures of synthesized compounds. However, all combined compounds showed reduced affinity toward the 5-HT_{2A} receptor.

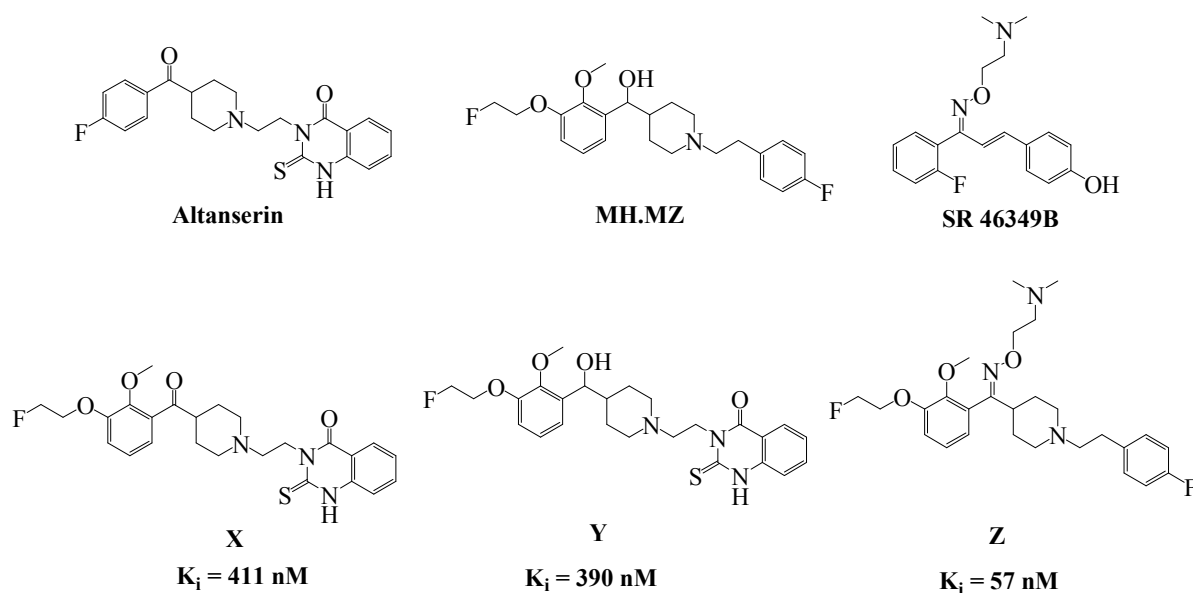


Figure 10: Structure of new 4-benzoylpiperidine derivatives combining elements of altanserin, MH.MZ and SR 46349B

One explanation for the reduced binding characteristics of (X) and (Y) is that altanserin probably binds to the 5-HT_{2A} receptor with the p-fluorobenzoyl moiety in a hydrophobic binding pocket. The remarkably reduced affinity of compounds (X) and (Y) indicates, that the additional space required by the fluoroethoxy group and the methoxy group is not tolerated in this hydrophobic binding pocket. These results demonstrate that [¹⁸F]MH.MZ can only bind to the 5-HT_{2A} receptor with the p-fluorophenylethyl residue in the hydrophobic binding pocket. In conclusion, MDL 100907 and altanserin probably bind *vice versa* in the binding pocket of the 5-HT_{2A} receptor.

5-HT_{1A}:

A second topic studied in this thesis is the 5-HT_{1A} receptor. The 5-HT_{1A} receptor system can already be visualized by [¹¹C]WAY 100635 and [¹⁸F]MPPF. However, Fiorino et al.³ reported about an outstanding high affine ($K_i = 0.021$ nM) and selective compound, 4-[3-[4-(o-methoxyphenyl)-piperazin-1-yl]propoxy]-4-azatricyclo-[5.2.1.0_{2,6}]dec-8-ene-3,5-dione, for the 5-HT_{1A} receptor subtype. By replacing the methoxy- by a fluoroethoxy group of the parent compound, three different reference compounds were obtained in the present thesis enabling a labelling strategy with [¹⁸F]FETos (Figure 11).

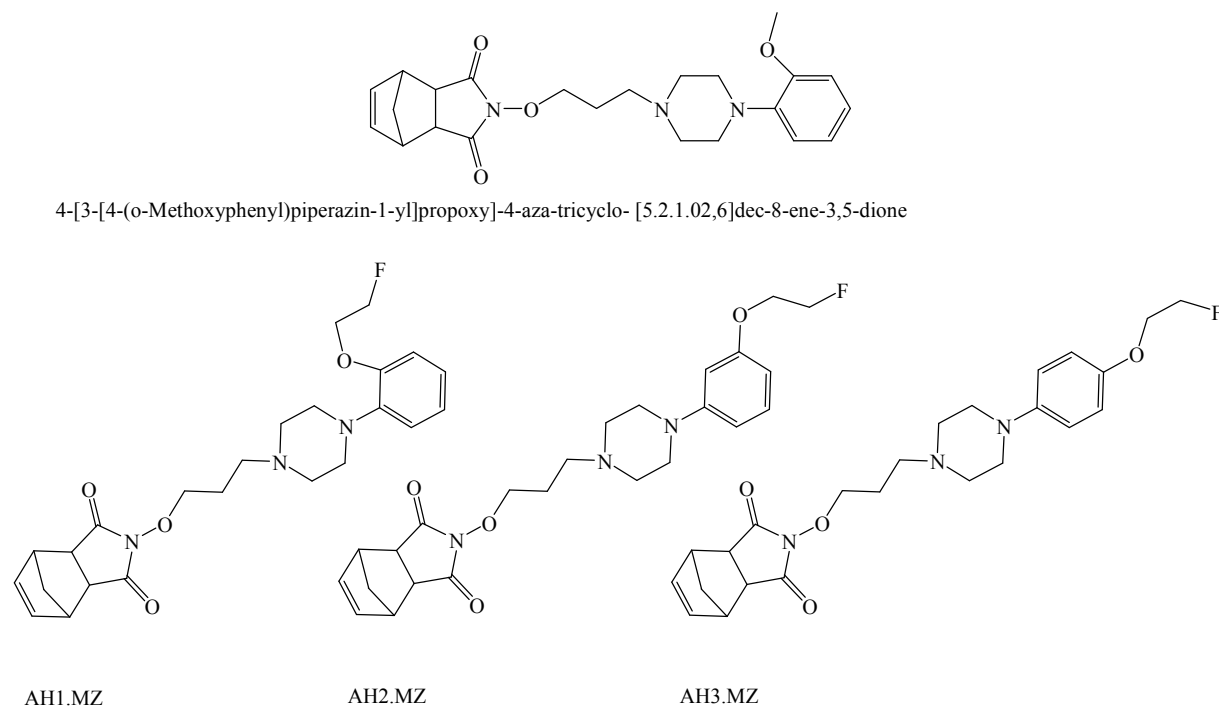


Figure 11: Structures of the original (above) and novel WAY 100635 derivatives (below)

In vitro evaluation of these ligands showed high to moderate affinities toward the 5-HT_{1A} receptor of AH1.MZ ($K_i = 4.2$ nM) and of AH2.MZ ($K_i = 30$ nM), but no affinity toward the 5-HT_{1A} receptor of the p-substituted fluoroethylated compound (AH3.MZ) ($K_i > 10.000$ nM). The receptor profile of AH1.MZ and AH2.MZ demonstrates selectivity within the 5-HT system. However, the outstanding affinity and selectivity of the literature reference compound 4-[3-[4-(o-methoxyphenyl)piperazin-1-yl]propoxy]-4-azatricyclo-[5.2.1.0^{2,6}]dec-8-ene-3,5-dione is mainly lost by introducing a fluoroethyl group. Nevertheless, compound AH1.MZ may provide potential for molecular imaging of the 5-HT_{1A} receptor system. Because of this potential, ¹⁸F-labelling via [¹⁸F]FETos to [¹⁸F]AH1.MZ was carried out and optimized resulting in radiochemical yields of >70%. The final formulation of the injectable solution including [¹⁸F]FETos synthon synthesis, radiosynthesis and a semi-preparative HPLC separation took no longer than 130 min and provided [¹⁸F]AH1.MZ with a purity >98% (Figure 12).

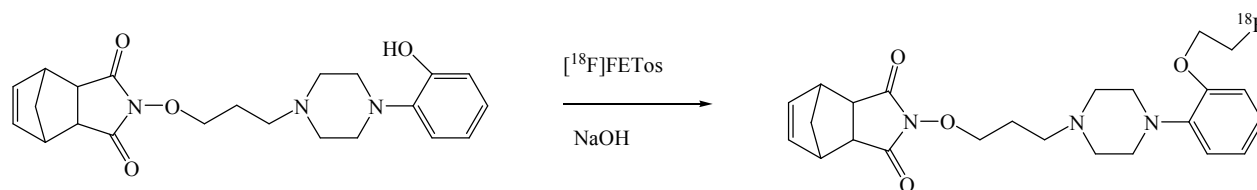


Figure 12: Radiosynthesis of [¹⁸F]AH1.MZ

These *in vitro* and ¹⁸F-labelling results should enable *ex vivo* biodistribution, autoradiography and *in vivo* μ PET studies of [¹⁸F]AH1.MZ.

5 Outlook

In the present thesis, a set of novel ^{18}F -labeled compounds to target postsynaptic serotonin receptors was synthesized and evaluated. The promising results may enable many prospective applications regarding molecular imaging of the 5-HT_{2A} receptors at least in rats. These developments originating from radiopharmaceutical chemistry are now ready to be considered for neuroscience research. Thereby, a comparison in both μPET and human scans of [^{18}F]altanserin and (R)-[^{18}F]MH.MZ should be accomplished to prove the superiority of (R)-[^{18}F]MH.MZ or [^{18}F]MH.MZ. For example, endurance performance experiments could be carried out compared with controls.

5-HT is known to be responsible for the feeling of happiness and it is proposed that sport increases serotonin levels. Therefore, physical training is recommended in depression.⁴ The involvement of SERT, the 5-HT_{1A/1B} and α_{1B} receptor as well as a changed serotonin metabolism in trained subjects could be obtained.^{4,5} Moreover, Meeusen et al. showed a dependency of a 5-HT_{2A/2C} antagonist (ritanserin) on endurance performance in humans.⁶ These facts give place to assume that with a high selective 5-HT_{2A} tracer differences in receptor occupancy could be detected in trained and controlled subjects by PET. This study would provide the first *in vivo* insight how deep physical training can affect our mood. Perhaps even the effect known as the “runner’s high” could be clarified.

Another issue, the involvement of the 5-HT_{2A} receptor in alcoholism could be investigated in addicted small subjects.

Furthermore, challenge studies of dopamine, serotonin and γ -aminobutyric acid (GABA) should be conducted and enhance our understanding of receptor cross talking. Due to the broad spectrum of PET-tracers existing in Mainz (5-HT_{2A}: [^{18}F]MH.MZ, D₂/D₃: [^{18}F]Fallypride; DAT: [^{18}F]PR04.MZ, GABA: [^{18}F]flumazenil) these experiments are conceivable for the first time.

Serotonin challenges against 5-HT_{2A} tracers similar to the known experiments of Jagoda et al., who tested the density of 5-HT_{1A} receptors and changes in endogenous 5-HT by [^{18}F]FPWAY, will be carried out in the close future.⁷ [^{18}F]MH.MZ, (R)-[^{18}F]MH.MZ and [^{18}F]VK-1 are the tracers of choice to possibly measure changes in endogenous serotonin levels by PET. These experiments should allow an insight how increased serotonin levels affect specifically the 5-HT_{2A} receptor and perhaps explain why increased serotonin levels by different mechanisms lead to different biological effects. For example, fluoxetine and

paroxetine, both SERT inhibitors and thus increasing the serotonin level, are applied in depression, whereas the serotonin releaser fenfluramin acts as an anorectic.

Supplementary, [^{18}F]AH1.MZ and [^{18}F]AH2.MZ, novel promising 5-HT_{1A} tracers, should be evaluated in more detail. Both show, in principle, good characteristics to perform PET scans of the 5-HT_{1A} receptor status. [^{18}F]AH2.MZ is within the serotonergic system the more valuable tracer (not published data).

In addition, ^{18}F -labelable derivatives of flibanserin, a drug to cure female sexual dysfunction (FSD) or hypoactive sexual desire disorder (HSDD) have already been synthesized, not shown in this thesis. Figure 13 shows the syntheses of new ^{18}F -labelable flibanserin derivatives already carried out.

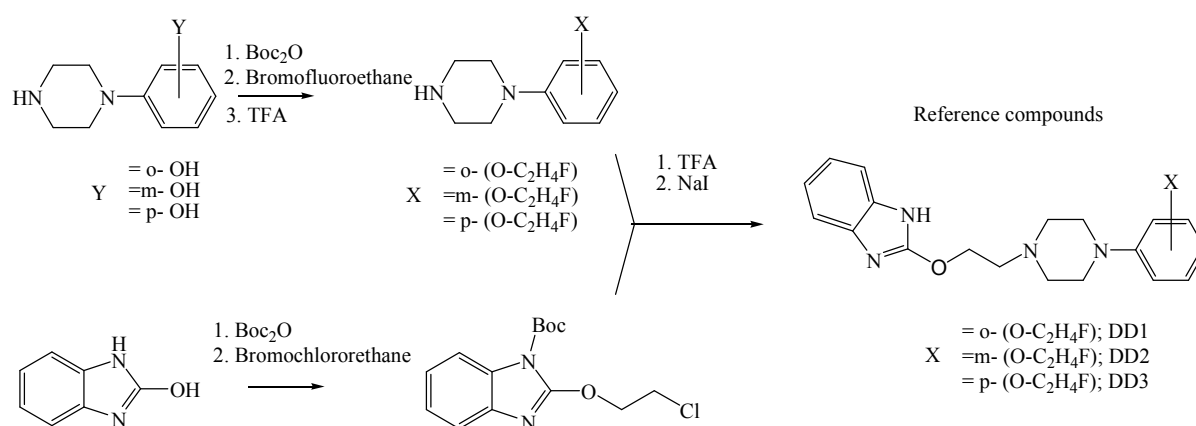


Figure 13: Synthesis of flibanserin derivatives (DD1, DD2, DD3)

The novel 5-HT_{2A} and 5-HT_{1A} tracers combined with in future labelled flibanserin derivatives could provide a better insight of the molecular basis of this drug.

Many other medical and biological experiments are imaginable. However, the future will show how deep the impact of [^{18}F]MH.MZ- as well as [^{18}F]AH.MZ derivatives on the molecular imaging in volunteers and in patients will be.

6 Epilogue

The American congress declared the last ten years of the 20th century to the „decade of the brain.” Exploring the human brain and its network of millions of neurons is probably one of the last Terra incognita. However, during the 21st century the field of neurosciences has to be and will be investigated in more detail. It will play a key role not only in academic but also in social-political areas. In a growing older population within the industrial countries with an increasing number of neurodegenerative and psychiatric illnesses the handle of these disorders will be a major task for social services due to the raising costs for the community. Otherwise a collapse of the health systems will not be avoidable. For example, even today an estimated 121 million people worldwide are affected by depression. Furthermore, AD is the most common neurodegenerative disease and is one of the most costly disorders to society, ranking third after cancer and heart disease. The prevalence of AD in Western societies appears to double every ten years after the age of 65, with estimates indicating that 16-29% of people aged over 85 are afflicted.⁸ In addition, the increasing interest in life-drugs improving living circumstances will enhance pharmaceutical companies to develop new products affecting the mind. The mentioned flibanserin (Ectris®) is only one of the promising pharmaceuticals with the potential to improve the life of many women today. Many other life-drugs will come into the market and may provide customers with the ability e.g. to augment their apprehension.

For these reasons, a deeper insight of neurologic processes has to be gained for therapeutic and pharmaceutical applications. How difficult this is, demonstrates the number of possible synaptic connections. A certain neuron can arrange several thousand connections with other neurons. However, the brain consists of 10^{12} neurons and thus 10^{15} synapses. Therefore, the array of possible combinations of synapses in the human brain is higher than the total number of atoms in the whole known universe.⁹ Hence, it is understandable that our knowledge of the brain, the mind und the behaviour is still limited, even of the possibility to image the working human brain *in vivo* or to analyse genetic substrates of the brain development.

Without any doubt both methods allow a deeper insight in the working brain. Nevertheless, there is still a lot to study. What are the reasons for schizophrenia, AD, drug addiction and many other interferences of the brain? How can they be cured? What is consciousness and how does it come into being? Maybe, some day answers to these questions could lead to the final conclusion whether free will exists or whether it is an illusion only created in our mind. Do we act deterministically as predicted by Einstein? So to speak,

Are we humans or are we dancers?

References

- 1 Andersen, K.; Liljefors, T.; Gundertofe, K.; Perregaard, J.; Bogeso, K.P. Development of a receptor-interaction model for serotonin 5-HT₂ receptor antagonists. *J. Med. Chem.* 1994, 37, 950-962
- 2 Laćan, G; Plenevaux, A; Rubins, D.J.; Way, B.M.; Defraiteur, C.; Lemaire, C.; Aerts, J.; Luxen, A.; Cherry, S.R.; Melega, W.P. Cyclosporine, a P-glycoprotein modulator, increases [¹⁸F]MPPF uptake in rat brain and peripheral tissues: microPET and ex vivo studies. *Eur J Nucl Med Mol Imaging* (2008) 35: 2256-2266.
- 3 F. Fiorino, E. Perissutti, B. Severino, V. Santagada, D. Cirillo, S. Terracciano, P. Massarelli, G. Bruni, E. Collavoli, C. Renner, G. Caliendo, New 5-Hydroxytryptamine_{1A} Receptor Ligands containing a Norbornene nucleus : Synthesis and In Vitro Pharmacological Evaluation. *J. Med. Chem.* 2005, 48, 5495–5503.
- 4 Greenwood, B.N.; Foley, T.E.; Day, E.W.H.; Burhans, D.; Brooks, L.; Campeau, S.; Fleshner, M. Wheel Running Alters Serotonin (5-HT) Transporter, 5-HT_{1A}, 5-HT_{1B}, and Alpha_{1B}-Adrenergic Receptor mRNA in the Rat Raphe Nuclei. *Biol. Psychiatry* (2005) 57, 559-568
- 5 Langfort, J.; Baranczuk, E.; Pawlak, D.; Chalimoniuk, M.; Lukacova, N.; Marsala, J.; Gorski, J. The Effect of Endurance Training on Regional Serotonin Metabolism in the Brain During Early Stage of Detraining Period in the Female Rat. *Cellular and Molecular Neurobiology* (2006) 26, 1327-1341
- 6 Meeusen, R.; Roeykens, J.; Mognus, I.I.; Keizer, H.; De Meirleir, K.; Endurance Performance in Humans The Effect of a Dopamine Precursor or a Specific Serotonin (5-HT_{2A/2C}) Antagonist. *Int. J. Sports Med.* (1997) 18, 571 - 577
- 7 Jagoda, E.M.; Lang, L.; Tokugawa, J.; Simmons, A.; Ma, Y.; Contoreggi, C.; Kiesewetter, D.; Eckelman, W.C. Development of 5-HT_{1A} receptor radioligands to determine receptor density and changes in endogenous 5-HT. *Synapse* (2006) 59, 330-341
- 8 http://en.wikipedia.org/wiki/Alzheimer#cite_note-173
- 9 Thompson, R.F. *Das Gehirn. Von der Nervenzelle zur Verhaltenssteuerung* 3.Auflage 2001 Spektrum Akademischer Verlag GmbH Heidelberg

8 Curriculum Vitae

Angaben zur Person:

Name: Matthias Manfred Herth
Adresse: Hermann-Löns-Str. 6,
65479 Raunheim
Geburtstag/Ort: 07.06.1980; Mainz



Schulbildung:

1991-2000 Frauenlob - Gymnasium
2000-2001 Zivildienst; Sozialstation Raunheim
2001-2006 Chemie-Studium an der Johannes Gutenberg-Universität Mainz
Abschluss: Diplom

Veröffentlichungen:

1. Herth, M.M.; Thorpe, M.R.; Ferrieri, R.A. *J. Label. Compd. Radiopharm.* **2005**, 48, 379
2. Thorpe, M.R.; Ferrieri, A.P.; Herth, M.M.; Ferrieri, R.A. *Planta* **2007**, 2, 541
3. Herth, M.M.; Debus, F.; Piel, M.; Palner, M. Knudsen, G.M.; Lüddens, H.; Rösch, F. *Bioorg. Med. Chem. Lett.* **2008**, 18, 1515
4. Mühlhausen, U.; Ermert, J.; Herth, M.M.; Coenen, H.H. *J. Label. Compd. Radiopharm.* **2009**, 52, 6
5. Herth, M.M.; Kramer, V.; Rösch, F. *J. Label. Compd. Radiopharm.* **2009**, DOI: 10.1002/jlcr.1589
6. Herth, M.M.; Piel, M.; Debus, F.; Schmitt, U.; Lüddens, H.; Rösch, F. *Nuclear Medicine and Biology* **2009**, DOI:10.1016/j.nucmedbio.2009.01.012
7. Herth, M.M.; Kramer, V.; Piel, M.; Palner, M.; Reiß, P.; Knudsen, G.M.; Rösch, F. *Bioorg. Med. Chem.* **2009**, DOI:10.1016/j.bmc.2009.03.021